Distribution Agreement

In presenting this thesis or dissertation as a partial fulfillment of the requirements for an advanced degree from Emory University, I hereby grant to Emory University and its agents the non-exclusive license to archive, make accessible, and display my thesis or dissertation in whole or in part in all forms of media, now or hereafter known, including display on the world wide web. I understand that I may select some access restrictions as part of the online submission of this thesis or dissertation. I retain all ownership rights to the copyright of the thesis or dissertation. I also retain the right to use in future works (such as articles or books) all or part of this thesis or dissertation.

Signature:

Racheal M. Spurlin	Date

Design and Synthesis of Chemical Modulators for Altered Activity of Nuclear Receptor Liver Receptor Homolog-1 and Synthesis of Spirocyclic Piperidines via Radical Hydroarylation

By

Racheal M. Spurlin

Doctor of Philosophy

Chemistry

Eric A. Ortlund, Ph.D.
Advisor

Nathan T. Jui, Ph.D.
Committee Member

Monika Raj, Ph.D.
Committee Member

William Wuest, Ph.D.
Committee Member

Accepted:

Dean of the Graduate School
Kimberly J. Arriola, Ph.D.

Date

Design and Synthesis of Chemical Modulators for Altered Activity of Nuclear Receptor Liver Receptor Homolog-1 and Synthesis of Spirocyclic Piperidines via Radical Hydroarylation

By

Racheal M. Spurlin

B.S., North Carolina State University, 2018

Advisor: Eric A. Ortlund, Ph.D.

A dissertation submitted to the Faculty of the
James T. Laney School of Graduate Studies of Emory University
in partial fulfillment of the requirements for the degree of
Doctor of Philosophy
in Chemistry
2023

Abstract

Design and Synthesis of Chemical Modulators for Altered Activity of Nuclear Receptor Liver Receptor Homolog-1 and Synthesis of Spirocyclic Piperidines via Radical Hydroarylation

By: Racheal M. Spurlin

Liver Receptor Homolog-1 (LRH-1) has been implicated in human disease, particularly inflammatory bowel syndrome and pancreatic and breast cancer, due to its upregulating of genes causing lipid metabolism and stereognosis in the gut, as well as proliferation, invasion, and metastasis of tumor cells. While creating modulators to alter the activity of LRH-1 is desirable, effectively and specifically targeting this protein is extremely challenging due to the hydrophobic nature of its binding pocket. From a high through-put screen a ligand with a [3.3.0] bicyclic scaffold was identified as an agonist for LRH-1. In past iterations of agonists, we have identified an agonist with low nanomolar binding affinity. Although this is a use tool for *in vitro* assays, we sought to improve certain pharmacodynamic and kinetic properties to create a molecule that has improved metabolic stability and solubility properties that shows efficacy *in vivo*.

We further sought to apply our knowledge of previously developed LRH-1 agonists to design antagonists and targeted protein degraders. Based on the structural insights from our agonist design using a [3.3.0] bicyclic scaffold, we developed a series of antagonists, where the lead compound alters the protein's conformation, preventing recruitment of coactivators. Additionally, using compounds from our program, we constructed a bifunctional molecule capable of stimulating degradation of LRH-1 through ubiquitinoylation. After rounds of optimization, we arrived at a successful degrader capable of downregulating LRH-1 target gene expression.

Design and Synthesis of Chemical Modulators for Altered Activity of Nuclear Receptor Liver Receptor Homolog-1 and Synthesis of Spirocyclic Piperidines via Radical Hydroarylation

By

Racheal M. Spurlin

B.S., North Carolina State University, 2018

Advisor: Eric A. Ortlund, Ph.D.

A dissertation submitted to the Faculty of the
James T. Laney School of Graduate Studies of Emory University
in partial fulfillment of the requirements for the degree of
Doctor of Philosophy
in Chemistry
2023

Acknowledgements

The pursuit a PhD is one never taken alone. I wouldn't be here without the Emory Chemistry community and my family and friends. Firstly, I'd like to thank Dr. Nate Jui for accepting me into his lab at Emory back in 2018. I wouldn't be a chemist today if it wasn't for you and your mentorship. Although I may not have ended where I started, I'd also like to thank Dr. Eric Ortlund for welcoming me into his lab after needing to find a new lab. It was very comforting to know that I could continue with my dissertation research. I also wouldn't be here without the guidance of my committee members. Graduate school has been rough in many ways, but Dr. Bill Wuest you've always been encouraging and making me, as well as others believe that I have the ability to do this. Also thank you to Dr. Raj for your deep insight during committee meetings.

I wouldn't be anywhere if it wasn't for my parents. They're constant support and guidance has led me to where I am today. You're help and love has come through in innumerable forms whether it was making sure I was eating or helping me explore Atlanta. Baloo you were always a happy face to come home to. I can't thank my little angel enough. My grandmother and aunt also have been widely supportive during this journey.

Labmates are irreplicable in my heart. Ciaran, Jeff, and Adam I wouldn't have made it past my first year if it wasn't for your mentorship. Thank you for teaching me how to run a project, where to look for help, and of course making mistakes seem small and inconsequential. Your belief that I could obtain a PhD is one of the few reasons why believed it was possible. Cam, you always had the best music and wouldn't shy away from a Broadway ballad to lighten the mood. Thank you for always being a listening ear and a great mentor. Kelly, I'm sorry for the times we shared a hood and I made it smell with all of the thiols. Thank you for teaching me how to use a Schlenk line and how to run a column. Our hood conversations were some of the most encouraging. Cecie,

Alyssa, and Amber we all joined the same lab at the same time. For better or for worse, we somehow all found the best path for us. My first year would have been insufferable, but you always validated me and somehow we made it through together.

Transitioning across campus to a new lab and a new environment was honestly terrifying. Sam it would have literally been impossible without you. You helped me in so many ways and taught me more biology than I ever thought I wanted to know. Jen you honestly keep this lab together. You're always a smiling face and happy to help whenever possible. Thank you, you very underappreciated lab mom. Zhenxin, we've been deskmates for a year. I'm sorry for consistently distracting you in order to procrastinate on my work, but your support has helped me through many hard times. Xu you've taught me that I know nothing about the English language other than what sounds right. You're a great scientist and mentor. Molly and Hannah, you both have young and bright faces in lab. I hope that through the troubles and trials of graduate school you both remember that a bad month doesn't reflect badly on you, science sometimes just sucks. You're both overly capable to obtain a PhD and I can't wait to be watching your defenses in the coming years.

To my community of friends outside of Emory: Emily, Elizabeth, Dawn, Erin, and Lauren. Thank you for always listening to me complain about science and work. For the nights of board games, laughs, and walks, it was nice to get out of the graduate school mindset and remember I am more than a student.

Amber you've always been more than a labmate. I can't believe we met on the first day of graduate school and you quickly became of my best friends. From our early mornings to late nights, and even starting fires, although it wasn't always easy, I wouldn't change our time together for anything. Here's to more camping trips and wild adventures in the future.

Table of Contents

List of Figures

List of Schemes

List of Tables

List of abbreviations

AcOH	acetic acid
AF-1	active function surface-1
AF-2	active function surface-2
AhR	aryl hydrocarbon receptor
aMD	accelerated molecular dynamics
CRBN	cereblon
DBD	DNA-binding domain
DCM	dichloromethane
DLPC	diauroylphosphatidylchloline
DMF	dimethylformamide
DPPC	dipalmitoylphoatidylcholine
ER	estrogen receptor
EtOAc	ethyl acetate
FP	fluorescence polarization
FRET	fluorescence resonance energy transfer
Fsp3	fraction of sp3
FXR	farnesoid x receptor
GPCR	G protein-coupled receptors
GR	glucocorticoid receptor
H12	helix 12
HAT	hydrogen atom transfer
HATs	histone acetyltransferases

HBTU	hexafluorophosphate benzotriazole tetramethyl uronium
HCl	hydrochloric acid
HDAC	histone deacetylase corepressor
Hex	hexanes
HPLC	high pperformance liquid chromatography
HRE	hormone response element
IBD	inflammatory bowel disease
IP	intraperitoneal
IV	intravenous
KSV	Stern-volmer quenching constant
LBD	ligand binding domain
LBP	ligand binding pocket
LCMS	liquid-chromatography mass-spectrometry
LRH-1	liver receptor homolog-1
MD	molecular dynamics
MeCN	acetonitrile
MeOH	methanol
mpk	milligrams per kilogram
mRNA	messenger RNA
MTBE	methyl tert-butyl ether
NMO	*N*-methyl-morpholine *N*-oxide
NMR	nuclear magnetic resonance
NR	nuclear receptors

PC	photocatalyst
POI	protein of interest
PPAR	peroxisome proliferator-activated receptor
PROTAC	proteolysis targeting chimeric
PXR	pregnane x receptor
qPCR	quantitative PCR
RE	relative efficacy
RXR	retinoid x receptor
SET	single electron transfer
SF-1	Steroidogenic factor-1
S_NAR	aromatic cubstitution reaction
TBDPS	tert-butyldiphenylsilyl
TEA	triethylamine
TFA	trifluoroacetic acid
THF	tetrahydrofuran
TLC	thin layer chromatography
TPAP	tetrapropylammonium perrhuthenate
VHL	Von Hippel-Lindau

Chapter 1: Introduction to Nuclear Receptors

1.1 Small molecule modulation on biological processes

Over 95% of FDA approved drugs in 2019 targeted proteins.[1,2] These macromolecules are an essential unit for life due to their mediation of cellular and physiological processes. Although not all proteins are considered druggable, meaning they have the ability to bind and be regulated by small molecules, only 2% of druggable proteins are actually targeted. While there are a variety of different proteins regulated by small molecules, 70% of all approved pharmaceuticals target one of four major receptor superfamilies: G protein-coupled receptors (GPCRs), ion channels (transport proteins), kinases (enzymatic proteins), and nuclear receptors (transcription factors) (33%, 18%, 3%, and 16% respectively) (Figure 1.1).[3] Within these categories there are proteins considered to be "orphans" with no known endogenous ligand,[4] making the ability to create synthetic ligands to alter function essential for biological discovery and drug development.

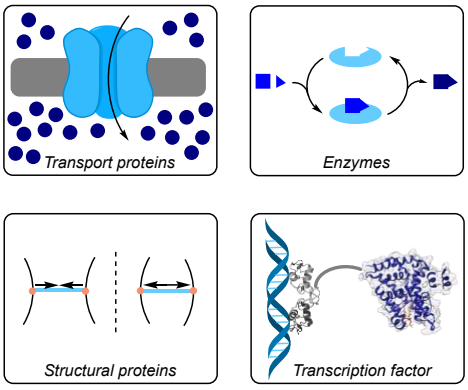

Figure 1.1 Differential regulation of protein function

Nature uses ligands to alter activity in two forms: activation or repression. Simply, agonist, or activators, help the protein complete its function, whereas as an antagonist, or inhibitors, stop or prevent the protein from completing its function.[4,5] The specific molecular process targeted depends on the desired physiological effect and the relation to native protein function. On a cellular level, this has been used to regulate the function of proteins. When designing synthetic ligands this basis can now be expanded upon in order to aid in the knowledge of protein function as well as in the development of new pharmaceuticals.

1.2 The role of nuclear receptors in the body

Approximately 16% of FDA approved drugs target nuclear receptors (NR).[3] NRs are a family of transcription factors. As the name suggests, transcription factors are a series of proteins that regulate the transcription of DNA to messenger RNA (mRNA).[4,6] Following binding to DNA, transcription factors recruit various coactivators or corepressors, which in turn alter the association of DNA to histones by appending various post translational modifications to histones. Coactivators, such as histone acetyltransferases (HATs), are recruited by transcription factors localizing them to DNA, as seen in Figure 1.2. Upon binding to a specific genetic sequence HATs acetylates lysine residues, breaking the electrostatic charge between the negative phosphate DNA backbone and the lysine residues. The unwound DNA is primed to be transcribed to mRNA via general transcriptional machinery, such as RNA polymerase. Conversely, corepressors, such as histone deacetylase (HDAC), deacetylate lysine residues in order to form electrostatic attraction between DNA and histones to form tightly wrapped chromatin.[7,8] Various coregulators allow for varied transcription, due to varied effects of DNA unwinding.[6]

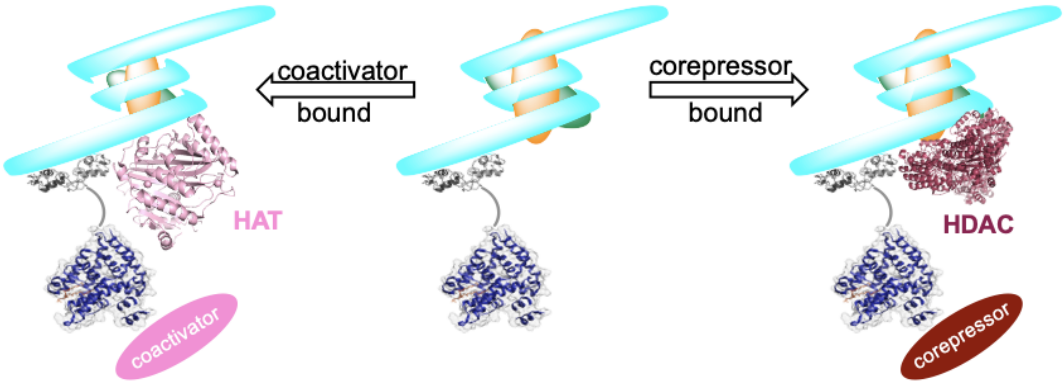

Figure 1.2: Recruitment of coregulators via transcription factors to regulate translation.

Although being able to control transcription is highly desirable for mitigating disease states, not all transcription factors have the ability to be modulated by small molecules. NRs are a family of transcription factors that are regulated by ligands. This allows for the unique and desired medicinal handle in order to regulate gene expression via small molecule modulators. NRs are

comprised of five domains. From the N- terminus to the C-terminus: A/B domain housing the active function surface-1 (AF-1), the DNA-binding domain (DBD) in the C domain, the D domain, the ligand-binding domain (LBD) within the E domain, and F domain containing the active function surface-2 (AF-2) (Figure 1.3).[9] The A/B region is an unstructured region that contains the first active function surface. This widely unconserved region can function independent of ligand regulation giving basal NR activity. The AF-1 is thought to be stabilized through interaction of the DNA via allosteric effects in the DBD. The DBD is highly conserved among NRs. Containing two zinc fingers this domain binds to specific sites on DNA called the hormone response element (HRE). Within domain D there is the hinge region, which is an unstructured peptide chain linking the DBD to the LBD in domain E. The LBD is the main focus of medicinal modulation. Holding the ligand binding pocket (LBP) where small molecules bind, causing a conformational change allowing for the binding of various coregulators via allosteric effects. This region in turn connects to the AF-2 region, moderately conserved across NRs, allowing for the binding of coregulators.[6,9]

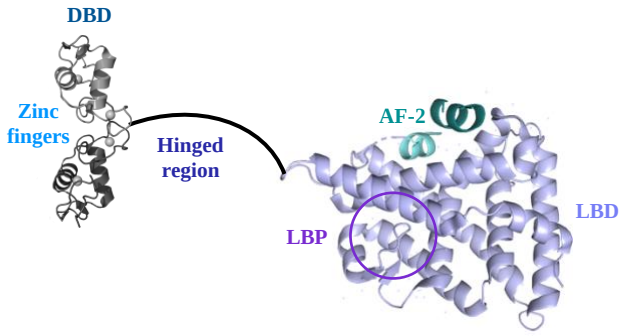

Figure 1.3: Nuclear receptor structure.
Labeled domains: DNA binding domain (DBD), Ligand binding domain (LBD), Ligand binding pocket (LBP), and active function surface-2 (AF-2).

All NRs have a similar molecular structure containing the five previously discussed domains, but they are classified into categories based on their signaling mechanism.[6] Type I nuclear receptors are unique in that they are maintained in the cytoplasm in complex with chaperone proteins until released by ligand binding. Traditionally, when the complex disassociates, the NR is shuttled into the nucleus where a homodimer (two of the same NR interact to function) forms

on a palindromic HRE to regulate transcription. The majority of Type I nuclear receptors are activated by various steroids in the body (such as the estrogen receptor (ER) or the glucocorticoid receptor (GR)).[6,10] Type III nuclear receptors, similarly, form a homodimer binding direct repeat HREs, but reside in the nucleus regardless of ligand binding. Upon ligand activation the corepressors are exchanged for coactivators starting the cascade of reactions for the occurrence of transcription.[11] Type II nuclear receptors work in a similar fashion, but function as a heterodimer (meaning two different nuclear receptors interact to function). Most commonly this heterodimer is formed with retinoid x receptor (RXR).[12,13] Finally, Type IV nuclear receptors have similar activity to Type II receptors, but function as a monomer.[14,15]

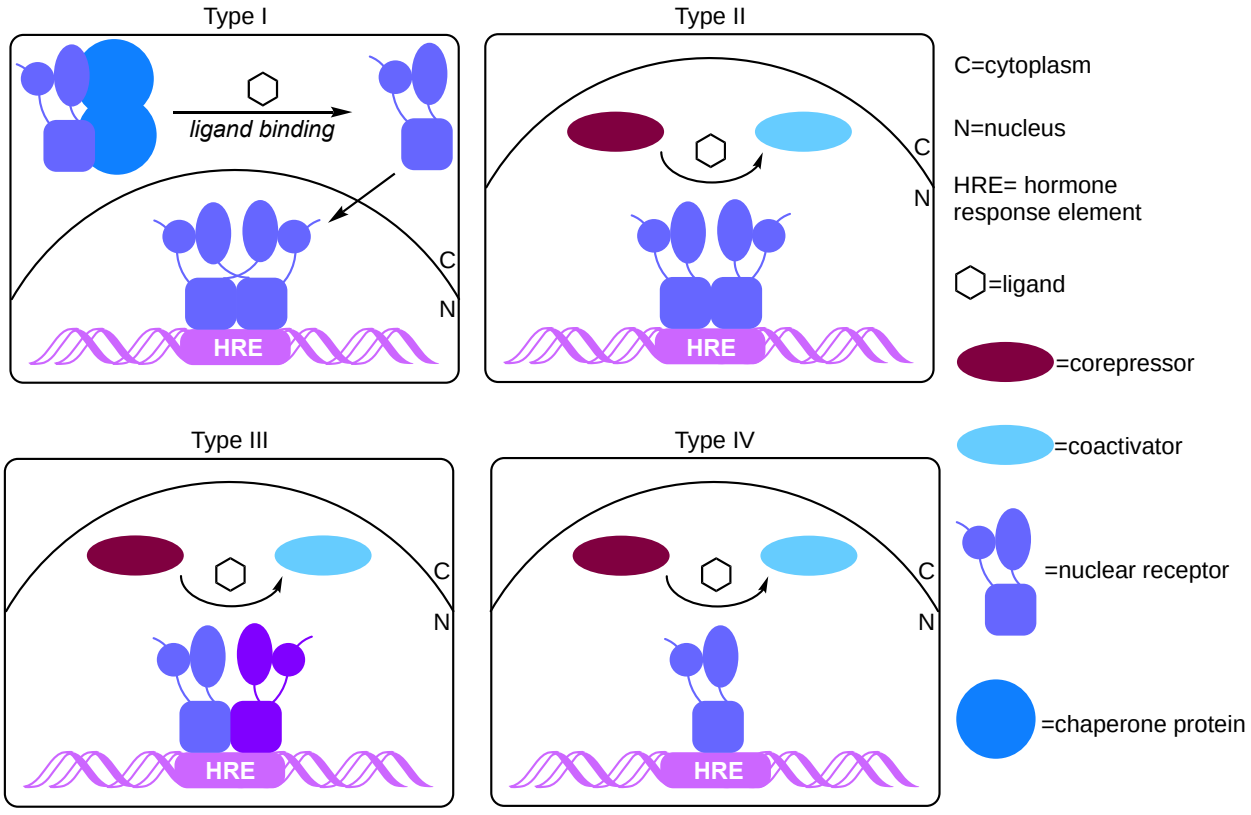

Figure 1.4: Type of nuclear receptors labeled via function

With knowledge on how nuclear receptors function, we are equipped to alter the activity of these unique proteins via small molecule binding. These small molecules are a valuable tool,

allowing for manipulation of genetic material from a chemical standpoint giving insight into biological mechanisms of disease states.

1.3 Liver Receptor Homolog-1 as a disease target

1.3.1 Liver Receptor Homolog-1 and it's role/regulations in the body

Liver Receptor Homolog-1 (LRH-1) or NR5A2 (nuclear receptor family 5 group A member 2) is a Type IV nuclear receptor primarily found in the liver, intestines, pancreas, and breast tissue. LRH-1 plays an essential role in cellular development, proliferation, and metabolic processes.[16–21] As a metabolic regulator, LRH-1 controls lipogenesis, steroidogenesis, and glucose transport and phosphorylation, allowing management of an organism's energy source.[17,21] Through these processes LRH-1 has been tied to a variety of disease states as a potential therapeutic including diabetes, inflammatory bowel disease (IBD), and cancer.

Due to LRH-1 having many roles within the body there are benefits for both its upregulation and downregulation. IBD affects 3.1 million people in the United States alone. Referring to the chronic inflammation of tissues in the colon, IBD, includes Crohn's and colitis.[22,23] It's been well reported that increasing the levels of LRH-1 activity can decrease inflammation in the gastrointestinal tract. LRH-1 regulates inflammation via transcriptional control of CYP11A1 and CYP11B1, which then induces the synthesis of glucocorticoids from cholesterol leading to a decrease in inflammation.[20,24,25] In IBD models, it has been well studied, that when LRH-1 is activated, intestinal tissues show a decrease in inflammation as well as an increase in tissue regeneration.[25,26]

LRH-1 has been termed a stem cell factor for its role in maintaining pluripotency during development and a crucial role in cellular regeneration in adults.[19,27] Due to its involvement in

these cellular processes it has been shown to play a role in many cancers, including breast, pancreatic, and colon via transcriptional regulation of genes, such as MMP9, c-Myc, and cyclin E that are involved in the proliferation, invasion, and metastasis of cancer cells.[21,28] In breast cancer, which effects one in nine women,[29] LRH-1 is an attractive target due to its transcriptional regulation of the enzyme aromatase. Aromatase catalyzes the reaction converting androgens (like testosterone) into estrogens. Estrogen activates the estrogen receptor α (ERα), another NR, that upregulates the transcription of various kinases such as PI3K and AKT, which promote cell proliferation, survival, and migration.[30] ERα also upregulates the transcription of LRH-1, creating a positive feedback loop between ERα and LRH-1. This loop not only leads to the upregulation of aromatase, but other genes like GREB1, cyclin E, and c-Myc.[28] Antagonizing LRH-1 would decrease the upregulation of transcriptional genes leading to invasion, proliferation, and metastasis of tumors resulting from the feedback loop.[16]

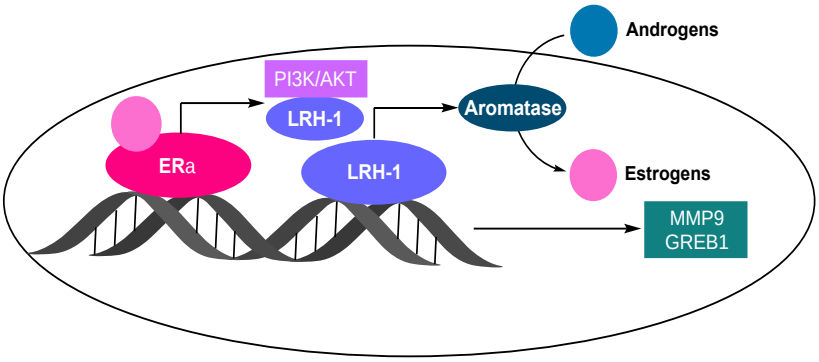

Figure 1.5: Mechanistic view of LRH-1's role in breast cancer cells

1.3.2 Small molecule manipulation of LRH-1

LRH-1 has been notably regulated by various phospholipids, including phosphatidylethanolamine, phosphatidylinositol, and phosphatidylcholines (Figure 1.6).[16] To date the most activating phospholipid for LRH-1 has been shown to be diauroylphosphatidylchloline (DLPC).[31,32] On the other hand, similar phospholipids such as dipalmitoylphoatidylcholine (DPPC), a phospholipid with a longer carbon chain, do not have an effect on LRH-1 activity.[33]

Although DLPC is an agonist for LRH-1, as a lipid it has poor solubility and is easily metabolized, remodeled, and sequestered in membranes making it a poor pharmacological tool. Furthermore, DLPC has low efficacy and potency in activating LRH-1.[16] Therefore, there would be a great benefit in creating synthetic ligands for LRH-1.

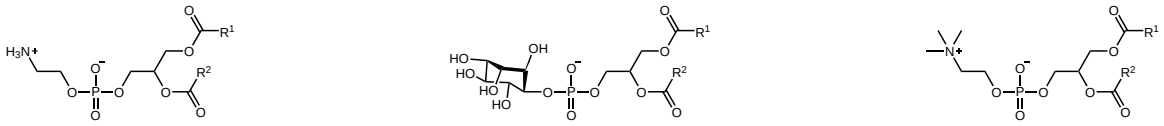

Figure 1.6: Medium chained lipids known to regulate LRH-1

In the hope of finding a synthetic agonist for LRH-1 Richard Whitby in collaboration with GSK preformed a high-throughput screen. From this screen, they identified GSK8470 via a fluorescence resonance energy transfer (FRET)-based biochemical assay as having the best potency (EC_{50} = 430 nM). To show further efficacy of this compound, messenger RNA (mRNA) levels were measured of one of the known transcription products of LRH-1, SHP, via quantitative PCR (qPCR). They found these levels, doubled in both a liver cell line (HepG2) and human hepatocytes in the presence of GSK8470.[34] Although this molecule exceeded DLPC (EC_{50} = >100 μM) in potency and efficacy the aniline is an acid labile moiety. Whitby, therefore, continued structure-activity relationship (SAR) around the bicyclooct-2-ene ring in order to improve both efficacy and potency. Some of the most substantial findings were the replacement of the aniline with a styrene and addition of an exo hydroxyl group to the [3.3.0] bicyclic structure which increased the activity by 1.7x.[35,36] This compound deemed RJW100 became the leading agonist that was then used in future SAR to continue to probe regions around the core to increase the agonist activity of LRH-1.

Although the changes between GSK8470 and RJW100 have great importance on LRH-1 activation and stability, the ability to crystalize RJW100 within the LBD proved unfruitful until 2016.[36] As seen in Figure 1.7, there are a few key observations: RJW100 assumed a different conformation with a near 180° rotation from GSK8470, attributed to the hydroxyl group forming a hydrogen bonding network to interact with H390, R393, T352, and D389 and the styrene replacement of the aniline creates pi T-stacking with H390, while the hexyl tail helps orient the compound pointing towards the entrance of the binding pocket.[16,36] This structure led the Jui lab to synthesize a series of molecules that would mimic the interactions seen in the LRH-1-DPLC crystal structure.[37] Flynn and coworkers embarked on a synthesizing a series of compounds in order to mimic the phospholipid interactions at the mouth of the pocket with the goal of enhancing allosteric activation of the protein to more faithfully mimic PL-like activation. Phosphate substitutions have been extensively studied as carboxylic acid isosteres. In order to find the optimal

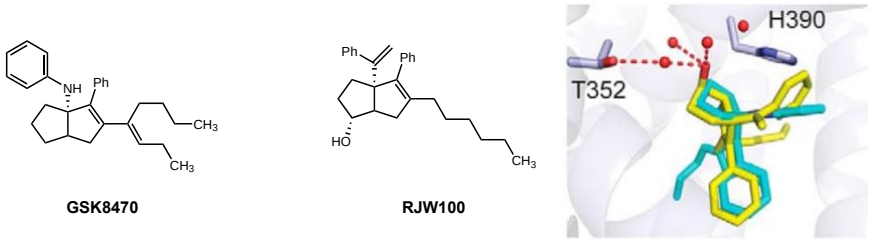

Figure 1.7: Structure of LRH-1 agonists from Richard Whitby

PDB of crystal structures: RJW100(yellow): 5L11; GSK8470(cyan): 3PLZ

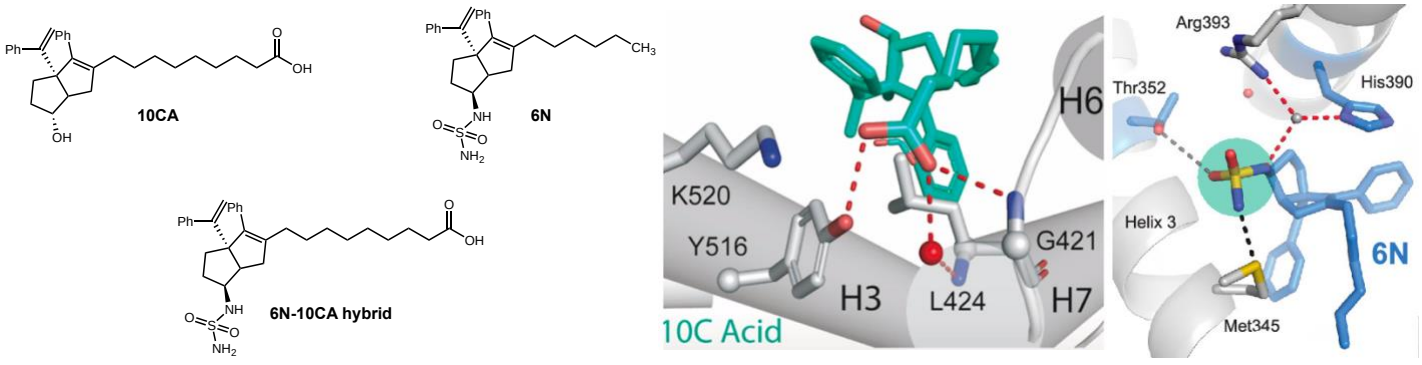

Figure 1.8: New agonist from SAR with corresponding crystal structures

PDB of crystal structures: 10CA(teal): 7JYD; 6N(blue): 6OQY

distance from the RJW100 core a series of tails were synthesized differing in carbon length, finding that the carboxylic acid on the tenth carbon (10CA) of the tail yields the highest LRH-1 activity.[38]

After interrogating the effects of the interactions at the mouth of the pocket, another series of molecules looked to probe interactions within the binding pocket. Mays et al. developed a series of 12 compounds that replaced the hydrogen bonding water network that the hydroxyl in RJW100 used, in order to make direct interactions with the amino acids. Within this series a sulfamide in the endo confirmation (compound 6N) was shown to displace the water network in order to made direct interactions with amino acids M345 and T352. This increased the potency (EC_{50}) to 15 nM, 1.3x higher than RJW100.[39] With the desire to make both the interactions deep within the pocket at the mouth of the pocket with the phospholipid mimic, a hybrid compound was created (6N-10CA hybrid).[40] This molecule increased both the efficacy and potency of previous small molecule modulators. Although a good modulator for LRH-1 in *in vitro* studies, this molecule is largely insoluble in aqueous solutions and has sites prone to oxidation.

The majority of research has focused on creating synthetic agonist for LRH-1, but there is also a need to decrease levels of LRH-1 transcriptional activity (as discussed in section 1.3.1). To date there have been few molecules described as antagonist or inverse agonists of LRH-1.[41–43]

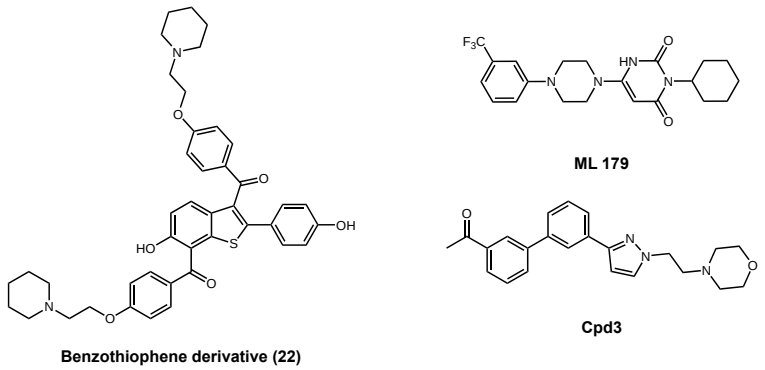

Figure 1.9: Structures of LRH-1 antagonists and inverse agonists

Most notably compounds from the Flettrick lab were first shown to decrease activity in cellular assays. Their current lead antagonist, Cpd3 has been shown to decrease LRH-1 transcriptional genes, such as SHP.[42] These molecules work with a micromolar IC_{50} and although there has yet to be a crystal

structure of these compounds bound in the pocket of LRH-1 or verification of their mechanism of action, the decrease of levels of LRH-1 activity in certain disease states shows promise for LRH-1 as a potential therapeutic.

Chapter 2: Lead optimization of Agonist Scaffold for LRH-1 for *in vivo* studies

2.1 Introduction

Nuclear receptors (NR) are a desirable drug target due to their ability to regulate gene transcription in response to small molecule ligands. The conformational change of the protein induced by ligand binding allows for the association of coregulator proteins, which in turn drives the recruitment of transcriptional machinery.[4,6] As a phospholipid-sensing regulator, liver receptor homolog-1 (LRH-1) favors the binding of hydrophobic molecules due to its large lipophilic binding pocket.[16,31] Although LRH-1 is a promising target as an inflammatory bowel disease (IBD) therapeutic due to its role in lipid metabolism and stereognosis,[17,18,21] the phospholipids that bind this NR are traditionally unfit for clinical and laboratory use for a myriad of reasons, including rapid metabolism, poor solubility, and low potency. Therefore, although small molecule modulators are highly desirable for this nuclear receptor, due to the hydrophobicity of the binding pocket many synthetic ligands also suffer from poor pharmacodynamic and kinetic properties.[16]

While there have been multiple generations of synthetic ligands for LRH-1 (Figure 2.1) starting with GSK8470, the current leading agonist for LRH-1 is a compound deemed as 6N-10CA hybrid.[34–36,38–40] While this molecule compared to its predecessors has higher potency and a low nanomolar binding affinity, it lacks many attributes desired for clinical use. The 6N-10CA hybrid has many labile moieties prone to oxidation, high lipophilicity leading to insolubility in aqueous solutions, has unselective activation between NRs within the same

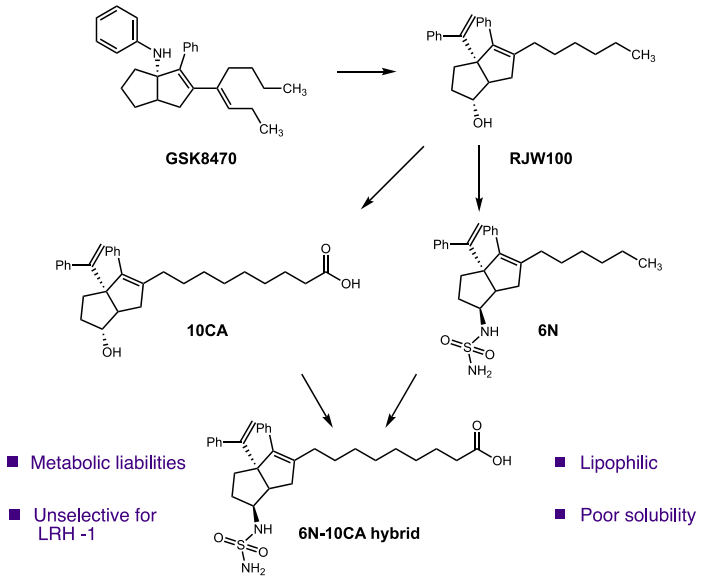

Figure 2.1: Evolution of [3.3.0] bicyclic LRH-1 agonists from GSK8470 to the current most potent compound (6N-10CA hybrid)

family, and requires a challenging synthesis limiting the scalability. We investigated probing these aspects of the molecule in order to improve the pharmacokinetic and dynamic properties.

2.2 Results and Discussion

2.2.1 Altering selectivity between LRH-1 and SF-1

Although LRH-1 has great potential to be a therapeutic target, due to conservation across of the ligand binding domain (LBD) within the NR5A family, creating a selective modulator has proven to be challenging. Steroidogenic factor-1 (SF-1), from the same family (NR5A) as LRH-1, contains 76% amino acid similarity of the LBD with LRH-1.[44] SF-1 is a strong regulator of sex determination as well as its overexpression being linked to a variety of rare cancers.[45–47] With high similarity of binding pockets, there is an interest and utility in creating a selective modulator between the two NRs.

There have been few molecules that have shown selectivity between the two homologous proteins. Whitby and coworkers described three molecules that have selectivity for one of the two proteins, RJW 101-103. Whereas RJW101 exhibits selectivity towards LRH-1, RJW102 and 103 are selective for SF-1 (Figure 2.2).[35] While their reason for selectivity remains unknown, in the series of compounds to displace the deep-pocket water interactions two molecules were found to be selective for LRH-1. Compounds 2N and 4N both show selectivity for LRH-1 over SF-1 (Figure 2.3B).[39] While there is selectivity between these two nuclear receptors, the potency for

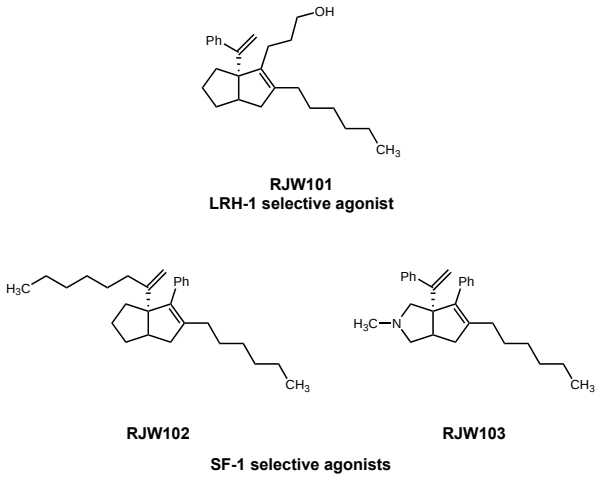

Figure 2.2: Structures of agonists found selective between the NR5A family developed by R.J. Whitby

LRH-1 is not comparable to that of 6N. Therefore, we proposed to increase the potency of these molecules by adding the carboxylic acid tail to create interactions at the mouth of the pocket.

The [3.3.0] bicyclic core was formed via the Whitby cyclization from a 1,6-enyne, phenylacetylene, and a dibrominated alkyl hydroxyl tail. After global deprotection, oxidization of the molecule occurred via TPAP and NMO followed by formation of a methyl ester. The formed carbonyl undergoes a reductive amination with ammonia, which due to the conformation of the core, solely forms the endo amine. The primary amine is either acylated to form the 2N-hybrid compound or reacted with an isocyanate for the formation of the 4N-hybrid compound (Scheme 2.1).

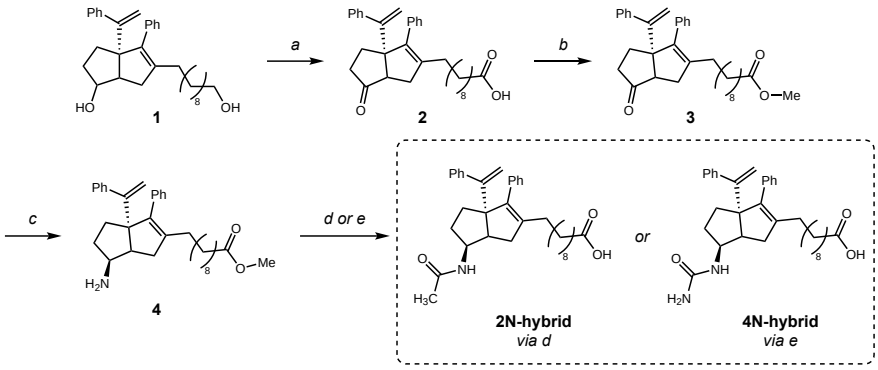

Scheme 2.1: Synthesis of compounds 2N-hybrid and 4N-hybrid

a tetrapropylammonium perrhuthenate,, H_2O, MeCN, 23 °C, 16 h; *b* MeOH, concentrated aqueous HCl, 23 °C, 16 h; *c* NH_3 (7 N in MeOH), titanium(IV) isopropoxide, 23 °C, 6 h; sodium borohydride, 16 h; *d* acetyl chloride, triethylamine, DCM 0 °C, 1 h; aqueous HCl 23 °C, 48 h; *e* (trimethylsilyl)isocyanate, triethylamine, MeCN 23 °C, 16 h; lithium hydroxide H_2O/THF °C, 16 h.

To evaluate the efficacy of the compounds we performed a luciferase reporter assay for both LRH-1 and SF-1, respectively. As seen in Figure 2.3C, in both cases the efficacy of the compound increased for LRH-1. Positively, when comparing the fold activation to SF-1 there is no significant increase in activation between the three concentrations, but unfortunately it took the max concentration of 10 μM to reach the full efficacy. Therefore, the selectivity was maintained while efficacy was increased, but potency of the molecule was not.

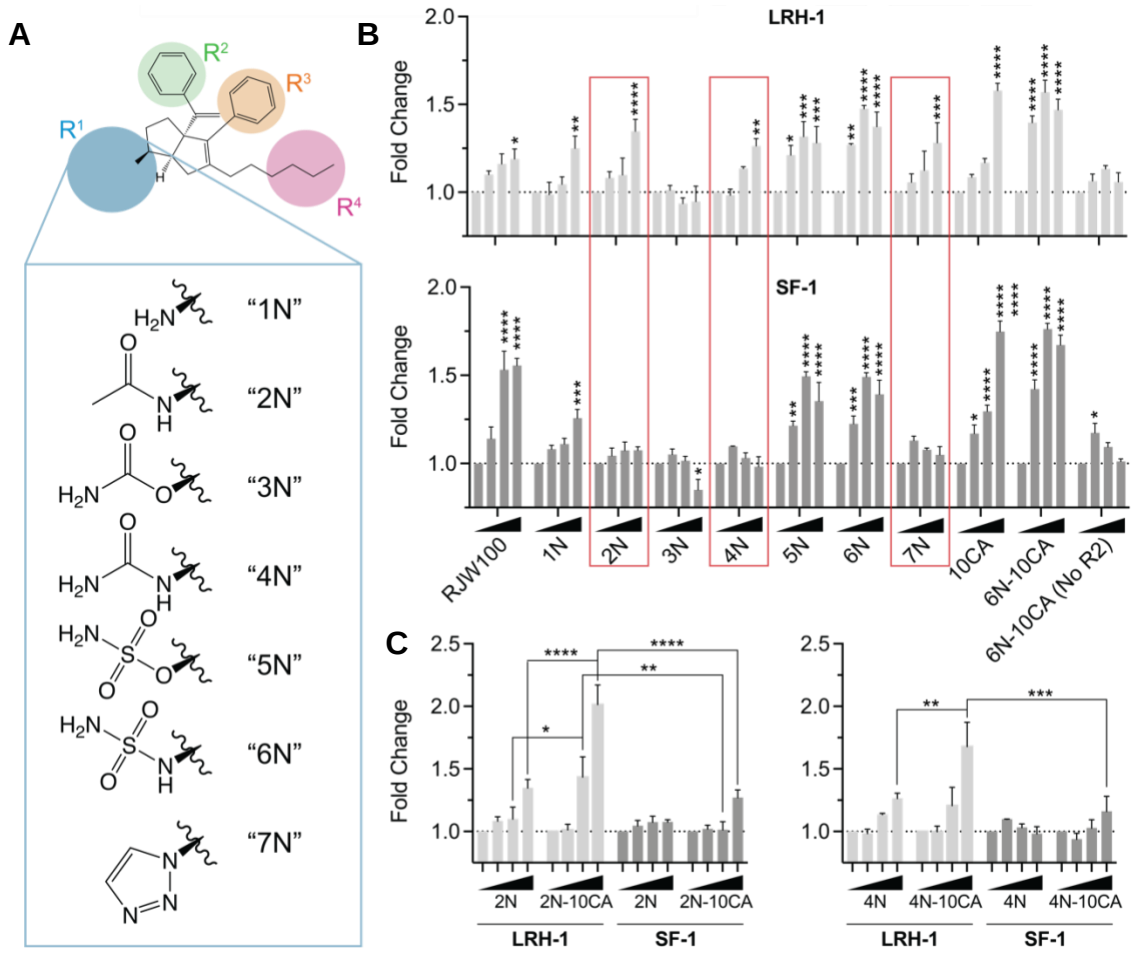

Figure 2.3: Small molecules show selectivity for LRH-1

(A) Chemical structures of small molecule agonists with R^1 modifications are shown. (B) LRH-1 (top) and SF-1 (bottom) luciferase reporter assays are shown. Four bars for each ligand represent (from left to right) DMSO (control), and small molecule at 0.1, 1, and 10 µM. Data normalized and analyzed relative to DMSO control: Two-Way ANOVA with Dunnett multiple comparison's test. *p<0.05, **p<0.01, ***p<0.001, ****p<0.0001. Boxed in red are ligands that demonstrate specificity for LRH-1. (C) Luciferase reporter assays were used to examine LRH-1 and SF-1 activation by 2N and 4N with 10CA tail modifications. Four bars for each ligand represent (from left to right) DMSO (control), and small molecule at 0.1, 1, and 10 µM. Data normalized and analyzed relative to DMSO control: Two-way ANOVA with Tukey multiple comparison's test. *p<0.05, **p<0.01, ***p<0.001, ****p<0.0001.

To determine possible off target activity of these molecules with NRs outside the NR5A family, we ordered a NR activity screen. Dosing at maximum efficacy we see minor activation for AhR, FXR, and PPARγ. PXR was fully activated to the reference, but no other nuclear receptor in the panel showed activation from the compounds (Figure 2.4). PXR is drug sensor responsible for the metabolism of small molecules, therefore the activation of PXR is not uncommon.[48,49]

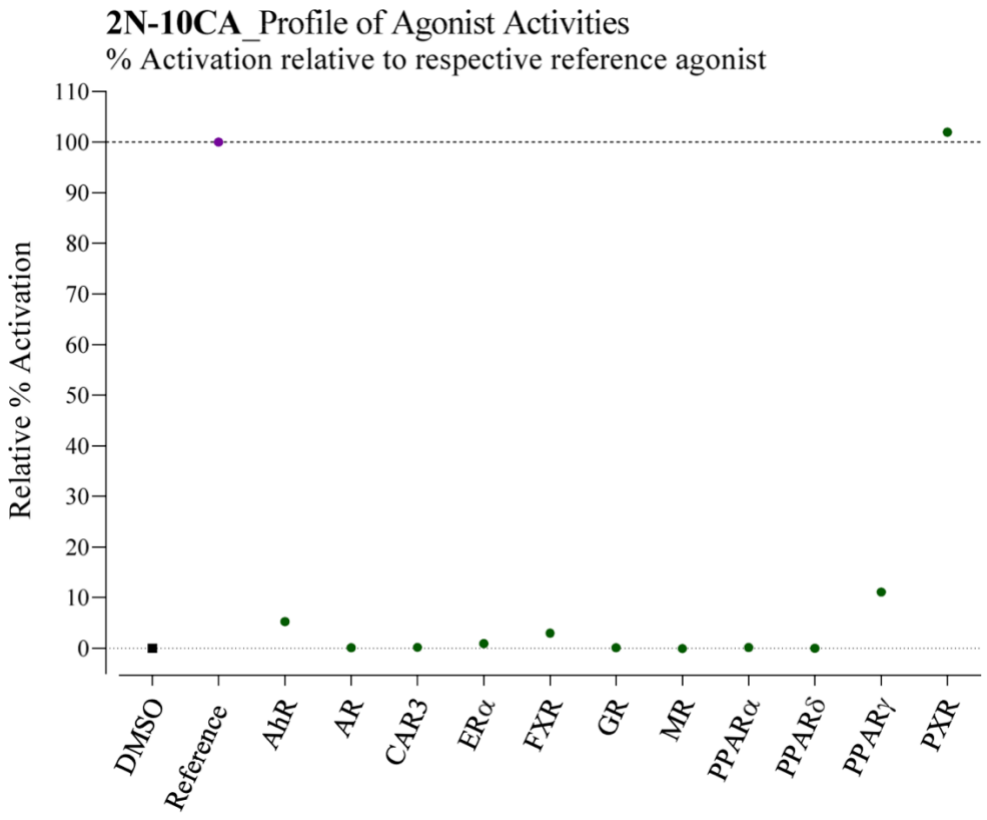

Figure 2.4: Activation comparison of a panel of nuclear receptors

2N-10CA was introduced to reporter cells at 10 μM and the activity of respective nuclear receptors was tested. Agonism was examined for all receptors, aside from RORγ, where inverse agonism was tested. Data was normalized to receptor activity by an agonist (or antagonist for RORγ) for each receptor added at a concentration corresponding to the EC_{100} (Or IC_{100} for RORγ).

Overall, we successfully maintained selectivity between two homologous proteins (LRH-1 and SF-1) in the same NR family. While there isn't monogamous selectivity across a range of NRs, we were also able to increase the efficacy via addition of the 10-carbon atom carboxylic acid tail. Through this we are interested in exploring further head groups to increase the potency of the molecule, while also maintaining selectivity within the NR5A family.

2.2.2 Synthesis of carboxylic acid bioisosteres series

The previously designed carboxylic acid used to mimic the polar interactions of phospholipids at the mouth of the pocket has been shown to increase potency, efficacy, and the thermal stability of LRH-1.[26,38] Although the acid is an important moiety on this pharmacophore,

carboxylic acids have been reported to be metabolically instable, toxic, as well as having limited passive diffusion across biological membranes. Therefore, it would be beneficial to create a series of bioisosteres to increase pharmacological properties, but also to further the phospholipid mimic at the mouth of the pocket.

A series of isosteres were synthesized (Scheme 2.2) in order to improve lipophilicity of the phospholipid mimics. The set of six isosteres were first interrogated in an *in vitro* system for potency, efficacy, and relative thermal stability. Via a fluorescence polarization (FP) competition assay previously developed for LRH-1[50] we found that while the tetrazole and serine isosteres bound with nearly identical affinity as the parent compound 10CA, all other isosteres lost some affinity for the protein (Figure 2.5A). This was also reflected in the thermal stabilization of LRH-1 (Figure 2.5B). When comparing the downstream gene expression via quantitative real-time polymerase chain reaction (qPCR) we see that there is a significant increase in both SHP and CYP7A1, two highly regulated genes of LRH-1, for the tetrazole. The sulfamate and serine isosteres saw about a two-fold increase for CYP7A1 (Figure 2.4D). Via a luciferase reporter we were able to determine the relative efficacy (RE) to 10CA, as well as the EC_{50}. As seen in Figure 2.4C, there are two compounds that show both an improvement in the efficacy and

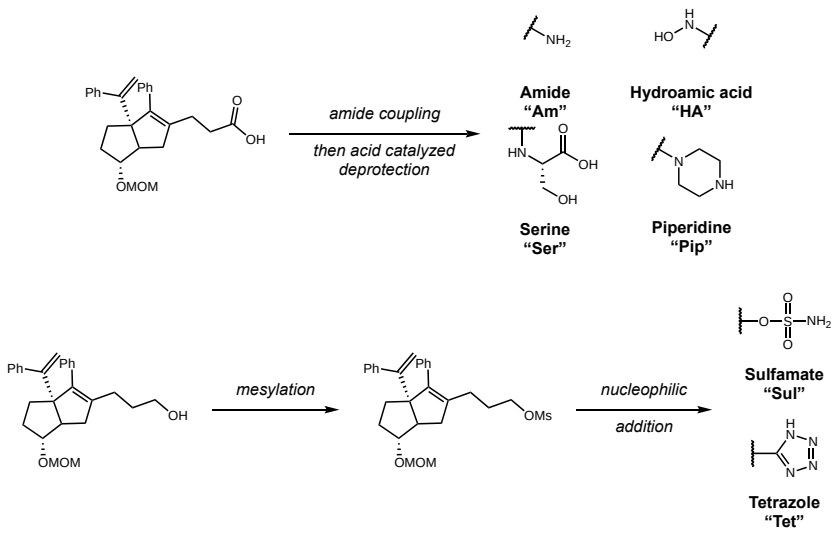

Scheme 2.2: Representative scheme of the synthesis of bioisosteres for LRH-1

potency (Tet and HA). The tetrazole alone shows both improved potency as well as an increase in target gene expression of cultured cells.

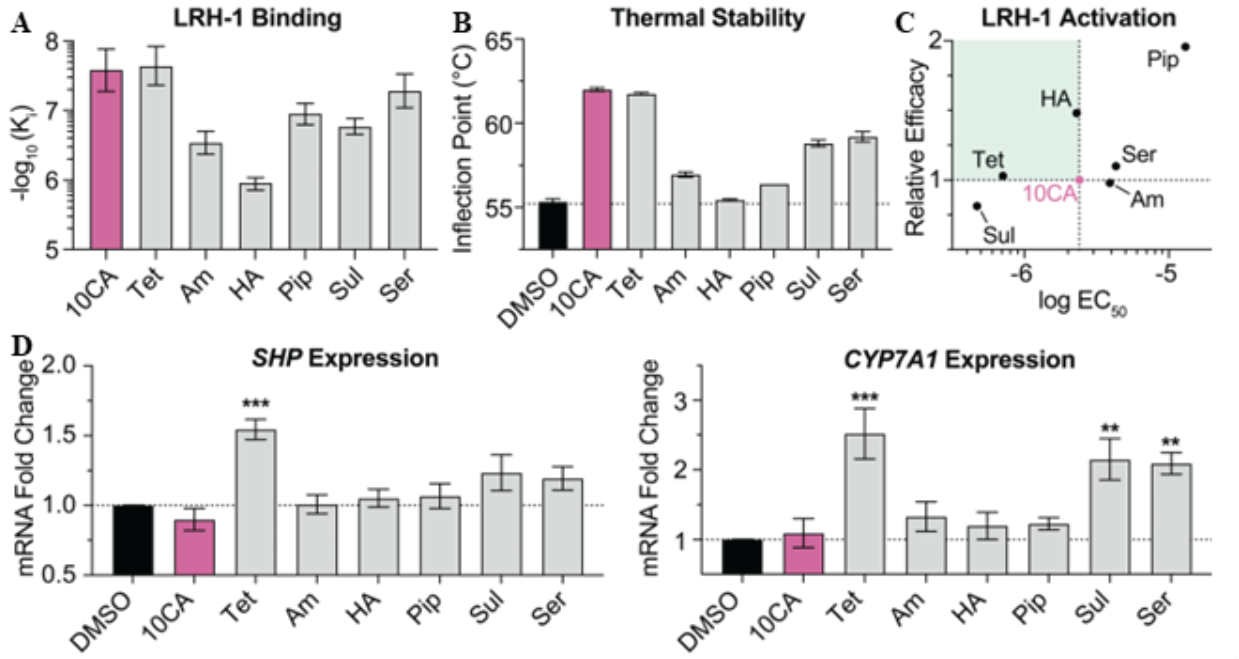

Figure 2.5: Tet isostere maintains high affinity while improving compound potency and increasing LRH-1 target gene expression

(A) FP competition assay showing binding of compounds to the LRH-1 LBD (K_i: inhibition constant). Data shown as mean +/- from two independent experiments. Error bars represent 95% confidence intervals. (B) Comparison of ligand-driven thermal stability of the LRH-1 LBD. The inflection point corresponds to the temperature at which the protein unfolds. Data shown as mean +/- SEM from two independent experiments. (C) Data from luciferase reporter assays. Relative efficacy (RE) was calculated by normalizing the fold change by that of 10CA. The quadrant representing improved potency and efficacy is shaded in green. Data shown as mean from three biological replicates. (D) RT-qPCR analysis of HepG2 cells treated with agonists (10 μM: Tet, Sul; 30 μM: 10CA, Am, HA, Pip, Ser) for 24 hrs. Data normalized to signal of DMSO control and shown as mean +/- SEM from four biological replicates. Brown-Forsythe and Welch one-way ANOVA with Dunnett multiple comparisons test **p<0.01, ***p<0.001

In order to investigate the mechanism of tetrazole mediated activity, a crystal structure was successfully solved of the LRH-1 LBD bound to Tet and a fragment of the coactivator TIF2 (Figure 2.6). Via this crystal structure we are able to identify the similarities of the tetrazole and 10CA within the pocket of LRH-1. The *exo* hydroxyl on the [3.3.0] core participated in hydrogen bonding to the polar residues within the pocket via a conserved hydrogen bonding network, as previously seen with both RJW100 and 10CA. On the other hand, at the mouth of the pocket we see an increase of interactions with polar residues. The tetrazole creates both direct and hydrogen bonding

interactions via water networks with amino acids G421, Y516, and K520. These interactions are attributed to an increased affinity for LRH-1.

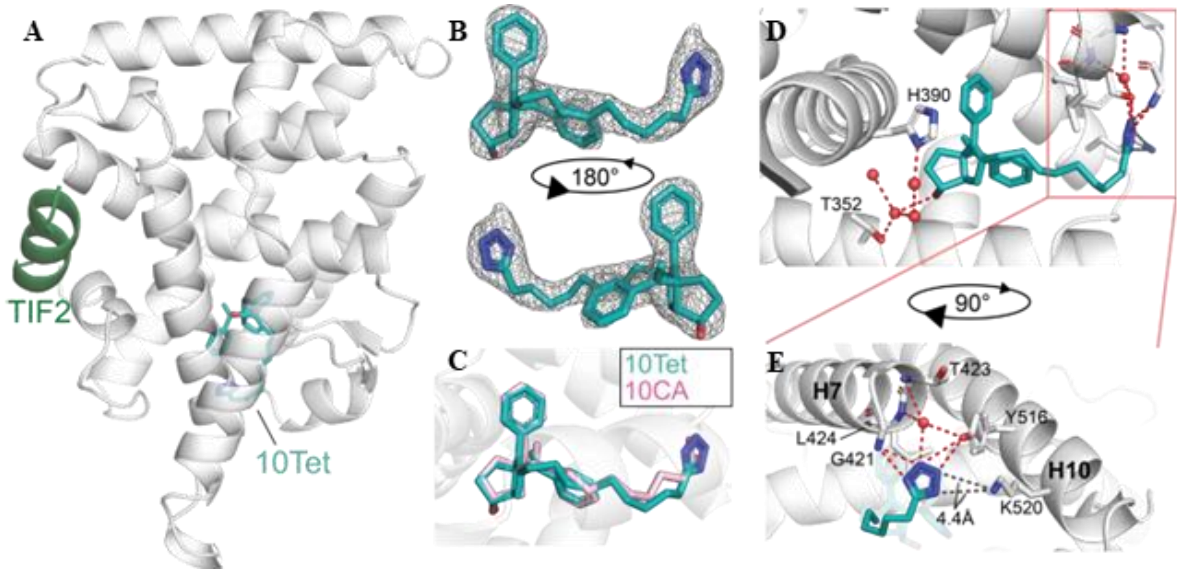

Figure 2.6: Crystal structure of LRH-1 LBD complexed with Tet and fragment of coactivator TIF2 reveals interactions at both regions of binding pocket

(A) Crystal structure of Tet (cyan) bound to the LRH-1 LBD (PDB 8F8M). TIF2 coactivator peptide is shown in green (B) Ligand $2F_O$-F_C map showing electron density for Tet contoured at 1σ. (C) Overlay of Tet (cyan) and 10CA (pink PDB 7JYD). (D) Key deep pocket interactions made by Tet (E) Pocket mouth interactions made by Tet. Sidechains (along with backbones of G421, T423, and L424) of engaged residues are shown as sticks (O-red, N=blue, S=yellow, C=white). Water molecules shown as spheres. Hydrogen bonds are represented as red dotted lines. Note that K520 is slightly out of hydrogen bonding range for the tetrazole (distance indicated with gray dotted lines).

Previously we have found that potency and efficacy of LRH-1 small molecule modulators can be increased by replacing the *exo* hydroxyl with an *endo* sulfamide displacing the hydrogen bonding water network within the LBD, while maintaining the effects given by the carboxylic acid.[40] Due to these prior results, we hypothesized that the addition of the sulfamide to the tetrazole structure would also increase the potency and efficacy of the molecule. As seen in Figure 2.7, the 6N-Tet exhibits an increase in binding, thermal stability, and SHP expression via qPCR, as well as improvements of both the efficacy and potency of the molecule via a luciferase reporter assay. Through the improved features we are now looking to scale up the compound in order to test the replacement of the carboxylic acid for an increase in metabolic stability, permeability, as well as pharmacokinetic studies.

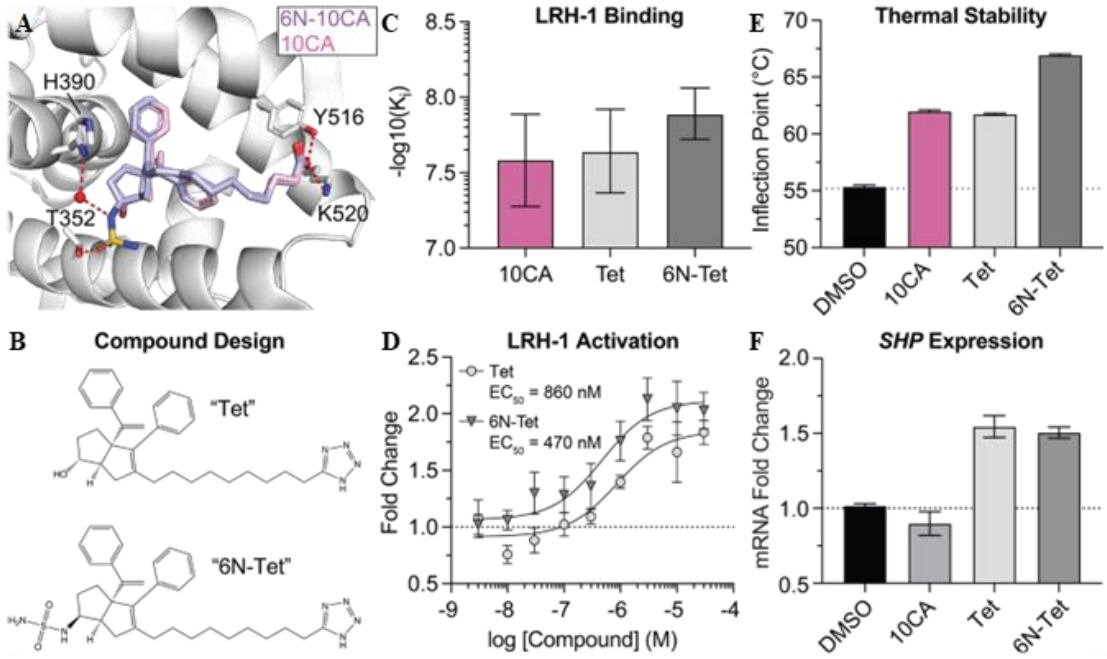

Figure 2.7: Addition of sulfamide improves compound affinity and potency while maintaining tail-mediated efficacy

(A) Overlay of 6N-10CA (purple; PDB 7TT8) and 10CA (pink; PDB 7JYD). Select residues that engage small molecules deep within the pocket and at the pocket mouth are indicated. Sidechains are shown as sticks (O=red, N=blue, S=yellow, C=white). Water molecules shown as shperes. Hydrogen bonds are represented as red dotted lined. (B) Chemical structures of Tet and hybrid molecule 6N-Tet, which incorporates the sulfamide moiety of LRH-1 small molecule agonist 6N. (C) FP competition assay showing binding of compounds to the LRH-1 LBD. K_i: inhibition constant. Data shown as mean +/- from two independent experiments. Error bars represent 95% confidence intervals. (D) Luciferase reporter assay comparing compound-driven activation of LRH-1. EC_{50}= half maximal effective concentration. Efficacies of Tet and 6N-tet wre 1.9 and 2.1, respectively. Data shown as mean from three (Tet) or five (6N-tet) biological replicates. (E) Comparison of ligand-driven thermal stability of the LRH-1 LBD. The inflection point corresponds to the temperature at which the protein unfolds. Data shown as mean +/- SEM from two independent experiments. (F) RT-qPCR analysis of HepG2 cells treated with agonists (Tet and 6N-tet- 10 μM, 10CA 30 μM) for 24 hrs. Data normalized to signal of DMSO control and shown as mean +/- SEM from two (DMSO and 6N-tet) or four (10CA and Tet) biological replicates

With the 6N-Tet isostere showing great efficacy for LRH-1, we sought to compare the activation of this molecule against a myriad of NRs. Unselective binding poses a problem in drug development due to potential off-target activation in undesired pathways. Unlike the 2N and 4N compounds, 6N-Tet activates both NRs in the NR5A family. Dosing at maximum efficacy, we see minor activation of PXR in the luciferase reporter, but overall we were able to maintain selectivity for the NR5A NRs (LRH-1 and SF-1), as seen in Figure 2.8.

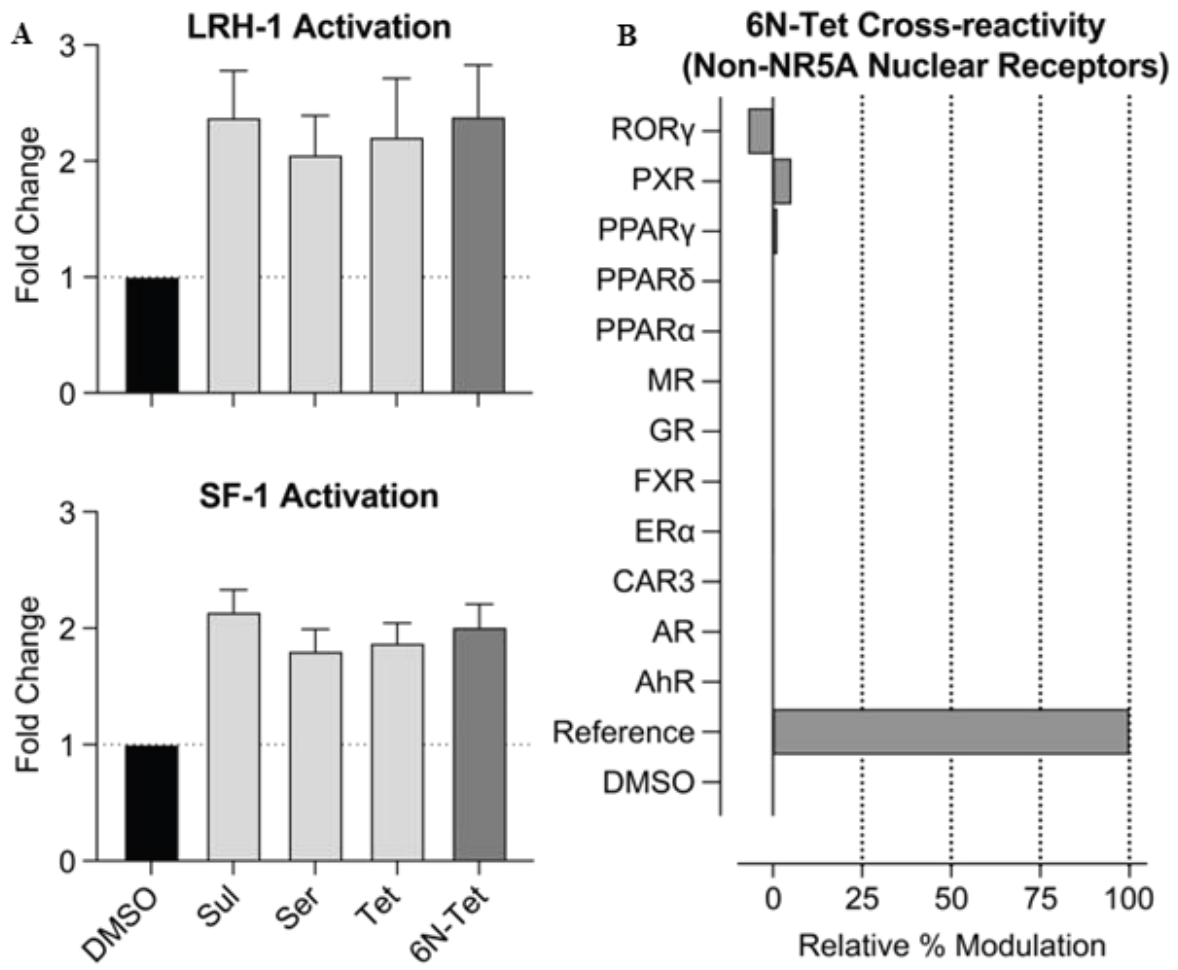

Figure 2.8: Small molecules show specificity for NR5A receptors

(A) LRH-1 and SF-1 luciferase reporter assays, indicating ligand-induced activity after addition of 10 μM of indicated small molecules. Data represented as means +/- SEM from four biological replicates (B) 6N-Tet was introduced to reporter cells at 2 μM and the activity of respective nuclear receptors was tested. Agonism was exmined for all receptors, aside from RORγ, where inverse agonism was tested. Data was normalized to receptor activity by an agonist (or antagonist for RORγ) for each receptor added at a concentration corresponding to the EC_{100} (Or IC_{100} for RORγ).

In this series of bioisosteres we successfully replaced the carboxylic acid for increased potency and efficacy in comparison to the parent compound. The identified tetrazole isostere utilizes hydrogen-bonding interactions with G421, Y516, and K520 giving rise to an increase of downstream gene expression. Upon addition of the sulfamide, potency was further increased (EC_{50}= 470 nm). Furthermore, selectivity of the compound is maintained for the NR5A family.

2.2.3 Addressing hydrophobicity of synthetic modulators via addition of heteroatoms

In 2000 Lipinski published his "rule of 5". According to his theory for a drug to be orally active, compounds should not be in violation of more than one of the following rules: no more than 5 hydrogen bond donors, no more than 10 hydrogen bond acceptors, a molecular mass less than 500 Da, and a partition coefficient (logP) no greater than 5.[51] Historically, many medicinal chemists have looked to these rules in order to design pharmaceuticals. While, many chemists no longer adhere strictly to these rules, they still provide a useful guide due to their relevance in various pharmacological effects. For instance, logP or aqueous solubility has effects on the transport, distribution, and metabolism of biological molecules.[52] The more lipophilic (higher logP) a molecule is the more readily a molecule is to be metabolized and excreted from the body.[52,53] As seen in Scheme 2.3 both 10CA and 6N-10CA have a computed logP (clogP) higher than 5. We sought to lower the logP by the incorporation of heteroatoms within the lipophilic structure.

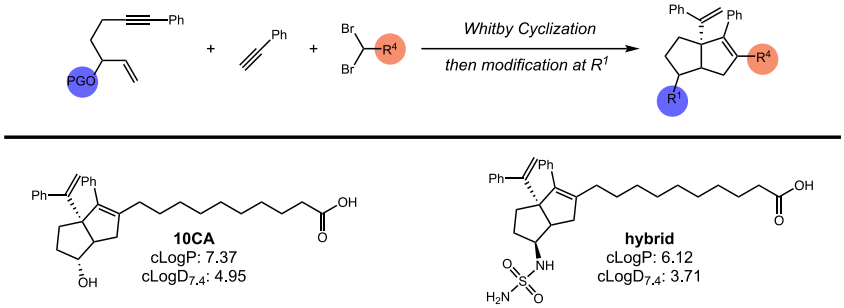

Scheme 2.3: Relative clopP of leading LRH-1 agonists

Upon first inquiring on where to incorporate heteroatoms we focused on two areas: the all carbon bicyclooct-2-ene core and the long lipophilic tail. When looking at previously made compounds by the Whitby group, we found incorporation of either a nitrogen or oxygen atom into the ring structure decreased activity (maximum RE 53% of RJW100's activity) (Scheme

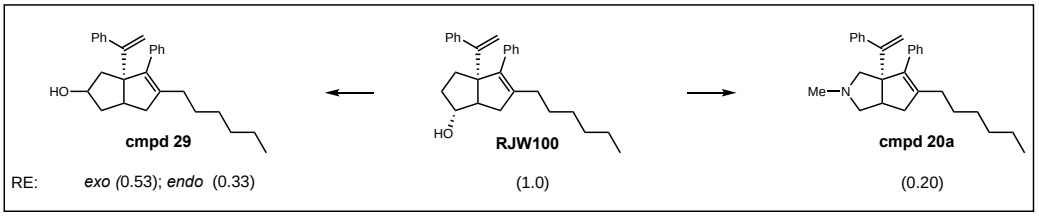

Scheme 2.4: Relative efficacy of compounds from Whitby lab

2.4).[35] Therefore, we sought to incorporate heteroatoms into the lipophilic tail. Via the proposed synthesis we could individually make two tails with either one or two oxygen atoms.

The deemed monoether tail was synthesized starting with the iodination of 6-bromohex-1-ene that then undergoes substitution by 1,5-pentanol. The hydroxyl is protected before ozonolysis of the terminal alkene resulting in the aldehyde used for dibromination. This dibromide within the Whitby cyclization gives the "tail" on the structure. The diether tail was also synthesized to a dibromide. Starting with the formation of di(1,3-dioxan-2-yl) methane before a copper catalyzed ring opening reaction to form the diol. The resulting diol was then able to undergo the traditional monoprotection, oxidation, and dibromination of the resulting aldehyde to form the tail (Scheme 2.5). These two tails were used in the Whitby cyclization to make both monoether (ME) and diether (DE) derivatives of 10CA and 6N-10CA hybrid via the same route as their parent compounds (Figure 2.9A).[38,40]

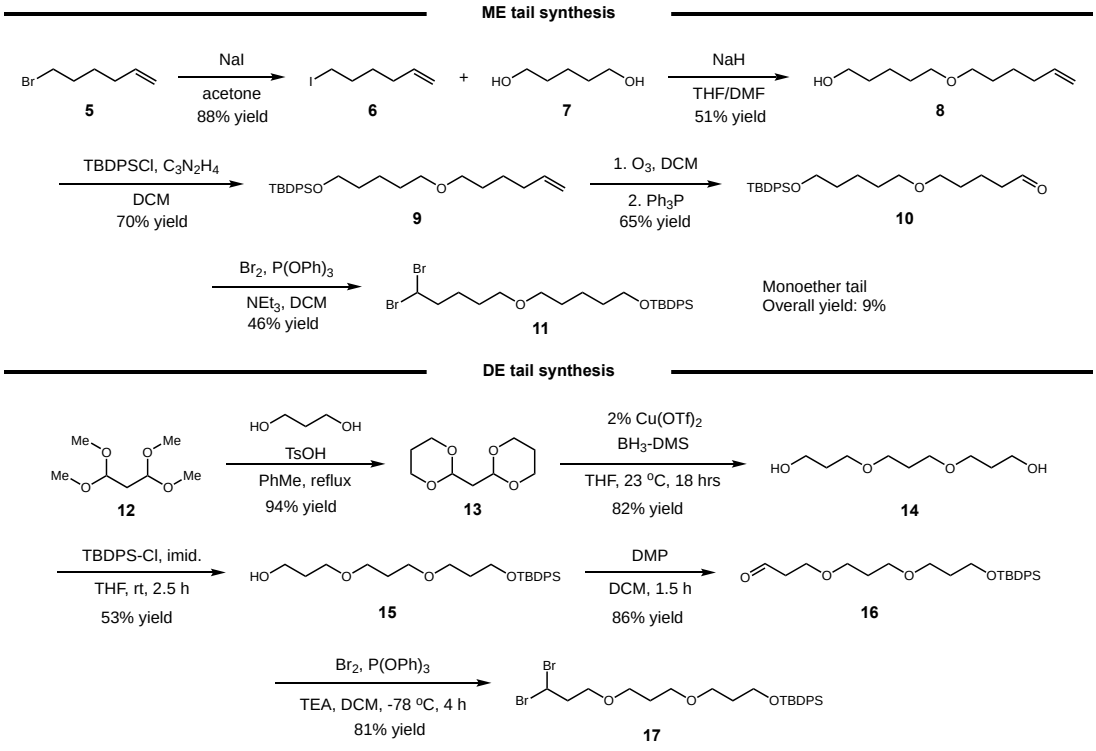

Scheme 2.5: Synthetic route for both monoether and diether tails

Due to the hydrophobic nature of LRH-1's binding pocket we expected a loss in potency of the ether compounds. Excitingly, with the ME derivatives of both 10CA and 6N-10CA, both potency and efficacy were maintained (Figure 2.9B). With each DE derivative there was some loss of potency due to the weakened binding to LRH-1. Although we still maintained desired activity with all molecules, we next wanted to look at specific pharmacokinetic properties of the molecules to find a candidate that would move forward in animal studies. The properties we initially focused on were solubility, cell permeability, and metabolic stability. As seen in Figure 2.9C, with each

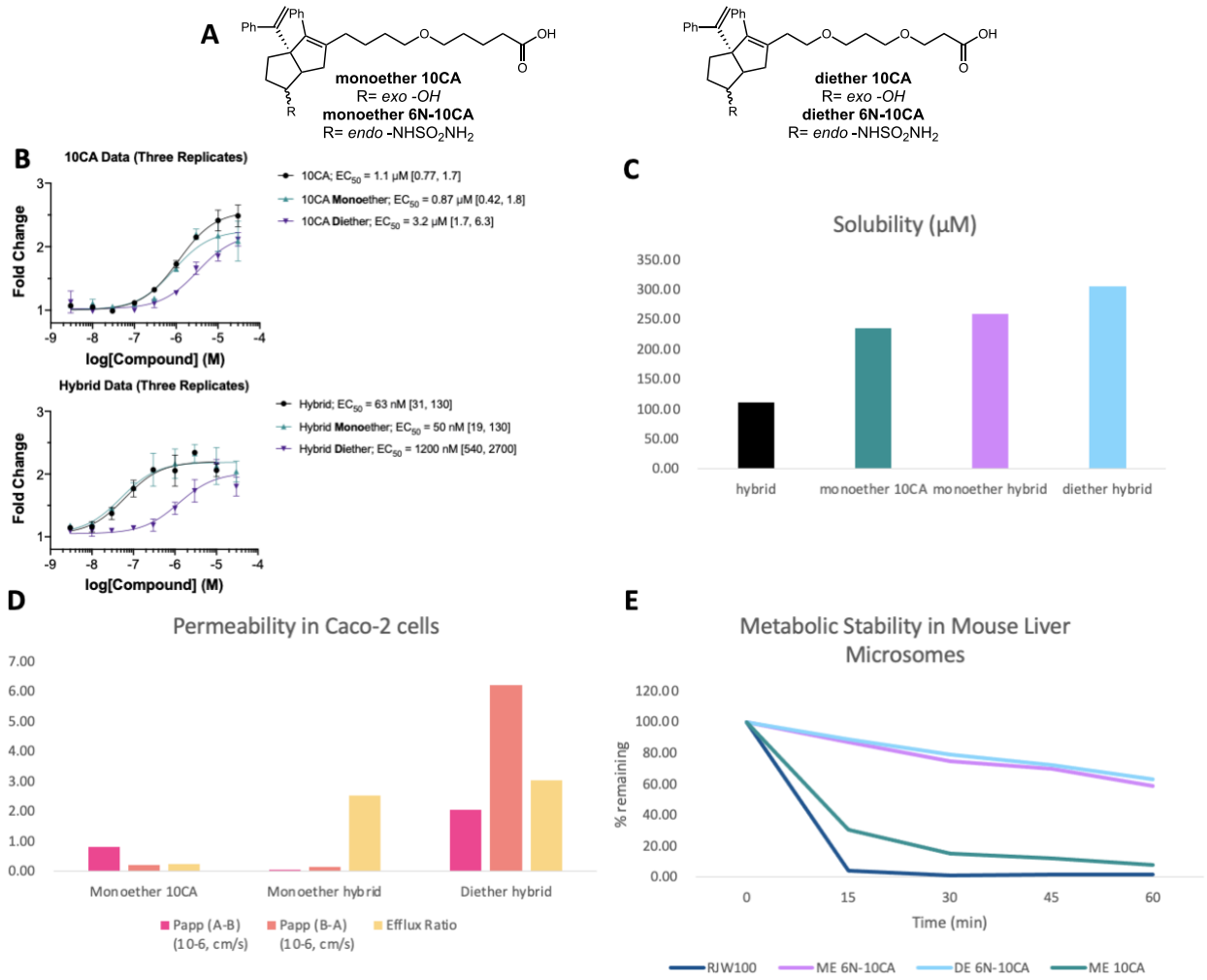

Figure 2.9: Pharmacokinetic studies of ether compounds

(A) Compound structures. (B) Luciferase reporter assay comparing compound-driven activation of LRH-1. EC_{50}= half maximal effective concentration. Data shown as mean from three biological replicates. (C) Aqueous solubility assay. (D) Permeability assay from Caco-2 cells (5µM compound). (E) Metabolic stability of compounds performed on mouse liver microsomes (2 µM compound).

added heteroatom in the tail we increased the solubility of the molecule. Furthermore, when exposed mouse liver microsomes the ether compounds were metabolized slower than RJW100. Both the 6N-10CA derivatives having longer lasting metabolic stability. Finally, we looked at the permeability of these compounds into Caco-2 cells. Although all compounds have some permeability into cells, the sulfamide containing compounds have high efflux ratios. With this in mind, we moved forward with the 6N-10CA derivatives for *in vivo* studies.

We first interrogated the distribution of the compound within wild-type mice tissues. Desiring efficacy in the GI tract, after five doses at 100 milligrams per kilogram (mpk) we collected the liver, colon, and plasma. As seen in Figure 2.10, there was a higher localization of the compound in the colon than the liver and plasma. Due to IBD causing inflammation in the colon, this was an exciting finding for our targeted disease model. From this we desired to look at plasma concentration. While most lipids are readily metabolized and excreted from the body, compounds found in the plasma can be circulated and utilized by the body over time. Testing plasma concentrations over 24 hours by three different modes of dosing (IP, oral, and IV) we can see that over time the monoether hybrid structure has the longest lasting plasma concentration,

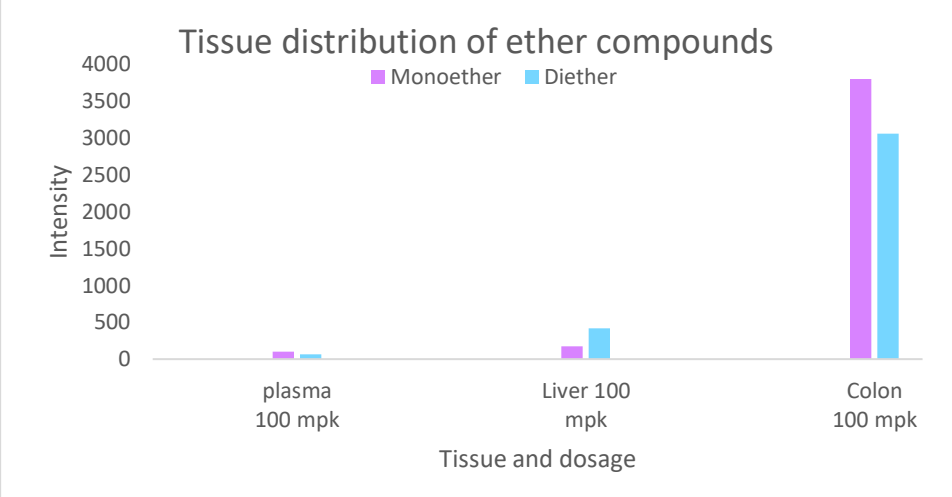

Figure 2.10: Tissue disstribution of ME and DE 6N-10CA compounds

Mice were dosed five times at 100 milligrams per kilogram (mpk) in am and pm. After the fifth dose the mice were sacked and the tissues were collected. Collected tissues were extracted and concentration of the compounds were calculated.

showing availability even after eight hours. With all of the data in mind, we moved forward to scale up on the monoether 6N-10CA hybrid to perform *in vivo* studies on out disease model.

Adding ethers into the 10-carbon lipophilic tail of the agonist compounds resulted in an increase of solubility and metabolic stability, while either maintaining or increasing the potency of the compounds.

2.3 Conclusion

Through this selection of molecules, we have seen that selectivity within the NR5A family as well as across NRs is possible via various headgroups. We've also created more soluble ether analogs as well as a series of bioisosteres. While either maintaining activity and binding of the molecule or addressing certain metabolic instabilities we have successfully created a modulator for *in vivo* studies to more accurately probe the role of LRH-1 in IBD.

2.4 Future directions/studies

We've successfully altered known metabolic liabilities of the molecule, while maintaining potency and efficacy. Currently, we are designing a new series of compounds to address remaining liabilities. Styrenes are known to be metabolized by cytochrome p450s via epoxidation of the alkene.[54,55] Therefore, we propose to cyclopropanate the styrene. While many attempts have been made for this cyclopropanation, we have only been able to cyclopropanate the alkene within the bicyclooct-2-ene core. Due to the fact the creation of the external styrene, through a nucleophilic addition to the zirconium, is essential in the mechanism for the Whitby reaction, we propose a new route.[35,56] The Pauson-Khand reaction has previously been used in order to make [3.3.0] core of the structure.[57] The resulting product of this reaction can be seen to undergo conjugate addition

with Gilman's reagent in order to add the cyclopropal group into the structure, similar to the method preformed by Yamashita.[58] With this reaction we also were able to change the enyne to accommodate a nitrogen atom. The cyclization of this enyne has previously been unsuccessful in the Whitby reaction, but cyclizes at 85% yield via the Pauson-Khand. Current studies are currently underway to find optimal condition for the 1,4-addition (Scheme 2.6).

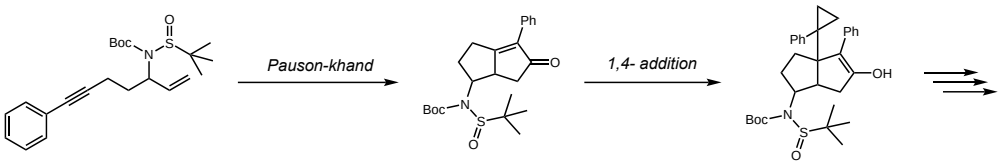

Scheme 2.6: Synthetic route for the addition of cyclopropanation

While we are also trying to improve the synthetic route of the molecule, we hope to address the poor efflux ratio associated with the structure. Due to the 10CA ME having a lower efflux ratio, we hypothesize that the sulfamide has a large effect. Sulfonamides have been well studied in early antibiotic research, especially their association with cell toxicity.[59] Therefore, we propose to alter the sulfamide in future iterations of compounds we hope to mitigate these effects.

2.5 Supplemental Information

2.5.1 Supplemental figures

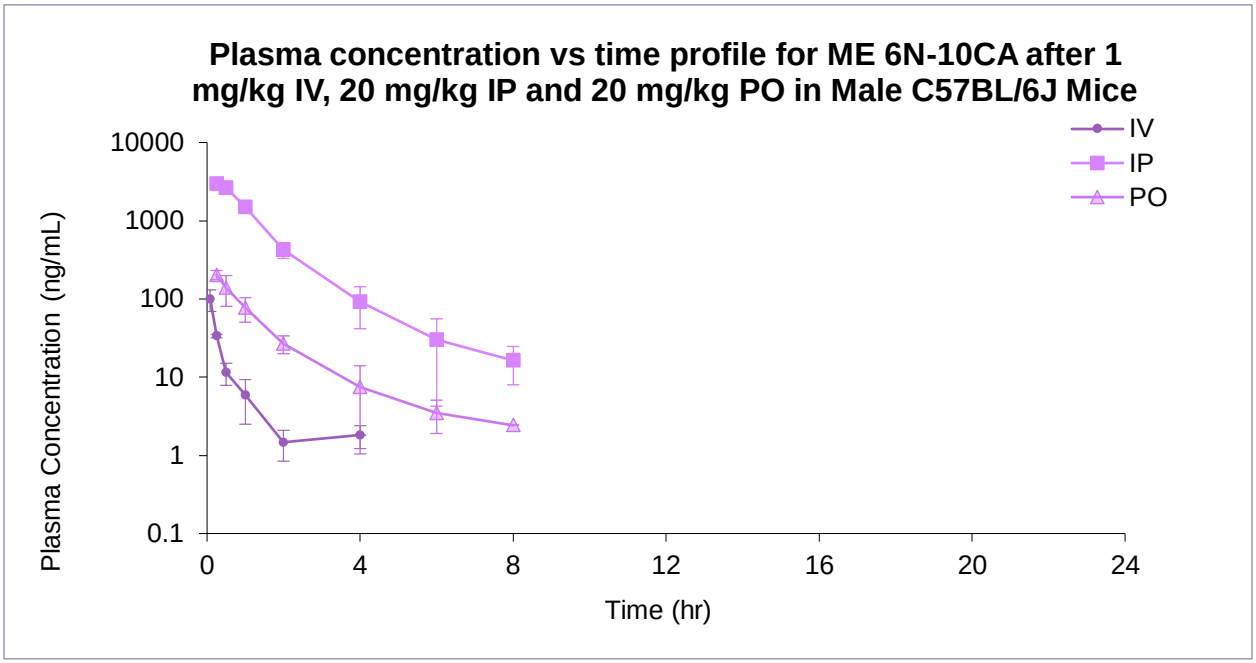

Figure 2.S3: pharmacokinetic data of monoether 6N-10CA

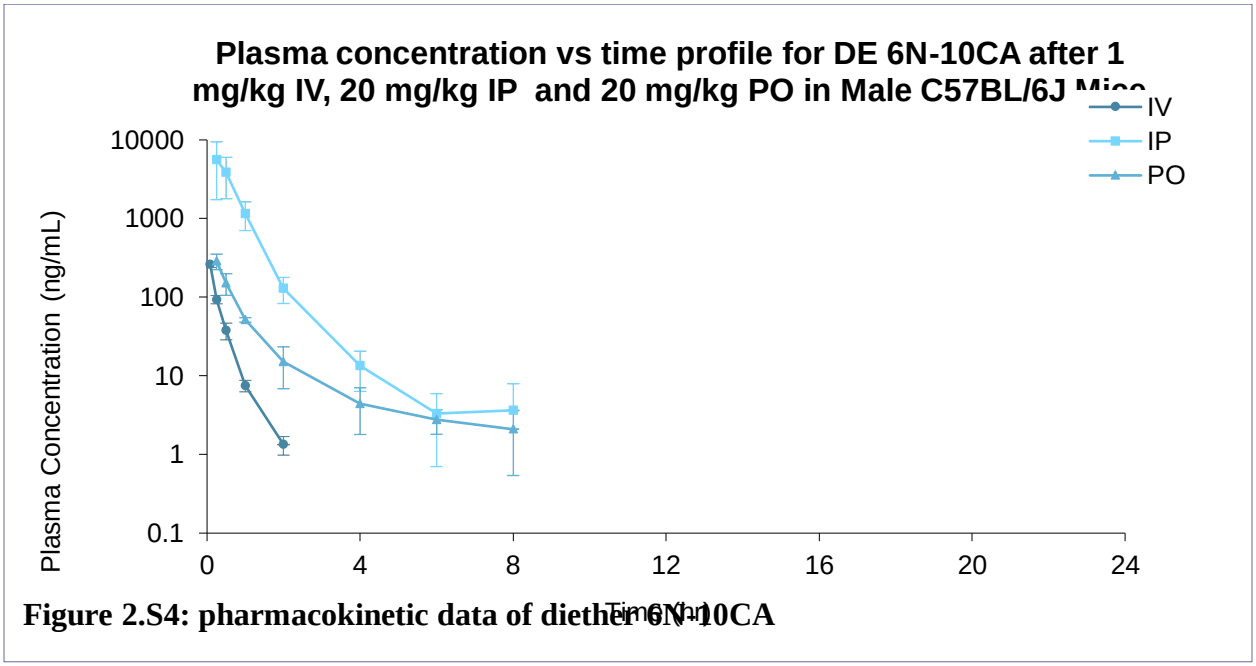

Figure 2.S4: pharmacokinetic data of diether 6N-10CA

2.5.2 Supporting information for section 2.2.1

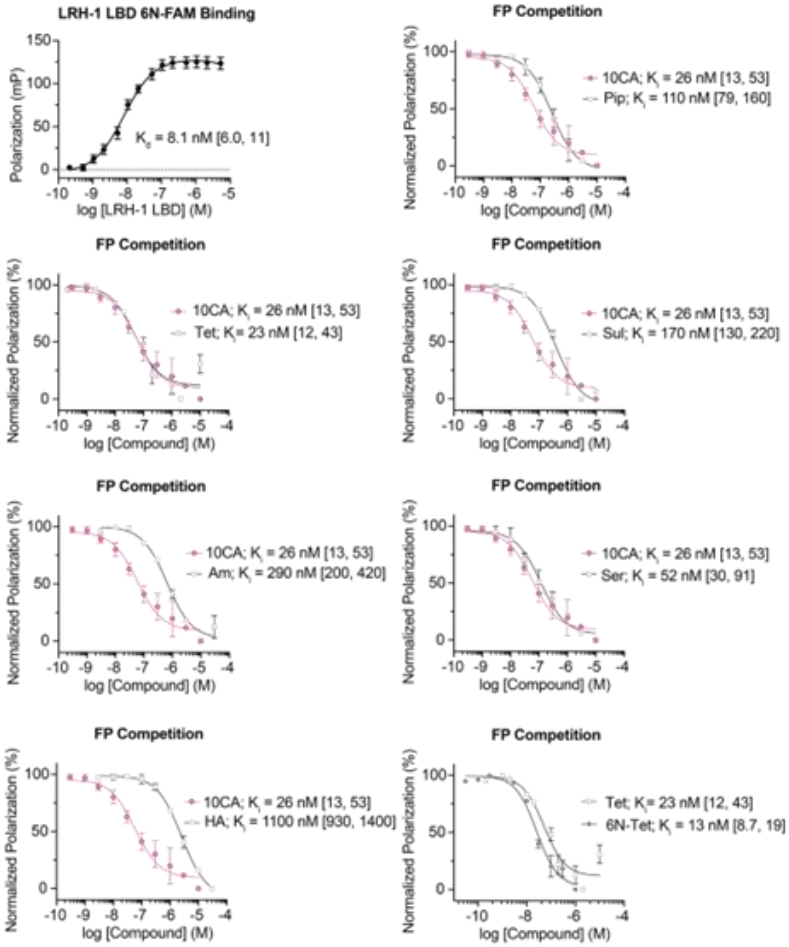

Figure 2.S1: FP binding and FP competition assays displayed independently. Top left curve represents the forward binding curve used to determine the binding affinity of 6N-FAM for the LRH-1 LBD. Data shown as means +/- SEM from eight independent experiments. K_d= dissociation constant. 95% confidence intervals are shown in brackets. The remaining curves represent FP competition assays used to determent compound K_i (inhibition constant) values. FP competition data shown as means +/- SEM from two independent experiments, with 95% confidence intervals shown in brackets. Polarization values were normalized for each independent experiment in such a way that the highest value =100 and the lowest value =0. K_i values reported here, along with associated confidence intervals, were used to construct graphs in the resulting figures.

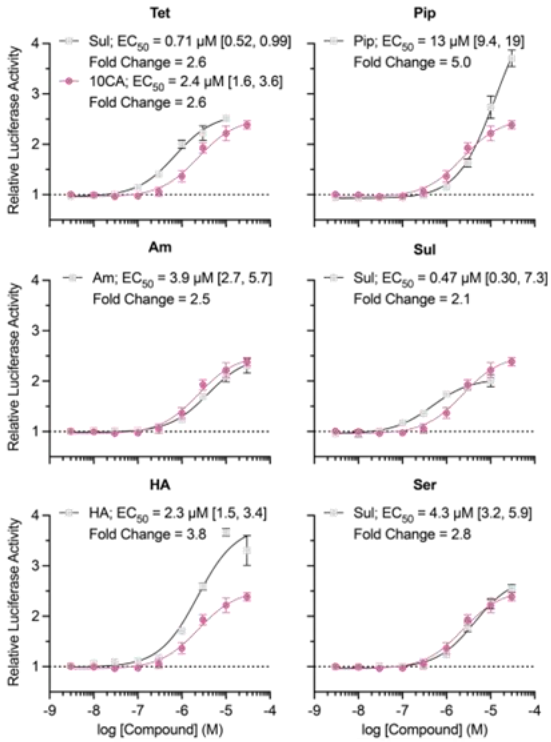

Figure 2.S2: Luciferase reporter assays displayed independently. Luciferase reporter assay (HeLa cells) showing effects of small molecules on LRH-1 activity Relative luciferase activity corresponds to the calculated span of the curve +1. Data were normalized relative to DMSO control and are shown as mean +/- SEM from three biological replicates. EC_{50}= half maximal effective concentration. 95% confidence intervals are shown in brackets. EC_{50} values reported here, along with relative luciferase activity normalized to that of 10CA, were used to construct respective figures.

Figure S2: Luciferase reporter assays displayed independently. Luciferase reporter assay (HeLa cells) LRH-1 LBD + Tet + TIF2	
Data Collection	
Space group	$P3_221$
Cell dimensions	
a, *b*, *c*, (Å)	89.2, 89.2, 105.7
α, β, γ (°)	90, 90, 120
Resolution (Å)	44.6 – 2.60 (2.69 – 2.60)
Average I/σ	12.1 (1.38)
Completeness (%)	97.7 (81.7)
CC1/2	0.937 (0.570)
Redundancy	11.2
Unique reflections	15066 (1235)
Refinement	
R-work/R-free (%)	20.1/22.4
No. atoms	
Protein	2041
Ligand	37
Water	29
B-factors	
Protein	68.1

Ligand	58.5
Water	62.7
R.M.S. deviations	
Bond length (Å)	0.002
Bond angles (°)	0.49
Ramachandran favored (%)	96.4
Ramachandran outliers (%)	0.00
Twin law	-h, -k, l
PDB accession code	8F8M

Table 2.S1: X-ray crystallography data collection and refinement

Biological information

Cell Culture. HeLa cells were cultured under standard conditions (5% CO_2, 37°C) in phenol red-free MEMα + 10% fetal bovine serum (FBS) – charcoal/dextran treated and were verified to be mycoplasma free with the LookOut® Mycoplasma PCR Detection Kit.

Protein purification of wildtype SF-1. E. coli strain BL21(DE3)-pLysS was transformed with the SF-1 LBD (amino acids 218-461) in the pLIC-His vector and cultured at 37°C to OD_{600} of 0.6 in Lysogeny Broth medium in the presence of chloramphenicol and ampicillin. Protein expression was induced with 0.5 mM isopropyl-1-thio-D-galactopyranoside (IPTG) for four hours at 32°C. Cell pellets were lysed in 125 mL NiA (500 mM NaCl, 25 mM imidazole, 5% glycerol, 20 mM Tris HCl pH 7.4, 0.5 mM TCEP) with lysozyme, phenylmethylsulfonyl fluoride (PMSF), and DNase followed by sonication. Lysate was clarified by centrifugation in a Sorvall RC 6+ centrifuge at 16,000 x g for 45 minutes. Supernatant was flowed over a 5 mL HisTrap FF column (GE Healthcare, Little Chalfront, UK) and protein was eluted with NiB (NiA with 500 mM imidazole). To homogenize the lipid population, SF-1 was incubated overnight with DLPC. Size exclusion chromatography (SEC) into assay buffer (150 mM NaCl, 20 mM Tris HCl pH 7.4, 5% glycerol)

was used as a final purification step. Protein was concentrated to ~3 mg/mL, flash frozen, and stored at -80 °C for use in assays.

Protein purification of CysLite SF-1. CysLite SF-1 (amino acids 218-461, C247S, C412S) in the pLic-His vector was used for crystallization. This protein was purified as described for wildtype SF-1 through the HisTrap column; after elution from the HisTrap column, the 6X-His tag was cleaved overnight using tobacco etch virus protease. Cleaved protein was flowed over a second HisTrap column and the flowthrough was collected, concentrated to ~3 mg/mL, flash frozen, and stored at -80 °C for use in crystallization.

Fluorescence Polarization. FP assays were performed as described previously. Briefly, experiments were conducted in black, polystyrene, non-binding surface 384-well plates (Corning Inc., Corning, NY) with 30 mL volumes in assay buffer (150 mM NaCl, 20 mM Tris-HCl, 5% glycerol, pH 7.4). Binding affinity for 6N-FAM was determined using 10 nM 6N-FAM and protein concentrations ranging from 1^{-10} - 5^{-5} M. Plates were incubated overnight at 4 °C and centrifuged at 2,000 x *g* for 2 minutes before polarization measurement. Polarization was monitored on a Neo plate reader (Biotek, Winooski, VT) at an excitation/emission wavelength of 485/528 nm. Plates were incubated overnight at 4 °C and centrifuged at 2,000 x *g* for 2 minutes before polarization measurement. Nine technical replicates were conducted over three experiments and compiled binding data were baseline-corrected to wells with no protein and fit with a one-site binding curve in GraphPad Prism version 7 (GraphPad, Inc., La Jolla, CA). 6N conjugated to fluorescein amidite (FAM) (10 nM/well – 0.8 times the affinity of SF-1 for 6N-FAM) was incubated with SF-1 LBD (25 nM/well – 60% of the forward binding B_{max}). Unlabeled compounds were added at concentrations indicated in figures with DMSO in each well held constant at 6.7% v/v. Each experiment was performed two or three times with four technical replicates each. Technical

replicates were averaged and normalized independently prior to final data analysis. Using GraphPad Prism (version 9), data were fit to a one-site, fit K_i curve, assuming a final probe concentration of 10 nM and probe affinity determined with forward binding assays (WT: 12.3 nM, M268L: 19.3 nM, T272V: 10.9 nM, Y436F: 9.9 nM, K440A: 5.5 nM).

Luciferase Reporter. LRH-1 reporter assays were conducted as described previously. Briefly, HeLa cells were seeded at ~7,500 cells per well in 96-well plates (white-walled, clear bottom) in MEMα + 10% FBS. Once cells reached 80-90% confluence, they were transfected with LRH-1 (in pCI vector, 5 ng/well) or SF-1 (in pcDNA vector, 5 ng/well), a reporter plasmid with an NR5A response element derived from the SHP promoter cloned upstream of firefly luciferase (in pGL3-Basic vector, 50 ng/well), and a plasmid expressing Renilla luciferase constitutively from a CMV promoter (1 ng/well). Cells were transfected with FuGENE at a ratio of 3:1 (FuGENE:DNA). Twenty-four hours after transfection, compounds were diluted in Opti-MEM and introduced to cells at final concentrations indicated in figures (final DMSO concentration was 0.37%). Luciferase signal was measured after ~24 hours using the DualGlo kit (Promega) with a BioTek Neo plate reader. Each experiment was conducted with three biological replicates, each with three technical replicates averaged prior to data analysis. Firefly luciferase signal for each well was divided by the well's Renilla signal intensity and then normalized relative to the DMSO control. Data were analyzed with GraphPad Prism (version 9) using a stimulating dose-response curve (Hill slope = 1). Data were excluded from analysis for cells treated with 3e-5 M of 6N and 6N-10CA, as the final signal showed a drastic decrease in overall signal, potentially indicating cell toxicity or compound insolubility.

RT-qPCR. RT-qPCR was performed as described previously. HepG2 cells were seeded at 400,000 cells per well in 24-well plates in DMEM + 10% FBS. When cells reached ~ 90% confluence, media was exchanged with media containing DMSO or compound at the desired concentration (final DMSO concentration: 0.3%). Small molecules were added concentrations indicated in figure legends. After 24 hours, media was decanted, cells were washed with phosphate buffered saline, and cells were collected in RLT lysis buffer (+ 1% 2-mercaptoethanol). Cells were stored at -80°C prior to RNA extraction. RNA was extracted from cells using the RNeasy® Mini Kit (QIAGEN), with on-column DNase digestion. RNA was reverse transcribed with the High-Capacity cDNA Reverse Transcription Kit (Applied Biosystems™). cDNA was quantified using Power SYBR Green PCR Master Mix (Applied Biosystems™), using human *ACTB* (Actin Beta) as a housekeeping gene. Ct values were calculated by resident software on the StepOne Plus thermocycler. Data were normalized using the ΔΔCt method. Each experiment was conducted with two or four biological replicates that were normalized independently for data analysis. Data were analyzed with GraphPad Prism, using a Brown-Forsythe and Welch One-Way ANOVA and Dunnett T3 Multiple Comparisons Test. Primers used for RT-qPCR were as follows:

hACTB.

forward 5’-AGGCACCAGGGCGTGAT-3’

reverse 5’-GCCCACATAGGAATCCTTCTGAC-3’

hSHP

forward 5’-GCTTAGCCCCAAGGAATATGC-3’

reverse 5’-GTTCCAGGACTTCACACAGC-3’

hCYP7A1

forward 5’-GAGAAGGCAAACGGGTGAAC-3’

reverse 5’-GGATTGGCACCAAATTGCAGA-3’

Thermal stability assays. Thermal stability of the LRH-1 LBD complexed with ligands was determined as described previously using a Tycho^{TM} NT.6 Nanotemper. LRH-1 LBD was incubated with 5-fold molar excess of ligand (final DMSO concentration was 1.4%) overnight at 4°C in assay buffer (150 mM NaCl, 20 mM Tris-HCl, 5% glycerol, pH 7.4). Complexes were centrifuged at high speed for five minutes and then loaded into capillaries Tryptophan/tyrosine fluorescence was monitored at wavelengths 330 and 350 nm over a 30°C/min gradient (35°C – 95°C). The inflection point was determined with Tycho^{TM} NT.6 software. Two separate experiments were conducted with three technical replicates, which were averaged and plotted using GraphPad Prism (version 9).

Protein purification. LRH-1 LBD was expressed and purified as described previously Briefly, BL21(DE3) *E. coli* cells were transformed with human LRH-1 LBD (residues 299-541) with an N-terminal 6xHis tag in a pMCSG7 vector. Cells were grown at 37°C in liquid broth until OD_{600} 0.6. Protein expression was induced with 1 mM IPTG for 4 hours at 30°C. Cells were centrifuged and stored at -80°C. The cell pellet was resuspended in lysis buffer (20 mM Tris-HCl, 150 mM NaCl, 5% glycerol, 25 mM imidazole, 0.2 mM phenylmethylsulfonyl fluoride, DNase, lysozyme, pH 7.4) and lysed via sonication. Protein was isolated with Ni^{2+} affinity chromatography. Human LRH-1 LBD purifies bound to bacterial phospholipids when expressed in *E. coli* We removed co-purified bacterial lipids for LRH-1 LBD used in FP competition assays by incubating the protein with four-fold molar excess of DLPC overnight at 4°C. LBD was then purified with size-exclusion chromatography (SEC) into assay buffer (150 mM NaCl, 20 mM Tris-HCl, 5 % glycerol, pH 7.4). LRH-1 LBD used for thermal stability assays was purified in a similar manner but was not

complexed with DLPC prior to SEC purification. LRH-1 LBD used for crystallography was incubated with TEV protease to remove the 6xHis tag and subjected to a second round of Ni^{2+}affinity chromatography before being complexed with Tet (see below). All protein was stored at -80°C until use.

X-ray crystallography. LRH-1 LBD-Tet crystals were generated as described previously. Briefly, cleaved (6xHis tag removed) LRH-1 LBD was incubated with Tet at four-fold molar excess overnight at 4°C. The complex was then purified via SEC into crystallization buffer (150 mM NaCl, 100 mM ammonium acetate, 1 mM EDTA, 2 mM CHAPS, 1 mM DTT, pH 7.4) and incubated with a peptide corresponding to human TIF2 NR box 3 ($^{+}H_3N$-KENALLRYLLDKDD-CO_2^-) at four-fold molar excess, along with an additional two-fold molar excess of Tet, for two hours at room temperature. The complex was then concentrated to ~ 7 mg/mL and crystals were generated via hanging drop vapor diffusion in crystallant containing 0.1 M tri-Na citrate – pH 4.6, 10-14% tert-butanol, and 0-7.5% glycerol at 4°C. Crystals were flash frozen in liquid N_2 using cryoprotectant consisting of crystallant supplemented with 30% glycerol. Data were collected remotely from the Southeast Regional Collaborative Access Team (SER-CAT) at the Advanced Photon Source (Argonne National Laboratories, Chicago, IL). Data were processed using HKL2000 and phased with molecular replacement, using PDB 4DOS as the search model. Structure refinement was performed with Phenix and Coot Additional refinement was performed with PDB-REDO. Twinning was detected with xtriage in Phenix, and we used the recommended twin law (-h,-k,l) during refinement. Final figures were constructed with PyMOL (Schrödinger, LLC), which was also used to predict hydrogen bonds between the ligand and pocket mouth.

Cross-reactivity studies. Reporter assays comparing LRH-1 and SF-1 activity were conducted as above. However, for experiments testing SF-1 activity, cells were transfected with SF-1 in a pcDNA vector (5 ng/well). Cells were transfected with FuGENE at a ratio of 4:1 (FuGENE:DNA). Cells were treated with 10 μM of compound for 24 hours (final DMSO concentration was 0.37%). Reporter assays assessing cross-reactivity with non-NR5A receptors were conducted by INDIGO Biosciences, Inc. Reporter cells expressed either the native receptor (AhR, AR, ERα, GR, and MR) or a receptor hybrid in which the native N-terminal DBD has been replaced with that of the yeast Gal4 DBD (RORγ, CAR3, FXR, PPARα, PPARδ, PPARγ, and PXR). Huh7 (AhR), CV-1 (AR), CHO (CAR3, ERα, FXR, GR, PPARα, PPARδ, and PPARγ), or HEK293 (RORγ, MR, and PXR) cells were used in studies. A gene encoding Firefly luciferase was downstream of a receptor-specific genetic response element or the Gal4 upstream activation sequence. All reference compounds used, aside from ursolic acid (RORγ inverse agonists), were agonists and were as follows: ursolic acid (RORγ), MeBio (AhR), 5α-Dihydro-11- ketoTestosterone (AR), CITCO (CAR3), 17β-estradiol (ERα), GW4064 (FXR), dexamethasone (GR), aldosterone (MR), GW7647 (PPARα), GW0742 (PPARδ), rosiglitazone (PPARγ), and rifampicin (PXR). Experiments were run in triplicate in 96-well plates (medium = cell recovery medium). Assay plates were incubated for 24 hours and then the treatment media was discarded. Luciferase Detection Reagent was added and relative bioluminescence was measured. All graphical manipulations were performed using GraphPad Prism software.

Chemical synthesis

General information

All reactions were carried out in flame-dried glassware, equipped with a stir bar and under a nitrogen atmosphere with dry solvents under anhydrous conditions, unless otherwise noted. Solvents used in anhydrous reactions were purified by passing over activated alumina and storing under argon. Yields refer to chromatographically and spectroscopically (^{1}H NMR) homogenous materials, unless otherwise stated. Reagents were purchased at the highest commercial quality and used without further purification, unless otherwise stated. n-Butyllithium (n-BuLi) was used as a 2.5 M solution in hexanes (Aldrich), was stored at 4°C and titrated prior to use. Organic solutions were concentrated under reduced pressure on a rotary evaporator using a water bath. Chromatographic purification of products was accomplished using forced-flow chromatography on 230-400 mesh silica gel. Thin-layer chromatography (TLC) was performed on 250μm SiliCycle silica gel F-254 plates. Visualization of the developed chromatogram was performed by fluorescence quenching or by staining using $KMnO_4$, *p*-anisaldehyde, or ninhydrin stains.

^{1}H and ^{13}C NMR spectra were obtained from the Emory University NMR facility and recorded on a Bruker Avance III HD 600 equipped with cryo-probe (600 MHz), INOVA 600 (600 MHz), INOVA 500 (500 MHz), INOVA 400 (400 MHz), VNMR 400 (400 MHz), or Mercury 300 (300 MHz), and are internally referenced to residual protio solvent signals. Data for ^{1}H NMR are reported as follows: chemical shift (ppm), multiplicity (s = singlet, d = doublet, t = triplet, q = quartet, m = multiplet, dd = doublet of doublets, dt = doublet of triplets, ddd= doublet of doublet of doublets, dtd= doublet of triplet of doublets, b = broad, etc.), coupling constant (Hz), integration, and assignment, when applicable. Data for decoupled ^{13}C NMR are reported in terms of chemical shift and multiplicity when applicable. Liquid Chromatography Mass Spectrometry (LC-MS) was performed on an Agilent 6120 mass spectrometer with an Agilent

1220 Infinity liquid chromatography inlet. Preparative High-Pressure Liquid chromatography (Prep-HPLC) was performed on an Agilent 1200 Infinity Series chromatograph using an Agilent Prep-C18 30 x 250 mm 10 μm column, or an Agilent Prep-C18 21.2 x 100 mm, 5 μm column.

Synthesis of 6N-10CA has been previously reported.[40] Synthetic methods for 1-7N have also been previously published along with RJW100.[39] The carboxylic acid derivate (10CA) was synthesized as previously described.[38]

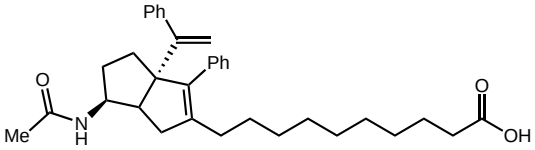

10-((3a*R*,6*S*)-6-acetamido-3-phenyl-3a-(1-phenylvinyl)-1,3a,4,5,6,6a-hexahydropentalen-2-yl)decanoic acid (**2N-10CA**): To a flame-dried reaction vial equipped with a stirbar backfilled to a nitrogen atmosphere was added 10-((3a*R*,6*S*)-6-amino-3-phenyl-3a-(1-phenylvinyl)-1,3a,4,5,6,6a-hexahydropentalen-2-yl)decanoic acid (prepared as previously reported)[40] (0.03 mmol, 1.0 equiv, 14.4 mg) in DCM (280 μL). The reaction vial was cooled to 0 °C before the dropwise addition of acetyl chloride (0.04 mmol, 1.5 equiv, 3.0 μL) and triethylamine (0.09 mmol, 3.0 equiv, 11.6 μL), respectively. The reaction stirred for 1 hour warming to room temperature before being quenched with water. The organic layer was then removed and the aqueous layer was reextracted (3x) with DCM. The combined organic layers were dried with $NaSO_4$, filtered, and concentrated via rotary evaporation. The crude oil was redissolved in dioxanes (500 μL) with 2 drops of HCl. After 48 hours the reaction showed consumption of starting material. The reaction was then diluted in EtOAc and washed with water (2x). The organic layer was dried with $NaSO_4$, filtered, and concentrated via rotary evaporation. The oil

was purified via flash chromatography (50-100% EtOAc/Hexanes) to give the title compound (4.3 mg, 42% yield) as a clear oil.

^{1}H NMR (600 MHz, cdcl$_3$) δ 7.33 – 7.27 (m, 5H), 7.23 (dd, *J* = 7.2, 2.5 Hz, 5H), 5.37 (d, *J* = 8.1 Hz, 1H), 5.05 (d, *J* = 1.4 Hz, 1H), 5.01 (d, *J* = 1.5 Hz, 1H), 4.25 (dtd, *J* = 10.6, 8.5, 6.2 Hz, 1H), 2.66 (td, *J* = 8.6, 2.0 Hz, 1H), 2.29 (t, *J* = 7.5 Hz, 2H), 2.04 (tdd, *J* = 17.6, 7.8, 3.6 Hz, 3H), 1.98 (s, 3H), 1.86 (dtd, *J* = 11.8, 6.0, 2.3 Hz, 1H), 1.75 (td, *J* = 12.3, 5.9 Hz, 1H), 1.66 (td, *J* = 6.4, 2.3 Hz, 1H), 1.60 (t, *J* = 7.2 Hz, 2H), 1.35 (ddt, *J* = 16.7, 11.4, 5.7 Hz, 2H 3?), 1.31 – 1.20 (m, 13H).

^{13}C NMR (151 MHz, $CDCl_3$) δ 175.83, 169.75, 154.33, 143.47, 142.97, 139.31, 136.89, 129.84, 129.48, 128.85, 128.02, 127.82, 127.68, 127.57, 126.77, 114.99, 69.03, 53.26, 47.48, 35.25, 33.34, 32.06, 31.63, 29.97, 29.71, 29.68, 29.24, 29.20, 29.09, 28.96, 28.06, 24.67, 23.33, 22.70.

LRMS (APCI) m/z: $[M+H]^+$ calc'd. for $C_{34}H_{44}NO_3$: 514.7, found 514.4

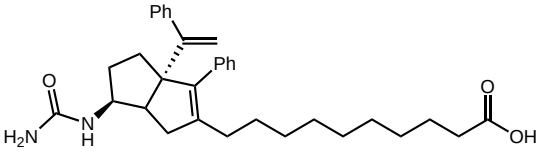

10-((3a*R*,6*S*)-3-phenyl-3a-(1-phenylvinyl)-6-ureido-1,3a,4,5,6,6a-hexahydropentalen-2-yl)decanoic acid (**4N-10CA**): To a flame-dried reaction vial equipped with a stirbar backfilled to a nitrogen atmosphere was added 10-((3a*R*,6*S*)-6-amino-3-phenyl-3a-(1-phenylvinyl)-1,3a,4,5,6,6a-hexahydropentalen-2-yl)decanoic acid (0.04 mmol, 1.0 equiv, 20 mg) (prepared as previously reported)[40] dissolved in dry MeCN. Triethylamine (0.08 mmol, 2.0 equiv, 11 μL) was added followed by (trimethylsilyl)isocyanate (0.08 mmol, 2.0 equiv, 11 μL). The reaction proceeded overnight at ambient temperatures before being pushed through a silica plug and concentrated. The crude material was purified via flash chromatography (100% EtOAc). The crude oil was redissolved in a 1:1 mixture of H_2O/THF (400 μL) with LiOH (0.06 mg, 3.0 equiv,

1.5 mg). After 16 hours the reaction showed consumption of starting material. The reaction was then diluted in EtOAc and washed with water (2x). The organic layer was dried with $NaSO_4$, filtered, and concentrated via rotary evaporation. The oil was purified via flash chromatography (10% MeOH/DCM) to give the title compound (3.0 mg, 15% yield) as a clear oil.

^{1}H NMR (500 MHz, cdcl$_3$) δ 7.34 – 7.29 (m, 8H), 7.19 (d, *J* = 7.2 Hz, 2H), 5.09 (s, 1H), 4.92 (s, 1H), 4.60 (br. s, 1H), 2.52 (s, 1H), 2.33 (dt, *J* = 17.7, 9.5 Hz, 2H), 2.12 (dt, *J* = 15.2, 8.0 Hz, 1H), 2.04 – 1.88 (m, 2H), 1.77 – 1.66 (m, 4H), 1.59 (d, *J* = 7.4 Hz, 4H), 1.32 (d, *J* = 62.4 Hz, 13H).

^{13}C NMR (151 MHz, $CDCl_3$) δ 169.75, 154.33, 134.81, 129.78, 127.90, 127.73, 127.72, 126.77, 58.51, 50.91, 40.95, 37.11, 34.68, 33.71, 33.44, 32.49, 30.18, 30.05, 29.46, 29.38, 29.26, 29.09, 27.10, 26.72, 26.56, 25.91, 25.29, 24.76, 23.19, 22.71, 22.67, 20.71, 19.74.

LRMS (APCI) m/z: $[M+H]^+$ calc'd. for $C_{33}H_{43}N_2O_3$: 515.7, found 515.3

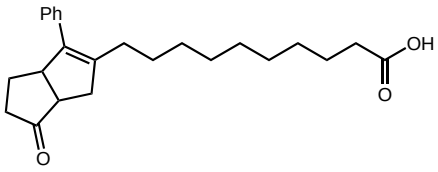

10-(6-oxo-3-phenyl-1,3a,4,5,6,6a-hexahydropentalen-2-yl)decanoic acid (**S1**): To reaction vial equipped with a stirbar was added 10-(6-hydroxy-3-phenyl-1,3a,4,5,6,6a-hexahydropentalen-2-yl)decanoic acid (0.6 mmol, 1.0 equiv, 206 mg) (prepared as previously reported)[57] dissolved in DCM (11.2 mL). Dess-Martin Periodinane (0.7 mmol, 1.2 equiv, 284 mg) was added and the reaction proceeded overnight at ambient temperatures before being pushed through a silica plug. The filtrate was concentrated and the crude material was purified via flash chromatography (50% EtOAc/Hex) to give the title compound (154.4 mg, 75% yield) as a clear oil.

^{1}H NMR (600 MHz, $CDCl_3$) δ 7.38 (dd, *J* = 8.3, 6.9 Hz, 2H), 7.27 (m, 1H), 7.18 – 7.16 (m, 2H), 3.95 (d, *J* = 7.1 Hz, 1H), 2.38 – 2.34 (m, 3H), 2.20 (td, *J* = 7.1, 2.6 Hz, 2H), 2.18 – 1.97 (m, 3H), 1.85 (ddt, *J* = 13.0, 9.2, 1.7 Hz, 1H), 1.71 – 1.60 (m, 4H), 1.58 – 1.51 (m, 1H), 1.45 – 1.18 (m, 12H).

^{13}C NMR (151 MHz, $CDCl_3$) δ 141.04, 137.38, 137.03, 128.31, 128.22, 126.65, 68.11, 50.99, 48.82, 39.43, 36.17, 33.76, 29.41, 29.31, 29.26, 29.15, 29.01, 28.98, 28.88, 28.65, 28.43, 27.99, 24.67, 23.98.

LRMS (APCI) m/z: $[M+H]^+$ calc'd. for $C_{24}H_{33}O_3$: 369.5, found 369.3.

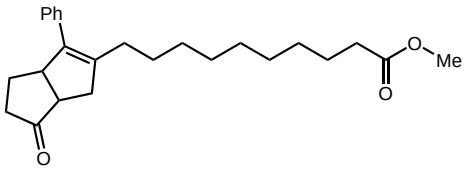

methyl 10-(6-oxo-3-phenyl-1,3a,4,5,6,6a-hexahydropentalen-2-yl)decanoate (**S2**):): To reaction vial equipped with a stirbar was added **S1** (0.2 mmol, 1.0 equiv, 77.2 mg) dissolved in methanol (2 mL). Two drops of hydrochloric acid was added to the reaction and was stirred overnight at ambient temperatures before being concentrated. The crude material was purified via flash chromatography (5-10% EtOAc/Hex) to give the title compound (79.7 mg, 96% yield) as a clear oil.

^{1}H NMR (600 MHz, $CDCl_3$) δ 7.40 – 7.36 (m, 2H), 7.28 – 7.26 (m, 1H), 7.18 – 7.16 (m, 2H), 3.95 (t, *J* = 6.9 Hz, 1H), 3.68 (s, 3H), 2.84 – 2.65 (m, 2H), 2.31 (t, *J* = 7.6 Hz, 2H), 2.26 – 1.90 (m, 5H), 1.89 – 1.82 (m, 1H), 1.62 (p, *J* = 7.5 Hz, 2H), 1.38 (dt, *J* = 8.8, 6.0 Hz, 1H), 1.34 – 1.13 (m, 12H).

^{13}C NMR (151 MHz, $CDCl_3$) δ 174.35, 141.04, 137.36, 137.04, 128.31, 128.22, 126.65, 51.45, 50.98, 48.80, 39.43, 36.16, 34.11, 29.46, 29.33, 29.30, 29.21, 29.12, 28.01, 24.95, 23.98.

LRMS (APCI) m/z: $[M+H]^+$ calc'd. for $C_{25}H_{35}O_3$: 383.6, found 383.3.

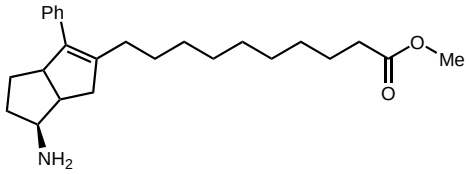

methyl 10-((6*S*)-6-amino-3-phenyl-1,3a,4,5,6,6a-hexahydropentalen-2-yl)decanoate (**S3**): To a flame-dried reaction vial equipped with a stirbar backfilled to a nitrogen atmosphere was added **S2** (0.2 mmol, 1.0 equiv, 67.6 mg) dissolved in dry ethanol. Titanium (IV) isopropoxide (0.3 mmol, 1.5 equiv, 80.4 μL) was added followed by ammonia 7N in methanol (3.53 mmol, 20 equiv, 504 μL). The reaction proceeded for 6 hours at ambient temperatures, turning yellow, before the addition of sodium borohydride (0.53 mmol, 3 equiv, 20 mg) at 0 ºC. The reaction proceed overnight warming to room temperature before being poured into a separatory funnel. The mixture was partitioned between water and EtOAc. The organic layer was collected and washed with brine (2x). The crude material was pushed through a silica plug (10-50% EtOAc/Hex + 1% TEA then 100% EtOAc+ 1% TEA). The oil was then dissolved in dry benzene under nitrogen and was used without further purification in subsequent steps.

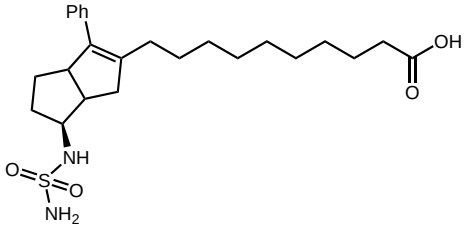

10-((6*S*)-3-phenyl-6-(sulfamoylamino)-1,3a,4,5,6,6a-hexahydropentalen-2-yl)decanoic acid (**6N-10CA (no R2)**): An oven-dried vial was charged with a stirbar, ^{t}BuOH (1.23 mmol, 91.7 mg), and DCM (11.2 ml) then evacuated under reduced pressure and backfilled with nitrogen

three times and cooled to 0 ºC. Chlorosulfonyl isocyanate (1.125 mmol, 97 µl) was then added dropwise via syringe and the solution allowed to warm to 23 ºC over 90 minutes. A 1.63 ml portion of this solution was added slowly via syringe to a solution of **S3** (0.15 mmol, 1.0 equiv 57 mg) and triethylamine (0.297 mmol, 2.0 equiv, 41 µl) in DCM (1.47 ml) at 0 ºC under nitrogen. This combined solution was allowed to warm to 23 ºC gradually 16 h then diluted with EtOAc. The diluted solution was washed with three times with NH_4Cl then H_2O and brine. The organic layer was dried over Na_2SO_4, filtered, and filtrate concentrated under reduced pressure to collect the crude material. The crude material was dissolved in dioxane (508 µL). The solution was frozen in an ice bath and then allowed to slowly warm to 23 ºC. As soon was the entire solution had re-melted, cold concentrated HCl (169 µL) was added so the solution was 3:1 HCl: Dioxane. The solution was allowed to slowly warm to 23 ºC and continue reacting at 40 °C until starting material was consumed by TLC. The reaction solution was diluted with EtOAc and washed four times with H_2O then twice with brine. The organic layer was dried over Na_2SO_4, filtered, and filtrate concentrated under reduced pressure to collect the crude material. This crude material was purified by flash chromatography on silica with 30-45% EtOAc/hexanes to collect the title compound (4.4 mg, 7% yield).

^{1}H NMR (600 MHz, $CDCl_3$) δ 7.26 (t, *J* = 7.6 Hz, 2H), 7.17 – 7.14 (m, 1H), 7.12 – 7.09 (m, 2H), 4.96 (d, *J* = 7.8 Hz, 1H), 4.55 (s, 2H), 3.76 (dtd, *J* = 10.2, 7.8, 5.5 Hz, 1H), 3.55 (t, *J* = 8.7 Hz, 1H), 2.97 – 2.90 (m, 1H), 2.46 (d, *J* = 7.4 Hz, 2H), 2.28 (t, *J* = 7.2 Hz, 2H), 2.12 (ddd, *J* = 15.1, 9.4, 6.8 Hz, 1H), 1.98 (dt, *J* = 14.5, 7.3 Hz, 1H), 1.78 (dtd, *J* = 11.4, 5.8, 2.4 Hz, 1H), 1.61 – 1.47 (m, 2H), 1.45 – 1.32 (m, 2H), 1.29 – 1.15 (m, 14H).

^{13}C NMR (151 MHz, $CDCl_3$) δ 139z.18, 138.38, 137.61, 128.46, 128.15, 126.47, 57.96, 53.11, 41.21, 36.95, 33.29, 30.64, 29.71, 29.12, 28.99, 28.58, 28.43, 28.31, 28.29, 27.91, 27.82, 24.20.

LRMS (APCI) m/z: $[M+H]^+$ calc'd. for $C_{24}H_{37}N_2O_4S$: 449.6, found 448.8.

2.5.3 Supporting information for 2.2.2

General coupling procedure: A flame-dried vial was charged with a stir bar and 1,1'-carbinyliimidazole (CDI). The vial was placed under vacuum and backfilled 3x with nitrogen before the addition of the substrate dissolved in dry THF. The reaction stirred at room temperature for 1.5 h. The amine was added to the solution and the reaction proceeded for 16 h. The reaction mixture was then diluted in ethyl acetate and washed with water twice. The organic layer was then dried with magnesium sulfate, filtered, and concentrated via rotary evaporation. The resulting residue was purified to afford the product.

General deprotection procedure: In a reaction vial the substrate was dissolved in acetonitrile. A few drops of hydrochloric acid was added at room temperature and the reaction proceeded until complete by TLC (30 minutes- 2 h). The crude mixture was concentrated and purified to afford the product.

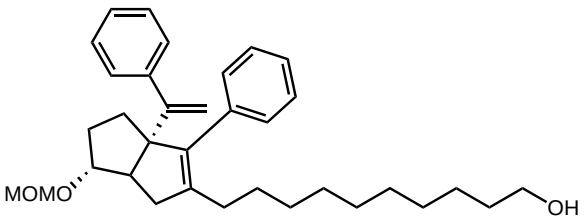

10-((3a*R*,6*R*)-6-(methoxymethoxy)-3-phenyl-3a-(1-phenylvinyl)-1,3a,4,5,6,6a-hexahydropentalen-2-yl)decan-1-ol: The title compound was prepared according to the reported procedure and the NMR data were consistent with those previously reported.[38]

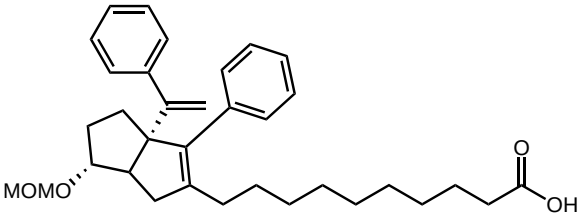

10-((3a*R*,6*R*)-6-(methoxymethoxy)-3-phenyl-3a-(1-phenylvinyl)-1,3a,4,5,6,6a-hexahydropentalen-2-yl)decanoic acid (**S4**)**:** The title compound was prepared according to the reported procedure and the NMR data were consistent with those previously reported.[38]

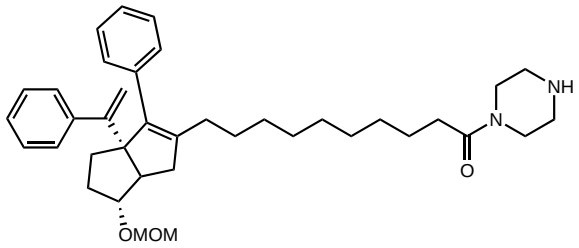

10-((3a*R*,6*R*)-6-(methoxymethoxy)-3-phenyl-3a-(1-phenylvinyl)-1,3a,4,5,6,6a-hexahydropentalen-2-yl)-1-(piperazin-1-yl)decan-1-one (**S5**): Following the general coupling procedure, the reaction of **S4** (27.6 mg, 0.05 mmol), CDI (9.7 mg, 0.06 mmol, 1.2 equiv), piperazine (94.7 mg, 1.1 mmol, 20 equiv) and THF (1.1 mL) provided the title compound as a clear oil (10.9 mg, 35% yield) after purification by flash chromatography (5-10% MeOH/DCM). **^{1}H NMR** (600 MHz, $CDCl_3$) δ 7.34 – 7.32 (m, 3H), 7.29 (dd, *J* = 7.1, 1.2 Hz, 2H), 7.26 – 7.23 (m, 3H), 7.22 – 7.19 (m, 2H), 5.05 (d, *J* = 1.4 Hz, 1H), 5.00 (d, *J* = 1.5 Hz, 1H), 4.60 – 4.57 (m,

2H), 3.80 – 3.75 (m, 3H), 3.62 (s, 2H), 3.30 (s, 3H), 3.01 (t, *J* = 8.9 Hz, 3H), 2.42 (dd, *J* = 9.3, 1.7 Hz, 1H), 2.32 (dt, *J* = 15.6, 8.4 Hz, 4H), 2.08 – 2.06 (m, 1H), 2.06 – 1.98 (m, 4H), 1.77 – 1.71 (m, 1H), 1.68 – 1.57 (m, 6H), 1.34 – 1.26 (m, 10H).

^{13}C NMR (151 MHz, $CDCl_3$) δ 171.74, 154.55, 144.14, 141.34, 139.25, 137.50, 129.65, 127.85, 127.65, 126.63, 126.58, 114.89, 94.76, 86.75, 69.10, 55.18, 52.79, 49.46, 40.54, 33.17, 32.44, 31.46, 29.74, 29.71, 29.44, 29.43, 29.41, 27.86, 26.99, 25.22.

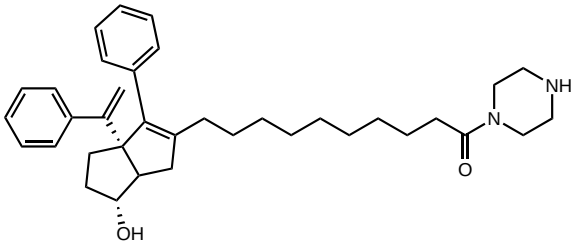

10-((3a*R*,6*R*)-6-hydroxy-3-phenyl-3a-(1-phenylvinyl)-1,3a,4,5,6,6a-hexahydropentalen-2-yl)-1-(piperazin-1-yl)decan-1-one (**Pip**): Following the general deprotection procedure, the reaction of **S5** (5.5 mg, 0.01 mmol), 2 drops of HCl and acetonitrile (100 μL) provided the title compound as a clear oil (2.1 mg, 42% yield) after purification by flash chromatography (10% MeOH/DCM).

^{1}H NMR (600 MHz, $CDCl_3$) δ 7.37 (ddd, *J* = 5.4, 3.0, 1.0 Hz, 3H), 7.34 – 7.31 (m, 2H), 7.28 – 7.27 (m, 3H), 7.21 (dt, *J* = 7.1, 1.4 Hz, 2H), 5.09 (d, *J* = 1.5 Hz, 1H), 5.01 (d, *J* = 1.4 Hz, 1H), 3.97 (s, 3H), 3.85 (m, 2H), 3.78 – 3.62 (m, 5H), 3.57 – 3.48 (m, 3H), 3.31 (s, 1H), 3.29 – 3.18 (m, 2H), 2.40 – 2.27 (m, 6H), 2.15 (d, *J* = 4.8 Hz, 1H), 2.13 – 2.08 (m, 4H), 2.08 – 2.02 (m, 2H), 1.76 – 1.66 (m, 2H), 1.37 – 1.29 (m, 5H).

^{13}C NMR (151 MHz, $CDCl_3$) δ 154.55, 144.21, 141.14, 139.19, 137.37, 129.72, 127.77, 127.67, 126.70, 126.63, 115.09, 82.08, 69.35, 55.75, 53.49, 40.25, 34.03, 33.37, 32.13, 31.96, 29.74, 29.70, 29.67, 29.63, 29.61, 29.54, 29.41, 29.39, 29.33, 29.30, 29.28, 27.82, 27.76, 22.74.

LRMS (APCI) m/z[M+H]$^+$ calc'd for $C_{36}H_{50}N_2O_2$ [M+H]+ 542.4, found 542.8

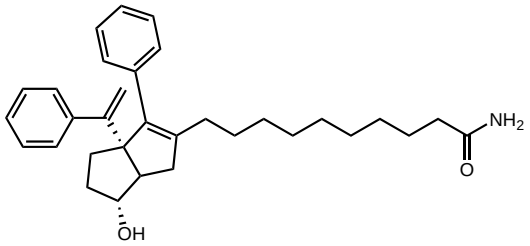

10-((3a*R*,6*R*)-6-hydroxy-3-phenyl-3a-(1-phenylvinyl)-1,3a,4,5,6,6a-hexahydropentalen-2-yl)decanamide (**Am**): **S4** was added to a scintillation vial (52 mg, 0.1 mmol, 1.0 equiv), equipped with a magnetic stir bar and dissolved in THF. Carbonyldiimidazole (35 mg, 0.2 mmol, 2 equiv) was added in small portions (effervesces) and stirred until completion was detected by LCMS (small portions of the activated ester was quenched with methanol to visualize reaction progress). Ammonia (as a 0.5N solution in dioxane, 100 µL, excess) was added to the reaction mixture, which was stirred at room temperature until completion as detected by TLC and LCMS. The reaction mixture was concentrated and the crude residue was passed through silica (50–100% EtOAc/Hex eluent), concentrated, and dissolved in acetonitrile. A magnetic stirrer was added, and two drops of concentrated HCl was added to the solution. After deprotection was complete (approximately 1 hr OH O NH2 204 as determined by TLC and LCMS), the reaction mixture was concentrated and purified on silica (50–100% EtOAc/Hex eluent) to give the title compound (10.1 mg, 54% yield).

^{1}H NMR (600 MHz, CDCl3) δ 7.40 – 7.15 (m, 10H), 5.35 (d, J = 36.9 Hz, 2H), 5.06 (s, 1H), 4.99 (s, 1H), 3.95 (s, 1H), 2.35 (dd, J = 16.8, 9.3 Hz, 1H), 2.29 (d, J = 8.8 Hz, 1H), 2.21 (t, J = 7.6 Hz, 2H), 2.12 – 1.95 (m, 4H), 1.74 – 1.60 (m, 6H), 1.42 – 1.14 (m, 11H).

^{13}C NMR (126 MHz, CDCl3) δ 175.2, 155.0, 143.7, 141.9, 138.9, 137.8, 129.7, 127.8, 127.7, 127.6, 126.7, 126.6, 116.4, 86.0, 70.1, 54.0, 40.2, 35.9, 34.0, 32.1, 29.6, 29.6, 29.3, 29.2, 29.2, 27.3, 25.5.

LRMS (APCI) m/z[M+H]$^+$ calc'd for $C_{32}H_{41}NO_2$ [M+H]+ 472.3, found 471.8

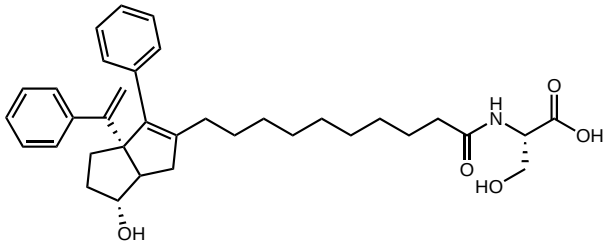

(10-((3a*R*,6*R*)-6-hydroxy-3-phenyl-3a-(1-phenylvinyl)-1,3a,4,5,6,6a-hexahydropentalen-2-yl)decanoyl)-*L*-serine (**Ser**): Following the general deprotection procedure, the reaction of **S6** (11.8 mg, 0.02 mmol), 2 drops of HCl and acetonitrile (410 μL) provided the title compound as a clear oil (2.1 mg, 42% yield) after purification by flash chromatography (10% MeOH/DCM).

^{1}H NMR (500 MHz, $CDCl_3$) δ 7.42 – 7.07 (m, 10H), 6.76 (s, 1H), 5.05 (s, 1H), 4.99 (s, 1H), 4.57 (s, 1H), 4.10 – 3.77 (m, 5H), 2.39 – 2.18 (m, 4H), 2.14 – 1.94 (m, 6H), 1.77 – 1.55 (m, 5H), 1.38 – 1.09 (m, 11H).

^{13}C NMR (151 MHz, $CDCl_3$) δ 154.58, 144.10, 141.15, 139.31, 137.36, 129.71, 127.82, 127.78, 127.69, 126.75, 126.66, 115.00, 44.80, 40.20, 32.11, 31.94, 29.72, 29.57, 29.37, 29.21, 27.66, 23.13, 22.71, 14.13.

LRMS (APCI) m/z[M+H]$^+$ calc'd for $C_{35}H_{44}NO_5$ [M–H]– 558.3, found 558.3

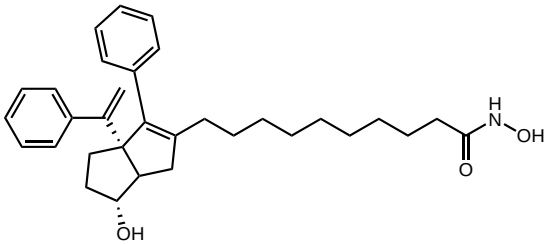

***N*-hydroxy-10-((3a*R*,6*R*)-6-hydroxy-3-phenyl-3a-(1-phenylvinyl)-1,3a,4,5,6,6a-hexahydropentalen-2-yl)decanamide** (**HA**): Following the general deprotection procedure, the reaction of **S7** (22.9 mg, 0.04 mmol), 2 drops of HCl and acetonitrile (1.0 mL) provided the title compound as a clear oil (12.9 mg, 66% yield) after purification by flash chromatography (10% MeOH/DCM).

^{1}H NMR (600 MHz, $CDCl_3$) δ 7.38 – 7.30 (m, 4H), 7.28 – 7.26 (m, 3H), 7.22 (dt, *J* = 6.4, 1.4 Hz, 3H), 5.09 (d, *J* = 1.5 Hz, 1H), 5.02 (d, *J* = 1.5 Hz, 1H), 3.99 – 3.95 (m, 1H), 2.54 – 2.45 (m, 2H), 2.40 – 2.30 (m, 3H), 2.22 – 2.16 (m, 2H), 2.13 – 1.99 (m, 6H), 1.76 – 1.62 (m, 4H), 1.62 – 1.54 (m, 2H), 1.39 – 1.27 (m, 10H).

^{13}C NMR (151 MHz, $CDCl_3$) δ 154.59, 144.16, 141.13, 139.26, 137.39, 129.71, 127.79, 127.74, 127.66, 126.69, 126.63, 115.02, 82.16, 69.35, 55.83, 40.21, 34.05, 32.09, 29.98, 29.71, 29.65, 29.60, 29.45, 29.23, 29.18, 29.10, 29.07, 29.04, 27.71.

LRMS (APCI) m/z$[M+H]^+$ calc'd for $C_{32}H_{42}NO_3$ [M+H]+ 488.3, found 488.6

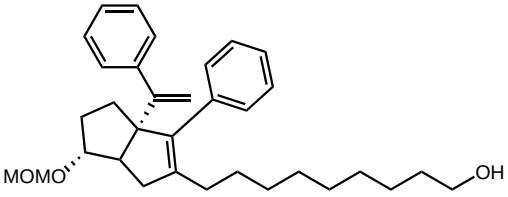

9-((3a*R*,6*R*)-6-(methoxymethoxy)-3-phenyl-3a-(1-phenylvinyl)-1,3a,4,5,6,6a-hexahydropentalen-2-yl)nonan-1-ol (**S7**): Hexahydropentalene formation was accomplished through slight modifaction of Whibty's procedure.[38,39] Prior to cyclization, all non-volatile

reagents were dried by azeotropic removal of water using benzene. A dry three-neck round bottom flask backfilled with nitrogen (3x) containing bis(cyclopentadienyl)zirconium(IV) dichloride (1.403 g, 4.8 mmol, 1.2 equiv) was dissolved in anhydrous, degassed tetrahydrofuran (THF, 16mL) and cooled to -78 °C. The resulting solution was treated with n-BuLi (2.5M in hexanes, 3.8 mL, 9.6 mmol, 2.4 equiv). The light yellow solution stirred for 45 minutes at -78 °C. A solution of *tert*-butyldimethyl((7-phenylhept-1-en-6-yn-3-yl)oxy)silane (921.2 mg, 4.0 mmol, 1 equiv) was added dropwise to the solution in anhydrous THF (16 mL). The solution stirred at -78 °C for 45 minutes before the bath was removed and the solution stirred at room temperature for 2.5 hours turning a salmon-colored mixture. The mixture was cooled to -78 °C before the addition of *tert*-butyl((10,10-dibromodecyl)oxy)diphenylsilane (2.45 g, 4.4 mmol, 1.1 equiv) in anhydrous THF (16 mL). followed immediately by freshly prepared lithium diisopropylamide (LDA, 4.4 mmol, 1.1 equiv) in anhydrous THF (16 mL). The red-solution stirred for 15 minutes before the addition of freshly prepared lithium phenylacetylide (1.5 mL, 14.4 mmol, 3.6 equiv) in anhydrous THF (16 mL). The reaction mixture continued at -78 °C for 1.5 h before being quenched with methanol (24 mL) and saturated aqueous sodium bicarbonate (24 mL). The resulting slurry was allowed to warm to room temperature before being diluted with ethyl acetate and being washed with water. The aqueous layer was reextracted with ethyl acetate (2x) before the combined organic layers were then washed with brine (2x). The resulting organic layer was dried with magnesium sulfate, filtered and concentrated via rotary evaporation. The resulting yellow slurry was then pushed through a short plug of silica (100% ethyl acetate eluent) and concentrated *in vacuo*. The crude product was then dissolved in THF and treated with tetrabutylammonium fluoride hydrate (3.0 equiv) overnight. The reaction mixture was concentrated and the diastereomers were purified and separated by

careful silica gel chromatography (20-40% EtOAc/Hexanes eluent) to afford the *exo* diastereomer in a RATIO.

^{1}H NMR (400 MHz, $CDCl_3$) δ 7.39 – 7.29 (m, 6H), 7.27 – 7.21 (m, 2H), 5.07 (d, *J* = 1.5 Hz, 1H), 5.02 (d, *J* = 1.5 Hz, 1H), 4.61 (d, *J* = 1.5 Hz, 1H), 3.66 (td, *J* = 6.6, 3.6 Hz, 3H), 3.33 (s, 3H), 2.46 – 2.41 (m, 1H), 2.34 (dd, *J* = 16.8, 9.2 Hz, 1H), 2.21 (td, *J* = 7.1, 2.7 Hz, 1H), 2.10 (d, *J* = 1.7 Hz, 1H), 2.08 – 2.01 (m, 4H), 1.72 – 1.63 (m, 2H), 1.61 – 1.48 (m, 8H), 1.40 – 1.20 (m, 10H).

^{13}C NMR (101 MHz, $CDCl_3$) δ 154.32, 143.95, 141.19, 139.03, 138.09, 137.30, 134.62, 128.92, 127.65, 127.47, 126.45, 126.39, 114.73, 94.52, 86.52, 68.90, 62.90, 55.38, 52.08, 39.45, 32.62, 32.58, 32.24, 31.25, 29.53, 29.45, 29.29, 29.20, 29.16, 29.13, 27.62, 25.52.

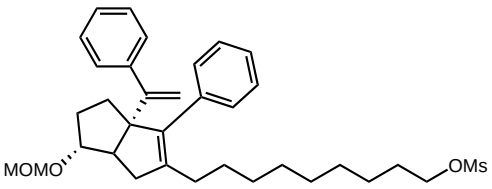

9-((3a*R*,6*R*)-6-(methoxymethoxy)-3-phenyl-3a-(1-phenylvinyl)-1,3a,4,5,6,6a-hexahydropentalen-2-yl)nonyl methanesulfonate (**S8**): A flame-dried round bottom flask equipped with a stir bar was backfilled (3x) with nitrogen gas before the addition of RMS-IV-162 (504.9 mg, 1.0 mmol, 1 equiv) in DCM (10 mL), methanesulfonyl chloride (160 μL, 2.0 mmol, 2 equiv), and triethylamine (290 μL, 2.0 mmol, 2 equiv). The reaction stirred for 60 minutes before the crude mixture was washed with water (1x). The aqueous layer was then extracted with DCM (2x) before the combined organic layers were dried with $MgSO_4$, filtered, and concentrated via rotary evaporation. The crude mixture was purified via flash

chromatography (10% EtOAc/Hex) to give the title compound (288.4 mg, 0.51 mmol, 51% yield) as a clear oil.

^{1}H NMR (600 MHz, Chloroform-*d*) δ 7.37 – 7.27 (m, 5H), 7.25 (t, *J* = 3.3 Hz, 3H), 7.23 – 7.17 (m, 2H), 5.05 (d, *J* = 1.5 Hz, 1H), 5.00 (d, *J* = 1.5 Hz, 1H), 4.60 – 4.57 (m, 2H), 4.21 (t, *J* = 6.6 Hz, 2H), 3.79 (p, *J* = 2.1 Hz, 1H), 3.31 (s, 3H), 2.99 (s, 3H), 2.43 – 2.41 (m, 1H), 2.33 (dd, *J* = 17.0, 9.2 Hz, 1H), 2.19 (td, *J* = 7.1, 2.6 Hz, 1H), 2.08 – 2.04 (m, 2H), 2.02 (ddd, *J* = 10.0, 7.2, 4.6 Hz, 2H), 1.73 (p, *J* = 6.8 Hz, 5H), 1.66 – 1.62 (m, 2H), 1.44 – 1.18 (m, 9H).

^{13}C NMR (151 MHz, $CDCl_3$) δ 154.46, 144.05, 141.20, 139.23, 137.41, 129.57, 127.77, 127.58, 127.50, 126.55, 126.51, 114.82, 94.68, 86.66, 70.08, 69.03, 55.09, 52.71, 40.47, 37.31, 32.36, 31.38, 29.63, 29.56, 29.24, 29.21, 29.06, 28.94, 27.73, 25.32.

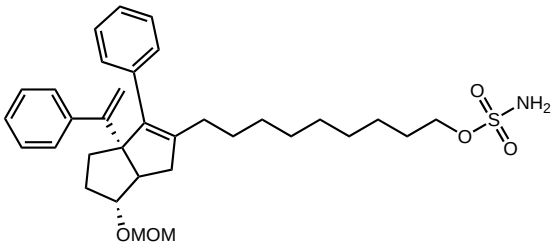

9-((3a*R*,6*R*)-6-(methoxymethoxy)-3-phenyl-3a-(1-phenylvinyl)-1,3a,4,5,6,6a-hexahydropentalen-2-yl)nonyl sulfamate (**S9**): An oven-dried vial backfilled with nitrogen was cooled to 0 °C before the addition of chlorosulfonyl isocyanate (0.5 mL, 5.744 mmol, 41 equiv) and formic acid (216 μL, 5.744 mmol, 41 equiv). The resulting solution (28 μL) was added to a solution of **RMS-IV-164** (70.6 mg, 0.144 mmol, 1 equiv) was dissolved in DMA. The reaction stirred for 24 h before being diluted in EtOAc and washed with water. The organic layer was dried with magnesium sulfate, filtered, and concentrated via rotary evaporation. The crude

mixture was purified via flash chromatography (5-30% EtOAc/Hexanes and then flushed with 100% EtOAc) to collect impure product taken to the next step without further purification.

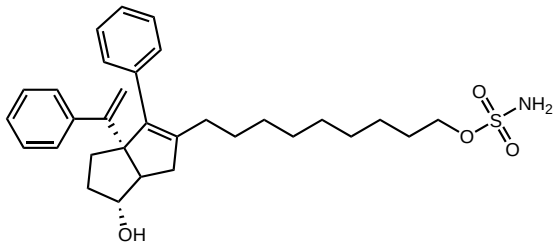

9-((3a*R*,6*R*)-6-hydroxy-3-phenyl-3a-(1-phenylvinyl)-1,3a,4,5,6,6a-hexahydropentalen-2-yl)nonyl sulfamate (**Sul**): Following the general deprotection procedure, the reaction of **AMJ-2-103** (37.9 mg, 0.07 mmol), 4 drops of HCl and acetonitrile (500 μL) provided the title compound as a clear oil (14.0 mg, 38% yield) after purification by reverse phase liquid chromatography using a 50-99% MeCN/H_2O gradient over 35 minutes to afford the title compound.

^{1}H NMR (500 MHz, Chloroform-*d*) δ 7.36 – 7.27 (m, 5H), 7.25 (d, *J* = 3.1 Hz, 3H), 7.21 – 7.17 (m, 2H), 5.07 (d, *J* = 1.4 Hz, 1H), 4.98 (d, *J* = 1.4 Hz, 1H), 4.79 (s, 2H), 4.19 (t, *J* = 6.6 Hz, 2H), 3.95 (d, *J* = 3.9 Hz, 1H), 2.36 (dd, *J* = 16.7, 9.3 Hz, 1H), 2.31 – 2.25 (m, 1H), 2.12 – 1.98 (m, 4H), 1.76 – 1.64 (m, 4H), 1.36 (dt, *J* = 19.7, 7.0 Hz, 3H), 1.30 – 1.19 (m, 11H).

^{13}C NMR (126 MHz, $CDCl_3$) δ 154.50, 144.07, 140.98, 139.13, 137.28, 129.61, 127.65, 127.63, 127.54, 126.58, 126.52, 114.93, 82.00, 71.43, 69.26, 55.73, 40.13, 33.90, 32.00, 29.51, 29.38, 29.13, 29.08, 28.84, 28.68, 27.62, 25.29.

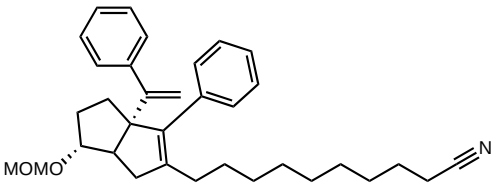

10-((3a*R*,6*R*)-6-(methoxymethoxy)-3-phenyl-3a-(1-phenylvinyl)-1,3a,4,5,6,6a-hexahydropentalen-2-yl)decanenitrile (**S10**): A flame-dried round bottom flask equppied with a stir bar was backfilled 3x with nitrogen. Sodium cyanide (250 mg, 5.1 mmol, 10 equiv) was quickly added before the addition of **S8** (288.4 mg, 0.51 mmol, 1 equiv) in DMF (5.1 mL). A vent needle to a saturated KOH solution was added before heating the reaction to 110 ^{o}C. After 10 minutes the reaction showed completion by TLC and was cooled to room temperature before being diluted with EtOAc. The solution was washed with saturated KOH (2x), water (1x), and brine (3x). The resulting organic layer was dried with $MgSO_4$, filtered, and concentrated via rotary evaporation. The crude mixture was purified by flash chromatography to give the title compound (224.8 mg, 0.45 mmol, 89% yield) as a clear oil.

^{1}H NMR (600 MHz, Chloroform-*d*) δ 7.35 – 7.29 (m, 6H), 7.26 – 7.24 (m, 2H), 7.22 – 7.20 (m, 2H), 5.05 (d, *J* = 1.4 Hz, 1H), 5.01 (d, *J* = 1.5 Hz, 1H), 4.59 (d, *J* = 2.6 Hz, 2H), 3.80 – 3.78 (m, 1H), 3.31 (s, 3H), 2.43 (dt, *J* = 9.2, 1.7 Hz, 1H), 2.32 (t, *J* = 7.1 Hz, 3H), 2.03 (dtd, *J* = 12.6, 7.2, 6.2, 2.9 Hz, 4H), 1.74 (ddt, *J* = 6.8, 4.7, 2.3 Hz, 1H), 1.67 – 1.62 (m, 4H), 1.45 – 1.39 (m, 3H), 1.33 (t, *J* = 7.0 Hz, 2H), 1.30 – 1.18 (m, 9H).

^{13}C NMR (151 MHz, $CDCl_3$) δ 154.45, 144.05, 141.17, 139.24, 137.40, 129.56, 127.76, 127.57, 127.56, 126.54, 126.50, 119.75, 114.81, 94.67, 86.64, 69.02, 55.08, 52.70, 40.46, 32.35, 31.37, 29.61, 29.52, 29.17, 29.11, 28.66, 28.55, 27.71, 25.28, 17.04.

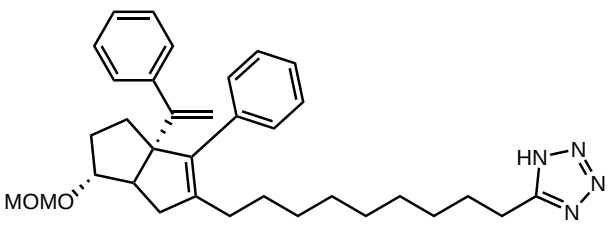

5-(9-((3a*R*,6*R*)-6-(methoxymethoxy)-3-phenyl-3a-(1-phenylvinyl)-1,3a,4,5,6,6a-hexahydropentalen-2-yl)nonyl)-1*H*-tetrazole (**S11**): A round bottom flask was charged with a stir bar and **S10** (112.4 mg, 0.23 mmol, 1.0 equiv) in toluene (500 μL). Trimethylsilyl azide (81 μL, 0.46 mmol, 2 equiv) and dibutyltin oxide (5.7 mg, 0.023 mmol, 0.1 equiv) were added to the reaction vial before heating to reflux. After 48 hours the reaction was cooled to room temperature and concentrated before being redissolved in methanol (10 mL). The reaction was reconcentrated before being dissolved in EtOAc and washed with saturated sodium bicarbonate (2x). The organic layer was dried with magnesium sulfate, filtered, and concentrated. The crude reaction mixture was purified by flash chromatography (50% EtOAc/Hex then 10% MeOH/DCM) to give the title compound (53.3 mg, 0.1 mmol, 43% yield) as a clear oil.

^{1}H NMR (400 MHz, Chloroform-*d*) δ 7.27 (m, 8H), 7.18 – 7.13 (m, 2H), 5.01 (d, *J* = 1.4 Hz, 1H), 4.96 (d, *J* = 1.6 Hz, 1H), 4.63 – 4.56 (m, 2H), 3.76 (t, *J* = 3.1 Hz, 1H), 3.31 (s, 3H), 2.97 (t, *J* = 7.7 Hz, 2H), 2.38 (d, *J* = 9.1 Hz, 1H), 2.27 (dd, *J* = 17.1, 8.9 Hz, 1H), 2.01 – 1.93 (m, 5H), 1.81 – 1.74 (m, 2H), 1.67 – 1.56 (m, 2H), 1.19 – 1.13 (m, 12H).

^{13}C NMR (101 MHz, $CDCl_3$) δ 154.20, 143.91, 141.04, 139.29, 137.19, 129.47, 127.61, 127.56, 127.52, 127.49, 126.50, 126.46, 125.59, 114.83, 94.48, 86.89, 68.96, 54.97, 52.60, 40.24, 32.22, 31.22, 29.53, 29.28, 28.87, 28.82, 28.76, 28.66, 28.59, 27.46, 27.29, 23.40.

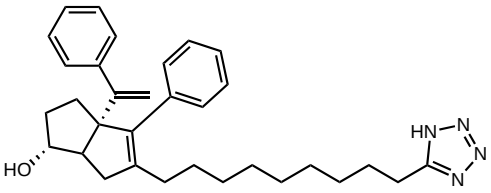

(1*R*,3a*R*)-5-(9-(1*H*-tetrazol-5-yl)nonyl)-4-phenyl-3a-(1-phenylvinyl)-1,2,3,3a,6,6a-hexahydropentalen-1-ol (**Tet**): Following the general deprotection procedure, the reaction of **S11** (37.6 mg, 0.07 mmol), 2 drops of HCl and acetonitrile (500 μL) provided the title compound as a clear oil (20.0 mg, 57% yield) after purification by flash chromatography (0-2% MeOH/DCM).

^{1}H NMR (400 MHz, Chloroform-*d*) δ 7.27 (t, *J* = 7.7 Hz, 5H), 7.21 (t, *J* = 3.8 Hz, 3H), 7.16 (d, *J* = 7.4 Hz, 2H), 5.03 (d, *J* = 7.8 Hz, 1H), 4.95 (d, *J* = 4.3 Hz, 1H), 3.95 (d, *J* = 4.2 Hz, 1H), 2.95 (t, *J* = 7.7 Hz, 1H), 2.31 – 2.23 (m, 1H), 2.10 – 1.89 (m, 2H), 1.84 – 1.59 (m, 2H), 1.38 – 1.14 (m, 12H).

^{13}C NMR (151 MHz, $CDCl_3$) δ 154.46, 144.04, 141.08, 139.38, 137.30, 129.68, 127.79, 127.75, 127.69, 126.73, 126.68, 115.04, 82.34, 72.97, 69.31, 55.89, 49.45, 40.10, 34.12, 32.07, 29.46, 29.18, 29.09, 28.99, 28.93, 28.87, 27.73, 27.57.

LRMS (APCI) m/z$[M+H]^+$ calc'd for C32H41N4O [M+H]+ 497.3, found 497.9

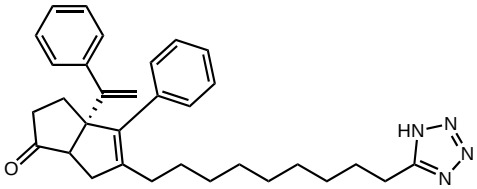

(3a*R*)-5-(9-(1*H*-tetrazol-5-yl)nonyl)-4-phenyl-3a-(1-phenylvinyl)-3,3a,6,6a-tetrahydropentalen-1(2*H*)-one (**S12**): In a round bottom flask **Tet** (18.9 mg, 0.04 mmol, 1 equiv) was dissolved in DCM (760 μL). Dess-Martin Periodinate (21.2 mg, 0.05 mg, 1.2 equiv) was added and the reaction proceeded open to air. After completion the mixture was diluted in MTBE pushed through a plug of celite before being concentrated via rotary evaporation to give the title compound as a yellow oil (21.1 mg, quant.).

^{1}H NMR (400 MHz, $CDCl_3$) δ 7.35 – 7.29 (m, 6H), 7.28 – 7.22 (m, 4H), 5.23 (d, *J* = 1.4 Hz, 1H), 5.14 (d, *J* = 1.3 Hz, 1H), 3.04 (t, *J* = 7.6 Hz, 2H), 2.54 (d, *J* = 7.6 Hz, 1H), 2.51 – 2.27 (m, 3H), 2.24 – 2.10 (m, 3H), 1.96 (dd, *J* = 13.8, 6.8 Hz, 1H), 1.85 (tt, *J* = 15.1, 7.6 Hz, 4H), 1.43 – 1.29 (m, 12H).

^{13}C NMR (101 MHz, $CDCl_3$) δ 152.68, 144.54, 142.17, 137.68, 136.22, 134.61, 128.77, 128.08, 128.03, 128.01, 127.50, 127.45, 127.02, 126.91, 115.30, 65.34, 55.63, 38.31, 37.60, 29.52, 29.33, 28.80, 28.60, 28.38, 28.28, 28.22, 28.11, 27.13, 27.02, 23.15.

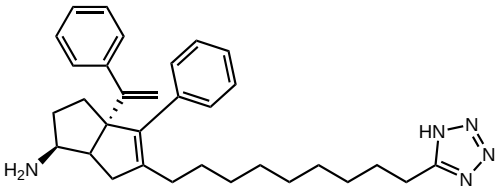

(1*S*,3a*R*)-5-(9-(1*H*-tetrazol-5-yl)nonyl)-4-phenyl-3a-(1-phenylvinyl)-1,2,3,3a,6,6a-hexahydropentalen-1-amine (**S12**): To a flame-dried round bottom equipped with a stir bar and backfilled (3x) with nitrogen **S11** (18 mg, 0.04 mmol, 1 equiv) dissolved in dry ethanol (400 μL) was added. Titanium isopropoxide (18 μL, 0.06 mmol, 1.5 equiv) was added to the reaction followed by ammonia (7N in methanol) (120 μL, 0.8 mmol, 20 equiv). The reaction stirred overnight before the addition of sodium borohydride (4.5 mg, 0.12 mmol, 3 equiv). The reaction mixture stirred for another hour before being diluted in ethyl acetate and extracted (2x) with sat. Rochelle's salt. The organic layer was dried with magnesium sulfate, filtered, and concentrated via rotary evaporation. The crude mixture was then purified via flash chromatography (10-20% MeOH/DCM) to give the title compound (7.8 mg, 39% yield) as a yellow oil.

^{1}H NMR (600 MHz, MeOD) δ 7.35 – 7.31 (m, 5H), 7.29 – 7.26 (m, 3H), 7.21 – 7.17 (m, 2H), 5.10 (d, *J* = 1.2 Hz, 1H), 4.93 (d, *J* = 1.2 Hz, 1H), 3.51 (ddd, *J* = 11.9, 9.0, 5.8 Hz, 1H), 2.87 (t, *J* = 7.5 Hz, 3H), 2.73 (dd, *J* = 9.1, 2.7 Hz, 1H), 2.30 (dd, *J* = 17.8, 9.1 Hz, 1H), 2.24 (d, *J* = 2.8 Hz, 1H), 2.14 (ddd, *J* = 13.7, 9.2, 6.8 Hz, 1H), 2.08 – 1.97 (m, 4H), 1.91 – 1.78 (m, 2H), 1.76 – 1.71 (m, 3H), 1.27 – 1.16 (m, 11H).

^{13}C NMR (151 MHz, MeOD) δ 155.35, 144.86, 143.56, 140.73, 137.50, 130.96, 129.07, 128.92, 128.74, 128.26, 116.61, 70.88, 54.94, 47.17, 35.92, 34.13, 30.60, 30.53, 30.40, 30.18, 30.12, 30.07, 29.94, 29.20, 28.44, 24.89.

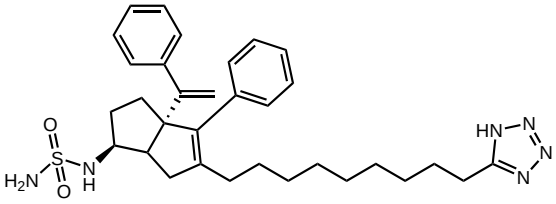

***N*-((1*S*,3a*R*)-5-(9-(1*H*-tetrazol-5-yl)nonyl)-4-phenyl-3a-(1-phenylvinyl)-1,2,3,3a,6,6a-hexahydropentalen-1-yl)-sulfanoylamine** (**6N-Tet**): **S12** was added to a reaction vial in EtOH (314 μL). H_2O (160 μL) was added followed by sulfamide (7.6 mg, 0.09 mmol, 5 equiv) and triethylamine (6.5 μL, 0.05 mmol, 3 equiv). The reaction proceeded for 16 hours at reflux before being cooled to room temperature. The reaction mixture was concentrated via rotatory evaporation. The crude mixture was then purified via flash chromatography (10-20% MeOH/DCM) to give the title compound (2.1 mg, 35% yield) as a yellow oil.

^{1}H NMR (400 MHz, $cdcl_3$) δ 7.27 (d, *J* = 10.6 Hz, 7H), 7.20 – 7.15 (m, 3H), 5.07 (s, 1H), 4.96 (s, 1H), 4.70 (br. s, 2H), 3.81 (s, 1H), 2.96 (s, 2H), 2.60 (t, *J* = 8.6 Hz, 1H), 2.45 (d, *J* = 17.6 Hz, 1H), 2.19 – 1.90 (m, 7H), 1.73 (dd, *J* = 20.7, 7.6 Hz, 7H), 1.40 (t, *J* = 7.1 Hz, 10H).

2.5.4 Supporting information for 2.2.3

General Cyclization procedure:

Hexahydropentalene formation was accomplished through slight modification of Whitby's procedure.[38,40,57,60] Prior to cyclization, all non-volatile reagents were dried by azeotropic removal of water using benzene. A dry round bottom flask containing bis(cyclopentadienyl)zirconium(IV) dichloride (1.2 equiv) under nitrogen, was dissolved in anhydrous, degassed tetrahydrofuran (THF, 8 mL/mmol enyne) and cooled to -78 °C. The resulting mixture was treated with n-BuLi (2.4 equiv) and the light yellow solution was stirred for 45 minutes. A solution of **(**(5-(methoxymethoxy)hept-6-en-1-yn-1-yl)benzene) or (tertbutyldimethyl((7-phenylhept-1-en-6-yn-3-yl)oxy)silane) (1.0 equiv) in anhydrous, degassed THF (8 mL/mmol) was added. The resulting salmon-colored mixture was stirred at -78 °C for 45 minutes before the cooling bath was removed. The reaction mixture continued to stir at room temperature for an additional 2.5 hours. The reaction mixture was then cooled to -78 °C and the required 1,1-dibromoether tail (**S17** or **S22**) (1.1 equiv) was added as a solution in anhydrous THF (8 mL/mmol enyne) followed by freshly prepared lithium diisopropylamide (LDA, 1.0 M, 1.1 equiv.). After 15 minutes, a freshly prepared solution of lithium phenylacetylide (3.6 equiv) in anhydrous THF (8 mL/ mmol enyne) was added dropwise and the resulting rust-colored solution was stirred at -78 °C for 1.5 hours. The reaction was quenched with methanol and saturated aqueous sodium bicarbonate slowly warming to room temperature, affording a light yellow slurry. The slurry was poured onto water and extracted with

ethyl acetate four times. The combined organic layers were washed with brine, dried withNa_2SO_4, and concentrated in vacuo. The resulting yellow oil was passed through a short plug of silica (100% EtOAc eluent) and concentrated. The crude product was dissolved in THF and treated with either HCl or TBAF. The resulting solution stirred at room temperature for 16 h. The reaction mixture was concentrated and the diastereomers were purified and separated by flash chromatography.

General Oxidation procedure

To a solution starting material (1.0 equiv) in acetonitrile (0.1 M) was added tetrapropylammonium perruthenate (TPAP) (0.1 equiv), N-methylmorpholine N-oxide (NMO) (10 equiv), and water (10 equiv) and stirred at room temperature overnight. The reaction solution was then filtered through a pad of silica with (100% EtOAc) and concentrated. The resulting mixture was purified by flash chromatography to give the title compound.

General methylation procedure

To a solution of the desired carboxylic acid (1.0 equiv) in methanol (0.1 M) was added three drops of concentrated HCl and stirred at room temperature overnight. Reaction solution was then concentrated in vacuo and filtered through a pad of silica to collect the title compound.

General reductive amination

To a flame-dried screw top test tube charged with a stir bar backfilled (3x) was added carbonyl compound (1.0 equiv.) and ethanol (0.1 M). Ammonia (7 M in methanol, 5.0 or 20.0 equiv) then titanium(IV) isopropoxide (1.5 equiv) were added via syringe and stirred at room temperature for 6 hours. The test tube cap was then removed and sodium borohydride (3.0 equiv) added portion-

wise. The resulting solution was stirred at room temperature for 30 minutes before being diluted with EtOAc. The solution was adjusted to a pH of 1 with 1M HCl. The layers were separated and the aqueous layer was extracted 3x with EtOAc. The combined organic layers were then dried over Na_2SO_4, filtered, and concentrated in vacuo before being purified by flash chromatography to give the title compound.

General deprotection procedure

A reaction vial was charged with a stir bar and starting material (1.0 equiv) dissolved in dioxane and a few drops of concentrated HCl was then added. The reaction was gradually heated to 40 °C before being diluted with EtOAc and washed with 3 x 5 mL 0.5 M aqueous HCl, 5 ml water, and 5 mL brine. The organic layer was then dried over Na_2SO_4, filtered, and concentrated in vacuo to give the title compound after flash chromatography.

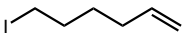

6-iodohex-1-ene (**S13**): To a round bottom flask under nitrogen flow was added sodium iodide (93.68 g, 5 eqivalents, 625 mmol), acetone (300 mL) and 6-bromo-1-hexene (125 mmol, 1 eq, 16.75 mL). The suspension was stirred and heated to reflux for 18h. The reaction was then loaded onto a silica plug, eluted with hexanes, 1:1 hexanes and MTBE, and MTBE (75 mL each). The organics were concentrated to a colorless oil (21.9 g, 104 mmol, 83%).

^{1}H NMR (600 MHz, Chloroform-*d*) δ 5.76 (ddtd, *J* = 17.0, 10.2, 6.7, 1.5 Hz, 1H), 4.99 (dp, *J* = 17.1, 1.7 Hz, 1H), 4.94 (dp, *J* = 10.2, 1.6 Hz, 1H), 3.17 (td, *J* = 7.0, 1.5 Hz, 2H), 2.05 (qd, *J* = 7.3, 1.5 Hz, 2H), 1.85 – 1.76 (m, 2H), 1.48 (pd, *J* = 7.5, 1.5 Hz, 2H).

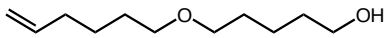

5-(hex-5-en-1-yloxy)pentan-1-ol (**S14**): Sodium hydride (60% in mineral oil, 3.46 g, 86 mmol, 1 eq) was added to a flame dried round bottom flask under positive nitrogen pressure followed by 115 mL of DMF and 115 mL of THF. This was cooled to 0°C and then 1,5-pentane diol (27.2 mL, 3.0 eq, 260 mmol) was added dropwise. The resulting solution was stirred for 20 minutes, then 6-iodohex-1-ene **(S13)** was added dropwise. The reaction was stirred overnight and allowed to warm to room temperature. In the morning, saturated ammonium chloride was added to quench the reaction and then the mixture was extracted with ethyl acetate (3x 100 mL). The organics was combined, dried, and concentrated to provide a crude oil that was purified by silica chromatography (0-20% EtOAc:hexanes) to yield the title compound (8.01 g, 43 mmol, 50% yield).

^{1}H NMR (600 MHz, Chloroform-*d*) δ 5.80 (ddtd, *J* = 16.9, 10.1, 6.7, 0.9 Hz, 1H), 5.00 (dtd, *J* = 17.1, 2.6, 1.5 Hz, 1H), 4.94 (ddq, *J* = 10.1, 2.2, 1.1 Hz, 1H), 3.64 (td, *J* = 6.5, 0.9 Hz, 2H), 3.40 (tdd, *J* = 6.6, 3.8, 0.9 Hz, 4H), 2.06 (tdd, *J* = 7.8, 6.4, 1.3 Hz, 2H), 1.63 – 1.55 (m, 6H), 1.47 – 1.40 (m, 4H).

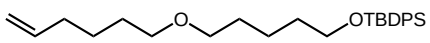

***tert*-butyl((5-(hex-5-en-1-yloxy)pentyl)oxy)diphenylsilane** (**S15**): 8.01 g of 5-(hex-5-en-1-yloxy)pentan-1-ol **(S14)** (43 mmol) was dissolved in 400 mL of dry THF, followed by 4.39 g imidazole (1.5 eq, 64.5 mmol). The mixture was stirred for 5 minutes until it was homogeneous and then TBDPS-Cl (1.2 eq, 51.6 mmol, 13.42 mL) was added dropwise. Stirred overnight at room temperature. The reaction was concentrated to approximately 150 mL and passed through a celite

plug to remove imidazolium salts. The filtrate was then concentrated to a clear oil that was purified by silica chromatography (1-7% EtOAc/hexanes) (12.9 g, 30.37 mmol, 70% yield).

^{1}H NMR (600 MHz, Chloroform-*d*) δ 7.69 – 7.64 (m, 4H), 7.44 – 7.35 (m, 6H), 5.80 (ddt, *J* = 16.9, 10.2, 6.7 Hz, 1H), 5.00 (dq, *J* = 17.1, 1.7 Hz, 1H), 4.94 (ddt, *J* = 10.2, 2.5, 1.2 Hz, 1H), 3.65 (t, *J* = 6.5 Hz, 2H), 3.38 (dt, *J* = 9.3, 6.6 Hz, 4H), 2.10 – 2.03 (m, 2H), 1.62 – 1.51 (m, 6H), 1.48 – 1.37 (m, 4H), 1.04 (s, 9H).

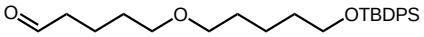

5-((5-((*tert*-butyldiphenylsilyl)oxy)pentyl)oxy)pentanal (**S16**): 9.59 mmol (4.06 g) of **S15** was dissolved in 150 mL of dry DCM and the reaction cooled to -78 °C. Next, ozone was bubbled through the reaction while stirring until a blue color persisted. Oxygen was then bubbled through the reaction to flush remaining ozone and then 3 equivalents (7.73 g) of triphenylphosphine was added. The reaction was warmed to room temperature and stirred for 3 hours. The solvent was removed in vacuo and the resulting oil purified by silica chromatography (0-20% EtOAc/hexanes). 3.083 g, 76%

^{1}H NMR (600 MHz, Chloroform-*d*) δ 9.76 (t, *J* = 1.8 Hz, 1H), 7.71 – 7.60 (m, 4H), 7.46 – 7.33 (m, 6H), 3.66 (t, *J* = 6.5 Hz, 2H), 3.39 (dt, *J* = 18.5, 6.5 Hz, 4H), 2.45 (td, *J* = 7.3, 1.8 Hz, 2H), 1.75 – 1.67 (m, 2H), 1.64 – 1.51 (m, 6H), 1.45 – 1.36 (m, 2H), 1.04 (s, 9H).

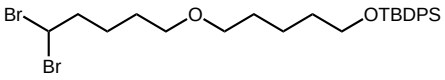

***tert*-butyl((5-((5,5-dibromopentyl)oxy)pentyl)oxy)diphenylsilane** (**S17**): Under nitrogen, a solution of triphenylphosphite (2.35 mL, 9 mmol, 1.1 equiv) in DCM (50 mL) was cooled to -78 °C. Bromine (0.48 mL, 9 mmol, 1.1 equiv) and triethylamine (1.32 mL, 9 mmol, 1.1 equiv) were

sequentially added dropwise at -78 °C. The reaction was stirred for 5 minutes, then **S16** (5.8 g, 14 mmol, 1.0 equiv) was added as a solution in DCM (10 mL) via syringe at -78 °C. The reaction was stirred for 5 h and allowed to warm to ambient temperature. The whole reaction was then poured over a pad of silica. The filtrate was concentrated and purified on a short plug of silica with 5% MTBE in hexanes to afford the title compound as a clear, colorless oil (3.35 g, 72%).

^{1}H NMR (600 MHz, Chloroform-*d*) δ 7.64 (dt, *J* = 8.0, 1.4 Hz, 4H), 7.44 – 7.31 (m, 6H), 5.67 (td, *J* = 6.2, 1.1 Hz, 1H), 3.63 (td, *J* = 6.5, 1.2 Hz, 2H), 3.42 – 3.29 (m, 4H), 2.38 (dddt, *J* = 7.6, 6.1, 4.2, 2.0 Hz, 2H), 1.66 – 1.46 (m, 9H).

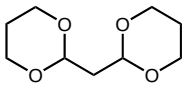

di(1,3-dioxan-2-yl)methane (**S18**): The title compound was prepared according to the reported procedure (17.6 g, 94%) and the NMR data were consistent with those previously reported.[61]

3,3'-(propane-1,3-diylbis(oxy))bis(propan-1-ol) (**S19**): A dry 3-neck round bottom flask charged with a stir bar was removed from a drying oven and sealed with septum stoppers before being connected to a vacuum line. The flask was allowed to cool to room temperature under vacuum. Once cool, Di(1,3-dioxan-2-yl)methane (21 g, 111.85 mmol, 1.0 equiv) and freshly prepared $Cu^{II}(OTf)_2$ (810 mg, 2.24 mmol, 2% loading) were added to the flask under positive nitrogen pressure. The flask was resealed with a septum stopper. The atmosphere was exchanged by applying vacuum and backfilling with N_2 (this process was conducted a total of three times). Degassed tetrahydrofuran (THF, 65 ml/mmol Di(1,3-dioxan-2-yl)methane) was delivered to the flask and the resulting solution was cooled to 0°C. Once cool, BH_3·DMS (37.1 ml, 391.5 mmol,

3.5 equiv) was added. The resulting mixture was allowed to stir overnight while warming to rt. The reaction was quenched with MeOH and subjected to a short celite plug. The resulting crude mixture was concentrated *in vacuo* and subjected to silica gel chromatography (5-15% MeOH/EtOAc) to afford the title compound (13.3 g, 62%). The title compound's NMR data were consistent with those previously reported.[62]

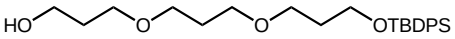

2,2-dimethyl-3,3-diphenyl-4,8,12-trioxa-3-silapentadecan-15-ol (**S20**): To a solution of tripropylene glycol (13.3 g, 69.2 mmol, 1.3 equiv) and imidazole (3.62 g, 53.2 mmol, 1 equiv) in anhydrous THF (800 ml) in an oven-dried flask under nitrogen at r.t. was added *tert*-butyl(chloro)diphenylsilane (13.85 ml, 53.2 mmol, 1 equiv) and stirred for 2.5 h. The resulting solution was concentrated *in vacuo* and subjected to silica gel chromatography (20-50% EtOAc/Hexanes) to afford the title compound (12.3 g, 54%).

^{1}H NMR (600 MHz, Chloroform-*d*) δ 7.67 – 7.65 (m, 4H), 7.43 – 7.35 (m, 6H), 3.77 – 3.73 (m, 4H), 3.61 – 3.58 (m, 2H), 3.54 (t, *J* = 6.4 Hz, 2H), 3.49 (t, *J* = 6.4 Hz, 2H), 3.46 (t, *J* = 6.3 Hz, 2H), 2.42 (s, 1H), 1.85 – 1.78 (m, 6H), 1.04 (d, *J* = 0.6 Hz, 9H).

^{13}C NMR (151 MHz, Chloroform-*d*) δ 135.56, 133.99, 129.54, 127.60, 70.46, 68.46, 67.76, 67.63, 62.35, 60.84, 32.72, 31.96, 30.07, 26.86, 19.24.

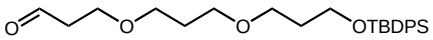

2,2-dimethyl-3,3-diphenyl-4,8,12-trioxa-3-silapentadecan-15-al (**S21**): To a solution of 2,2-dimethyl-3,3-diphenyl-4,8,12-trioxa-3-silapentadecan-15-ol (**S20**) (12.3 g, 28.6 mmol, 1 equiv) in anhydrous THF (500 ml) in an oven-dried flask under nitrogen at 0°C was added Dess-Martin Periodinane (14.5 g, 34.3 mmol, 1.2 equiv) and allowed to warm to room temperature and stirred for 1.5 h. The reaction mixture was then filtered through a pad of celite. The resulting solution was concentrated *in vacuo* and subjected to silica gel chromatography (20-50% EtOAc/Hexanes) to afford the title compound (10.5 g, 86%).

^{1}H NMR (600 MHz, Chloroform-*d*) δ 9.77 (td, *J* = 2.0, 0.7 Hz, 1H), 7.69 – 7.64 (m, 4H), 7.44 – 7.34 (m, 6H), 3.74 (dt, *J* = 8.1, 6.1 Hz, 4H), 3.54 (t, *J* = 6.4 Hz, 2H), 3.49 (t, *J* = 6.4 Hz, 2H), 3.45 (t, *J* = 6.3 Hz, 2H), 2.66 – 2.61 (m, 2H), 1.81 (dp, *J* = 8.0, 6.4 Hz, 4H), 1.04 (s, 9H).

^{13}C NMR (151 MHz, Chloroform-*d*) δ 201.30, 135.56, 133.99, 129.55, 127.61, 68.25, 67.58, 64.47, 60.83, 43.87, 32.75, 29.98, 26.85, 19.24.

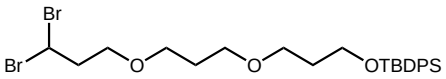

15,15-dibromo-2,2-dimethyl-3,3-diphenyl-4,8,12-trioxa-3-silapentadecane (**S22**): To a cold solution of triphenyl phosphite (7.1 g, 27.0 mmol, 1.1 equiv) in anhydrous dichloromethane (350 mL) maintained at -78°C under N_2 flow, bromine (1.4 ml, 27.0 mmol, 1.1 equiv) was dropped in. Anhydrous triethylamine (4.1 mL, 29.5 mmol, 1.2 equiv) and 2,2-dimethyl-3,3-diphenyl-4,8,12-trioxa-3-silapentadecan-15-al (10.5 g, 24.5 mmol, 1 equiv) were added to the faint orange solution. The reaction mixture was stirred for 4 h and allowed to warm to room temperature after 3 h. The resulting solution was concentrated *in vacuo* and subjected to silica gel chromatography (10-30% MTBE/Hexanes) to afford the title compound (10.9 g, 78%).

^{1}H NMR (600 MHz, Chloroform-*d*) δ 7.68 – 7.65 (m, 4H), 7.44 – 7.40 (m, 2H), 7.40 – 7.36 (m, 4H), 5.82 (t, *J* = 6.7 Hz, 1H), 3.75 (t, *J* = 6.1 Hz, 2H), 3.55 (t, *J* = 6.4 Hz, 2H), 3.52 – 3.44 (m, 6H), 2.61 (q, *J* = 5.9 Hz, 2H), 1.86 – 1.77 (m, 4H), 1.05 (s, 9H).

^{13}C NMR (151 MHz, Chloroform-*d*) δ 135.57, 133.98, 129.55, 128.35, 127.61, 77.23, 77.02, 76.81, 68.18, 68.05, 67.64, 67.58, 60.84, 45.59, 43.09, 32.76, 29.99, 27.25, 20.21.

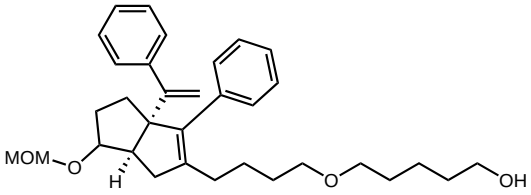

5-(4-((3aR,6aR)-6-(methoxymethoxy)-3-phenyl-3a-(1-phenylvinyl)-1,3a,4,5,6,6a-hexahydropentalen-2-yl)butoxy)pentan-1-ol (**S23**): According to the general cyclization procedure, **S17** (2.50 g, 4.4 mmol) was reacted with enyne (1.20 g, 4 mmol) before being treated with 5 equivalents of tetrabutylammonium fluoride to give the title compound (1.2 g, 5:1 dr, 60% yield over 2 steps) as a yellow oil after purification by flash chromatography (0-50% EtOAc/Hex eluent).

^{1}H NMR (600 MHz, Chloroform-*d*) δ 7.32 – 7.25 (m, 3H), 7.24 – 7.20 (m, 5H), 7.18 (dt, *J* = 8.1, 1.5 Hz, 2H), 5.02 (q, *J* = 2.5, 2.0 Hz, 1H), 4.98 (q, *J* = 2.4, 1.9 Hz, 1H), 4.60 – 4.54 (m, 2H), 3.79 – 3.73 (m, 1H), 3.66 – 3.57 (m, 4H), 3.34 (td, *J* = 6.6, 1.3 Hz, 2H), 3.28 (d, *J* = 1.3 Hz, 3H), 2.39 (dq, *J* = 9.6, 1.8 Hz, 1H), 2.26 (dddd, *J* = 9.8, 7.0, 3.1, 1.2 Hz, 1H), 2.03 – 1.96 (m, 3H), 1.60 – 1.52 (m, 8H), 1.49 – 1.34 (m, 8H).

LRMS (APCI) m/z$[M+H]^+$ calc'd for $C_{33}H_{44}O_4$: 505.3, found 473.3 (**13a** - $CH_3O^{\bullet}$)

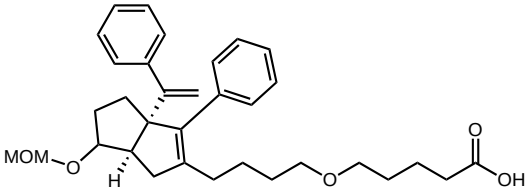

5-(4-((3aR,6aR)-6-(methoxymethoxy)-3-phenyl-3a-(1-phenylvinyl)-1,3a,4,5,6,6a-hexahydropentalen-2-yl)butoxy)pentanoic acid (**S24**): A solution of **S23** (504 mg, 1 eq) in 50 mL acetonitrile was treated with tetrapropylammonium perruthenate (TPAP, 0.1 equiv, 17.55 mg), N-Methylmorpholine-N-Oxide (NMO, 10 equiv, 1.17 g), and water (10 equiv, 180 microliters). The reaction mixture was allowed to stir overnight at room temperature. The reaction mixture was passed through celite, concentrated and purified on silica (0-65% EtOAc (containing 0.1% AcOH)/hexanes eluent) to provide the title compound. 70 mg, 13%

^{1}H NMR (600 MHz, Chloroform-*d*) δ 7.38 – 7.28 (m, 4H), 7.28 – 7.25 (m, 3H), 7.25 – 7.22 (m, 2H), 5.06 (d, *J* = 1.2 Hz, 1H), 5.04 (t, *J* = 1.2 Hz, 1H), 4.64 (s, 2H), 3.81 (dd, *J* = 4.5, 2.6 Hz, 1H), 3.42 (q, *J* = 5.8 Hz, 2H), 3.37 (dd, *J* = 6.1, 1.2 Hz, 5H), 2.39 (t, *J* = 7.6 Hz, 2H), 1.71 – 1.59 (m, 4H), 1.56 – 1.41 (m, 5H), 1.36 – 1.23 (m, 10H).

^{13}C NMR (151 MHz, $CDCl_3$) δ 154.47, 144.05, 137.50, 129.58, 127.85, 127.71, 127.66, 126.65, 114.90, 104.61, 94.51, 86.79, 70.37, 70.21, 69.71, 55.06, 52.80, 40.46, 33.66, 33.58, 32.37, 31.58, 29.67, 29.43, 28.98, 28.62, 24.49, 21.80, 21.58.

LRMS (APCI) m/z$[M+H]^+$ calc'd for $C_{33}H_{42}O_5$: 519.3, found 487.3 (**14a** - $CH_3O^{\bullet}$)

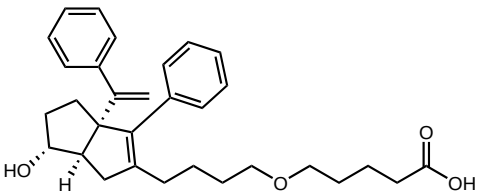

5-(4-((3aR,6aR)-6-hydroxy-3-phenyl-3a-(1-phenylvinyl)-1,3a,4,5,6,6a-hexahydropentalen-2-yl)butoxy)pentanoic acid (**S25**): 70 mg of **S24** was dissolved in 200 mL DCM and then 5 drops of TFA was added. The reaction was stirred at room temp until complete by TLC and HPLC. The reaction was then concentrated and purified by silica chromatography (30-100% EtOAc/Hexanes w/ 1% AcOH). 27 mg, 42%

^{1}H NMR: ^{1}H NMR (600 MHz, Chloroform-*d*) δ 7.35 – 7.28 (m, 5H), 7.24 – 7.18 (m, 5H), 5.06 (d, *J* = 1.3 Hz, 1H), 5.00 (d, *J* = 1.4 Hz, 1H), 3.95 (s, 1H), 3.39 (t, *J* = 6.2 Hz, 2H), 3.34 (t, *J* = 6.3 Hz, 2H), 2.39 (t, *J* = 7.3 Hz, 2H), 2.34 – 2.28 (m, 1H), 2.12 – 1.98 (m, 4H), 1.77 – 1.57 (m, 11H), 1.52 – 1.45 (m, 1H), 1.42 (q, *J* = 7.6, 7.2 Hz, 1H).

^{13}C NMR (151 MHz, $CDCl_3$) δ 154.57, 144.10, 140.82, 139.51, 137.32, 129.68, 127.80, 127.74, 127.70, 126.69, 126.68, 114.99, 82.03, 70.54, 70.28, 69.30, 55.79, 40.09, 33.99, 33.71, 32.06, 29.72, 29.65, 29.44, 28.99, 24.47, 21.67.

LRMS (APCI) m/z$[M+H]^+$ calc'd for $C_{31}H_{38}O_4$: 475.3, found 475.3

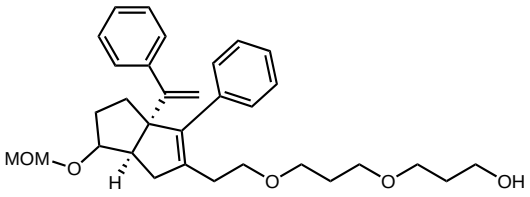

3-(3-(2-((3aR,6aR)-6-(methoxymethoxy)-3-phenyl-3a-(1-phenylvinyl)-1,3a,4,5,6,6a-hexahydropentalen-2-yl)ethoxy)propoxy)propan-1-ol (**S26**): According to the general cyclization procedure, **S22** (2.50 g, 4.4 mmol) was reacted with enyne (1.20 g, 4 mmol) before being treated with 5 equivalents of tetrabutylammonium fluoride to give the title compound (1.24 g, 7:1 dr, 61% yield over 2 steps) as a yellow oil after purification by flash chromatography (0-50% EtOAc/Hex eluent).

^{1}H NMR: ^{1}H NMR (600 MHz, Chloroform-*d*) δ 7.32 (ddq, *J* = 6.0, 2.3, 1.3 Hz, 2H), 7.28 – 7.25 (m, 2H), 7.26 – 7.19 (m, 6H), 5.03 (q, *J* = 1.3 Hz, 1H), 4.98 (dd, *J* = 2.0, 1.3 Hz, 1H), 4.58 – 4.53 (m, 2H), 3.76 – 3.75 (m, 1H), 3.58 – 3.54 (m, 2H), 3.48 – 3.44 (m, 2H), 3.42 – 3.35 (m, 4H), 3.27 (d, *J* = 2.0 Hz, 3H), 2.40 (ddt, *J* = 11.0, 7.1, 1.7 Hz, 2H), 2.36 – 2.25 (m, 3H), 2.07 (d, *J* = 16.9 Hz, 1H), 1.78 (dddt, *J* = 7.8, 5.9, 3.4, 1.8 Hz, 5H), 1.67 – 1.58 (m, 2H).

LRMS (APCI) m/z[M+H]$^+$ calc'd for $C_{32}H_{42}O_5$: 507.3, found 475.3 (**S26** - $CH_3O^{\bullet}$)

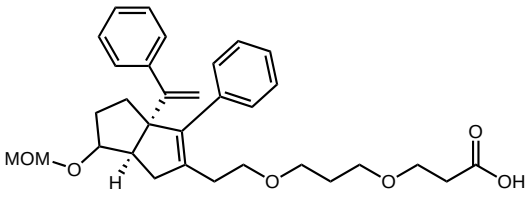

3-(3-(2-((3aR,6aR)-6-(methoxymethoxy)-3-phenyl-3a-(1-phenylvinyl)-1,3a,4,5,6,6a-hexahydropentalen-2-yl)ethoxy)propoxy)propanoic acid (**S27**): A solution of **S26** (504 mg, 1 eq) in 50 mL acetonitrile was treated with tetrapropylammonium perruthenate (TPAP, 0.1 equiv, 17.55 mg), N-Methylmorpholine-N-Oxide (NMO, 10 equiv, 1.17 g), and water (10 equiv, 180 microliters). The reaction mixture was allowed to stir overnight at room temperature. The reaction mixture was passed through celite, concentrated and purified on silica (20-80% EtOAc (containing 0.1% AcOH)/hexanes eluent) to provide the title compound. (285 mg, 45%).

^{1}H NMR (600 MHz, Chloroform-*d*) δ 7.35 – 7.30 (m, 2H), 7.29 – 7.25 (m, 2H), 7.24 – 7.20 (m, 6H), 5.03 (d, *J* = 1.4 Hz, 1H), 4.98 (d, *J* = 1.4 Hz, 1H), 4.61 – 4.55 (m, 2H), 3.80 – 3.74 (m, 1H), 3.67 – 3.63 (m, 2H), 3.52 – 3.46 (m, 2H), 3.42 – 3.34 (m, 5H), 3.29 (t, *J* = 1.0 Hz, 2H), 2.57 (td, *J* = 6.2, 1.4 Hz, 2H), 2.39 (dt, *J* = 9.3, 1.6 Hz, 1H), 2.35 – 2.29 (m, 2H), 2.26 (dt, *J* = 13.8, 6.5 Hz, 1H), 2.11 – 2.08 (m, 1H), 2.08 – 2.04 (m, 2H), 2.01 – 1.96 (m, 1H), 1.78 (pd, *J* = 6.4, 1.6 Hz, 2H), 1.74 – 1.67 (m, 1H), 1.67 – 1.58 (m, 2H).

LRMS (APCI) m/z calc'd for $C_{32}H_{40}O_6$: 521.3, found 489.3 (**S27** - $CH_3O^{\bullet}$)

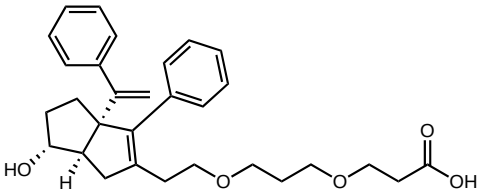

3-(3-(2-((3aR,6aR)-6-hydroxy-3-phenyl-3a-(1-phenylvinyl)-1,3a,4,5,6,6a-hexahydropentalen-2-yl)ethoxy)propoxy)propanoic acid (**DE 10CA**): 125 mg of **S27** was dissolved in 10 mL acetonitrile and 5 drops of 12M HCl. Reaction stirred for 10 minutes, then concentrated and purified by prep HPLC (15-75% ACN in water, 0.1% formic acid modifier, 30 minute gradient). 97 mg, 85%

^{1}H NMR (600 MHz, Chloroform-*d*) δ 7.37 (dd, *J* = 6.6, 2.9 Hz, 2H), 7.32 (t, *J* = 7.3 Hz, 2H), 7.28 (d, *J* = 7.8 Hz, 6H), 5.09 (s, 1H), 5.03 (s, 1H), 4.01 – 3.93 (m, 1H), 3.70 (t, *J* = 6.2 Hz, 2H), 3.54 (t, *J* = 6.3 Hz, 2H), 3.44 (qd, *J* = 9.2, 4.6 Hz, 4H), 2.61 (t, *J* = 6.1 Hz, 2H), 2.42 – 2.33 (m, 2H), 2.31 (dd, *J* = 12.6, 6.9 Hz, 2H), 2.14 (d, *J* = 17.2 Hz, 1H), 1.83 (p, *J* = 6.3 Hz, 2H), 1.74 (tt, *J* = 10.9, 5.5 Hz, 1H), 1.49 (pd, *J* = 7.1, 3.4 Hz, 1H), 1.43 (q, *J* = 7.7, 6.6 Hz, 1H), 1.36 (p, *J* = 3.5 Hz, 1H).

LRMS (APCI) m/z$[M+H]^+$ calc'd for $C_{30}H_{36}O_5$: 477.3, found 477.3

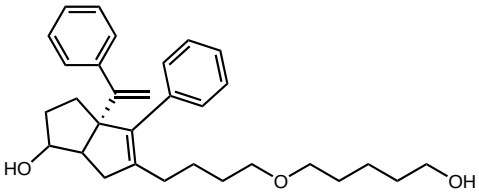

(3a*R*)-5-(4-((5-hydroxypentyl)oxy)butyl)-4-phenyl-3a-(1-phenylvinyl)-1,2,3,3a,6,6a-hexahydropentalen-1-ol (**S28**): According to the general cyclization procedure, **S17** (2.50 g, 4.4

mmol) was reacted with enyne (1.20 g, 4 mmol) before being treated with three drops of HCl to give the title compound (1.21 g, 66% yield over 2 steps) as a yellow oil after purification by flash chromatography (0-65% EtOAc/Hex eluent).

^{1}H NMR (600 MHz, Chloroform-*d*) δ 7.35 – 7.30 (m, 5H), 7.25 (m, 2H), 7.20 (t, *J* = 6.8 Hz, 3H), 5.07 (d, *J* = 1.6 Hz, 1H), 4.99 (dp, *J* = 1.5 Hz, 1H), 3.95 (m, 1H), 3.65 (t, *J* = 6.6 Hz, 3H), 3.38 (t, *J* = 6.4 Hz, 4H), 3.33 (t, *J* = 6.3 Hz, 2H), 2.64 (d, *J* = 17.3 Hz, 1H), 2.47 (t, *J* = 8.7 Hz, 1H), 2.42 – 2.24 (m, 2H), 2.14 – 1.94 (m, 6H), 1.76 – 1.64 (m, 4H), 1.59 (dd, *J* = 10.7, 4.6 Hz, 4H), 1.55 – 1.46 (m, 1H).

LRMS (APCI) m/z[M+H]$^+$ calc'd for $C_{31}H_{41}O_3$: 461.7, found 461.3

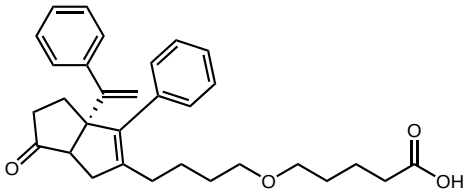

5-(4-((3a*R*)-6-oxo-3-phenyl-3a-(1-phenylvinyl)-1,3a,4,5,6,6a-hexahydropentalen-2-yl)butoxy)pentanoic acid (**S29**): According to the oxidation general procedure, **S28** (1.21 g, 2.63 mmol) was reacted with TPAP (92.4 mg, 0.26 mmol), NMO (3.07 g, 26 mmol), water (473μL, 473 mg, 26 mmol), and acetonitrile (40 mL) to give the title compound (529 mg, 43% yield) as an oil after purification by flash chromatography (0-65% EtOAc/Hex).

^{1}H NMR (600 MHz, $CDCl_3$) δ 7.40 – 7.31 (m, 6H), 7.24 (m, 4H), 5.24 (dt, *J* = 3.8, 1.4 Hz, 1H), 5.13 (q, *J* = 1.6 Hz, 1H), 3.39 (tdd, *J* = 6.2, 3.6, 1.4 Hz, 2H), 3.32 (qd, *J* = 5.1, 1.9 Hz, 2H), 2.52 – 2.48 (m, 1H), 2.40 (tdd, *J* = 7.5, 3.7, 1.5 Hz, 2H), 2.37 – 2.29 (m, 2H), 2.15 – 2.08 (m, 4H), 2.07 – 1.99 (m, 2H), 1.93 (ddd, *J* = 16.5, 8.3, 2.9 Hz, 1H), 1.75 – 1.69 (m, 2H), 1.66 – 1.58 (m, 2H), 1.49 – 1.40 (m, 2H), 1.35 (qd, *J* = 7.9, 4.3 Hz, 2H).

^{13}C NMR (151 MHz, $CDCl_3$) δ 177.36, 153.15, 144.47, 142.49, 137.82, 136.55, 128.98, 128.28, 128.17, 127.65, 127.15, 127.02, 115.36, 70.51, 70.31, 65.48, 55.56, 38.64, 37.52, 33.47, 29.70, 28.91, 28.37, 24.32, 21.69.

LRMS (APCI) m/z$[M+H]^+$ calc'd for $C_{31}H_{37}O_4$: 473.6, found 473.3

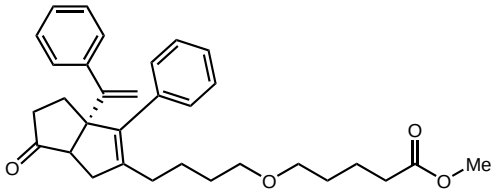

methyl 5-(4-((3a*R*)-6-oxo-3-phenyl-3a-(1-phenylvinyl)-1,3a,4,5,6,6a-hexahydropentalen-2-yl)butoxy)pentanoate (**S30**): According to the methylation general procedure, **S29** (529 mg, 1.1 mmol) was reacted with HCl in methanol to give the title compound (545 mg, quantitative yield) as a yellow oil.

^{1}H NMR (600 MHz, $CDCl_3$) δ 7.40 – 7.36 (m, 2H), 7.33 (tt, *J* = 8.0, 1.4 Hz, 3H), 7.30 – 7.26 (m, 3H), 7.25 – 7.22 (m, 2H), 5.24 (d, *J* = 1.3 Hz, 1H), 5.13 (d, *J* = 1.3 Hz, 1H), 3.68 (s, 3H), 3.37 (t, *J* = 6.4 Hz, 2H), 3.32 – 3.29 (m, 2H), 2.49 (d, *J* = 7.8 Hz, 1H), 2.35 (t, *J* = 7.5 Hz, 3H), 2.33 – 2.27 (m, 1H), 2.17 – 2.08 (m, 4H), 2.05 (dd, *J* = 13.5, 6.4 Hz, 2H), 1.94 (dd, *J* = 16.5, 7.8 Hz, 1H), 1.73 – 1.66 (m, 2H), 1.62 – 1.55 (m, 3H), 1.44 (ddd, *J* = 13.1, 8.2, 5.8 Hz, 2H), 1.38 – 1.30 (m, 2H).

^{13}C NMR (151 MHz, $CDCl_3$) δ 174.05, 153.19, 144.47, 142.51, 137.80, 136.57, 128.99, 128.28, 128.16, 127.65, 127.14, 127.02, 115.35, 70.47, 70.32, 65.47, 55.52, 51.48, 38.71, 37.50, 33.83, 29.76, 29.73, 29.14, 28.39, 24.33, 21.75.

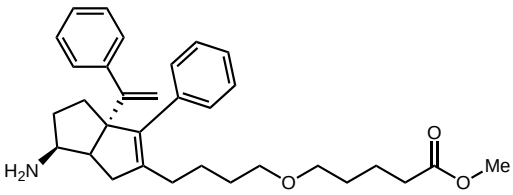

methyl 5-(4-((3a*R*,6*S*)-6-amino-3-phenyl-3a-(1-phenylvinyl)-1,3a,4,5,6,6a-hexahydropentalen-2-yl)butoxy)pentanoate (**S31**): According to the reductive amination general procedure **S30** (545 mg, 1.13 mmol) was reacted with Ammonia (816 μL, 5.65 mmol), Ti(O*i*Pr)$_4$ (517 μL, 1.7 mmol), and $NaBH_4$ (128 mg, 3.4 mmol) in ethanol (11 mL) to give the title compound (235 mg, 42% yield) as a clear oil after purification by flash chromatography (0-10% MeOH/DCM).

^{1}H NMR (600 MHz, $CDCl_3$) δ 7.35 – 7.32 (m, 2H), 7.30 (d, *J* = 7.5 Hz, 2H), 7.27 (dd, *J* = 5.0, 2.0 Hz, 4H), 7.22 – 7.20 (m, 2H), 5.08 (d, *J* = 1.4 Hz, 1H), 4.95 (d, *J* = 1.5 Hz, 1H), 3.68 (s, 3H), 3.39 (t, *J* = 6.4 Hz, 2H), 3.35 (td, *J* = 6.3, 1.6 Hz, 2H), 3.33 – 3.29 (m, 1H), 2.50 (dd, *J* = 17.4, 2.2 Hz, 1H), 2.44 (td, *J* = 8.9, 2.2 Hz, 1H), 2.35 (t, *J* = 7.5 Hz, 2H), 2.16 – 2.00 (m, 4H), 1.85 – 1.79 (m, 1H), 1.70 (qd, *J* = 7.1, 5.0 Hz, 4H), 1.60 (dq, *J* = 9.8, 6.5 Hz, 2H), 1.55 – 1.45 (m, 6H).

^{13}C NMR (151 MHz, $CDCl_3$) δ 174.07, 155.05, 144.20, 142.49, 139.84, 137.08, 129.78, 127.75, 127.69, 127.62, 126.65, 126.58, 115.08, 70.56, 70.32, 69.52, 55.31, 51.49, 49.07, 34.48, 34.02, 33.83, 33.22, 29.81, 29.61, 29.15, 24.58, 21.78.

LRMS (APCI) m/z$[M+H]^+$ calc'd for $C_{32}H_{42}NO_3$: 488.7, found 488.3

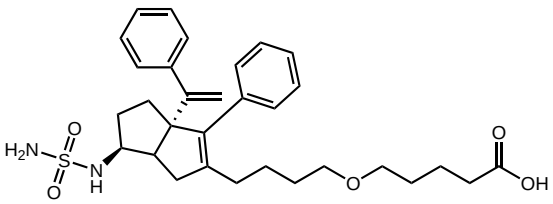

5-(4-((3a*R*,6*S*)-3-phenyl-3a-(1-phenylvinyl)-6-(sulfamoylamino)-1,3a,4,5,6,6a-hexahydropentalen-2-yl)butoxy)pentanoic acid (**ME 6N-10CA**): **S31** was added to a reaction vial in EtOH (0.1M). H_2O (0.05 M) was added followed by sulfamide (5 equiv) and triethylamine (3 equiv). The reaction proceeded for 16 hours at reflux before being cooled to room temperature. The reaction mixture was concentrated via rotatory evaporation. The crude mixture was then purified via flash chromatography (10-20% MeOH/DCM) to give the title compound as a yellow oil.

^{1}H NMR (600 MHz, $CDCl_3$) δ 7.35 – 7.31 (m, 3H), 7.32 – 7.29 (m, 2H), 7.28 (d, *J* = 5.8 Hz, 3H), 7.20 – 7.17 (m, 2H), 5.71 – 5.66 (m, 1H), 5.13 (d, *J* = 1.2 Hz, 1H), 4.92 (d, *J* = 1.2 Hz, 1H), 4.76 – 4.66 (br. s, 2H), 3.81 (m, 1H), 3.52 – 3.40 (m, 4H), 2.66 (td, *J* = 9.1, 2.4 Hz, 1H), 2.49 (dd, *J* = 17.7, 2.4 Hz, 1H), 2.42 (td, *J* = 7.5, 1.3 Hz, 2H), 2.21 – 2.14 (m, 5H), 2.00 (dt, *J* = 9.8, 5.3 Hz, 2H), 1.84 (dq, *J* = 14.7, 7.3 Hz, 1H), 1.80 – 1.69 (m, 3H), 1.68 – 1.62 (m, 2H), 1.60 – 1.50 (m, 3H).

^{13}C NMR (151 MHz, $CDCl_3$) δ 177.19, 154.33, 143.88, 142.75, 139.44, 136.68, 129.85, 127.90, 127.69, 127.58, 126.88, 126.78, 115.76, 70.03, 69.58, 68.72, 57.06, 47.05, 35.37, 33.03, 32.77, 31.28, 30.94, 29.81, 29.71, 28.51, 24.93, 21.71.

LRMS (APCI) m/z$[M+H]^+$ calc'd for $C_{31}H_{41}N_2O_5S$: 553.7, found 553.3

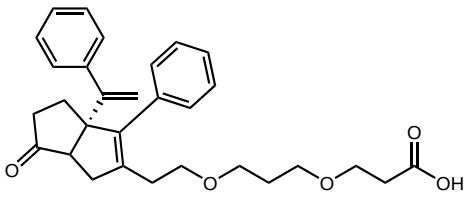

3-(3-(2-((3a*R*)-6-oxo-3-phenyl-3a-(1-phenylvinyl)-1,3a,4,5,6,6a-hexahydropentalen-2-yl)ethoxy)propoxy)propanoic acid (**S32**): According to the methylation general procedure, **S31**

(403.4 mg, 0.85mmol) was reacted with HCl in methanol to give the title compound (299 mg, 70% yield) as a yellow oil after purification by flash chromatography (30% EtOAc/Hex).

^{1}H NMR (600 MHz, $CDCl_3$) δ 7.38 (d, *J* = 4.4 Hz, 4H), 7.36 – 7.31 (m, 1H), 7.31 – 7.28 (m, 3H), 7.25 (dd, *J* = 7.5, 1.9 Hz, 2H), 5.27 (s, 1H), 5.15 (s, 1H), 3.72 (t, *J* = 6.1 Hz, 2H), 3.52 (q, *J* = 5.9 Hz, 2H), 3.45 – 3.32 (m, 4H), 2.62 (t, *J* = 6.1 Hz, 2H), 2.50 (d, *J* = 7.8 Hz, 1H), 2.43 (dd, *J* = 14.2, 7.1 Hz, 1H), 2.39 (d, *J* = 16.6 Hz, 1H), 2.29 (ddt, *J* = 20.5, 13.4, 6.9 Hz, 2H), 2.19 – 2.08 (m, 2H), 2.08 – 2.01 (m, 1H), 1.97 (dd, *J* = 16.6, 7.8 Hz, 1H), 1.85 – 1.75 (m, 2H).

^{13}C NMR (151 MHz, $CDCl_3$) δ 174.03, 152.96, 142.48, 141.53, 139.42, 136.31, 129.07, 128.26, 128.17, 127.67, 127.25, 127.05, 115.51, 68.76, 68.21, 67.57, 65.46, 55.67, 38.89, 37.55, 34.70, 30.31, 29.92, 28.37.

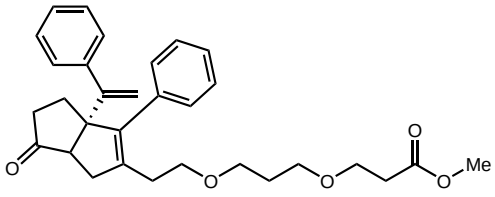

methyl 3-(3-(2-((3a*R*)-6-oxo-3-phenyl-3a-(1-phenylvinyl)-1,3a,4,5,6,6a-hexahydropentalen-2-yl)ethoxy)propoxy)propanoate (**S33**): According to the methylation general procedure, **S32** (403.4 mg, 0.85mmol) was reacted with HCl in methanol to give the title compound (299 mg, 70% yield) as a yellow oil after purification by flash chromatography (30% EtOAc/Hex).

^{1}H NMR (600 MHz, $CDCl_3$) δ 7.38 (d, *J* = 4.3 Hz, 4H), 7.34 (h, *J* = 4.4 Hz, 1H), 7.31 – 7.28 (m, 3H), 7.25 (dd, *J* = 7.6, 2.0 Hz, 2H), 5.27 (s, 1H), 5.15 (s, 1H), 3.70 (m, 4H), 3.48 (tt, *J* = 6.5, 3.2 Hz, 2H), 3.48 (dtt, *J* = 7.5, 3.1, 1.4 Hz) 1H), 3.37 (dddd, *J* = 31.9, 16.1, 9.2, 6.7 Hz, 4H), 2.58 (t,

J = 6.4 Hz, 2H), 2.48 (d, *J* = 7.8 Hz, 1H), 2.44 – 2.35 (m, 2H), 2.30 (dq, *J* = 13.6, 6.8 Hz, 2H), 2.17 – 2.01 (m, 3H), 1.98 (dd, *J* = 16.5, 7.9 Hz, 1H), 1.78 (p, *J* = 6.4 Hz, 2H).

^{13}C NMR (151 MHz, $CDCl_3$) δ 172.10, 152.99, 142.52, 141.34, 139.50, 136.32, 129.07, 128.26, 128.15, 127.66, 127.23, 127.03, 115.50, 68.56, 68.01, 67.69, 66.12, 65.46, 55.59, 51.65, 50.92, 38.86, 37.51, 34.93, 30.40, 29.97, 28.40.

LRMS (APCI) m/z$[M+H]^+$ calc'd for $C_{31}H_{37}O_5$: 489.6, found 489.3

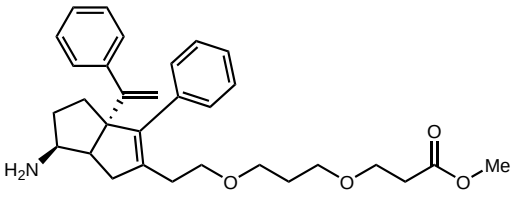

methyl 3-(3-(2-((3a*R*,6*S*)-6-amino-3-phenyl-3a-(1-phenylvinyl)-1,3a,4,5,6,6a-hexahydropentalen-2-yl)ethoxy)propoxy)propanoate (**S34**): According to the reductive amination general procedure **S33** (299.1 mg, 0.6 mmol) was reacted with Ammonia (1.7 mL, 12.2 mmol), Ti(O*i*Pr)$_4$ (272 μL, 261.4 mg, 0.92 mmol), and $NaBH_4$ (68.1 mg, 1.8 mmol) in ethanol (6 mL) to give the title compound (210.8 mg, 67% yield) as an orange oil after purification by flash chromatography (0-10% Methanol/DCM).

^{1}H NMR (600 MHz, Chloroform-*d*) δ 7.53 – 7.36 (m, 2H), 7.31 (dd, *J* = 8.3, 6.5 Hz, 3H), 7.29 – 7.25 (m, 3H), 7.19 (dq, *J* = 5.3, 2.9, 2.5 Hz, 2H), 5.18 (d, *J* = 1.5 Hz, 1H), 5.07 (d, *J* = 1.6 Hz, 1H), 3.93 – 3.86 (m, 1H), 3.75 – 3.66 (m, 3H), 3.65 (s, 3H), 3.60 – 3.51 (m, 3H), 3.48 (ddd, *J* = 9.2, 5.6, 3.2 Hz, 1H), 2.89 – 2.75 (m, 1H), 2.70 (dd, *J* = 9.7, 6.7 Hz, 1H), 2.66 – 2.58 (m, 2H), 2.54 (ddd, *J* = 16.2, 6.8, 4.4 Hz, 2H), 2.24 – 2.16 (m, 1H), 2.00 – 1.94 (m, 3H), 1.93 – 1.79 (m, 2H), 1.73 (dq, *J* = 15.9, 6.0 Hz, 2H), 1.49 – 1.38 (m, 1H).

^{13}C NMR (151 MHz, $CDCl_3$) δ 172.18, 143.78, 141.27, 139.69, 136.61, 129.70, 127.84, 127.70, 126.76, 115.24, 69.44, 68.83, 67.98, 67.66, 66.10, 51.68, 50.87, 34.91, 34.18, 32.69, 29.98, 29.93. **LRMS** (APCI) m/z$[M+H]^+$ calc'd for $C_{31}H_{40}NO_4$: 490.6, found 490.3

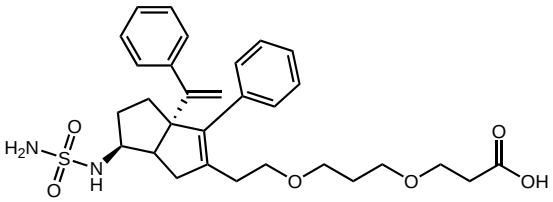

3-(3-(2-((3a*R*,6*S*)-3-phenyl-3a-(1-phenylvinyl)-6-(sulfamoylamino)-1,3a,4,5,6,6a-hexahydropentalen-2-yl)ethoxy)propoxy)propanoic acid (**DE 6N-10CA**): **S34** (26.3 mg, 0.05 mmol, 1.0 equiv) was added to a reaction vial in EtOH (500 μL). H_2O (1.0 mL) was added followed by sulfamide (24 mg, 0.25 mmol, 5 equiv) and triethylamine (21 μL, 0.15 mmol, 3 equiv). The reaction proceeded for 16 hours at reflux before being cooled to room temperature. The reaction mixture was concentrated via rotatory evaporation. The crude mixture was then purified via flash chromatography (10-20% MeOH/DCM) to give the title compound (19.9 mg, 70% yield) as a yellow oil.

^{1}H NMR (600 MHz, $CDCl_3$) δ 7.41 – 7.39 (m, 2H), 7.33 (t, *J* = 7.2 Hz, 2H), 7.28 (t, *J* = 1.0 Hz, 8H), 5.45 (d, *J* = 9.0 Hz, 1H), 5.11 (d, *J* = 1.4 Hz, 1H), 5.09 (d, *J* = 1.6 Hz, 1H), 4.76 (br. s, 2H), 3.87 (t, *J* = 8.7 Hz, 1H), 3.77 – 3.72 (m, 2H), 3.69 (td, *J* = 9.6, 5.3 Hz, 1H), 3.64 (dt, *J* = 9.7, 6.3 Hz, 2H), 3.58 (dt, *J* = 10.5, 6.3 Hz, 1H), 3.53 (td, *J* = 9.6, 4.9 Hz, 2H), 2.63 (dddd, *J* = 30.5, 17.3, 9.8, 6.6 Hz, 4H), 2.53 (d, *J* = 17.2 Hz, 1H), 2.05 (tt, *J* = 12.4, 4.9 Hz, 2H), 1.96 – 1.84 (m, 3H), 1.42 – 1.36 (m, 2H).

^{13}C NMR (151 MHz, $CDCl_3$) δ 175.22, 175.12, 153.75, 143.31, 140.71, 140.25, 136.41, 129.47, 128.02, 127.81, 127.68, 126.87, 126.83, 115.11, 68.76, 68.69, 67.69, 67.57, 65.84, 56.69, 34.78, 34.60, 32.69, 31.45, 29.78, 29.73, 20.40.

LRMS (APCI) m/z$[M+H]^+$ calc'd for $C_{30}H_{39}N_2O_6S$: 555.7, found 555.3

Chapter 3: Degradation of Liver Receptor Homolog-1 Nuclear Receptor via Proteolysis Targeting Chimeras (PROTACs)

3.1 Introduction

Due to nuclear receptor's (NR) role in the production of transcriptional genes there is a great desire to be able to regulate their output. While in many cases the transcriptional genes are controlled and used in cellular regulation, in some cases such as cancer, the regulatory pathways malfunction resulting in proliferation and metathesis of tumors.[17,19,28] Therefore, there is a great desire to be able to be able to manipulate NRs via small molecule ligands.

Liver receptor homolog-1 (LRH-1) has previously been shown to be upregulated in certain cancer models, including breast and pancreatic.[17,28] Particularly in breast cancer, LRH-1 has been linked to a positive feedback loop with estrogen receptor α (ERα). This loop leads to the increase in transcriptional genes such as GREB1 and CYP7A1 that are associated with the proliferation of tumors.[28] Within this model there would be a great benefit to decreasing the gene products resulting from LRH-1 transcriptional activity. While some antagonists show utility in *in vitro* models, their specific mechanism of action for downregulation unknown.[42] We desired to make a modulator designed with a known mechanism to show LRH-1's role in cancer models.

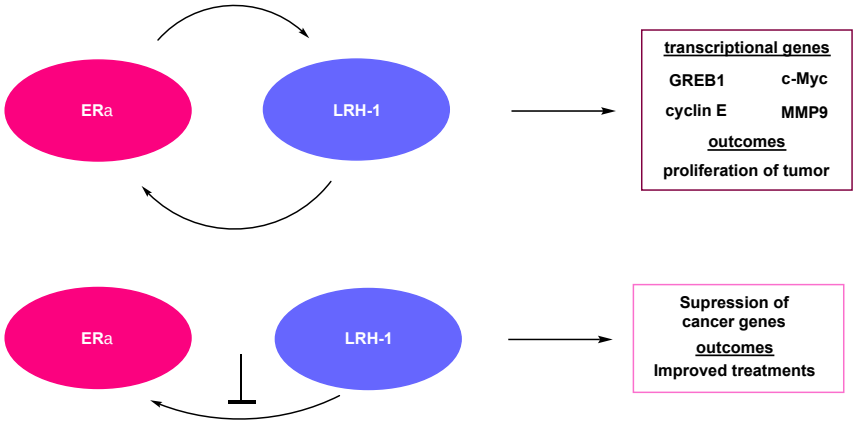

Figure 3.1: LRH-1's role in cancer

While creating an antagonist for LRH-1 is a specifically challenging due in part to the hydrophobic binding pocket, we started to investigate the use of chemical probes for degradation. In 2001 Craig Crews, Kathleen Sakamoto, and Ray Deshaies showed *in vitro* degradation of a protein of interest (POI) by linking a small molecule binder of their POI to an Ubiquitin ligase (E3

ligase) ligand.[63] Via this bivalent molecule, the POI is brought into close proximity to an E3 ligase. E3 ligases are unique in cellular processes due to their ability to catalyze ubiquitin transfer of proteins. Similar to how NRs recruit other machinery to generate transcription, E3 ligases recruit other machinery for ubiquinylation. E3 ligases recruit E2 ligases, which are primed with ubiquitin from E1 ligases. The formed E2/E3 ligase complex transfers ubiquitin onto lysine residues of the POI. Upon disassociation of the complex, the POI is now primed for degradation by the proteosome (Figure 3.2).[64–66] This method is deemed proteolysis targeting chimeras

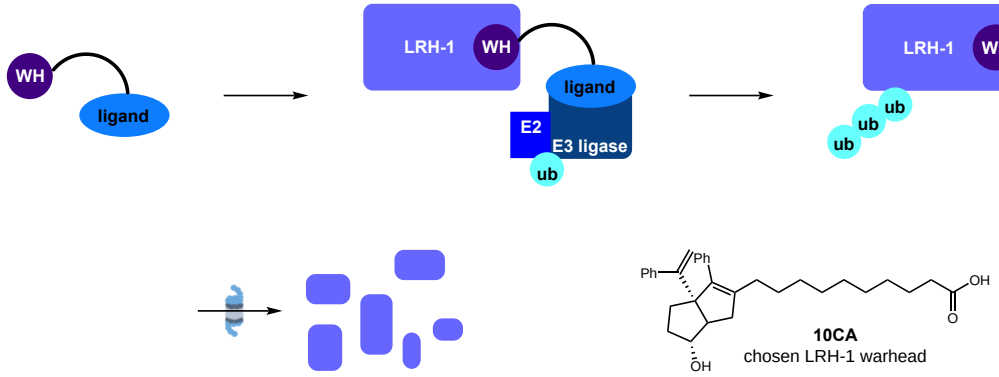

Figure 3.2: Mechanism of action of PROTACs with proposed LRH-1 warhead

(PROTACs).[63] With the ability to make selective binders to proteins this gives us the ability to selectively degrade a POI.[67] While other methods can knockdown levels of LRH-1, PROTACs gives us a unique handle to specifically degrade LRH-1 via small molecule binding.

From previous studies there are two main E3 ligases utilized in PROTACs.[64,68] The first is CRBN bound by thalidomide and its derivatives. The other E3 ligase Von Hippel-Lindau (VHL) binds (S,R,S)-AHPC-Me. Both of these receptors are found within the nucleus and cytoplasm of cells. We designed our PROTACs to connect from the primary

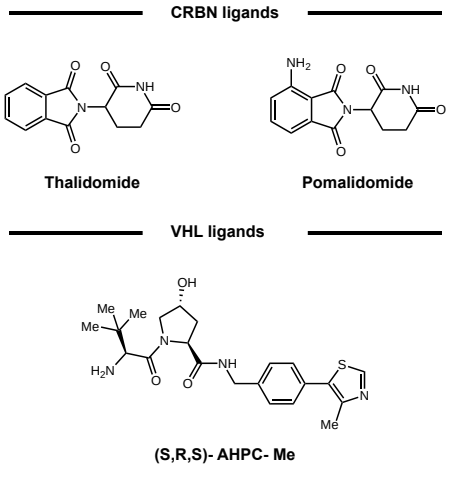

Scheme 3.1: Ligands for E3 ligase CRBN and VHL

amines within the ligand, which are unessential for protein binding. When looking at the warheads available for LRH-1, we proposed to use a modulator containing the ten-carbon carboxylic acid as a linking point to the warhead. Due to the carboxylic acid being at the mouth of the pocket, from previous studies, we proposed short to medium linkers would be suitable for ubiquitin transfer.

3.2 Results and discussion

Linkers have been shown to be very important in PROTAC systems. While a linker that is too short may not be amenable to the formation of the tertiary complex, a linker too long in length would create a flimsy complex. Therefore, linker length is an important aspect to making these bivalent molecules.[69] With this in mind, we synthesized a library of PROTACs differing in linker length.

The library of LRH-1 PROTACs synthesized contained thalidomide as the E3 ligase ligand. We specifically chose the thalidomide derivative, pomalidomide, due to the aniline that could be used as a handle to add a linker. The ligand was synthesized via an intramolecular cyclization of (*tert*-butoxycarbonyl)glutamine to form the glutaramide ring. The ring formation was followed by the insertion into fluorophthalic anhydride. The fluorine was primed to undergo

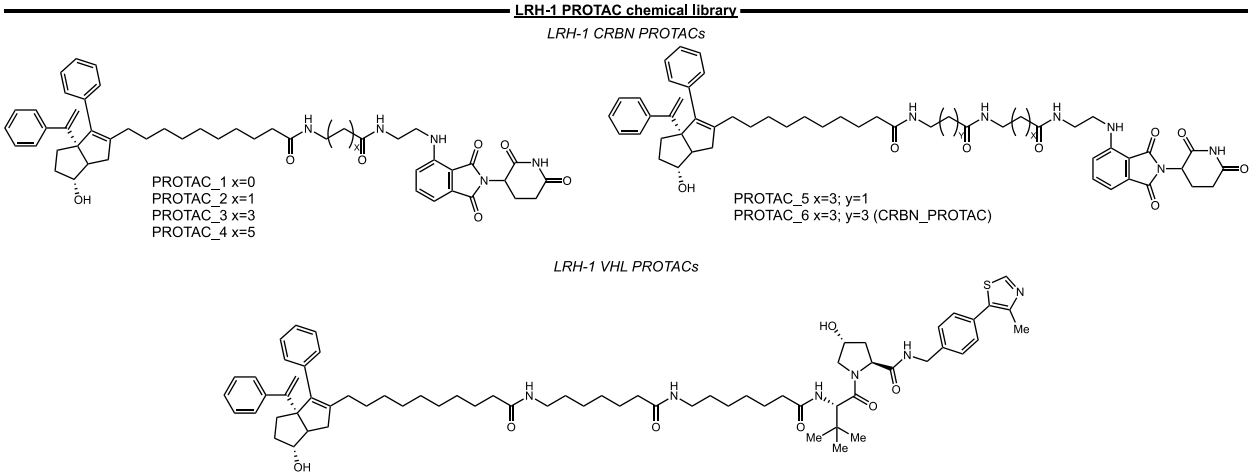

Scheme 3.2: PROTAC library of CRBN and VHL E3 ligase ligands

a microwave assisted S_NAR with ethane-1,2-diamine to yield the E3 ligase ligand, pomalidomide. The resulting primary amine was used to link to the chosen warhead for LRH-1 10CA. We also synthesized a single VHL PROTAC for comparison of the two E3 ligases.

One of the most important aspects of a PROTAC is binding to the POI. Due to the added linkage to create the bivalent compounds, we first verified the binding of the library to LRH-1. Via a fluorescence polarization (FP)[50] assay the inhibition constant (K_i) of the compounds ranged from 3.1 to 0.31 μM, compared to the unattached warhead 10CA at 5.3 nM. Although affinity for LRH-1 was lost, we still have the required binding to LRH-1.

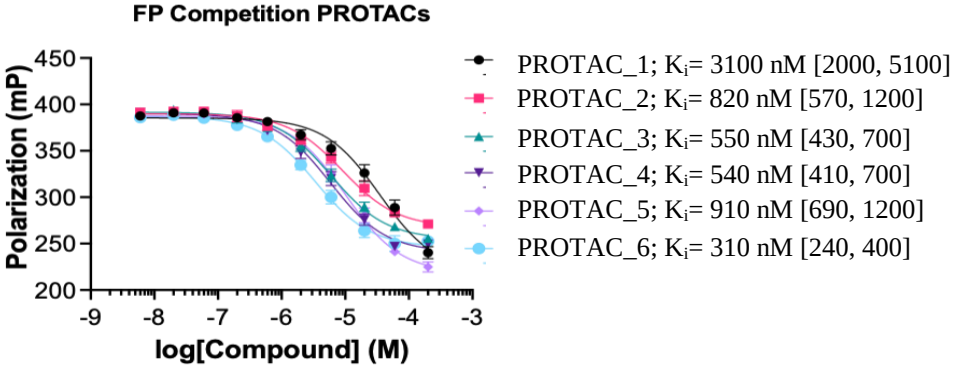

Figure 3.3: Binding affinty of CRBN PROTAC library

FP competition assay showing binding of compounds to the LRH-1 LBD (K_i: inhibition constant). Data shown as mean +/- from two independent experiments. Error bars represent 95% confidence intervals.

In order to check the efficacy of these molecules, we then looked at the levels of messenger RNA (mRNA) of highly regulated gene products of LRH-1 via quantitative PCR (qPCR). Where the shortest linker seemed to have no effect on gene expression, all other linkers decrease the transcription of both SHP and CYP7A1 (Figure 3.4). The linker with the largest change is PROTAC_2, but the most stable downregulation PROTAC_3. Through controls of both an agonist (6N-10CA) and unlinked pomalidomide (negative control), it supports that you need both the LRH-1 ligand and the CRBN ligand (pomalidomide) linked as a bivalent compound downregulation in gene expression. Notably at higher concentrations of PROTACs mRNA levels increase. We propose this phenomenon comes from the “hook effect” where the bivalent

compound is bound to either LRH-1 or CRBN, but not both at the same time due to the higher concentrations.[65]

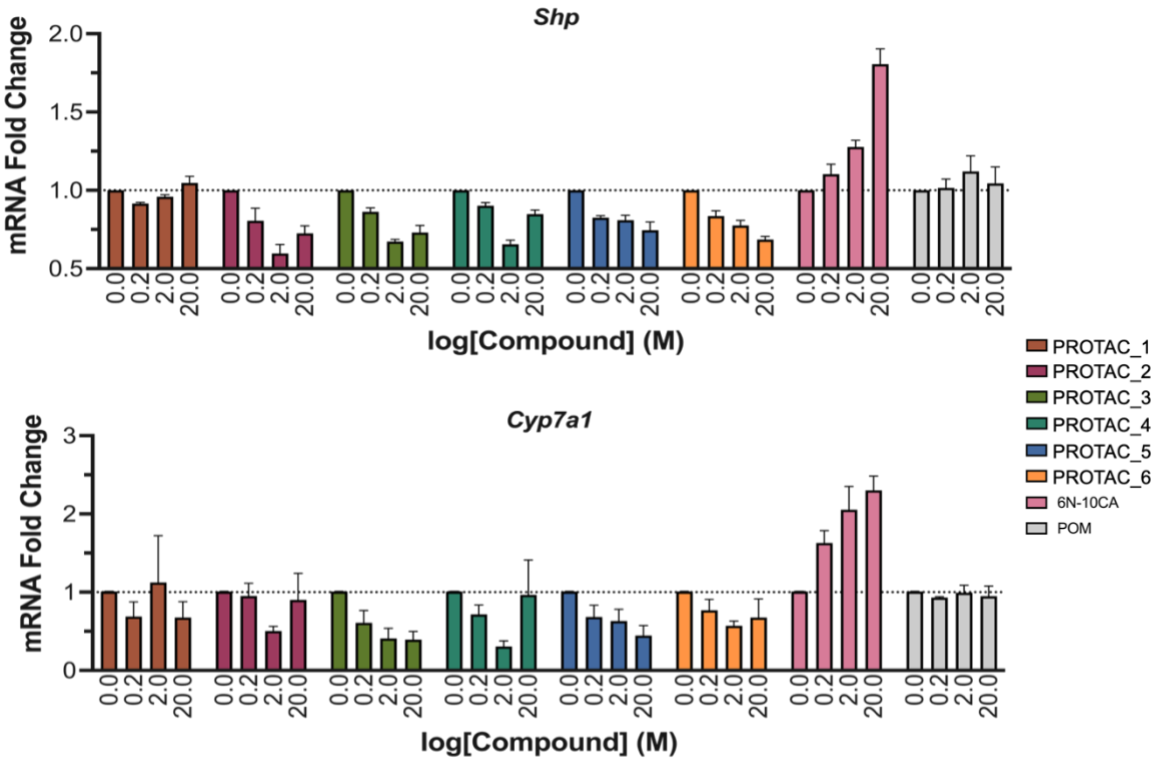

Figure 3.4: Downstream gene expression of LRH-1 from CRBN PROTACs

RT-qPCR analysis of HepG2 cells treated with CRBN PROTACs (PROTACs 1-6 at 0.2-20 μM) for 24 hrs. Data normalized to signal of DMSO control and shown as mean +/- SEM from four biological replicates

To verify the mechanism of action we sought to show degradation of LRH-1 *in vitro*. We first tested degradation via Western blot. Initially looking at both the VHL PROTAC and CRBN PROTAC (PROTAC_6) at a single time point (24 hrs) from the nuclear extract of the cells, we see complete loss of LRH-1 in both PROTACs versus the DMSO control (Figure 3.5). This excitingly supported our mechanism of action. Although in this one replicate we were able to see the loss of LRH-1, in further replicates the data was inconsistent. Therefore, we started to look at other methods in order to help support our mechanism of action. The

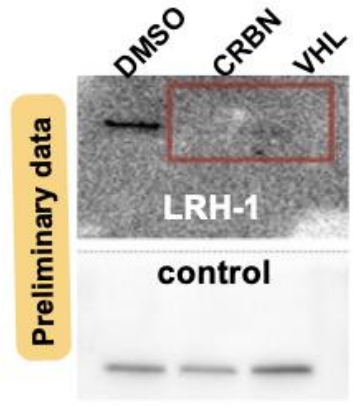

Figure 3.5: Western blot for LRH-1 with PROTACs of both VHL and CRBN PROTACs

first area that we looked was the Venus degradation assay, an *in vitro* assay that links the POI to a fluorescent probe. Once the protein is degraded the complex would no longer emit fluorescence. Unfortunately, from this assay, we don't observe the loss of fluorescence (Figure S1). Although this is contradictory to the western blot results, in this assay we have to overexpress LRH-1, causing an influx of protein. Therefore, if any LRH-1 was degraded in small amounts we may not be able to observe it. Further studies are now underway to optimize the western blot, as well as looking into more whole cells assays to show loss of protein, such as proteomics.

Finally, we wanted to look at a model that represented our disease target. In this study we looked at the mRNA levels of genes that are proliferatory of tumors, within a breast cancer cell line (Figure 3.6). Through this we see a decrease of gene expression for all tested PROTACs, even

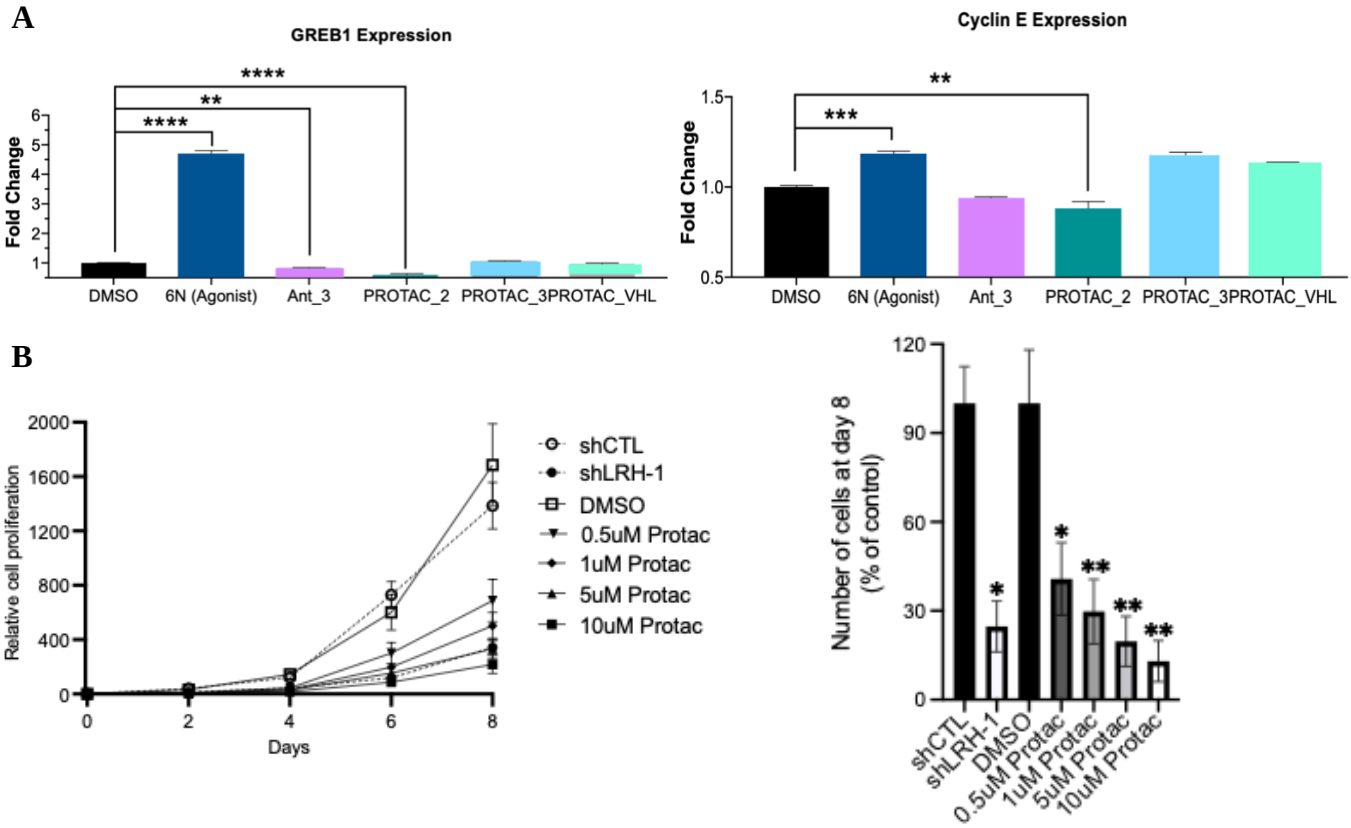

Figure 3.6: PROTAC utility in cancer models

(A) RT-qPCR analysis of HepG2 cells treated with CRBN PROTACs (PROTACs 1-6 at 10 μM) for 24 hrs. Data normalized to signal of DMSO control and shown as mean +/- SEM from four biological replicates. (B) cell proliferation assay in MCF7 cells for 8 days at concentrations ranging from 0.5-10 μM from three biological replicates.

showing a greater decrease than a synthetic LRH-1 antagonist (Ant_3). In seeing this effect we hoped to also see the same phenotypic response. The Gévry lab tested cell proliferation with the current leading CRBN PROTAC (PROTAC_3). In a breast cancer cell line they were able to see that the rate of proliferation of MCF-7 cells drastically decreased, reaching the same levels as an LRH-1 knockout model at 5 μM over an eight day period.

3.3 Conclusion/Future studies

Through these studies we have been able to successfully downregulate LRH-1 gene expression via a bivalent molecule linking LRH-1 to an E3 ligase. While preliminary studies show the loss of LRH-1 via western blot, we are continuing with more replicates to confirm the initial results. This model shows promise in breast cancer cell lines, with the downregulation of tumor proliferating genes, as well as showing decreased proliferation in the presence of PROTACs for up to 72 hrs. In future studies we hope to show the promise of LRH-1 as a target for cancer therapeutics.

3.4 Supplemental Information

Supporting figures

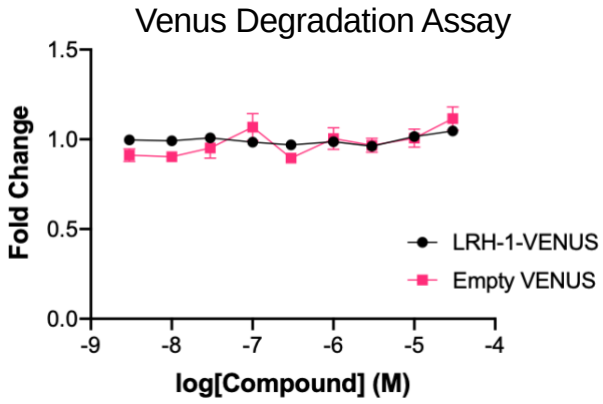

Figure 3.S1: Venus degradation assay with PROTAC_6

Biological information

Cell Culture. HeLa cells were cultured under standard conditions (5% CO_2, 37°C) in phenol red-free MEMα + 10% fetal bovine serum (FBS) – charcoal/dextran treated and were verified to be mycoplasma free with the LookOut® Mycoplasma PCR Detection Kit.

Protein purification. LRH-1 LBD was expressed and purified as described previously Briefly, BL21(DE3) *E. coli* cells were transformed with human LRH-1 LBD (residues 299-541) with an N-terminal 6xHis tag in a pMCSG7 vector. Cells were grown at 37°C in liquid broth until OD_{600} 0.6. Protein expression was induced with 1 mM IPTG for 4 hours at 30°C. Cells were centrifuged and stored at -80°C. The cell pellet was resuspended in lysis buffer (20 mM Tris-HCl, 150 mM NaCl, 5% glycerol, 25 mM imidazole, 0.2 mM phenylmethylsulfonyl fluoride, DNase, lysozyme, pH 7.4) and lysed via sonication. Protein was isolated with Ni^{2+} affinity chromatography. Human LRH-1 LBD purifies bound to bacterial phospholipids when expressed in *E. coli* We removed co-purified bacterial lipids for LRH-1 LBD used in FP competition assays by incubating the protein

with four-fold molar excess of DLPC overnight at 4°C. LBD was then purified with size-exclusion chromatography (SEC) into assay buffer (150 mM NaCl, 20 mM Tris-HCl, 5 % glycerol, pH 7.4). LRH-1 LBD used for thermal stability assays was purified in a similar manner but was not complexed with DLPC prior to SEC purification. All protein was stored at -80°C until use.

Fluorescence Polarization. FP assays were performed as described previously. Briefly, experiments were conducted in black, polystyrene, non-binding surface 384-well plates (Corning Inc., Corning, NY) with 30 mL volumes in assay buffer (150 mM NaCl, 20 mM Tris-HCl, 5% glycerol, pH 7.4). Binding affinity for 6N-FAM was determined using 10 nM 6N-FAM and protein concentrations ranging from 1^{-10} - 5^{-5} M. Plates were incubated overnight at 4 °C and centrifuged at 2,000 x *g* for 2 minutes before polarization measurement. Polarization was monitored on a Neo plate reader (Biotek, Winooski, VT) at an excitation/emission wavelength of 485/528 nm. Plates were incubated overnight at 4 °C and centrifuged at 2,000 x *g* for 2 minutes before polarization measurement. Nine technical replicates were conducted over three experiments and compiled binding data were baseline-corrected to wells with no protein and fit with a one-site binding curve in GraphPad Prism version 7 (GraphPad, Inc., La Jolla, CA). 6N conjugated to fluorescein amidite (FAM) (10 nM/well – 0.8 times the affinity of SF-1 for 6N-FAM) was incubated with SF-1 LBD (25 nM/well – 60% of the forward binding B_{max}). Unlabeled compounds were added at concentrations indicated in figures with DMSO in each well held constant at 6.7% v/v. Each experiment was performed two or three times with four technical replicates each. Technical replicates were averaged and normalized independently prior to final data analysis. Using GraphPad Prism (version 9), data were fit to a one-site, fit K_i curve, assuming a final probe concentration of 10 nM and probe affinity determined with forward binding assays.

RT-qPCR. RT-qPCR was performed as described previously. HepG2 cells were seeded at 400,000 cells per well in 24-well plates in DMEM + 10% FBS. When cells reached ~ 90% confluence, media was exchanged with media containing DMSO or compound at the desired concentration (final DMSO concentration: 0.3%). Small molecules were added concentrations indicated in figure legends. After 24 hours, media was decanted, cells were washed with phosphate buffered saline, and cells were collected in RLT lysis buffer (+ 1% 2-mercaptoethanol). Cells were stored at -80°C prior to RNA extraction. RNA was extracted from cells using the RNeasy® Mini Kit (QIAGEN), with on-column DNase digestion. RNA was reverse transcribed with the High-Capacity cDNA Reverse Transcription Kit (Applied Biosystems™). cDNA was quantified using Power SYBR Green PCR Master Mix (Applied Biosystems™), using human *ACTB* (Actin Beta) as a housekeeping gene. Ct values were calculated by resident software on the StepOne Plus thermocycler. Data were normalized using the ΔΔCt method. Each experiment was conducted with two or four biological replicates that were normalized independently for data analysis. Data were analyzed with GraphPad Prism, using a Brown-Forsythe and Welch One-Way ANOVA and Dunnett T3 Multiple Comparisons Test. Primers used for RT-qPCR were as follows:

hACTB.

forward 5’-AGGCACCAGGGCGTGAT-3’

reverse 5’-GCCCACATAGGAATCCTTCTGAC-3’

hSHP

forward 5’-GCTTAGCCCCAAGGAATATGC-3’

reverse 5’-GTTCCAGGACTTCACACAGC-3’

hCYP7A1

forward 5’-GAGAAGGCAAACGGGTGAAC-3’

reverse 5’-GGATTGGCACCAAATTGCAGA-3’

Chemical information

General information

All reactions were carried out in flame-dried glassware, equipped with a stir bar and under a nitrogen atmosphere with dry solvents under anhydrous conditions, unless otherwise noted. Solvents used in anhydrous reactions were purified by passing over activated alumina and storing under argon. Yields refer to chromatographically and spectroscopically (^{1}H NMR) homogenous materials, unless otherwise stated. Reagents were purchased at the highest commercial quality and used without further purification, unless otherwise stated. n-Butyllithium (n-BuLi) was used as a 2.5 M solution in hexanes (Aldrich), was stored at 4°C and titrated prior to use. Organic solutions were concentrated under reduced pressure on a rotary evaporator using a water bath. Chromatographic purification of products was accomplished using forced-flow chromatography on 230-400 mesh silica gel. Thin-layer chromatography (TLC) was performed on 250μm SiliCycle silica gel F-254 plates. Visualization of the developed chromatogram was performed by fluorescence quenching or by staining using $KMnO_4$, *p*-anisaldehyde, or ninhydrin stains.

^{1}H and ^{13}C NMR spectra were obtained from the Emory University NMR facility and recorded on a Bruker Avance III HD 600 equipped with cryo-probe (600 MHz), INOVA 600 (600 MHz), INOVA 500 (500 MHz), INOVA 400 (400 MHz), VNMR 400 (400 MHz), or Mercury 300 (300 MHz), and are internally referenced to residual protio solvent signals. Data for ^{1}H NMR are reported as follows: chemical shift (ppm), multiplicity (s = singlet, d = doublet, t = triplet, q = quartet, m = multiplet, dd = doublet of doublets, dt = doublet of triplets, ddd= doublet of doublet

of doublets, dtd= doublet of triplet of doublets, b = broad, etc.), coupling constant (Hz), integration, and assignment, when applicable. Data for decoupled ^{13}C NMR are reported in terms of chemical shift and multiplicity when applicable. Liquid Chromatography Mass Spectrometry (LC-MS) was performed on an Agilent 6120 mass spectrometer with an Agilent 1220 Infinity liquid chromatography inlet. Preparative High-Pressure Liquid chromatography (Prep-HPLC) was performed on an Agilent 1200 Infinity Series chromatograph using an Agilent Prep-C18 30 x 250 mm 10 μm column, or an Agilent Prep-C18 21.2 x 100 mm, 5 μm column.

General boc deprotection procedure: In a reaction vial the substrate was dissolved in DCM. TFA was added dropwise at room temperature while the reaction stirred. The reaction proceeded until shown complete by TLC (15-45 minutes). The crude mixture was concentrated and purified to afford the product.

General amide coupling procedure: A flame-dried vial was charged with a stir bar and HBTU (1.1 equiv). The vial was placed under vacuum and backfilled 3x with nitrogen before the addition of primary amine substrate (1 equiv) dissolved in DMF, carboxylic acid (1.1 equiv) and diisopropylethylamine (5 equiv). The resulting mixture stirred until shown complete by TLC. The reaction mixture was then diluted with EtOAc and washed with water. The aqueous layer was extracted with EtOAc (2x). The combined organic layers were dried over magnesium sulfate, filtered, and concentrated via rotary evaporation. The residue was purified to afford the product.

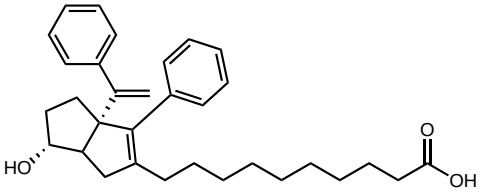

10-((3a*R*,6*R*)-6-hydroxy-3-phenyl-3a-(1-phenylvinyl)-1,3a,4,5,6,6a-hexahydropentalen-2-yl)decanoic acid (**10CA**): The title compound was prepared according to the reported procedure and the NMR data were consistent with those previously reported.[38]

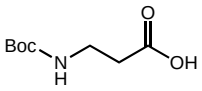

3-((*tert*-butoxycarbonyl)amino)propanoic acid (**S1**): A round bottom flask was charged with a stir bar, beta-alanine (500 mg, 5.6 mmol, 1 equiv), and NaOH (224 mg, 5.6 mmol, 1 equiv). The solids were dissolved in 2:1 dioxanes/H_2O solution (28 mL) before being cooled to 0 ^oC. Di-*tert*-butyl dicarbonate (1.3 g, 6.2 mmol, 1.1 equiv) was added to the reaction mixture and the reaction proceeded for 12 h slowly warming to room temperature. After completion, the reaction was diluted with EtOAc and washed with water. The aqueous layer was pHed to 2 with 1M HCl then reextracted with EtOAc (3x). The combined organic layers were dried with sodium sulfate, filtered, and concentrated to give the title compound (1.0 g, 5.3 mmol, 95% yield) without any further purification. The title compound matched previously reported spectra.[70]

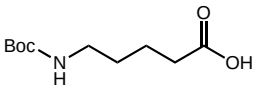

5-((*tert*-butoxycarbonyl)amino)pentanoic acid (**S2**): A round bottom flask was charged with a stir bar, 5-aminovaleric acid hydrochloride (500 mg, 3.3 mmol, 1 equiv), and NaOH (130 mg, 3.3

mmol, 1 equiv). The solids were dissolved in 2:1 dioxanes/H_2O solution (16.1 mL) before being cooled to 0 ^oC. Di-*tert*-butyl decarbonate (781 mg, 3.6 mmol, 1.1 equiv) was added to the reaction mixture and the reaction proceeded for 12 h slowly warming to room temperature. After completion, the reaction was diluted with EtOAc and washed with water. The aqueous layer was pHed to 2 with 1M HCl then reextracted with EtOAc (3x). The combined organic layers were dried with sodium sulfate, filtered, and concentrated to give the title compound (532.2 mg, 2.4 mmol, 74% yield) without any further purification. The title compound matched previously reported spectra.[71]

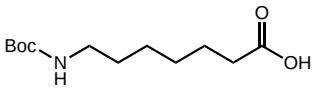

7-((*tert*-butoxycarbonyl)amino)heptanoic acid (**S3**): A round bottom flask was charged with a stir bar, 7-aminoheptanoic acid (225 mg, 1.5 mmol, 1.0 equiv), and NaOH (60 mg, 1.5 mmol, 1.0 equiv). The solids were dissolved in 2:1 dioxanes/H_2O solution (7.7 mL) before being cooled to 0 ^oC. Di-*tert*-butyl decarbonate (371 mg, 1.7 mmol, 1.1 equiv) was added to the reaction mixture and the reaction proceeded for 12 h slowly warming to room temperature. After completion, the reaction was diluted with EtOAc and washed with water. The aqueous layer was pHed to 2 with 1M HCl then reextracted with EtOAc (3x). The combined organic layers were dried with sodium sulfate, filtered, and concentrated to give the title compound (303.2 mg, 1.2 mmol, 82% yield) without any further purification. The title compound matched previously reported spectra.[72]

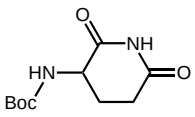

***tert*-butyl (2,6-dioxopiperidin-3-yl)carbamate** (**S4**): A round bottom flask was charged with a stir bar, Boc-L-glutamine (12.3 g, 50 mmol, 1.0 equiv), carbonyldiimidazole (8.9 g, 55 mmol, 1.1 equiv), and 4-dimethylaminopyridine (1.2 g, 10 mmol, 0.2 equiv). The solids were dissolved in THF (500 mL) before the flask was fixed with a reflux condenser and set to reflux for 16 h. After the reaction was cooled to room temperature the mixture was concentrated to give a cream solid. The solid was washed with THF and filtered to give the title compound (4.4 g, 19 mmol, 39% yield) as a white solid. The title compound matched previously reported spectra.[73]

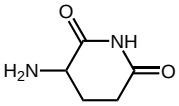

3-aminopiperidine-2,6-dione (**S5**): Following the general boc deprotection procedure, the reaction of **S4** (4.8 g, 21 mmol, 1.0 equiv). TFA (20 mL), and DCM (20 mL) provided the title compound (2.7 g, 21 mmol, quant.) after an hour. The crude mixture was moved forward without any additional purification.[73]

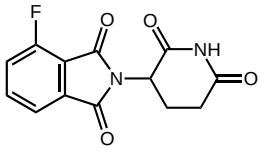

2-(2,6-dioxopiperidin-3-yl)-4-fluoroisoindoline-1,3-dione (**S6**): A round bottom flask was charged with a stir bar and **S5** (2.7 g, 21 mmol, 1 equiv). The solid was dissolved in acetic acid (140 mL) before the addition of 3-fluorophthalic anhydride (3.8 g, 23 mmol, 1.1 equiv). The reaction mixture was set to reflux for 16 h before being cooled to room temperature. The resulting mixture was diluted with EtOAc and pHed to ~6 using saturated aqueous sodium bicarbonate. The aqueous layer was extracted (3x) with EtOAc and the combined organic layers were dried with

sodium sulfate, filtered, and concentrated to give the title compound (2.4 g, 8.8 mmol, 41% yield) as a purple solid. The title compound matched previously reported spectra.[74]

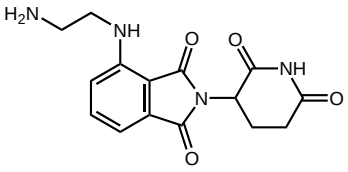

4-((2-aminoethyl)amino)-2-(2,6-dioxopiperidin-3-yl)isoindoline-1,3-dione (**S7**): To a vial charged with a stir bar, **S6** (55 mg, 0.2 mmol, 1.0 equiv), boc-ethylene diamine (32 μL, 0.2 mmol, 1 equiv), diisopropylamine (209 μL, 1.2 mmol, 6.0 equiv), and NMP (2 mL). The reaction was heated microwave irradiation at 90 °C for 50 minutes. The cooled reaction mixture was diluted with EtOAc and washed with water. To the aqueous layer 1M HCl was added until the pH was 1 and then was reextracted with EtOAc (3x). The combined organic layers were dried with sodium sulfate, filtered, and concentrated before being purified by flash chromatography (50% EtOAc/Hex) to give the intermediate. The resulting intermediate was dissolved in a 1:1 mixture of TFA/DCM. The reaction stirred for 2h before being concentrated to give the title compound (74.5 mg, 0.13 mmol, 64% yield) as the TFA salt. The title compound matched previously reported spectra.[74]

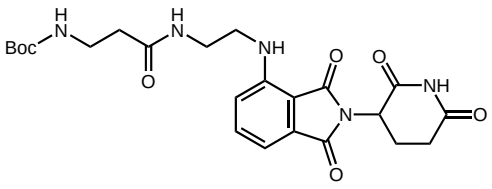

***tert*-butyl (3-((2-((2-(2,6-dioxopiperidin-3-yl)-1,3-dioxoisoindolin-4-yl)amino)ethyl)amino)-3-oxopropyl)carbamate** (**S8**): Following the general amide coupling procedure, the reaction of **S7** (24.8 mg, 0.06 mmol, 1.0 equiv), **S1** (12.5 mg, 0.07 mmol, 1.1 equiv), HBTU (25 mg, 0.07

mmol, 1.1 equiv), diisopropylethylamine (53 μL, 0.3 mmol, 5.0 equiv), and DMF (600 μL) provided the title compound (29.3 mg, 0.06 mmol, Quant.) as a yellow solid.

^{1}H NMR (600 MHz, Methanol-d_4) δ 7.59 (dd, *J* = 8.6, 7.1 Hz, 1H), 7.15 (d, *J* = 8.6 Hz, 1H), 7.09 (d, *J* = 7.1 Hz, 1H), 5.10 (dd, *J* = 12.6, 5.5 Hz, 1H), 3.52 – 3.45 (m, 4H), 3.34 (t, *J* = 6.7 Hz, 2H), 2.93 – 2.86 (m, 1H), 2.81 – 2.71 (m, 2H), 2.40 (t, *J* = 6.7 Hz, 2H), 2.15 (ddt, *J* = 13.1, 5.8, 3.0 Hz, 1H), 1.43 (s, 9H).

^{13}C NMR (151 MHz, MeOD) δ 173.29, 173.14, 170.19, 169.31, 167.88, 156.90, 146.71, 135.86, 132.56, 116.67, 110.73, 110.08, 78.73, 48.81, 41.55, 38.28, 36.58, 35.89, 31.22, 27.32, 22.41.

LRMS (**EI**) m/z $[M]^+$ calc'd for $C_{23}H_{30}N_5O_7$, 488.2, found 432.2 (**S8**-*t*Bu)

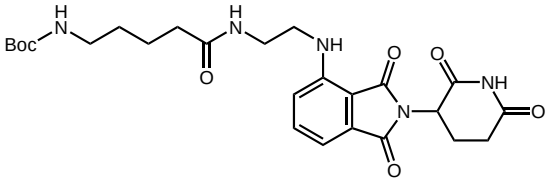

***tert*-butyl (5-((2-((2-(2,6-dioxopiperidin-3-yl)-1,3-dioxoisoindolin-4-yl)amino)ethyl)amino)-5-oxopentyl)carbamate** (**S9**): Following the general amide coupling procedure, the reaction of **S7** (39.3 mg, 0.09 mmol, 1.0 equiv), **S2** (21.7 mg, 0.1 mmol, 1.1 equiv), HBTU (37.9 mg, 0.1 mmol, 1.1 equiv), diisopropylethylamine (80 μL, 0.5 mmol, 5.0 equiv), and DMF (920 μL) provided the title compound (38.2 mg, 0.07 mmol, 82% yield) as a yellow solid.

^{1}H NMR (600 MHz, Methanol-d_4) δ 7.59 (dd, *J* = 8.5, 7.1 Hz, 1H), 7.16 (d, *J* = 8.6 Hz, 1H), 7.09 (d, *J* = 7.0 Hz, 1H), 5.09 (dd, *J* = 12.5, 5.5 Hz, 1H), 3.76 (p, *J* = 6.6 Hz, 1H), 3.50 (t, *J* = 5.7 Hz, 2H), 3.45 (t, *J* = 6.4 Hz, 2H), 3.26 (q, *J* = 7.4 Hz, 1H), 3.05 (t, *J* = 6.9 Hz, 2H), 2.94 – 2.84 (m, 1H), 2.82 – 2.69 (m, 2H), 2.22 (t, *J* = 7.4 Hz, 2H), 2.14 (tdd, *J* = 8.1, 6.1, 3.1 Hz, 1H), 1.63 (p, *J* = 7.5 Hz, 2H), 1.45 (s, 9H). (No NH peaks observed)

^{13}C NMR (151 MHz, MeOD) δ 176.57, 171.62, 170.61, 169.27, 148.12, 137.23, 133.97, 118.04, 112.10, 111.46, 55.15, 53.79, 50.20, 43.80, 42.70, 40.92, 39.73, 35.80, 32.21, 30.41, 28.78, 24.57, 18.70, 17.27, 13.15.

LRMS (**EI**) m/z $[M]^+$ calc'd for $C_{25}H_{39}N_6O_7$, 516.2, found 516.3

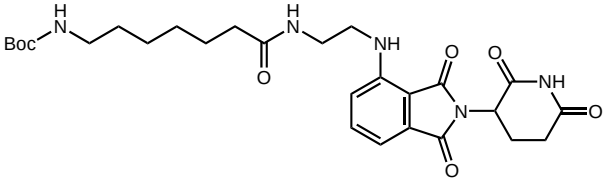

***tert*-butyl (7-((2-((2-(2,6-dioxopiperidin-3-yl)-1,3-dioxoisoindolin-4-yl)amino)ethyl)amino)-7-oxoheptyl)carbamate** (**S10**): Following the general amide coupling procedure, the reaction of **S7** (21.3 mg, 0.06 mmol, 1 equiv), **S3** (17.2 mg, 0.07 mmol, 1.1 equiv), HBTU (25 mg, 0.07 mmol, 1.1 equiv), diisopropylethylamine (52 μL, 0.3 mmol, 5 equiv), and DMF (600 μL) provided the title compound (32 mg, 0.06 mmol Quant.) as a yellow solid.

^{1}H NMR (600 MHz, Methanol-d_4) δ 7.59 (dd, J = 8.6, 7.1 Hz, 1H), 7.16 (d, J = 8.6 Hz, 1H), 7.09 (d, J = 7.1 Hz, 1H), 5.10 (dd, J = 12.7, 5.5 Hz, 1H), 3.51 (t, J = 5.6 Hz, 2H), 3.46 (t, J = 5.7 Hz, 2H), 3.03 (t, J = 7.1 Hz, 2H), 2.91 (ddd, J = 16.8, 13.8, 5.3 Hz, 1H), 2.83 – 2.71 (m, 2H), 2.21 (t, J = 7.5 Hz, 2H), 2.18 – 2.10 (m, 1H), 1.62 (p, J = 7.4 Hz, 2H), 1.46 (s, 9H), 1.34 (p, J = 3.5 Hz, 6H).

^{13}C NMR (151 MHz, MeOD) δ 176.83, 174.67, 171.58, 170.56, 169.27, 158.52, 148.13, 137.22, 133.93, 118.03, 112.08, 111.39, 79.45, 50.17, 42.74, 41.26, 39.77, 37.00, 32.20, 30.75, 29.87, 28.79, 27.51, 26.84, 23.78.

LRMS (**EI**) m/z $[M]^+$ calc'd for $C_{27}H_{38}N_5O_7$, 544.3, found 544.4

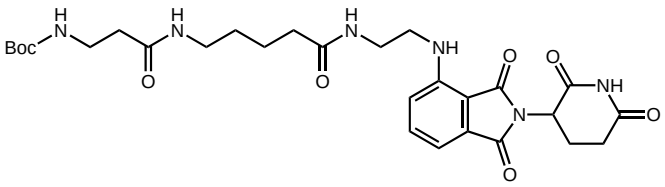

***tert*-butyl (3-((5-((2-((2-(2,6-dioxopiperidin-3-yl)-1,3-dioxoisoindolin-4-yl)amino)ethyl)amino)-5-oxopentyl)amino)-3-oxopropyl)carbamate** (**S11**): Following the general amide coupling procedure, the reaction of **S14** (16.9 mg, 0.03 mmol, 1 equiv), **S1** (6.6 mg, 0.04 mmol, 1.1 equiv), HBTU (13.3 mg, 0.04 mmol, 1.1 equiv), diisopropylethylamine (27 μL, 0.2 mmol, 5 equiv), and DMF (300 μL) provided the title compound (5.6 mg, 0.01 mmol, 32% yield) as a yellow solid.

^{1}H NMR (600 MHz, Methanol-d_4) δ 7.56 (dd, *J* = 8.5, 7.1 Hz, 1H), 7.13 (d, *J* = 8.5 Hz, 1H), 7.06 (d, *J* = 7.1 Hz, 1H), 5.06 (dd, *J* = 12.6, 5.5 Hz, 1H), 3.48 (t, *J* = 6.0 Hz, 2H), 3.42 (t, *J* = 6.0 Hz, 2H), 3.29 – 3.27 (m, 2H), 3.15 (t, *J* = 7.0 Hz, 2H), 2.89 – 2.82 (m, 1H), 2.78 – 2.67 (m, 2H), 2.33 (t, *J* = 6.8 Hz, 2H), 2.20 (t, *J* = 7.4 Hz, 2H), 2.14 – 2.07 (m, 1H), 1.65 – 1.57 (m, 2H), 1.48 (p, *J* = 7.0 Hz, 2H), 1.42 (s, 9H).

^{13}C NMR (151 MHz, MeOD) δ 175.08, 173.25, 172.42, 170.25, 169.21, 167.87, 146.74, 135.83, 131.88, 116.64, 110.69, 109.70, 78.72, 48.79, 41.30, 38.54, 38.32, 36.68, 35.92, 35.08, 30.80, 28.36, 27.34, 22.73, 22.40.

LRMS (**EI**) m/z $[M]^+$ calc'd for $C_{28}H_{39}N_6O_8$, 587.3, found 587.3

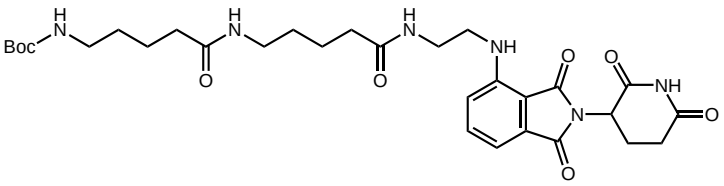

***tert*-butyl (5-((5-((2-((2-(2,6-dioxopiperidin-3-yl)-1,3-dioxoisoindolin-4-yl)amino)ethyl)amino)-5-oxopentyl)amino)-5-oxopentyl)carbamate** (**S12**): Following the general amide coupling procedure, the reaction of **S14** (16.9 mg, 0.03 mmol, 1 equiv), **S2** (7.6 mg, 0.04 mmol, 1.1 equiv), HBTU (13.3 mg, 0.04 mmol, 1.1 equiv), diisopropylethylamine (27 μL, 0.2 mmol, 5 equiv), and DMF (300 μL) provided the title compound (6.0mg, 0.01 mmol, 33% yield) as a yellow solid.

^{1}H NMR (600 MHz, Methanol-d_4) δ 7.59 (dd, *J* = 8.6, 7.1 Hz, 1H), 7.16 (d, *J* = 8.5 Hz, 1H), 7.09 (d, *J* = 7.1 Hz, 1H), 5.09 (dd, *J* = 12.6, 5.5 Hz, 1H), 3.50 (t, *J* = 5.7 Hz, 2H), 3.45 (t, *J* = 5.7 Hz, 2H), 3.17 (t, *J* = 6.9 Hz, 2H), 3.06 (t, *J* = 6.9 Hz, 2H), 2.93 – 2.85 (m, 1H), 2.81 – 2.68 (m, 2H), 2.21 (dt, *J* = 19.2, 7.4 Hz, 4H), 2.17 – 2.09 (m, 1H), 1.70 – 1.57 (m, 4H), 1.50 (ddd, *J* = 15.3, 12.7, 7.0 Hz, 4H), 1.45 (s, 9H).

^{13}C NMR (151 MHz, MeOD) δ 175.08, 174.52, 173.24, 170.24, 169.20, 167.86, 146.74, 135.83, 132.59, 116.64, 110.69, 110.07, 78.44, 54.43, 48.79, 42.38, 41.33, 39.51, 38.52, 38.33, 35.27, 35.09, 30.80, 28.44, 27.38, 22.84, 22.77, 22.40.

LRMS (**EI**) m/z $[M]^+$ calc'd for $C_{30}H_{43}N_6O_8$, 615.3, found 615.4

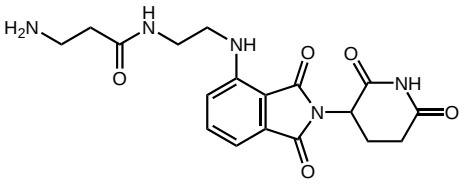

3-amino-*N*-(2-((2-(2,6-dioxopiperidin-3-yl)-1,3-dioxoisoindolin-4-yl)amino)ethyl)propenamide (**S13**): Following the general boc deprotection procedure, the reaction of **S8** (29.3 mg, mmol, 1.0 equiv) and 1:1 solution of TFA/DCM (2 mL) provided the title

compound (23.2 mg, Quant.) as the TFA salt as a dark yellow oil. The product was moved on without any further purification.

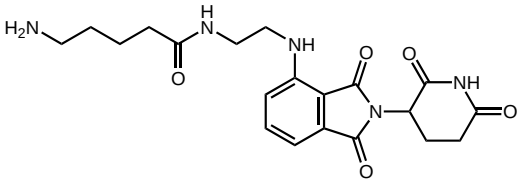

5-amino-*N*-(2-((2-(2,6-dioxopiperidin-3-yl)-1,3-dioxoisoindolin-4-yl)amino)ethyl)pentanamide (**S14**): Following the general boc deprotection procedure, the reaction of **S9** (28.2 mg, 0.05 mmol, 1 equiv) and 1:1 solution of TFA/DCM (2 mL) provided the title compound (33.8 mg, Quant) as the TFA salt as a dark yellow oil. The product was moved on without any further purification.

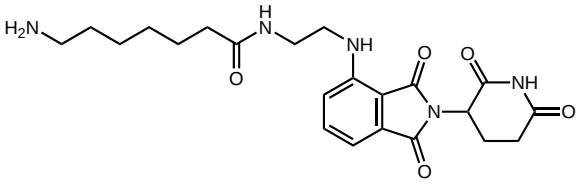

7-amino-*N*-(2-((2-(2,6-dioxopiperidin-3-yl)-1,3-dioxoisoindolin-4-yl)amino)ethyl)heptanamide (**S15**): Following the general boc deprotection procedure, the reaction of **S10** (35 mg, 1.0 equiv) and 1:1 solution of TFA/DCM (2 mL) provided the title compound (38 mg, quant.) as the TFA salt as a yellow oil. The product was moved on without any further purification.

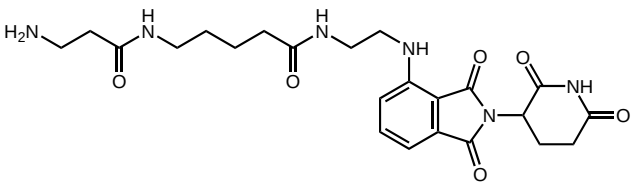

5-(3-aminopropanamido)-*N*-(2-((2-(2,6-dioxopiperidin-3-yl)-1,3-dioxoisoindolin-4-yl)amino)ethyl)pentanamide (**S16**): Following the general boc deprotection procedure, the reaction of **S11** (5.6 mg, 0.01 mmol, 1.0 equiv) and 1:1 solution of TFA/DCM (2 mL) provided the title compound (6.3 mg, Quant) as the TFA salt as a yellow oil. The product was moved on without any further purification.

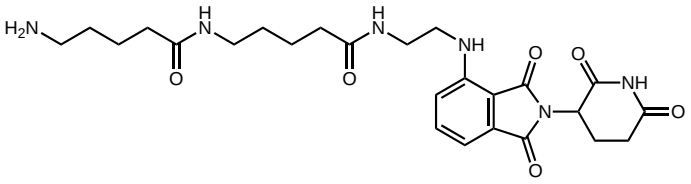

5-amino-*N*-(5-((2-((2-(2,6-dioxopiperidin-3-yl)-1,3-dioxoisoindolin-4-yl)amino)ethyl)amino)-5-oxopentyl)pentanamide (**S17**): Following the general boc deprotection procedure, the reaction of **S12** (20 mg, 1.0 equiv) and 1:1 solution of TFA/DCM (2 mL) provided the title compound (Quant) as the TFA salt as a yellow oil. The product was moved on without any further purification.

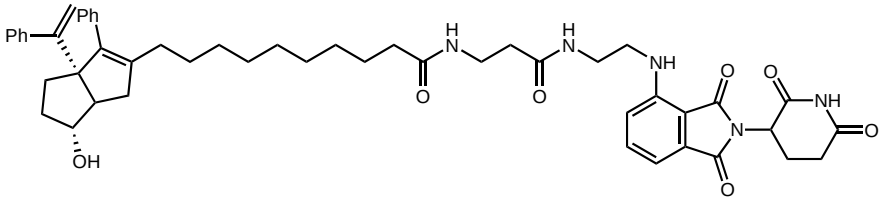

***N*-(3-((2-((2-(2,6-dioxopiperidin-3-yl)-1,3-dioxoisoindolin-4-yl)amino)ethyl)amino)-3-oxopropyl)-10-((3a*R*,6*R*)-6-hydroxy-3-phenyl-3a-(1-phenylvinyl)-1,3a,4,5,6,6a-hexahydropentalen-2-yl)decanamide** (**PROTAC_2**): Following the general amide coupling procedure, the reaction of **10CA** (28.4 mg, 0.06 mmol, 1.1 equiv), **S13** (18.9 mg, 0.05 mmol, 1 equiv), HBTU (22.8 mg, 0.06 mmol, 1.1 equiv), diisopropylethylamine (40 μL, 0.22 mmol, 4.0

equiv), and DMF (550 μL) provided the title compound (5.8 mg, 0.007 mmol, 14% yield) as a yellow solid after flash chromatography (5-10% MeOH/DCM).

^{1}H NMR (400 MHz, Chloroform-*d*) δ 7.47 (t, *J* = 7.9 Hz, 1H), 7.31 – 7.24 (m, 6H), 7.16 (d, *J* = 7.4 Hz, 3H), 7.08 (d, *J* = 7.1 Hz, 1H), 6.91 (d, *J* = 8.6 Hz, 1H), 5.03 (s, 1H), 4.96 (s, 1H), 4.92 – 4.86 (m, 2H), 3.91 (s, 1H), 3.48 (s, 4H), 3.39 (d, *J* = 6.1 Hz, 3H), 2.89 – 2.65 (m, 4H), 2.41 (d, *J* = 6.7 Hz, 3H), 2.28 (d, *J* = 16.8 Hz, 2H), 2.10 – 1.90 (m, 9H), 1.65 (d, *J* = 4.8 Hz, 2H), 1.47 (dd, *J* = 11.1, 7.0 Hz, 3H), 1.41 (d, *J* = 6.7 Hz, 1H), 1.15 (s, 11H).

^{13}C NMR (151 MHz, $CDCl_3$) δ 172.86, 171.03, 169.50, 168.48, 167.43, 154.60, 146.61, 144.16, 141.13, 139.27, 137.41, 136.34, 132.52, 129.71, 127.79, 127.72, 127.65, 126.68, 126.62, 116.68, 114.98, 112.10, 110.48, 82.08, 69.33, 55.82, 48.96, 42.46, 40.19, 38.79, 36.45, 35.69, 35.62, 34.08, 32.09, 31.93, 31.42, 29.71, 29.61, 29.46, 29.37, 29.26, 29.23, 29.17, 27.72, 25.68, 22.77, 18.65, 17.34, 14.20, 14.12.

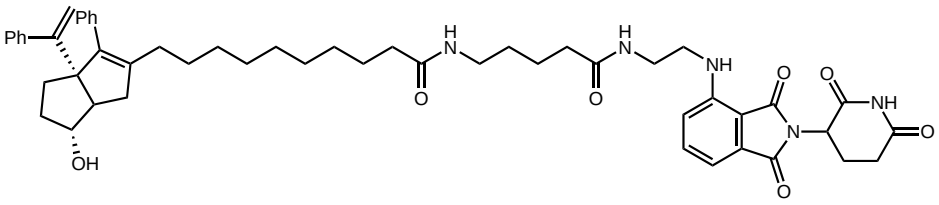

***N*-(5-((2-((2-(2,6-dioxopiperidin-3-yl)-1,3-dioxoisoindolin-4-yl)amino)ethyl)amino)-5-oxopentyl)-10-((3a*R*,6*R*)-6-hydroxy-3-phenyl-3a-(1-phenylvinyl)-1,3a,4,5,6,6a-hexahydropentalen-2-yl)decanamide** (**PROTAC_3**): Following the general amide coupling procedure, the reaction of **S14** (14.4 mg, 0.03 mmol, 1.0 equiv), **10CA** (16.5 mg, 0.03 mmol, 1.0 equiv), HBTU (13.2 mg, 0.03 mmol, 1.0 equiv), diisopropylethylamine (24 μL, 0.13 mmol, 4.0 equiv), and DMF (350 μL) provided the title compound (10 mg, 0.01 mmol, 33% yield) as a yellow oil after flash chromatography (5-10% MeOH/DCM).

^{1}H NMR (600 MHz, Chloroform-*d*) δ 7.49 (d, *J* = 7.3 Hz, 1H), 7.35 – 7.27 (m, 3H), 7.19 (d, *J* = 6.5 Hz, 3H), 7.10 (t, *J* = 6.3 Hz, 1H), 6.97 (dd, *J* = 9.4, 4.7 Hz, 1H), 6.42 (t, *J* = 5.3 Hz, 1H), 5.30 (d, *J* = 5.0 Hz, 1H), 5.05 (d, *J* = 4.8 Hz, 1H), 4.98 (d, *J* = 5.0 Hz, 1H), 4.91 (dt, *J* = 12.2, 5.1 Hz, 1H), 3.93 (s, 1H), 3.72 (t, *J* = 6.7 Hz, 1H), 3.48 (d, *J* = 5.6 Hz, 4H), 3.46 – 3.43 (m, 3H), 3.22 (t, *J* = 6.3 Hz, 2H), 2.81 – 2.71 (m, 2H), 2.33 – 1.97 (m, 13H), 1.65 (h, *J* = 6.8, 6.0 Hz, 9H), 1.35 – 1.17 (m, 25H).

^{13}C NMR (151 MHz, $CDCl_3$) δ 174.71, 173.70, 171.69, 169.38, 168.72, 167.52, 153.65, 146.74, 144.17, 141.55, 139.85, 137.41, 136.28, 132.50, 129.71, 127.79, 127.65, 126.67, 126.61, 116.82, 114.96, 112.37, 110.36, 82.07, 69.34, 55.81, 48.93, 42.12, 40.20, 38.77, 38.57, 36.77, 35.53, 34.08, 32.09, 31.43, 29.70, 29.66, 29.61, 29.46, 29.36, 29.28, 29.26, 29.24, 28.86, 27.73, 25.78, 22.78, 22.59, 22.58, 18.63, 17.28, 14.12, 6.84, 4.90.

LRMS (LCMS): m/z: $[M+H]^+$ calc'd. for $C_{62}H_{63}N_5O_7$: 870.1, found 873.0

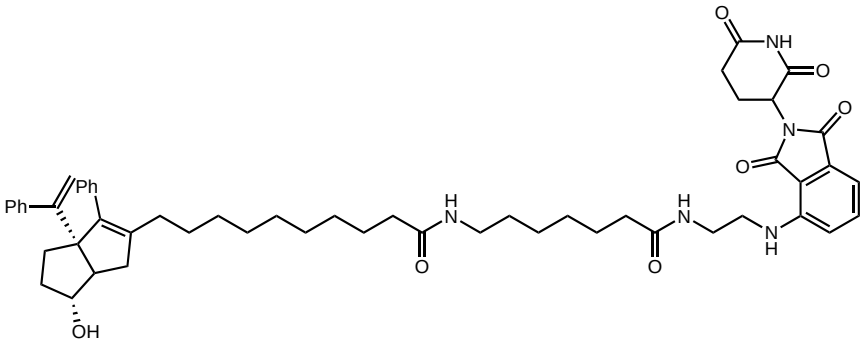

***N*-(7-((2-((2-(2,6-dioxopiperidin-3-yl)-1,3-dioxoisoindolin-4-yl)amino)ethyl)amino)-7-oxoheptyl)-10-((3a*R*,6*R*)-6-hydroxy-3-phenyl-3a-(1-phenylvinyl)-1,3a,4,5,6,6a-hexahydropentalen-2-yl)decanamide** (**PROTAC_4**): Following the general amide coupling procedure, the reaction of **S15** (19 mg, 0.05 mmol, 1 equiv), **10CA** (23.6 mg, 0.05 mmol, 1.1 equiv), HBTU (18.9 mg, 0.05 mmol, 1.1 equiv), diisopropylethylamine (33 μL, 0.22 mmol, 4.0

equiv), and DMF (480 μL) provided the title compound (5.8 mg, 0.03 mmol, 51% yield) as a yellow oil after flash chromatography (5-10% MeOH/DCM).

^{1}H NMR (600 MHz, Chloroform-*d*) δ 7.51 (dd, *J* = 8.6, 7.1 Hz, 1H), 7.35 – 7.29 (m, 5H), 7.27 – 7.25 (m, 3H), 7.21 (dd, *J* = 6.9, 1.7 Hz, 2H), 7.10 (d, *J* = 7.1 Hz, 1H), 7.02 (d, *J* = 8.6 Hz, 1H), 5.07 (d, *J* = 1.4 Hz, 1H), 5.00 (d, *J* = 1.4 Hz, 1H), 4.96 – 4.92 (m, 1H), 3.97 – 3.95 (m, 1H), 3.72 (pd, *J* = 6.6, 4.1 Hz, 5H), 3.50 – 3.45 (m, 3H), 3.18 (dt, *J* = 7.5, 3.7 Hz, 6H), 2.90 – 2.85 (m, 1H), 2.81 – 2.74 (m, 1H), 2.37 – 2.28 (m, 2H), 2.17 (dt, *J* = 15.3, 7.6 Hz, 3H), 2.10 – 1.97 (m, 5H), 1.73 – 1.66 (m, 2H), 1.62 – 1.57 (m, 4H), 1.32 – 1.24 (m, 13H).

^{13}C NMR (151 MHz, $CDCl_3$) δ 174.46, 173.74, 171.34, 169.28, 168.75, 167.51, 154.56, 146.73, 144.08, 141.08, 139.14, 137.33, 136.24, 132.33, 129.62, 127.70, 127.64, 127.57, 126.59, 126.53, 116.86, 114.87, 111.71, 110.06, 81.99, 69.26, 56.25, 55.46, 48.81, 43.42, 42.19, 40.13, 39.24, 38.79, 36.66, 36.14, 33.98, 32.01, 31.30, 29.56, 29.45, 29.23, 29.19, 29.14, 29.06, 28.28, 27.68, 26.08, 25.81, 25.26, 22.63, 18.47, 17.07, 12.47.

LRMS

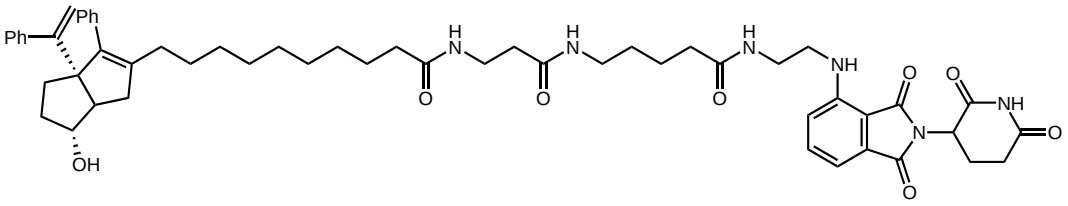

***N*-(3-((5-((2-((2-(2,6-dioxopiperidin-3-yl)-1,3-dioxoisoindolin-4-yl)amino)ethyl)amino)-5-oxopentyl)amino)-3-oxopropyl)-10-((3a*R*,6*R*)-6-hydroxy-3-phenyl-3a-(1-phenylvinyl)-1,3a,4,5,6,6a-hexahydropentalen-2-yl)decanamide** (**PROTAC_5**): Following the general amide coupling procedure, the reaction of **10CA** (9.5 mg, 0.02 mmol, 1.1 equiv), **S16** (6.3 mg, 0.01 mmol, 1.0 equiv), HBTU (7.6 mg, 0.02 mmol, 1.1 equiv), diisopropylethylamine (10 μL, 0.06

mmol, 4.0 equiv), and DMF (150 μL) provided the title compound (5.0 mg, 0.005 mmol, 53% yield) as a yellow oil after flash chromatography (5-10% MeOH/DCM).

^{1}H NMR (500 MHz, cdcl$_3$) δ 7.81 (d, *J* = 28.7 Hz, 2H), 7.50 – 7.42 (m, 4H), 7.33 – 7.28 (m, 1H), 7.19 (d, *J* = 7.3 Hz, 2H), 7.09 (d, *J* = 7.0 Hz, 1H), 6.93 (d, *J* = 8.4 Hz, 1H), 5.05 (s, 1H), 4.98 (s, 1H), 4.91 (s, 1H), 3.94 (s, 1H), 3.46 (s, 6H), 3.20 (s, 2H), 2.86 (d, *J* = 12.7 Hz, 1H), 2.73 (d, *J* = 11.3 Hz, 2H), 2.40 (s, 3H), 2.26 – 1.94 (m, 10H), 1.69 – 1.60 (m, 6H), 1.50 (dd, *J* = 14.3, 6.9 Hz, 3H), 1.42 (d, *J* = 6.5 Hz, 2H), 1.20 (s, 11H).

^{13}C NMR (151 MHz, CDCl$_3$) δ 146.61, 136.24, 129.70, 127.79, 127.72, 127.66, 126.70, 117.12, 116.86, 112.22, 112.00, 82.09, 82.05, 69.33, 55.77, 53.97, 48.97, 46.33, 42.07, 40.07, 38.92, 35.76, 31.93, 29.70, 29.37, 29.18, 28.58, 22.69, 14.12.

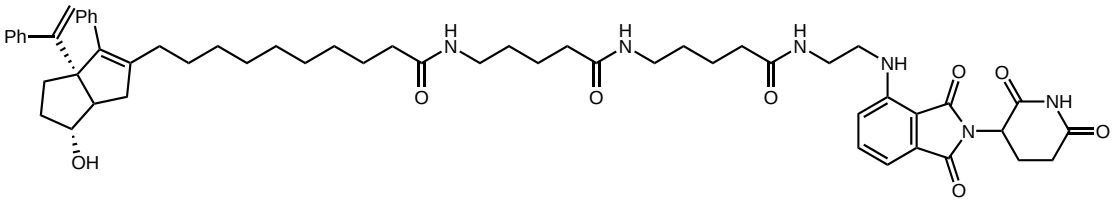

***N*-(5-((5-((2-((2-(2,6-dioxopiperidin-3-yl)-1,3-dioxoisoindolin-4-yl)amino)ethyl)amino)-5-oxopentyl)amino)-5-oxopentyl)-10-((3a*R*,6*R*)-6-hydroxy-3-phenyl-3a-(1-phenylvinyl)-1,3a,4,5,6,6a-hexahydropentalen-2-yl)decanamide** (**PROTAC_6**): Following the general amide coupling procedure, the reaction of **S17** (12 mg, 0.02 mmol, 1.0 equiv), **10CA** (12.1 mg, 0.03 mmol, 1.1 equiv), HBTU (9.7 mg, 0.03 mmol, 1.1 equiv), diisopropylethylamine (16 μL, 0.09 mmol, 4.0 equiv), and DMF (230 μL) provided the title compound (5.1 mg, 0.005 mmol, 23% yield) as a yellow oil after flash chromatography (5-10% MeOH/DCM).

^{1}H NMR (600 MHz, Chloroform-*d*) δ 7.43 (t, *J* = 8.1 Hz, 1H), 7.24 (dt, *J* = 14.0, 7.0 Hz, 4H), 7.12 (d, *J* = 7.4 Hz, 1H), 7.04 (d, *J* = 6.9 Hz, 1H), 6.90 (d, *J* = 8.8 Hz, 1H), 6.35 (s, 2H), 5.23 (d, *J* = 2.3 Hz, 0H), 4.98 (s, 1H), 4.92 (s, 0H), 4.85 (d, *J* = 11.9 Hz, 1H), 3.87 (s, 0H), 3.62 – 3.54 (m, 1H), 3.41 (d, *J* = 16.7 Hz, 4H), 2.81 (d, *J* = 15.3 Hz, 1H), 2.68 (p, *J* = 14.2, 13.7 Hz, 2H), 2.34 – 2.19 (m, 2H), 2.14 (d, *J* = 7.6 Hz, 2H), 2.08 (dt, *J* = 15.0, 7.3 Hz, 4H), 2.03 – 1.86 (m, 1H), 1.74 – 1.47 (m, 31H), 1.16 (d, *J* = 31.3 Hz, 26H).

^{13}C NMR (151 MHz, $CDCl_3$) δ 174.82, 173.68, 171.22, 169.40, 168.76, 167.51, 153.78, 146.29, 135.84, 132.06, 129.71, 127.79, 127.72, 127.65, 126.28, 117.19, 114.32, 111.94, 110.56, 82.61, 69.33, 55.80, 48.96, 41.35, 40.20, 38.75, 38.64, 38.48, 36.33, 35.74, 35.20, 34.09, 32.09, 31.93, 31.03, 29.71, 29.25, 28.80, 27.72, 25.82, 24.68, 22.81, 22.70, 22.55, 14.13.

LRMS (LCMS): m/z: $[M+H]^+$ calc'd. for $C_{57}H_{72}N_6O_8$: 969.2, found 969.6

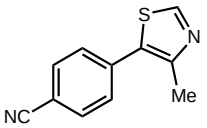

4-(4-methylthiazol-5-yl)benzonitrile: 4-bromobenzonitrile (1.8 g, 10 mmol), palladium (II) acetate (22.5 mg, 1 mmol), and potassium acetate (2.0 g, 20 mmol) in a round bottom charged with a stir bar were dissolved in DMA (40 mL) under nitrogen. To the mixture 4-methyl thiazole was added dropwise and stirred for 16h at 145ºC. After cooling to ambient temperatures, the reaction mixture was poured onto water and extracted with EtOAc (3x). The combined organic layers were washed with 1M LiCl and brine, dried with Na_2SO_4, and concentrated. The mixture was then purified on silica 40-60% EtOAc/Hexanes (1.8 g, 90% yield). The spectral data reported are consistent with literature.[75]

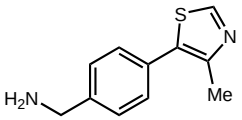

(4-(4-methylthiazol-5-yl)phenyl)methanamine: To a flame-dried round bottom equipped with a reflux condenser and a stir bar, 4-(4-methylthiazol-5-yl)benzonitrile (1.8 g, 9 mmol) was added and dissolved in THF (32 mL). The reaction was cooled to 0°C and followed by the addition of $LiAlH_4$ (682.2 mg, 18 mmol). The reaction was then heated to 70°C for 3.5h. After cooling the reaction to room temperature the reaction was diluted in ether and then cooled to 0°C before adding H_2O (1 mL), 15% aq. NaOH (1 mL), and H_2O (3mL) subsequentially. After returning to room temperature the reaction was poured onto water and extracted with EtOAc (3x), dried over Na_2SO_4, and finally concentrated to give the product (1.2 g, 66% yield). The spectral data reported are consistent with literature.[75]

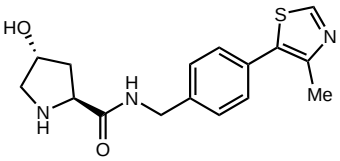

(2*S*,4*R*)-4-hydroxy-*N*-(4-(4-methylthiazol-5-yl)benzyl)pyrrolidine-2-carboxamide: (4-(4-methylthiazol-5-yl)phenyl)methanamine (864.9 g, 4.2 mmol), N-Boc-(2S, 4R)-4-hydroxyproline (1.1 g, 4.7 mmol), HBTU (1.8 g, 4.7 mmol), Hüing's base (1.5 mL, 8.4 mmol), DMF (42 mL). Following the general peptide coupling procedure, the compound was purified by a gradient of 50%-100% EtOAc/Hexanes and then a flush with 10% MeOH/DCM to give a yellow solid, which was then deprotonated by dissolving in a 1:1 mixture of TFA in DCM for 30 minutes when the reaction was complete by LCMS (837.3 mg, 67% yield). The spectral data reported are consistent with literature.[75]

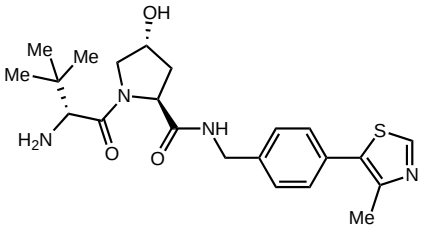

(2*S*,4*R*)-1-((*R*)-2-amino-3,3-dimethylbutanoyl)-4-hydroxy-*N*-(4-(4-methylthiazol-5-yl)benzyl)pyrrolidine-2-carboxamide: (2*S*,4*R*)-4-hydroxy-*N*-(4-(4-methylthiazol-5-yl)benzyl)pyrrolidine-2-carboxamide (837.3 g, 2.7 mmol), Boc-*tert*- Leucine (686.9 mg, 2.97 mmol), HBTU (1.12 mg, 2.97 mmol), Hüing's base (2.4 mL, 13.5 mmol), DMF (27 mL). Following the general peptide coupling procedure, the compound was purified by a gradient of 50%-100% EtOAc/Hexanes and then a flush with 10% MeOH/DCM to give a light-yellow ssolid, which was then deprotonated by dissolving in a 1:1 mixture of TFA in DCM for 30 minutes when the reaction was complete by LCMS (162.8 mg, 14% yield). The spectral data reported are consistent with literature.[75]

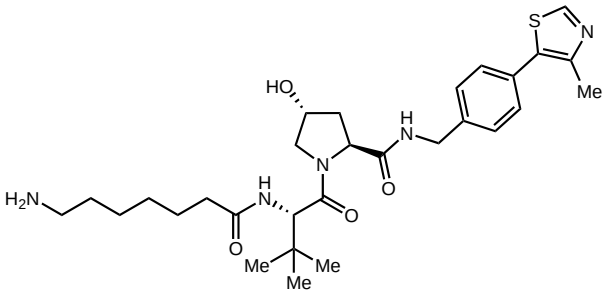

(2*S*,4*R*)-1-((*S*)-2-(7-aminoheptanamido)-3,3-dimethylbutanoyl)-4-hydroxy-*N*-(4-(4-methylthiazol-5-yl)benzyl)pyrrolidine-2-carboxamide: (2*S*,4*R*)-1-((*R*)-2-amino-3,3-dimethylbutanoyl)-4-hydroxy-*N*-(4-(4-methylthiazol-5-yl)benzyl)pyrrolidine-2-carboxamide (162.8 mg, 0.36 mmol), 7-((*tert*-butoxycarbonyl)amino)heptanoic acid (98 mg, 0.4 mmol), HBTU (151.7 mg, 0.4 mmol), Hüing's base (251 μL, 1.44 mmol), DMF (3.6 mL).Following the general peptide coupling procedure, the compound was purified by a gradient of 50%-100%

EtOAc/Hexanes and then a flush with 10% MeOH/DCM to give a light yellow solid, which was then deprotonated by dissolving in a 1:1 mixture of TFA in DCM for 45 minutes when the reaction was complete by LCMS (52.2 mg, 26% yield).

^{1}H NMR (400 MHz, Methanol-*d*4) δ 9.37 (s, 1H), 7.46 (m, 4H), 4.69 – 4.28 (m, 5H), 2.88 (t, *J* = 7.6 Hz, 2H), 2.51 (s 3H), 1.62 (q, *J* = 7.4 Hz, 4H), 1.43 – 1.33 (m, 4H), 1.01 (s, 9H).

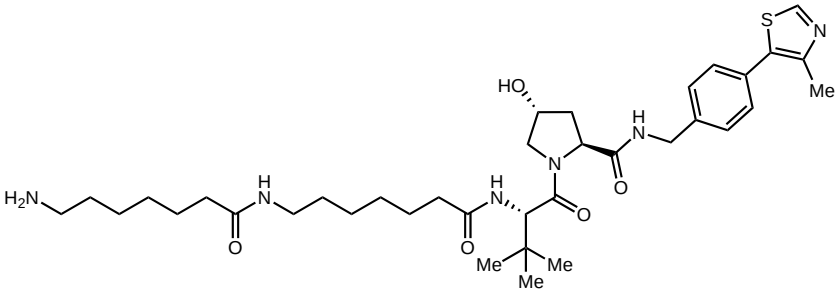

(2*S*,4*R*)-1-((*S*)-2-(7-(7-aminoheptanamido)heptanamido)-3,3-dimethylbutanoyl)-4-hydroxy-*N*-(4-(4-methylthiazol-5-yl)benzyl)pyrrolidine-2-carboxamide: (2*S*,4*R*)-1-((*S*)-2-(7-aminoheptanamido)-3,3-dimethylbutanoyl)-4-hydroxy-*N*-(4-(4-methylthiazol-5-yl)benzyl)pyrrolidine-2-carboxamide (52.2 mg, 0.09 mmol), 7-((*tert*-butoxycarbonyl)amino)heptanoic acid (33 mg, 0.13 mmol), HBTU (51 mg, 0.13 mmol), Hüing's base (84 μL, 0.48 mmol), DMF (2 mL). Following the general peptide coupling procedure, the compound was purified by a gradient of 50%-100% EtOAc/Hexanes and then a flush with 10% MeOH/DCM to give a light yellow solid, which was then deprotonated by dissolving in a 1:1 mixture of TFA in DCM for 20 minutes when the reaction was complete by LCMS (25.0 mg, 39% yield).

^{1}H NMR (600 MHz, CD_3OD) δ 9.04 (s, 1H), 7.53 – 7.40 (m, 4H), 5.53 – 5.45 (br. s, 3H), 4.70 – 4.26 (m, 5H), 4.03 – 3.91 (m, 1H), 3.87 (dd, *J* = 60.2, 10.9 Hz, 2H), 3.33 (s, 3H), 3.17 (d, *J* = 6.1 Hz, 2H), 2.93 (d, *J* = 7.8 Hz, 2H), 2.51 (d, *J* = 4.3 Hz, 3H), 2.37 – 2.00 (m, 7H), 1.73 – 1.24 (m, 14H), 1.05 (s, 9H).

^{13}C NMR (151 MHz, Methanol-*d*4) δ 174.60, 174.55, 173.08, 170.95, 151.94, 146.75, 139.20, 132.58, 129.65, 129.10, 128.98, 127.64, 69.70, 59.43, 57.62, 56.59, 53.74, 53.39, 42.29, 39.26, 38.88, 37.56, 35.43, 35.13, 28.87, 28.53, 28.21, 26.97, 26.30, 25.70, 25.53, 25.27, 14.03.

LRMS (LCMS): m/z: $[M+H]^+$ calc'd. for $C_{36}H_{56}N_6O_5S$: 684.9, found 687.3

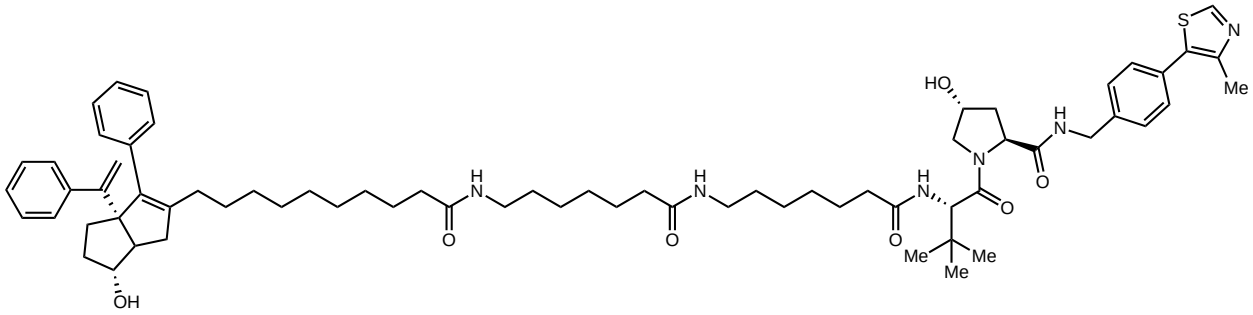

(2*S*,4*R*)-4-hydroxy-1-((2*S*)-2-(7-(7-(10-((3a*R*,6*R*)-6-hydroxy-3-phenyl-3a-(1-phenylvinyl)-1,3a,4,5,6,6a-hexahydropentalen-2-yl)decanamido)heptanamido)heptanamido)-3,3-dimethylbutanoyl)-*N*-(4-(4-methylthiazol-5-yl)benzyl)pyrrolidine-2-carboxamide: (2*S*,4*R*)-1-((*S*)-2-(7-(7-aminoheptanamido)heptanamido)-3,3-dimethylbutanoyl)-4-hydroxy-*N*-(4-(4-methylthiazol-5-yl)benzyl)pyrrolidine-2-carboxamide (18.3 mg, 0.025 mmol), 10-(6-*exo*-hydroxy-3-phenyl-3a-(1-phenylvinyl)-1,3a,4,5,6,6a-hexahydropentalen-2- yl)decanoic acid (13 mg, 0.028 mmol), HBTU (11 mg, 0.028 mmol), Hüing's base (18 μL, 0.1 mmol), DMF (250 μL). Following the general peptide coupling procedure, the compound was purified by HPLC on an

Agilent 1200 Infinity Series chromatograph using an Agilent Prep-C18 30 x 250 nm 10 μm column, with a linear gradient using water and 0.1% formic acid (FA) (Solvent A) and MeCN and 0.1% FA (Solvent B); t=0 min, 30% B, t=20 min, 99% B, flow rate 40mL/min, to afford the desired compound (2.7 mg, 9s% yield).

^{1}H NMR (600 MHz, Chloroform-*d*) δ 8.55 (s, 1H), 7.29 – 7.16 (m, 7H), 7.13 – 7.02 (m, 3H), 4.93 (d, *J* = 1.4 Hz, 1H), 4.86 (d, *J* = 1.4 Hz, 1H), 4.61 (t, *J* = 8.1 Hz, 1H), 4.48 – 4.37 (m, 3H), 4.23 (dd, *J* = 15.0, 5.3 Hz, 1H), 3.98 (s, 1H), 3.82 (s, 1H), 3.46 (dd, *J* = 11.3, 3.4 Hz, 1H), 3.08 (dq, *J* = 13.0, 6.8 Hz, 4H), 2.23 – 2.10 (m, 3H), 2.07 – 1.84 (m, 7H), 1.50 (d, *J* = 39.9 Hz, 41H), 1.20 – 1.02 (m, 40H), 0.81 (s, 9H).

^{13}C NMR (151 MHz, $CDCl_3$) δ 174.72, 150.34, 129.71, 129.54, 128.14, 127.79, 127.72, 127.65, 126.67, 125.78, 115.94, 114.50, 82.88, 70.62, 68.81, 59.58, 57.49, 56.86, 55.81, 43.77, 40.23, 39.12, 38.70, 36.88, 36.50, 35.94, 34.83, 33.97, 32.10, 29.70, 29.53, 29.39, 29.28, 29.12, 28.51, 28.14, 27.77, 26.42, 26.29, 26.15, 25.82, 25.46, 25.23, 16.05, 14.14.

LRMS (LCMS): m/z: $[M+H]^+$ calc'd. for $C_{68}H_{94}N_6O_7S$: 1139.6, found 1162.3 (+Na).

Chapter 4: Repurposing agonist scaffold for LRH-1 antagonism

4.1 Introduction

The downregulation of LRH-1 has been recently studied as having great therapeutic potential in cancer models. Although, this is an extremely beneficial research field, in most models there is a complete knockdown of LRH-1.[17,18,28] Therefore, the use of being able to downregulate the downstream gene expression of LRH-1, while maintaining the protein would be highly beneficial.

Creating an LRH-1 antagonist is difficult, due to the lack of a crystal structure in the inactive state. There is an innate destabilization of helix 12 (H12), the helix that interacts with coregulators, that is often associated with nuclear receptor (NR) antagonism.[16] The Flettrick lab developed a series of molecules that successfully showed the downregulation of LRH-1 regulated genes. Although these molecules have some efficacy *in vitro*, the specific mechanism of action for these molecules is still unknown.[42]

Antagonists have been designed in a variety of ways. For NRs, we have a unique ability to prevent activity by blocking the interaction of coactivators at the active function surface-2 (AF-2). This has been exhibited with ERα, a well known target of various cancers. They repurposed the native ligand for ERα, estrogen, into an antagonist.[76] From crystal structures, the phenol in estrogen helps orient the molecule and attributes to the potency by making contacts within the pocket.[76,77] Tamoxifen was a synthetically developed antagonist for LRH-1. Similarly to estrogen, the phenol is used to orient the molecule within the pocket, as well as giving it its

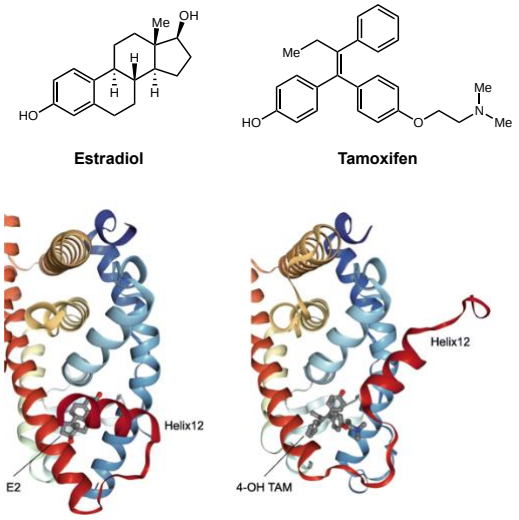

Figure 4.1: Structure of ER with estradiol and tamoxifen in the binding pocket
E2 PDB: 1ERE; 4-OH TAM PDB: 3ERT

potency. When comparing the crystal structures of the two bound in pocket there is a large difference in the position of H12 (Figure 4.1).[77] Within the agonist bound scaffold of the protein the H12 is folded into the structure stabilizing the protein, whereas in the antagonist bound scaffold, the helix is pushed out of conformation by the dimethylamine, disrupting the binding of coactivators.[77,78] We sought to utilize this design in order to develop LRH-1 antagonists.

When attempting to repurpose the bicyclooct-2-ene agonist scaffold in 6N for LRH-1 we see that the sulfamide provides a good deal of potency to the molecule. On the other hand, the phenyl group at the bridge, is uniquely positioned in close proximity to H12. This is where the propose to add steric bulkiness onto the molecule in order to disrupt the binding of coactivators to the LRH-1 scaffold.

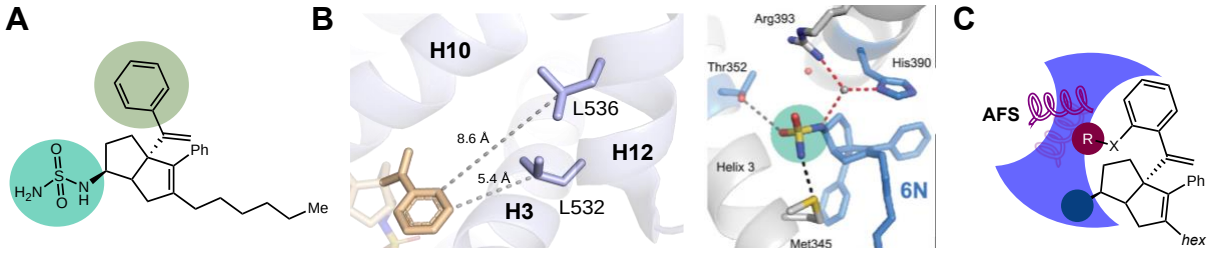

Figure 4.2: Design of LRH-1 antagonism from repurposing agonist scaffold

(A) 6N structure (B) 6N bound to LRH-1 LBD PDB:6OQY. (C) Proposed design for new LRH-1 antagonists.

4.2 Results and discussion

The series of antagonists were synthesized with the bicyclooct-2-ene core from the leading LRH-1 agonists. Formation of the core occurred via the Whitby cyclization from a 1,6-enyne, acetylene derivative, and dibromo alkane tail. In this series, we designed the molecules to have rigid moieties in order to disrupt the interactions at the AF-2. We specifically synthesized an

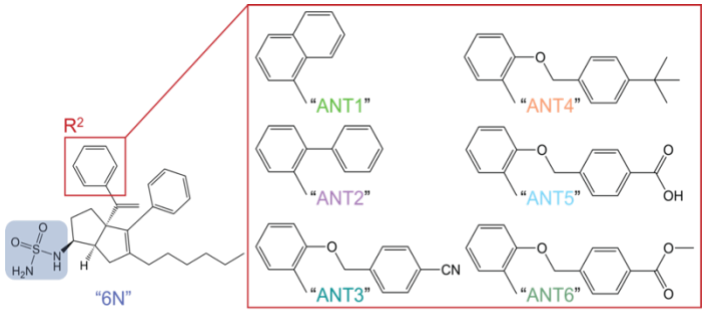

Figure 4.3: Series of new LRH-1 antagonists

alkyne to have ortho reactivity via a protected phenol in order to create functionality at this position for benzylation with 4-(bromomethyl)benzonitrile for the formation of ANT3 or to be triflated and cross-coupled with phenylboronic acid (ANT2). ANT1 was synthesized via the Whitby cyclization with ethynylnapthalene. We first tested these three antagonists. From preliminarily gene expression studies we found ANT3 to be the leading antagonist, spurring the synthesis of ANT4-6 to add polarity and/or steric hinderance on the H12.

With each structure we expected a significant loss in binding and a decrease in thermal stability, due to the added moieties on the styrene. As seen in Figure 4.4A, there is at least a 10-fold decrease in the binding affinity, but most remained in the mid to high nM range. As expected,

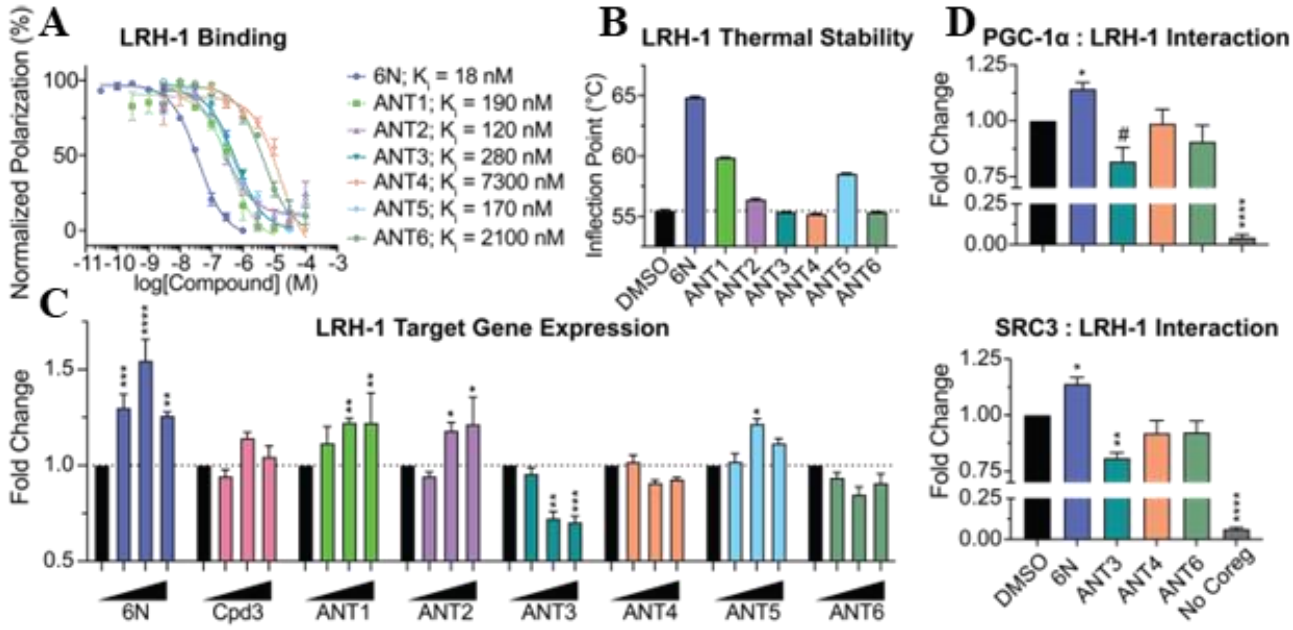

Figure 4.4: Modifications to 6N disrupts LRH-1 activity

(A) FP competition assay showing binding of 6N and 6N analogs to the LRH-1 LBD. K_i: inhibition constant. 95% confidence intervals are shown in brackets. Data were normalized relative to the well with the highest and lowest signal and (B) Comparison of ligand-driven thermal stability of the LRH-1 LBD. The inflection point corresponds to the temperature at which the protein unfolds. (C) Luciferase reporter assay (HeLa cells), comparing the effect of small molecules on LRH-1 activity. Doses correspond to 1.0 e-7, 1.0 e-6, and 1.0 e-5 M (ANT1 and ANT2), 5.0 e-8, 5.0 e-7, and 5.0 e-6 M (6N), or 1.0 e-6, 1.0 e-5, and 1.5 e-5 M (ANT3-ANT6). Two-way ANOVA with Dunnett multiple comparisons test, *p < 0.05, **p < 0.01, ***p < 0.001, ****p < 0.0001. Data are shown as mean ± SEM from three independent experiments (FP), three independent experiments (thermal shift), or three biological replicates (luciferase). Data normalized to signal of DMSO (no agonist) control for luciferase reporter and thermal shift assays. (D) Split luciferase assay (U2OS cells) testing compound-mediated interaction between LRH-1 and coactivators PGC-1α (top) and SRC3 (bottom). Transfected cells were treated with 5.0 e-6 (6N) or 1.0 e-5 (ANT3, ANT4, and ANT6) of indicated small molecules for 24 hours. "No Coreg" control indicates signal from cells transfected with LRH-1 fused to fragment of luciferase (NLuc1) and an empty NLuc2 vector. Data normalized to signal of DMSO (no agonist) control and shown as mean + SEM from four biological replicates. One sample t and Wilcoxon test, #p < 0.1, *p < 0.05, **p < 0.01, ****p < 0.0001.

we also see a decrease in the thermal stability of the protein due to the small molecule's alteration of the protein confirmation. In order to compare the decrease of transcriptional activity, all antagonists were compared via a luciferase reporter assay. In this assay there is a significant decrease of activity from ANT3. While ANT1 and ANT2 showed minor activation of LRH-1 transcriptional activity, similarly to known agonist 6N, ANT4-6 had no effect on the transcriptional activity (Figure 4.4C). Furthermore, ANT3 had significant decrease, while the current best known antagonists for LRH-1, Cpd3, had no effect within this assay (previously shown antagonism by qPCR).[42] Finally, we looked into supporting the proposed mechanism of action of disrupting the binding between LRH-1 and coactivators. As seen in Figure 4.4D, two coactivator were tested via a split luciferase assay. Through this assay there is a significant decrease in the interactions of both coactivators PGC-1α and SRC3.

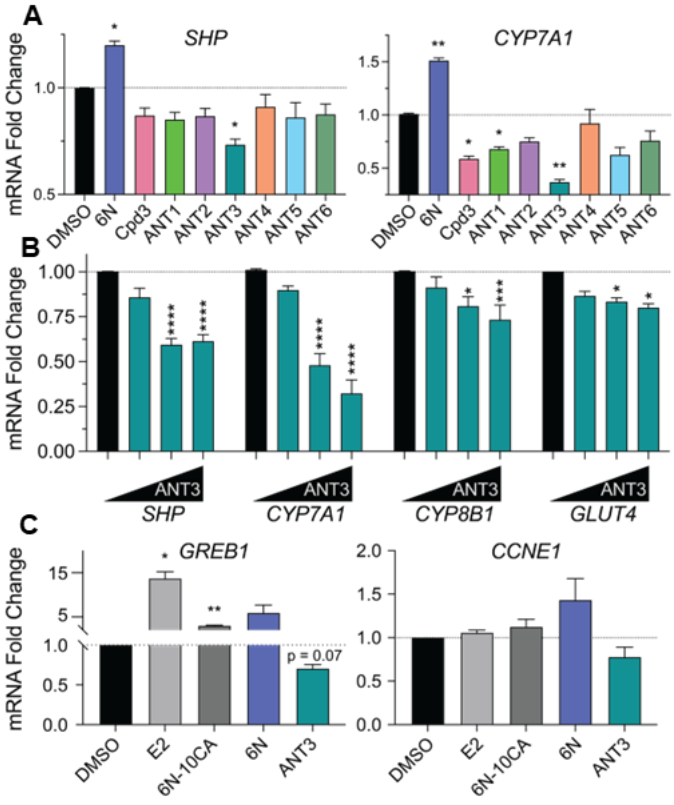

Figure 4.5: ANT3 decreases the expression of LRH-1 target genes in HepG2 cells

(A) RT-qPCR analysis of compound-mediated mRNA levels of *SHP* and *CYP7A1* in HepG2 cells treated with indicated small molecules (10 μM) for 24 hours. Brown-Forsythe and Welch One-Way ANOVA with Dunnett T3 Multiple Comparisons Test, *p < 0.05, **p < 0.01. (B) RT-qPCR analysis of indicated genes in HepG2 cells treated with ANT3 (1.0 e-6, 1.0 e-5, and 2.0 e-5 M) for 24 hours. Data normalized to signal of DMSO control (black) and shown as mean + SEM from three biological replicates. Two-Way ANOVA with Dunnett Multiple Comparisons Test, *p < 0.05, **p < 0.01, ***p < 0.001, ****p < 0.0001. **C.** RT-qPCR analysis of compound-mediated mRNA levels of *GREB1* and *CCNE1* in MCF-7 cells in charcoal-stripped media treated with indicated small molecules (10 μM) for 24 hours. Brown-Forsythe and Welch One-Way ANOVA with Dunnett T3 Multiple Comparisons Test, *p < 0.05, **p < 0.01.

We desired to look at this system in a direct biological context. Therefore, we performed quantitative PCR (qPCR) to calculate the levels of mRNA that resulted from LRH-1 activity. Specially, we looked at two gene, SHP and CYP7A1, because they are highly regulated by LRH-1 in

HepG2 cells (a liver cell line). From this study we found that in our hands, ANT3 is the only compound that shows a significant decrease in SHP expression and has the largest decrease in CYP7A1 expression. Furthermore, ANT3 showed decreased expression of CYP8B1 and GLUT4 when compared to the DMSO control. In a breast cancer cell line, MCF-7, ANT3 shows a minor decrease in the gene products GREB1 and CCNE1 (cyclin E) that are involved in the proliferation of tumor cells. From this data, we have support for the efficacy of the repurposed scaffold having an effect in cancer cell lines.

After supporting antagonism from biological data, we further investigated the mechanism of action. Due to the destabilization of H12 on the LRH-1 structure, crystallization efforts have been unfruitful. Therefore, we turned to molecular dynamics (MD) as a mechanism to model the structure in the binding pocket. As seen in Figure 4.6, there are two possible sites of interaction from the 6N crystal structure. From there accelerated MD (aMD), on the LRH-1 LBD we see that

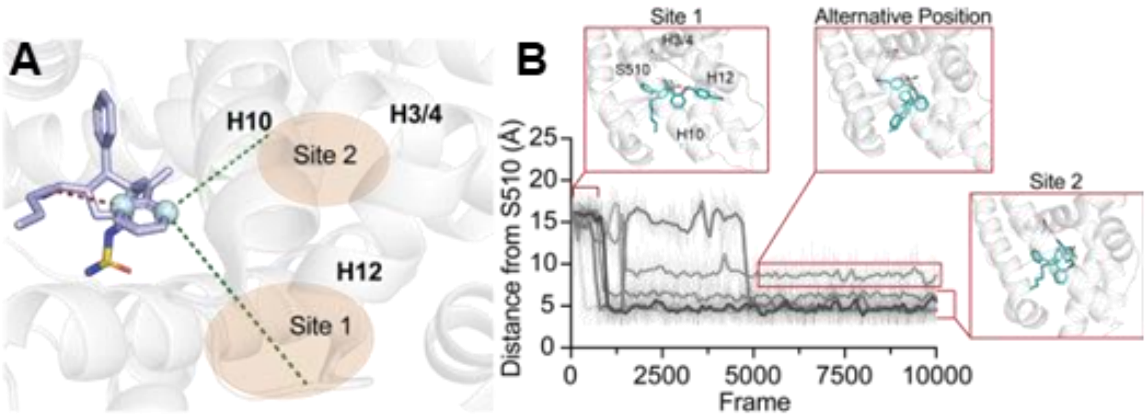

Figure 4.6: ANT3 orientation and effect on LRH-1 conformation

(A) Potential starting positions for the ANT3 modification are indicated. The carbons on the structure of 6N (PDB 6OQY; light purple), where the modification extends from, are marked with light blue spheres. The red dotted line shows an orientation that would likely clash with the compound and was thus excluded from consideration as a starting point. Green dotted lines indicate directions with room in the protein for modification without considerable rearrangement of neighboring residue side chains. These regions are marked as "Site 1" and "Site 2." Site 1 was chosen as the starting position for aMD simulations because it was in a region with no secondary structure, and thus permitted the greatest potential for ligand rearrangement. (B) Accelerated molecular dynamics simulations (6 x 1000-ns) of the LRH-1 LBD bound to ANT3. Each simulation is represented by a line (dark line = averaged values; light line = values from individual frames). The position of ANT3 is shown in three sites. Site 1 corresponds to the starting position near the loop between H10 and H12. Site 2 corresponds to the position where the ligand was stably oriented for five of six simulations. "Alternative Position" reflects the orientation of ANT3 in one of the six simulations. Time spent in each orientation is determined by measuring the distance between the ANT3 modification and S510 (side chain shown as sticks). Ten thousand frames were used for analysis for each simulation.

the preferred orientation for the benzonitrile moiety was site 2 (indicated in Figure 4.6B). As seen in Figure S1, the nitrile is coordinated by several residues within the pocket.

Lastly, with the added benzonitrile group on the structure there was a great loss in the binding affinity of the compound. From previous studies, we have found that the addition of a carboxylic acid on a 10-carbon tail increases the potency of the compound to the LRH-1 LBD, due to contact with amino acids Y516 and K520 at the mouth of the pocket.[38,40] Due to this we synthesized a new compound ANT3-10CA (Figure 4.7). This compound increased the binding affinity for LRH-1. Although the affinity was increased for the compound, there was no increase in potency or efficacy.

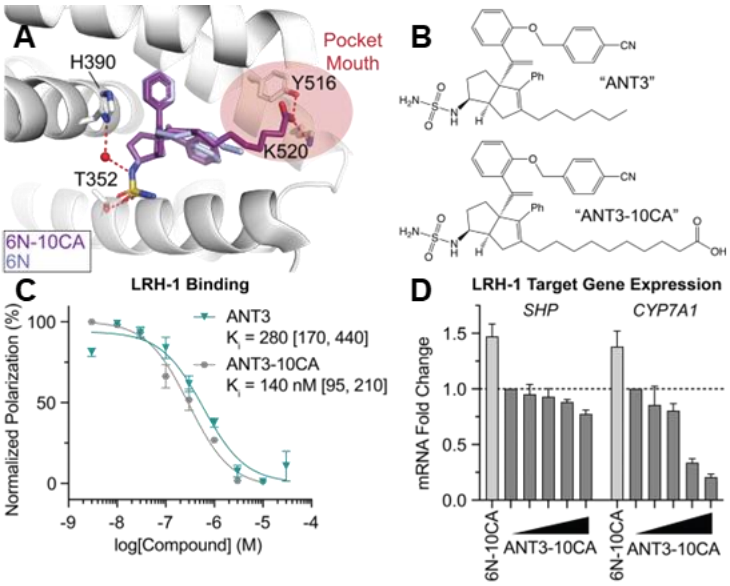

Figure 4.7: The addition of mouth-contacting groups enhances affinity while maintaining antagonism

(A) Overlay of 6N (PDB 6OQY; light purple) and 6N-10CA (PDB 7TT8; dark purple). Side chains of central residues responsible for deep pocket and pocket mouth (highlighted in red) binding are shown as sticks (O=red, N=blue, S=yellow). (B) Chemical structure of ANT3 and ANT3-10CA. (C) FP competition assay showing binding of ANT3 and ANT3-10CA to the LRH-1 LBD. K_i: inhibition constant. 95% confidence intervals are shown in brackets. Data were normalized relative to the well with the highest and lowest signal and shown as mean ± SEM from three independent experiments. (D) RT-qPCR analysis of indicated genes in HepG2 cells treated with 6N-10CA (light gray; 2.0 e-5) or ANT3-10CA (dark gray; from left to right: DMSO control, 1.0 e-7, 1.0 e-6, 1.0 e-6, and 2.0 e-5 M) for 24 hours. Data normalized to signal of DMSO control and shown as mean + SEM from three biological replicates. ANT3-10CA bound the LRH-1 LBD with a two-fold greater affinity in FP competition assays. While 6N-10CA enhanced *SHP* and *CYP7A1* mRNA levels, ANT3-10CA decreased both in a dose-dependent manner, showing a similar potency and efficacy as ANT3. This highlights both the utility of inclusion of the 10CA tail for improving compound binding and indicates that modifications in the R^2 group supersede the agonistic effects of favorable pocket mouth contacts.

4.3 Conclusion

In conclusion, we were able to alter the association of coactivators to LRH-1 via manipulation of H12. Through studies in a cancer cell line, we see a decrease in genes that are involved in the proliferation, invasion, and metastasis of tumors. This led to the creation of the first nanomolar binding LRH-1 antagonist.

4.4 Supplemental information

Supplemental figures

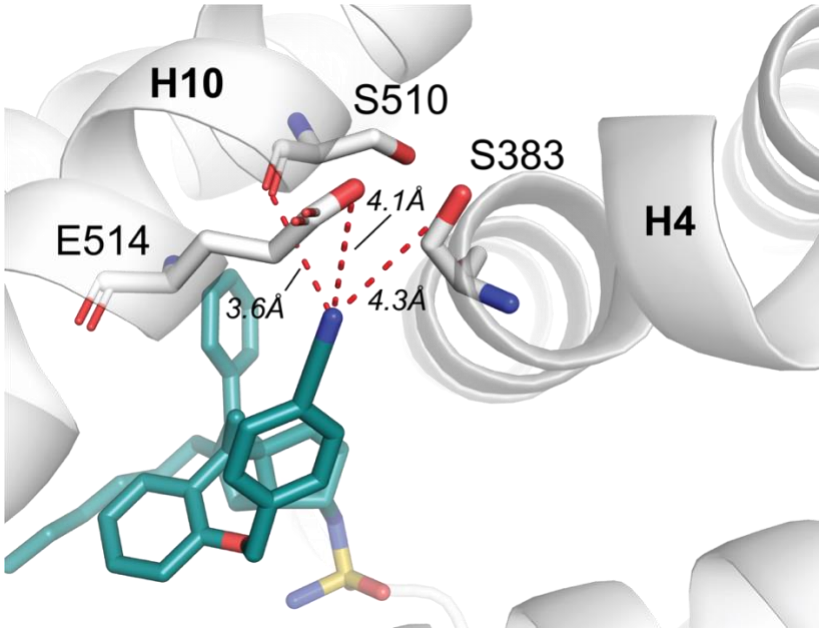

Supplemental figure 4.S1. ANT3 binding pose. Representation of ANT3 binding pose identified from aMD simulations. This also represents the starting position of ANT3 used for classical MD simulations. Residues near ANT3 are shown as sticks and distances between ANT3 benzonitrile and these residues are indicated (C=white or teal, O=red, N=blue, S=yellow).

Cell culture

HeLa and U2OS cells were cultured in phenol red-free MEMα + 10% fetal bovine serum (FBS) – charcoal/dextran treated (FBS-S), while HepG2 and MCF-7 cells were cultured in phenol red-free DMEM + 10% FBS. Cell lines were cultured under standard conditions (5% CO_2, 37°C) and were verified to be mycoplasma free with the LookOut® Mycoplasma PCR Detection Kit.

Data analysis and visualization

For biological replicates (cell-based experimental work) or independent experiments (*in vitro* work), technical replicates were averaged prior to data analysis. The number of biological replicates and independent experiments are indicated in figure legends. Bar charts, curves, and line graphs were constructed with GraphPad Prism version 9, structural figures were constructed with

either PyMol or VMD, and difference distance matrices were constructed with Bio3D. GraphPad Prism version 9 was used for all data analyses. All figures were constructed using Adobe Illustrator 2021 (Adobe Inc.). Values were consistently reported with two significant figures.

Protein expression and purification

LRH-1 LBD was expressed and purified as described previously. Briefly, BL21(DE3) *E. coli* cells were transformed with human LRH-1 LBD (residues 299-541) with an N-terminal 6xHis tag in a pMCSG7 vector. Bacteria were grown at 37°C in liquid broth until cells reached OD_{600} 0.6. Protein expression was then induced with 1 mM IPTG for 4 hours at 30°C. Cells were centrifuged and stored at -80°C. After one freeze-thaw cycle, the pellet was resuspended in lysis buffer (20 mM Tris-HCl, 150 mM NaCl, 5% glycerol, 25 mM imidazole, 0.2 mM PMSF, DNase, lysozyme, pH 7.4) and lysed via sonication. Lysate was subjected to Ni^{2+} affinity chromatography. For FP competition assays, co-purified bacterial lipids were exchanged with DLPC by incubating LRH-1 LBD with a four-fold molar excess of DLPC for 16 h at 4°C. Resulting complexes were then purified with size-exclusion chromatography (SEC) into assay buffer (150 mM NaCl, 20 mM Tris-HCl, 5 % glycerol, pH 7.4) and stored at -80°C. Protein used for thermal stability and peptide recruitment assays was purified similarly but was not complexed with DLPC before SEC purification.

Ligand binding

FP competition assays were performed as previously described. Briefly, experiments were conducted in black 384-well plates in assay buffer (150 mM NaCl, 20 mM Tris-HCl, 5% glycerol, pH 7.4). 6N conjugated to FAM (10 nM/well) was incubated with LRH-1 LBD (5 nM/well). Unlabeled compounds were added at concentrations indicated in the figures. Each experiment was performed three times with four technical replicates each. Technical replicates were averaged and

normalized independently before the final data analysis. Using GraphPad Prism (version 9), data were fit to a one-site, fit K_i curve, assuming a final probe concentration of 10 nM and probe affinity of 9 nM, based on forward binding assays for LRH-1 LBD and 6N-FAM recently reported (see **Supplemental figure 3.1**). Data were excluded from wells with 1.0 e-4 M ANT3 and 1.0 e-4 and 3.0 e-4 M ANT3-10CA, as the resulting points increased sharply after ligand saturation, distorting the curve fit.

Reporter assays

LRH-1 reporter assays were conducted as described previously. Briefly, HeLa cells were seeded at ~ 10,000 cells per well in 96-well plates (white-walled, clear bottom) in MEMα + 10% FBS-S. When cells reached 80-90% confluence, they were transfected with LRH-1 (5 ng/well), a reporter plasmid with an LRH-1 response element derived from the SHP promoter cloned upstream of firefly luciferase (50 ng/well), p300 in a pcDNA vector (or empty pcDNA vector) (10 ng/well), and a plasmid expressing Renilla luciferase constitutively from a CMV promoter (1 ng/well). Cells were transfected with FuGENE at a ratio of 4:1 (FuGENE: DNA). Twenty-four hours after transfection, compounds were diluted in Opti-MEM and introduced to cells at final concentrations indicated in figure legends (final DMSO concentration was 0.37%). After ~ 24 hours, the luciferase signal was measured using the DualGlo kit (Promega). Each experiment was conducted with three biological replicates, each with three technical replicates averaged before data analysis. Firefly luciferase signal for each well was divided by the well's Renilla signal intensity and normalized relative to the DMSO control. Data were analyzed with GraphPad Prism (version 9), using a stimulating dose-response curve (three parameters – Hill slope = 1).

Protein thermal stability

Thermal stability of the LRH-1 LBD complexed with ligands was determined using a Tycho™ NT.6 Nanotemper as described previously. LRH-1 LBD was incubated with a 5-fold molar excess of ligand (final DMSO concentration was 1.4%) overnight at 4 °C in assay buffer (150 mM NaCl, 20 mM Tris-HCl, 5% glycerol, pH 7.4). Samples were loaded into capillaries, and tryptophan/tyrosine fluorescence was monitored at wavelengths 330 and 350 nm over a 30 °C/min gradient (35°C – 95°C). The melting point (inflection point) was determined with Tycho™ NT.6 software. Three separate experiments were conducted in triplicate. Technical replicates were averaged, and data were plotted using GraphPad Prism (version 9).

Coregulator binding

U2OS cells were seeded at ~ 10,000 cells per well in 96-well plates (white-walled, clear bottom) in MEMα + 10% FBS. When cells reached 80-90% confluence, they were transfected with LRH-1 fused to the N-terminal fragment of NanoLuc luciferase (15 ng/well), coregulator (PGC-1α or SRC3) fused to the C-terminal fragment of NanoLuc luciferase (15 ng/well), and empty VENUS vector (15 ng/well; signal was used to verify that there was not notable compound cytotoxicity). Vectors were generated using LR Clonase™ II enzyme reaction (Invitrogen™). Cells were transfected with FuGENE at a ratio of 4:1 (FuGENE: DNA). Twenty-four hours after transfection, compounds were diluted in Opti-MEM and introduced to cells at a final concentration of 1.0 e-5 M. After ~ 24 hours, the NanoLuc luciferase substrate (Nano-Glo® Luciferase Assay System, Promega) was diluted 1:100 in phosphate-buffered saline and introduced to cells. After ~ two minutes, the bioluminescence was measured. Each experiment was conducted with four biological replicates, each with five technical replicates averaged before data analysis. Data were normalized relative to the signal from DMSO control cells, and a one sample t and Wilcoxon test was used to assess differences driven by compounds.

Gene expression analysis

RT-qPCR was performed as described previously. HepG2 cells were seeded at 400,000 cells per well in 24-well plates in DMEM + 10% FBS. When cells reached ~ 90% confluence, media was exchanged with media containing compound or DMSO at the desired concentration (final DMSO concentration: 0.1% for compounds 6N, Cpd3, and ANT1-3 tested at 10 μM; 0.2% for compounds ANT4-6; 0.2% for ANT3 tested at 1, 10, and 20 μM). Synthetic ligands were added at concentrations indicated in figure legends. Experimental setup for MCF-7 cells was similar, though cells were plated at 250,000 cells/well in 12-well plates in DMEM + 10% FBS-S (to strip the cells of exogenous estrogens). After 24 hours of compound treatment, cell media was decanted, cells were washed with PBS, and cells were collected in RLT (+ 1% 2-mercaptoethanol) lysis buffer. Cells were stored at -80°C.

RNA was extracted from cells using the RNeasy® Mini Kit (QIAGEN), with on-column DNAse digestion. RNA was reverse transcribed with the High-Capacity cDNA Reverse Transcription Kit (Applied Biosystems™). cDNA was quantified using Power SYBR Green PCR Master Mix (Applied Biosystems), using *ACTB* as a housekeeping gene. C_t values were calculated by resident software on the StepOne Plus thermocycler. Data were normalized using the ΔΔCt method. Each experiment was conducted with three biological replicates, corresponding to different passage numbers or cells passaged independently for at least one week. Data were analyzed with GraphPad Prism (version 9), using a Brown-Forsythe and Welch One-Way ANOVA and Dunnett T3 Multiple Comparisons Test (comparing ligands) or Two-way ANOVA and Dunnett Multiple Comparisons Test (dose-response). Primers used for RT-qPCR were as follows:

hACTB

forward 5'-AGGCACCAGGGCGTGAT-3'

reverse 5’-GCCCACATAGGAATCCTTCTGAC-3’

hSHP

forward 5’-GCTTAGCCCCAAGGAATATGC-3’

reverse 5’-GTTCCAGGACTTCACACAGC-3’

hCYP7A1

forward 5’-GAGAAGGCAAACGGGTGAAC-3’

reverse 5’-GGATTGGCACCAAATTGCAGA-3’

hCYP8B1

forward 5’-GAAGCGCATGAGGACCAA-3’

reverse 5’-TTGCATATTGCCCAAAGTCTAGT-3’

hGLUT4

forward 5’-ATCCTTGGACGATTCCTCATTGG-3’

reverse 5’-CAGGTGAGTGGGAGCAATCT-3’

hCCNE1

forward 5’-ATCAGCACTTTCTTGAGCAACA-3’

reverse 5’-TTGTGCCAAGTAAAAGGTCTCC-3’

Accelerated molecular dynamics simulations

Two complexes were prepared for aMD simulations: LRH-1-ANT3; and LRH-1-ANT5. TIF2 was excluded from complexes to more readily enable H12 repositioning. LRH-1 LBD complexes were generated by modeling ligands into the crystal structure of LRH-1-TIF2-PL (PDB 4PLE; chain A). Complexes included LRH-1 residues 299-540, and those with TIF2 contained residues 742-750 ($^{+}H_3N$-NALLRYLLD-CO_2^{-}) of TIF2. PDB 7JYE was used to add the two C-terminal residues (residues 539-540) of LRH-1 to complexes. To dock ligands, 6N was first guided

into the pocket using PDB 6OQ. Antagonists were then modeled using 6N as a template, building antagonist substituents using Maestro (Schrödinger, LLC). ANT modifications were positioned proximal to the loop between H10 and H12 to enable maximum mobility for repositioning in aMD simulations.

aMD was performed as described previously. After ligand docking, Maestro (Schrödinger, LLC) was used to optimize hydrogen bond assignments, add N- and C-terminal caps to LRH-1 and TIF2, and run initial minimization on the structure. Parameters for ligands were obtained using Antechamber in AmberTools20. Systems were set up using the xleap tool in AmberTools20 of Amber 2020, with ff14SB (protein), GAFF2 (ligand), and TIP3P (water) forcefields. Complexes were solvated in an octahedral box of TIP3P water with a 10 Å buffer around the protein complex. Complexes were neutralized with Na^+ and Cl^- ions, which were introduced to the system at physiological buffer conditions (150 mM NaCl).

For minimization, 5000 steps of steepest descent were used, followed by 5000 steps of conjugate gradient minimization. Minimizations were performed with 500 kcal/mol·Å2 restraints on all protein and ligand atoms. Restraints were removed on all atoms except the ligand and TIF2 peptides, and the protocol was repeated. Restraints were removed on all atoms except the ligand, and the protocol was repeated. Restraints were subsequently lowered to 100 kcal/mol·Å2 and removed from all atoms for two final rounds of minimization. Minimized systems were heated from 0 to 300 K with a 100-ps MD run, with constant volume periodic boundaries and 10 kcal/mol·Å2 restraints on all protein and ligand atoms.

A 10-ns equilibration was performed for all complexes with 10 kcal/mol·Å2 restraints on the protein and ligand atoms using the NPT ensemble. Restraints were lowered to 10 kcal/mol·Å2, and the protocol was repeated. Restraints were removed from all non-ligand atoms, and the

protocol was repeated with a 1 kcal/mol·Å2 restraint on the ligand. The water molecule critical for ligand engagement deep within the pocket for 6N was restrained along with the ligand.

We selected the parameters for potential energy threshold (E_P), dihedral energy threshold (E_D), dihedral energy boost (α_D), and total potential energy boost (α_P) using published guidelines and the instructions provided in the Amber 2020 manual. All aMD calculations and simulations were performed using Amber20. Six 1000-ns simulations were performed for complexes of LRH-1-ANT3 and LRH-1-ANT5 (no TIF2). Average dihedral energy ($Eavg_D$) and average total potential energy ($Eavg_P$) were obtained from classical MD simulations using the following calculations:

$\boldsymbol{\alpha_D}$: $0.2 * (3.5\ kcal/mol * N_{sr})$

$\mathbf{E_D}$: $Eavg_D + 3.5\ kcal/mol * N_{sr}$

$\boldsymbol{\alpha_P}$: $0.16\ kcal/mol * N_{atom}$

$\mathbf{E_P}$: $Eavg_P + (0.16\ kcal/mol * N_{atom})$

N_{sr} = number of total protein residues (caps included in the calculation)

N_{atom} = total number of atoms

Production trajectories of 1000-ns were obtained for unrestrained complexes in the NPT ensemble. All bonds between heavy atoms and hydrogens were fixed with the SHAKE algorithm. A cutoff distance of 10 Å was used to evaluate long-range electrostatics with particle mesh Ewald and for van der Waals forces. Structural averaging was performed using the CPPTRAJ module of AmberTools. Six 1000-ns simulations were run and concatenated with CPPTRAJ, with every tenth frame (total of 60,000 frames) used for data analysis. Water, salt, and terminal caps were removed for data analysis. CPPTRAJ was used for distance analysis between S510 (side chain oxygen) and

ANT3 (nitrogen on benzonitrile) or ANT5 (carbon of carboxylic acid). Data was graphed with Prism (version 9).

Classical molecular dynamics simulations

For classical molecular dynamics simulations, similar protocols were used to generate, minimize, and equilibrate systems. Complexes for these simulations included: i) apo LRH-1-TIF2; ii) LRH-1-6N-TIF2; iii) LRH-1-ANT1-TIF2; iv) LRH-1-ANT3-TIF2. Note that for LRH-1-ANT3-Tif2, the ligand was positioned so that the benzonitrile was oriented toward the cleft between H3/4 and H10, as this was the region where the ligand was stably oriented towards in five out of six accelerated simulations. Four 500-ns simulations were run and concatenated with CPPTRAJ, with every fifth frame (total of 40,000 frames) used for data analysis. Water, salt, and terminal caps were removed for data analysis.

Structural averaging and RMSF analysis was conducted with CPPTRAJ. Difference distance matrices were constructed with Bio3D. Dynamic networks were constructed from trajectories using the NetworkView plugin in VMD and the Carma program. Networks are built by defining all protein Cα atoms as nodes, using Cartesian covariance (calculated in Carma) to measure communication within the network. Pairs of nodes that reside within a 4.5 Å cutoff for 75% of the simulation are connected via an edge. Suboptimal paths between nodes were identified using the Floyd−Warshall algorithm. Matrices visualizing the number of paths between every residue on LRH-1-PGC-1α-ligand and Tif2 was determined using a loop script reported previously: ./subopt contact.dat loop 50 $i $j (i=source; j=sink; 50=cutoff). This was conducted for i = residues on AF-2 and j = all LRH-1 and TIF2 residues. Suboptimal paths were visualized with Prism (version 9) and VMD.

Chemical synthesis

General information

All reactions were carried out in flame-dried glassware, equipped with a stir bar and under a nitrogen atmosphere with dry solvents under anhydrous conditions, unless otherwise noted. Solvents used in anhydrous reactions were purified by passing over activated alumina and storing under argon. Yields refer to chromatographically and spectroscopically (^{1}H NMR) homogenous materials, unless otherwise stated. Reagents were purchased at the highest commercial quality and used without further purification, unless otherwise stated. n-Butyllithium (n-BuLi) was used as a 2.5 M solution in hexanes (Aldrich), was stored at 4°C and titrated prior to use. Organic solutions were concentrated under reduced pressure on a rotary evaporator using a water bath. Chromatographic purification of products was accomplished using forced-flow chromatography on 230-400 mesh silica gel. Thin-layer chromatography (TLC) was performed on 250μm SiliCycle silica gel F-254 plates. Visualization of the developed chromatogram was performed by fluorescence quenching or by staining using $KMnO_4$, *p*-anisaldehyde, or ninhydrin stains.

^{1}H and ^{13}C NMR spectra were obtained from the Emory University NMR facility and recorded on a Bruker Avance III HD 600 equipped with cryo-probe (600 MHz), INOVA 600 (600 MHz), INOVA 500 (500 MHz), INOVA 400 (400 MHz), VNMR 400 (400 MHz), or Mercury 300 (300 MHz), and are internally referenced to residual protio solvent signals. Data for ^{1}H NMR are reported as follows: chemical shift (ppm), multiplicity (s = singlet, d = doublet, t = triplet, q = quartet, m = multiplet, dd = doublet of doublets, dt = doublet of triplets, ddd= doublet of doublet of doublets, dtd= doublet of triplet of doublets, b = broad, etc.), coupling constant (Hz), integration, and assignment, when applicable. Data for decoupled ^{13}C NMR are reported in terms of chemical shift and multiplicity when applicable. Liquid Chromatography Mass Spectrometry (LC-MS) was

performed on an Agilent 6120 mass spectrometer with an Agilent 1220 Infinity liquid chromatography inlet. Preparative High-Pressure Liquid chromatography (Prep-HPLC) was performed on an Agilent 1200 Infinity Series chromatograph using an Agilent Prep-C18 30 x 250 mm 10 μm column, or an Agilent Prep-C18 21.2 x 100 mm, 5 μm column.

Methods and characterization data

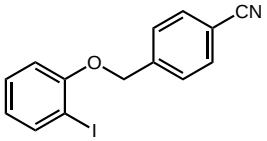

4-((2-iodophenoxy)methyl)benzonitrile (**S1**): A round bottom flask was charged with a stir bar, 2-iodophenol (10 g, 45.5 mmol, 1.1 equiv), K_2CO_3 (11.4 g, 82.6 mmol, 2.0 equiv), and 4-(bromomethyl)benzonitrile (8.1 g, 41.3 mmol, 1.0 equiv). Acetonitrile was added and the resulting orange mixture was stirred at 75 ^oC for 16 h before being cooled to room temperature. The reaction mixture was diluted with ethyl acetate and washed with brine (3x 200 mL) and a saturated sodium bicarbonate solution (3x 200 mL). The organic layer was dried over sodium sulfate, filtered, and concentrated via rotary evaporation. The title compound (13.4 g, 97% yield) was isolated as a tan solid after purification by flash column chromatography (10% EtOAc/Hex eluent).

^{1}HNMR (400 MHz, $CDCl_3$) δ 7.81 (dd, *J* = 7.8, 1.6 Hz, 1H), 7.69 (m, 2H), 7.66-7.61 (m, 2H), 7.30 (ddd, *J* = 8.2, 7.4, 1.6 Hz, 1H), 6.82 (dd, *J* = 8.2, 1.4 Hz, 1H), 6.76 (td, *J* = 7.6, 1.3 Hz, 1H), 5.18 (s, 2H).

^{13}CNMR (101 MHz, $CDCl_3$) δ 156.58, 141.93, 139.76, 132.46, 129.61, 127.32, 123.38, 118.77, 112.50, 111.69, 86.65, 69.72.

LRMS (**APCI**) m/z $[M+H]^+$ calc'd for $C_{14}H_{10}INO$, 335.1, found 335.1

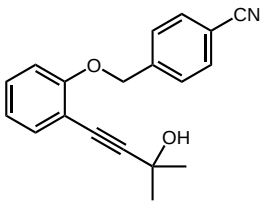

4-((2-(3-hydroxy-3-methylbut-1-yn-yl)phenoxy)methyl)benzonitrile (**S2**): A flame-dried 3-neck flask under vacuum was charged with a stir bar, bis(triphenylphosphine)palladium dichloride (256.9 mg, 0.4 mmol, 0.01 equiv), and copper iodide (209.2 mg, 1.1 mmol, 0.03 equiv). The flask was backfilled (3x) with nitrogen and triethylamine (366 mL) and **S1**(12.3 g, 36.6 mmol, 1.0 equiv) were added. The solution was sparged for 45 minutes before the addition of 2-methylbut-3-yn-2-ol (4.2 mL, 43.9 mmol, 1.2 equiv). The reaction was stirred under a nitrogen atmosphere at 60 ^{o}C for 16 h. The reaction was cooled to room temperature and diluted to ether before being filtered through a celite plug. The concentrate of the reaction was purified by flash column chromatography (20-40% EtOAc/Hex eluent) to afford the title compound as a tan solid (8.9 g, 84% yield).

^{1}HNMR (600 MHz, Chloroform-*d*) δ 7.68 (d, *J* = 8.3 Hz, 2H), 7.64 (d, *J* = 8.3 Hz, 2H), 7.42 (dd, *J* = 7.6, 1.7 Hz, 1H), 7.29 – 7.26 (m, 1H), 6.95 (td, *J* = 7.5, 1.0 Hz, 1H), 6.88 (dd, *J* = 8.3, 1.0 Hz, 1H), 5.19 (s, 2H), 1.63 (s, 6H).

^{13}CNMR (151 MHz, $CDCl_3$) δ 158.57, 142.38, 133.51, 132.23, 129.66, 127.10, 121.34, 118.19, 112.81, 112.46, 111.59, 98.36, 78.11, 69.21, 65.70, 31.48.

LRMS (**APCI**) m/z $[M+H]^+$ calc'd for $C_{19}H_{17}NO_2$, 291.4, found 291.1.

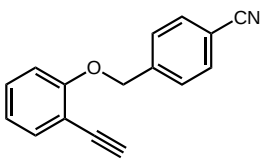

4-((2-ethynylphenoxy)methyl)benzonitrile (**S3**): To a round bottom flask charged with **S2** (1.2 g, 4.2 mmol, 1 equiv), finely powdered potassium hydroxide (712.5 mg, 12.7 mmol, 3 equiv), and a stir bar. The solids were dissolved in toluene (28 mL) before being fixed with a reflux condenser and refluxed for 4 h. After TLC showed completion the reaction was cooled to room temperature and filtered through a plug of celite. The yellow filtrate was concentrated and purified by flash chromatography (20% EtOAc/Hex) to afford the title compound as a tan solid (414.2 mg, 42% yield).

^{1}HNMR (600 MHz, Chloroform-*d*) δ 7.68 (d, *J* = 8.2 Hz, 2H), 7.60 (d, *J* = 8.3 Hz, 2H), 7.51 (dd, *J* = 7.6, 1.7 Hz, 1H), 7.31 – 7.27 (m, 1H), 6.96 (td, *J* = 7.5, 1.0 Hz, 1H), 6.86 (d, *J* = 8.3 Hz, 1H), 5.23 (s, 2H), 3.33 (s, 1H).

^{13}CNMR (151 MHz, $CDCl_3$) δ 159.08, 142.21, 134.31, 132.35, 130.15, 127.12, 121.33, 118.64, 112.46, 112.14, 111.62, 81.58, 79.68, 69.30.

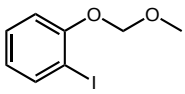

1-iodo-2-(methoxymethoxy)benzene (**S4**): A flame-dried 3-neck flask under vacuum was charged with a stir bar, K_2CO_3 (55.3 g, 400 mmol, 4 equiv) and 2-iodophenol (22.0 g, 100 mmol, 1 equiv). The flask was backfilled 3x with nitrogen before the addition of DMF (500 mL). The resulting solution was cooled to 0 ^{o}C before the addition of chloromethyl methyl ether (11.4 mL, 150 mmol, 1.5 equiv). The reaction stirred while warming to room temperature overnight. After 16 h, the reaction was cooled to 0 ^{o}C before being quench with water and being extracted with EtOAc (2x). The combined organic layers were washed with sodium bicarc (2x) before being dried, filtered, and concentrated. The crude material was columned 0-10% EtOAc/Hex to give the title product (11.9 g, 51% yield). The title compound matched previously reported spectra.[79]

^{1}HNMR (500 MHz, Chloroform-*d*) δ 7.78 (dd, *J* = 7.8, 1.6 Hz, 1H), 7.29 (ddd, *J* = 8.8, 7.4, 1.6 Hz, 1H), 7.08 (dd, *J* = 8.3, 1.4 Hz, 1H), 6.76 (td, *J* = 7.6, 1.4 Hz, 1H), 5.25 (s, 2H), 3.52 (s, 3H).

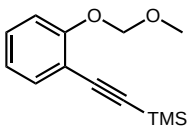

((2-(methoxymethoxy)phenyl)ethylnyl)trimethylsilane (**S5**): A flame-dried 3-neck flask under vacuum was charged with a stir bar, bis(triphenylphosphine)palladium dichloride (358 mg, 0.5 mmol, 0.01 equiv), and copper iodide (291 mg, 1.5 mmol, 0.03 equiv). The flask was backfilled (3x) with nitrogen and triethylamine (51 mL) and **S4** (11.9 g, 51 mmol, 1 equiv) were added. The solution was sparged for 45 minutes before the addition of trimethylsilylacetylene (8.0 mL, 56.1 mmol, 1.1 equiv). The reaction was stirred under a nitrogen atmosphere at 60 ^{o}C for 16 h. The reaction was cooled to room temperature and diluted to ether before being filtered through a celite plug. The concentrate of the reaction was purified by flash column chromatography (10% EtOAc/Hex eluent) to afford the title compound as a yellow oil (8.8 g, 75% yield). The title compound matched previously reported spectra.[79]

^{1}HNMR (500 MHz, Chloroform-*d*) δ7.44 (dd, *J* = 7.7, 1.7 Hz, 1H), 7.28 – 7.21 (m, 1H), 7.07 (dd, *J* = 8.3, 1.1 Hz, 1H), 6.95 (td, *J* = 7.6, 1.1 Hz, 1H), 5.25 (s, 2H), 3.54 (s, 3H), 0.26 (s, 9H).

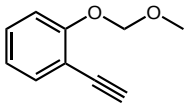

1-ethynyl-2-(methoxymethoxy)benzene (**S6**): A round bottom flask was charged with a stir bar and potassium fluoride (7.9 g, 135 mmol, 3.5 equiv). Methanol (125 mL) was added followed by **S5** (8.8 g, 37.6 mmol, 1.0 equiv). The reaction proceeded overnight at room temperature before

being concentrated. The crude mixture was resuspended in MTBE and was washed with water (3x). The organic layer was dried, filtered, and concentrated before the crude material was columned in 10% EtOAc/Hex to give the title compound (5.6 g, 91% yield) as a yellow oil. The title compound matched previously reported spectra.[79]

^{1}HNMR (500 MHz, Chloroform-*d*) δ 7.48 (dd, *J* = 7.6, 1.8 Hz, 1H), 7.34 – 7.28 (m, 1H), 7.14 (dd, *J* = 8.4, 1.1 Hz, 1H), 6.97 (td, *J* = 7.5, 1.1 Hz, 1H), 5.28 (s, 2H), 3.53 (s, 3H).

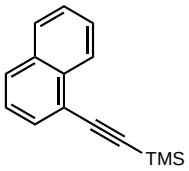

Trimethyl(napthalen-1-ylethynyl)silane (**S7**): A flame-dried 3-neck flask under vacuum was charged with a stir bar, bis(triphenylphosphine)palladium dichloride (281 mg, 0.4 mmol, 0.01 equiv), and copper iodide (228 mg, 1.2 mmol, 0.03 equiv). The flask was backfilled (3x) with nitrogen and triethylamine (40 mL) and 1-bromonapthalene (5.6 mL, 40 mmol, 1 equiv) were added. The solution was sparged for 45 minutes before the addition of trimethylsilylacetylene (6.8 mL, 48 mmol, 1.2 equiv). The reaction was stirred under a nitrogen atmosphere at 60 ^{o}C for 16 h. The reaction was cooled to room temperature and diluted to ether before being filtered through a celite plug. The concentrate of the reaction was purified by flash column chromatography (10% EtOAc/Hex eluent) to afford the title compound as a yellow oil (2.4 g, 27% yield). The title compound matched previously reported spectra.[80]

^{1}HNMR (500 MHz, Chloroform-*d*) δ 8.34 (d, *J* = 8.3 Hz, 1H), 7.83 (t, *J* = 8.6 Hz, 2H), 7.71 (dd, *J* = 7.2, 1.2 Hz, 1H), 7.58 (ddd, *J* = 8.3, 6.8, 1.4 Hz, 1H), 7.52 (ddd, *J* = 8.2, 6.9, 1.3 Hz, 1H), 7.41 (dd, *J* = 8.3, 7.1 Hz, 1H), 0.34 (s, 9H).

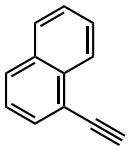

1-ethynylnapthalene (**S8**): A round bottom flask was charged with a stir bar and potassium fluoride (2.2 g, 38.5 mmol, 3.5 equiv). Methanol (37 mL) was added followed by **S7** (2.4 g, 11 mmol, 1.0 equiv). The reaction proceeded for 48 h at room temperature before being concentrated. The crude mixture was resuspended in MTBE and was washed with water (3x). The organic layer was dried, filtered, and concentrated before the crude material was columned in 10% EtOAc/Hex to give the title compound (1.5 g, 89% yield) as a yellow oil. The title compound matched previously reported spectra.[80]

^{1}HNMR (500 MHz, Chloroform-*d*) δ 8.38 (d, *J* = 8.3 Hz, 1H), 7.87 (d, *J* = 8.3 Hz, 2H), 7.75 (d, *J* = 7.0 Hz, 1H), 7.64 – 7.57 (m, 1H), 7.57 – 7.51 (m, 1H), 7.44 (t, *J* = 7.7 Hz, 1H), 3.49 (d, *J* = 1.4 Hz, 1H).

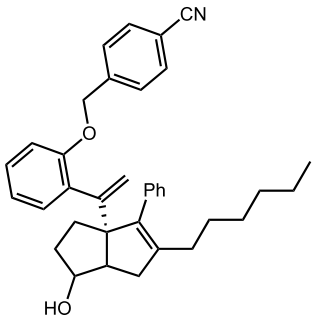

4-((2-(1-((3a*R*)-5-hexyl-1-hydroxy-4-phenyl-2,3,6,6a-tetrahydropentalen-3a(1*H*)-yl)vinyl)phenoxy)methyl)benzonitrile (**S9**): Hexahydropentalene formation was accomplished through slight modification of Whitby's procedure. Prior to cyclization, all non-volatile reagents were dried by azeotropic removal of water using benzene. A dry round bottom flask containing bis(cyclopentadienyl)zirconium(IV) dichloride (1.2 equiv) under nitrogen, was dissolved in

anhydrous, degassed tetrahydrofuran (THF, 8 mL/mmol enyne) and cooled to -78 °C. The resulting mixture was treated with n-BuLi (2.4 equiv) and the light yellow solution was stirred for 45 minutes. A solution of (tertbutyldimethyl((7-phenylhept-1-en-6-yn-3-yl)oxy)silane) (1.0 equiv) in anhydrous, degassed THF (8 mL/mmol) was added. The resulting salmon-colored mixture was stirred at -78 °C for 45 minutes before the cooling bath was removed. The reaction mixture continued to stir at room temperature for an additional 2.5 hours. The reaction mixture was then cooled to -78 °C and the required 1,1-dibromoheptane (1.1 equiv) was added as a solution in anhydrous THF (8 mL/mmol enyne) followed by freshly prepared lithium diisopropylamide (LDA, 1.0 M, 1.1 equiv.). After 15 minutes, a freshly prepared solution of lithium 4-((2-ethynylphenoxy)methyl)benzonitrile (3.6 equiv) in anhydrous THF (8 mL/ mmol enyne) was added dropwise and the resulting black solution was stirred at -78 °C for 1.5 hours. The reaction was quenched with methanol and saturated aqueous sodium bicarbonate slowly warming to room temperature, affording a light yellow slurry. The slurry was poured onto water and extracted with ethyl acetate four times. The combined organic layers were washed with brine, dried withNa_2SO_4, and concentrated in vacuo. The resulting yellow oil was passed through a short plug of silica (100% EtOAc eluent) and concentrated. The crude product was dissolved in THF and treated with either HCl or TBAF. The resulting solution stirred at room temperature for 16 h. The reaction mixture was concentrated and the diastereomers were purified and separated by flash chromatography. The mixture of stereoisomers were moved forward without further purification.

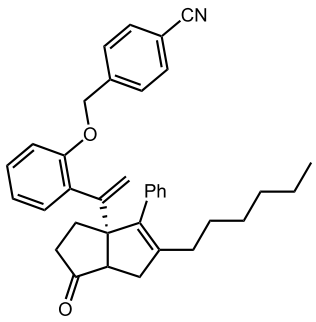

4-((2-(1-((3a*R*)-5-hexyl-1-oxo-4-phenyl-2,3,6,6a-tetrahydropentalen-3a(1*H*)-yl)vinyl)phenoxy)methyl)benzonitrile (S10): A scintillation vial was charged with a stir bar, **S9** (0.396 mmol, 205.0 mg), and MeCN (4 ml). The resulting solution stirred at 23 ºC then TPAP (0.0396 mmol, 13.9 mg) and NMO (3.96 mmol, 464.0 mg) added. The reaction solution continued to stir for 5 minutes before eluting through a plug of silica. The resulting crude material was then purified by flash chromatography on silica to collect the title compound (199.4 mg, quant.).

^{1}H NMR (400 MHz, $CDCl_3$) δ 7.63 (d, *J* = 8.3 Hz, 2H), 7.45 (d, *J* = 8.3 Hz, 2H), 7.34 – 7.19 (m, 6H), 7.11 (dd, *J* = 7.4, 1.8 Hz, 1H), 6.91 (td, *J* = 7.4, 1.1 Hz, 1H), 6.87 (dd, *J* = 8.4, 1.0 Hz, 1H), 5.35 (d, *J* = 1.7 Hz, 1H), 5.13 (d, *J* = 1.6 Hz, 1H), 5.08 (s, 2H), 2.62 (d, *J* = 7.2 Hz, 1H), 2.35 (d, *J* = 16.4 Hz, 1H), 2.24 – 1.91 (m, 7H), 1.31 – 1.11 (m, 8H), 0.83 (t, *J* = 7.0 Hz, 3H).

^{13}C NMR (101 MHz, $CDCl_3$) δ 155.39, 148.83, 145.03, 142.51, 137.57, 136.59, 132.44, 131.61, 130.80, 129.24, 128.55, 127.97, 127.51, 126.95, 120.84, 118.68, 116.14, 111.97, 111.72, 69.27, 66.14, 55.43, 37.92, 37.51, 31.58, 30.02, 29.36, 27.95, 27.84, 22.57, 14.09.

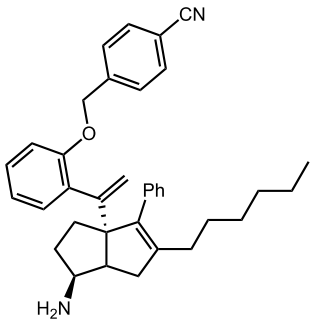

4-((2-(1-((1*S*,3a*R*)-1-amino-5-hexyl-4-phenyl-2,3,6,6a-tetrahydropentalen-3a(1*H*)-yl)vinyl)phenoxy)methyl)benzonitrile (S11): A reaction vial was charged with a stir bar, **S10** (0.899 mmol, 464.0 mg), and EtOH (6.5 ml). A solution of NH_3 in MeOH (7N, 35.96 mmol, 5.12 ml) followed immediately by $Ti(O^iPr)_4$ (1.35 mmol, 409 µl) was added and the vial sealed. The resulting solution was stirred at 23 ºC for 4.5 h before unsealing vial and adding $NaBH_4$ (2.7 mmol, 102.1 mg) and continuing stirring at 23 ºC for 16 h. Reaction was then diluted with EtOAc and saturated aqueous Rochelle's salt and sonicated for 5 min. The resulting slurry was washed twice with saturated aqueous Rochelle's salt, twice with H_2O, then brine. The organic layer was dried over Na_2SO_4, filtered, and filtrate concentrated under reduced pressure to collect the crude material. Crude material purified by flash chromatography on silica to collect the title compound (154.5 mg, 33% yield).

^{1}H NMR (400 MHz, $CDCl_3$) δ 7.66 – 7.61 (m, 2H), 7.48 (d, *J* = 8.0 Hz, 2H), 7.30 (dd, *J* = 6.6, 3.0 Hz, 2H), 7.24 – 7.17 (m, 4H), 7.12 (dd, *J* = 7.5, 1.8 Hz, 1H), 6.92 – 6.82 (m, 2H), 5.24 (d, *J* = 1.9 Hz, 1H), 5.07 (d, *J* = 3.4 Hz, 2H), 5.05 (d, *J* = 1.8 Hz, 1H), 3.17 (td, *J* = 9.7, 6.1 Hz, 1H), 2.53 (t, *J* = 8.4 Hz, 1H), 2.37 (d, *J* = 17.9 Hz, 1H), 2.19 – 2.01 (m, 3H), 1.75 (dtd, *J* = 11.7, 5.9, 2.1 Hz, 1H), 1.66 (ddd, *J* = 12.9, 6.1, 2.3 Hz, 1H), 1.55 (td, *J* = 12.3, 5.9 Hz, 1H), 1.44 – 1.13 (m, 9H), 0.85 (t, *J* = 6.9 Hz, 3H).

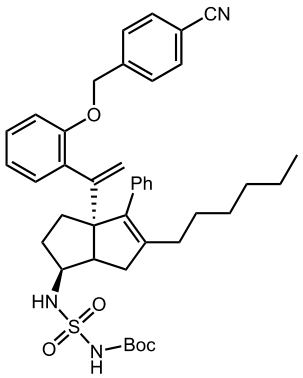

***tert*-butyl (*N*-((1*S*,3a*R*)-3a-(1-(2-((4-cyanobenzyl)oxy)phenyl)vinyl)-5-hexyl-4-phenyl-1,2,3,3a,6,6a-hexahydropentalen-1-yl)sulfamoyl)carbamate (S12):** An oven-dried vial was charged with a stir bar, ^{t}BuOH (2.2 mmol, 163.0 mg), and DCM (10.0 ml) then evacuated under reduced pressure and backfilled with nitrogen three times and cooled to 0 ºC. Chlorosulfonylisocyanate (2.0 mmol, 174 µl) was then added dropwise via syringe and the solution allowed to warm to 23 ºC over 35 minutes. A 1.89 ml portion of this solution was added slowly via syringe to a solution of **S11** (0.377 mmol, 195.0 mg) and Et_3N (0.566 mmol, 78 µl) in DCM (3.5 ml) at 0 ºC under nitrogen. This combined solution was allowed to warm to 23 ºC gradually over 16 h then diluted with EtOAc. The diluted solution was washed three times with 0.5 M HCl then H_2O and brine. The organic layer was dried over Na_2SO_4, filtered, and filtrate concentrated under reduced pressure to collect the crude material. Crude material purified by flash chromatography on silica to collect the title compound (98.6 mg, 38% yield).

^{1}H NMR (600 MHz, $CDCl_3$) δ 7.65 (d, *J* = 8.1 Hz, 2H), 7.48 (d, *J* = 7.9 Hz, 2H), 7.34 – 7.29 (m, 2H), 7.25 – 7.16 (m, 4H), 7.10 (dt, *J* = 7.4, 1.6 Hz, 1H), 6.91 (t, *J* = 7.4 Hz, 1H), 6.85 (d, *J* = 8.2 Hz, 1H), 5.28 (d, *J* = 1.7 Hz, 1H), 5.11 (s, 1H), 5.09 (d, *J* = 1.6 Hz, 1H), 3.70 (qd, *J* = 9.2, 6.5 Hz, 1H), 2.75 (t, *J* = 8.6 Hz, 1H), 2.43 (d, *J* = 17.4 Hz, 1H), 2.20 (dd, *J* = 17.3, 8.1 Hz, 1H), 2.15 – 2.10 (m, 2H), 1.78 (tdd, *J* = 8.9, 7.0, 6.3, 3.7 Hz, 1H), 1.68 (ddd, *J* = 13.3, 6.2, 2.7 Hz, 1H), 1.57 (td, *J* = 12.7, 12.2, 6.1 Hz, 1H), 1.46 (d, *J* = 1.5 Hz, 9H), 1.42 – 1.31 (m, 4H), 1.22 (td, *J* = 17.2, 9.8 Hz, 5H), 0.86 (t, *J* = 7.2 Hz, 3H).

^{13}C NMR (126 MHz, $CDCl_3$) δ 155.50, 150.24, 149.99, 143.67, 142.93, 138.64, 137.28, 132.53, 132.34, 130.51, 130.08, 129.89, 128.32, 127.86, 127.58, 126.74, 121.38, 118.82, 116.05, 84.34, 69.35, 58.35, 48.26, 34.91, 32.34, 31.70, 31.34, 29.95, 29.57, 29.35, 28.19, 28.12, 22.69, 14.19.

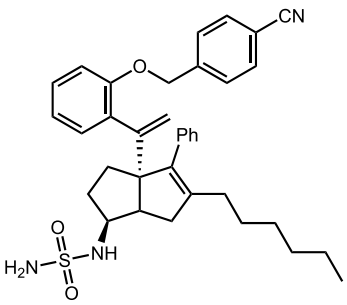

N-(3a-(1-(2-((4-cyanobenzyl)oxy)phenyl)vinyl)-5-hexyl-4-phenyl-1,2,3,3a,6,6a-hexahydropentalen-1-yl)sulfamide (Ant_3):A solution of 3:1 dioxane/concentrated aqueous HCl was frozen in an ice bath then allowed to slowly warm to 23 ºC. As soon as the entire solution had re-melted, 2.0 ml was transferred to a chilled (~0 ºC, but NOT in an ice bath) vial containing a stir bar and **S12** (0.14 mmol, 98.6 mg). The solution was allowed to slowly warm to 23 ºC and continue reacting for 20 h until **S12** was consumed. The reaction solution was diluted with EtOAc and washed four times with H_2O then twice with brine. The organic layer was dried over Na_2SO_4, filtered, and filtrate concentrated under reduced pressure to collect the crude material. This crude material was purified by flash chromatography on silica to collect the title compound (72.5 mg, 86%).

^{1}H NMR (500 MHz, $CDCl_3$) δ 7.66 – 7.62 (m, 2H), 7.50 – 7.46 (m, 2H), 7.32 – 7.26 (m, 2H), 7.27 – 7.17 (m, 4H), 7.09 (ddt, *J* = 7.3, 1.5, 0.5 Hz, 1H), 6.91 – 6.87 (m, 1H), 6.84 (ddt, *J* = 8.3, 1.0, 0.5 Hz, 1H), 4.48 (s, 1H), 4.38 (d, *J* = 8.3 Hz, 1H), 3.79 – 3.68 (m, 1H), 2.76 (t, *J* = 8.5 Hz, 1H), 2.37 (d, *J* = 17.2 Hz, 1H), 2.22 (dd, *J* = 17.2, 8.3 Hz, 1H), 2.10 (t, *J* = 7.5 Hz, 2H), 1.91 – 1.80 (m, 1H), 1.70 – 1.64 (m, 1H), 1.61 – 1.53 (m, 1H), 1.41 – 1.32 (m, 4H), 1.29 – 1.16 (m, 5H), 0.85 (t, *J* = 7.1 Hz, 3H).

^{13}C NMR (126 MHz, $CDCl_3$) δ 155.50, 150.15, 143.37, 142.95, 136.95, 132.55, 132.41, 130.45, 129.89, 128.30, 127.80, 127.59, 126.77, 120.95, 116.02, 69.52, 69.38, 57.15, 48.58, 34.91, 33.05, 31.71, 31.32, 29.95, 29.56, 28.24, 22.71, 14.20.

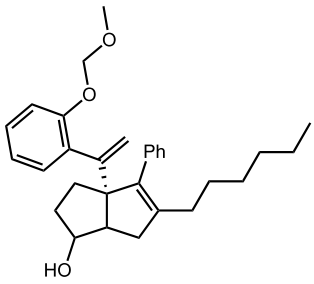

(3a*R*)-5-hexyl-3a-(1-(2-(methoxymethoxy)phenyl)vinyl)-4-phenyl-1,2,3,3a,6,6a-hexahydropentalen-1-ol (S13): Hexahydropentalene formation was accomplished through slight modification of Whitby's procedure.[38,40,57,60] Prior to cyclization, all non-volatile reagents were dried by azeotropic removal of water using benzene. A dry round bottom flask containing bis(cyclopentadienyl)zirconium(IV) dichloride (1.05 g, 3.6 mmol, 1.2 equiv) under nitrogen, was dissolved in anhydrous, degassed tetrahydrofuran (THF, 8 mL/mmol enyne) and cooled to -78 °C. The resulting mixture was treated with n-BuLi (2.9 mL, 7.2 mmol, 2.4 equiv) and the light yellow solution was stirred for 45 minutes. A solution of (tertbutyldimethyl((7-phenylhept-1-en-6-yn-3-yl)oxy)silane) (901.5 mg, 3.0 mmol, 1.0 equiv) in anhydrous, degassed THF (8 mL/mmol) was added. The resulting salmon-colored mixture was stirred at -78 °C for 45 minutes before the cooling bath was removed. The reaction mixture continued to stir at room temperature for an additional 2.5 hours. The reaction mixture was then cooled to -78 °C and the required 1,1-dibromoheptane (851.1 mg, 3.3 mmol, 1.1 equiv) was added as a solution in anhydrous THF (8 mL/mmol enyne) followed by freshly prepared lithium diisopropylamide (LDA, 1.0 M, 1.1 equiv.). After 15 minutes, a freshly prepared solution of lithium 4-((2-

ethynylphenoxy)methyl)benzonitrile (**S6**) (1.75 g, 10.8 mmol, 3.6 equiv) in anhydrous THF (8 mL/ mmol enyne) was added dropwise and the resulting black solution was stirred at -78 °C for 1.5 hours. The reaction was quenched with methanol and saturated aqueous sodium bicarbonate slowly warming to room temperature, affording a light yellow slurry. The slurry was poured onto water and extracted with ethyl acetate four times. The combined organic layers were washed with brine, dried withNa_2SO_4, and concentrated in vacuo. The resulting yellow oil was passed through a short plug of silica (100% EtOAc eluent) and concentrated. The crude product was dissolved in THF and treated with either HCl or TBAF. The resulting solution stirred at room temperature for 16 h. The reaction mixture was concentrated and the diastereomers were purified and separated by flash chromatography (10-30% EtOAc/Hex) to give the title compound as a mix of stereoisomers (960.4 mg, 72% yield)

Exo characteristic peaks: **^{1}H NMR** (600 MHz, $CDCl_3$) δ 7.44 – 7.41 (m, 1H), 7.36 – 7.34 (m, 2H), 7.30 – 7.27 (m, 2H), 7.22 (dddd, *J* = 8.2, 7.3, 3.9, 1.7 Hz, 2H), 7.05 (dd, *J* = 7.5, 1.8 Hz, 1H), 6.94 – 6.91 (m, 2H), 5.23 (d, *J* = 1.8 Hz, 1H), 5.11 (s, 2H), 5.06 (d, *J* = 1.8 Hz, 1H), 3.91 (t, *J* = 2.3 Hz, 1H), 2.66 (td, *J* = 8.4, 1.4 Hz, 1H), 2.61 – 2.46 (m, 3H), 2.28 – 2.11 (m, 3H), 2.09 – 2.04 (m, 2H), 1.85 – 1.78 (m, 1H), 1.75 (dtd, *J* = 12.0, 6.1, 4.3 Hz, 1H), 1.70 – 1.53 (m, 4H), 1.44 (dddd, *J* = 11.5, 10.4, 5.5, 2.3 Hz, 2H), 1.39 – 1.35 (m, 2H), 1.31 – 1.19 (m, 7H).

^{13}C NMR (151 MHz, $CDCl_3$) δ 154.28, 151.13, 143.32, 141.17, 139.12, 137.79, 133.61, 130.09, 129.97, 128.02, 127.54, 121.65, 115.03, 95.07, 81.75, 74.75, 69.51, 57.56, 56.31, 50.86, 39.69, 34.65, 33.18, 31.66, 31.18, 30.46, 29.91, 29.64, 29.48, 29.26, 28.03, 22.61, 14.10.

Endo characteristic peaks: **^{1}H NMR** (600 MHz, $CDCl_3$) δ 5.27 (d, *J* = 1.9 Hz, 1H), 5.09 (s, 2H), 5.03 (d, *J* = 1.9 Hz, 1H), 3.42 (s, 3H), 3.00 (dt, *J* = 12.9, 4.7 Hz, 1H).

^{13}C NMR (151 MHz, $CDCl_3$) δ 154.60, 139.51, 137.34, 132.87, 130.07, 129.81, 121.11, 115.67, 94.43, 69.30, 56.10, 52.13, 34.84, 28.23.

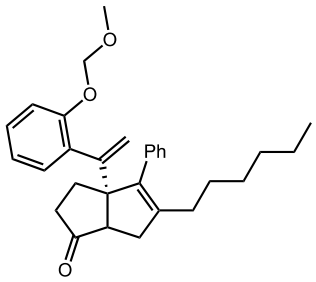

(3a*R*)-5-hexyl-3a-(1-(2-(methoxymethoxy)phenyl)vinyl)-4-phenyl-3,3a,6,6a-tetrahydropentalen-1(2*H*)-one (S14): A reaction vial was charged with a stir bar before the addition of **S13** (429.7, 0.96 mmol, 1.0 equiv) and Dess-Martin periodinane (489.7 mg, 1.15 mmol, 1.2 equiv) in dichloromethane (19.2 mL). The reaction stirred overnight before diluted with MTBE and being pushed through a plug of silica. The flow through was concentrated. The crude oil was purified via flash chromatography (10% EtOAc/Hex) to give the title compound (184.9 mg, 42% yield) as a clear oil.

^{1}H NMR (600 MHz, $CDCl_3$) δ 7.42 – 7.36 (m, 4H), 7.34 – 7.31 (m, 1H), 7.26 (ddd, *J* = 8.3, 7.4, 1.8 Hz, 1H), 7.11 (ddd, *J* = 16.0, 7.9, 1.4 Hz, 2H), 6.94 (td, *J* = 7.4, 1.1 Hz, 1H), 5.38 (d, *J* = 1.7 Hz, 1H), 5.15 (d, *J* = 6.8 Hz, 1H), 5.12 – 5.11 (m, 2H), 3.44 (s, 3H), 2.71 (d, *J* = 7.4 Hz, 1H), 2.43 (d, *J* = 16.3 Hz, 1H), 2.23 (ddd, *J* = 17.0, 7.2, 1.5 Hz, 2H), 2.12 (td, *J* = 7.3, 2.7 Hz, 2H), 2.07 – 1.96 (m, 3H), 1.34 – 1.24 (m, 4H), 1.21 (dt, *J* = 7.0, 2.1 Hz, 8H).

^{13}C NMR (151 MHz, $CDCl_3$) δ 154.56, 149.20, 144.80, 136.74, 131.92, 130.49, 129.28, 128.48, 127.93, 126.89, 121.16, 115.82, 113.98, 94.45, 66.03, 56.21, 37.95, 37.53, 31.58, 30.03, 29.39, 27.87, 27.63, 22.55, 14.06.

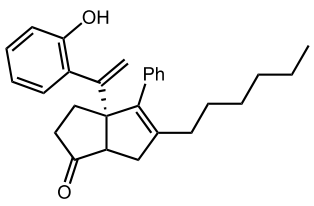

(3a*R*)-5-hexyl-3a-(1-(2-hydroxyphenyl)vinyl)-4-phenyl-3,3a,6,6a-tetrahydropentalen-1(2*H*)-one (S15): A reaction vial was charged with a stir bar and **S14** (163.7 mg, 0.4 mmol, 1.0 equiv) dissolved in dioxane (4.0 mL) and a few drops of concentrated HCl was then added. The reaction stirred overnight before being diluted with EtOAc and washed with 3 x 5 mL 0.5 M aqueous HCl, 5 ml water, and 5 mL brine. The organic layer was then dried over Na_2SO_4, filtered, and concentrated in vacuo to give the title compound (166.8 mg, Quant) after flash chromatography (10% Acetone/Hex).

^{1}H NMR (600 MHz, $CDCl_3$) δ 7.42 – 7.38 (m, 3H), 7.37 – 7.33 (m, 1H), 7.29 (d, *J* = 1.5 Hz, 1H), 7.22 (ddd, *J* = 8.1, 7.3, 1.7 Hz, 1H), 7.12 (dd, *J* = 7.6, 1.6 Hz, 1H), 6.94 (dd, *J* = 8.2, 1.1 Hz, 1H), 6.82 (td, *J* = 7.5, 1.2 Hz, 1H), 5.53 (d, *J* = 1.4 Hz, 1H), 5.33 (d, *J* = 1.4 Hz, 1H), 2.50 (d, *J* = 7.6 Hz, 1H), 2.38 – 2.34 (m, 1H), 2.16 – 2.01 (m, H), 1.96 (dd, *J* = 16.4, 7.5 Hz, 1H), 1.32 – 1.22 (m, 6H), 1.22 – 1.15 (m, 4H).

^{13}C NMR (151 MHz, $CDCl_3$) δ 152.15, 148.58, 145.93, 136.68, 136.41, 129.01, 128.97, 128.89, 128.29, 127.64, 127.28, 119.68, 118.24, 115.32, 65.95, 55.44, 38.64, 37.43, 31.54, 29.97, 29.38, 28.41, 27.66, 22.54, 14.05.

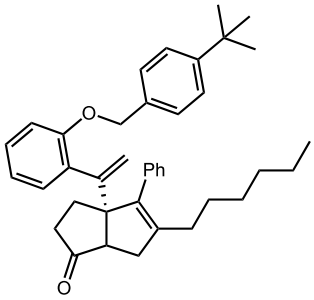

(3a*R*)-3a-(1-(2-((4-(*tert*-butyl)benzyl)oxy)phenyl)vinyl)-5-hexyl-4-phenyl-3,3a,6,6a-tetrahydropentalen-1(2*H*)-one (S16): To a flame-dried screw top vial with a stir bar backfilled (3x) was added **S15** (58.9 mg, 0.15 mmol, 1.0 equiv), 4-tertbutyl-benzyl benzoate (33 μL, 0.18 mmol, 1.2 equiv), and K_2CO_3 (41.5 mg, 0.3 mmol, 2 equiv) in DMF (1.5 mL). The reaction stirred for 72hrs at 70 °C before being cooled to room temperature. The crude mixture was diluted with EtOAc before being washed with water (2x). The organic layer was dried with Na_2SO_4, filtered, and concentrated. The crude material was purified via flash chromatography (0-10% EtOAc/Hex) to give the title compound (28.2 mg, 34% yield) as a clear oil.

^{1}H NMR (500 MHz, cdcl$_3$) δ 7.40 – 7.37 (m, 2H), 7.34 – 7.28 (m, 4H), 7.19 (ddd, *J* = 14.4, 7.9, 6.2 Hz, 3H), 7.08 (dd, *J* = 7.4, 1.8 Hz, 1H), 6.97 (dd, *J* = 8.4, 1.0 Hz, 1H), 6.90 (td, *J* = 7.4, 1.0 Hz, 1H), 5.32 (d, *J* = 1.7 Hz, 1H), 5.11 (d, *J* = 1.7 Hz, 1H), 5.06 – 4.98 (m, 2H), 2.67 (d, *J* = 7.1 Hz, 1H), 2.39 (d, *J* = 16.3 Hz, 1H), 2.22 – 2.15 (m, 2H), 2.14 – 2.09 (m, 2H), 2.06 – 1.92 (m, 3H), 1.35 (s, 9H), 1.31 – 1.14 (m, 6H).

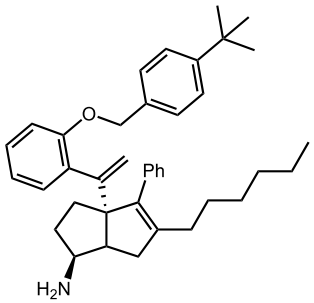

(1*S*,3a*R*)-3a-(1-(2-((4-(*tert*-butyl)benzyl)oxy)phenyl)vinyl)-5-hexyl-4-phenyl-1,2,3,3a,6,6a-hexahydropentalen-1-amine (S17): To a flame-dried screw top test tube charged with a stir bar backfilled (3x) was added **S16** (29 mg, 0.05 mmol, 1.0 equiv.) and ethanol (1.0 mL). Ammonia (7 M in methanol, 160 μL, 1.1 mmol, 20.0 equiv) then titanium(IV) isopropoxide (25 μL, 0.08 mmol, 1.5 equiv) were added via syringe and stirred at room temperature for 6 hours. The test tube cap was then removed and sodium borohydride (61 mg, 0.16 mmol, 3.0 equiv) added portion-wise. The resulting solution was stirred at room temperature for 30 minutes before being diluted with EtOAc. Saturated Rochelle's salt was added and the layers were separated and the aqueous layer was extracted 3x with EtOAc. The combined organic layers were then dried over Na_2SO_4, filtered, and concentrated in vacuo before being purified by flash chromatography (50% EtOAc/Hex + 1% TEA) to give the title compound (9.7 mg, 35% yield) as a clear oil.

^{1}H NMR (500 MHz, cdcl$_3$) δ 7.38 (d, *J* = 8.0 Hz, 3H), 7.33 (td, *J* = 5.8, 2.9 Hz, 5H), 7.25 – 7.18 (m, 1H), 7.15 (q, *J* = 6.9 Hz, 2H), 7.09 (dd, *J* = 7.4, 1.8 Hz, 1H), 6.94 (d, *J* = 8.2 Hz, 1H), 6.86 (t, *J* = 7.5 Hz, 1H), 5.23 (d, *J* = 1.9 Hz, 1H), 5.04 (d, *J* = 1.9 Hz, 1H), 5.02 (d, *J* = 5.0 Hz, 3H), 3.49 (s, 1H), 3.19 (td, *J* = 9.4, 6.1 Hz, 1H), 2.58 (t, *J* = 8.6 Hz, 1H), 2.36 (d, *J* = 17.5 Hz, 1H), 2.19 – 2.09 (m, 3H), 1.77 – 1.69 (m, 0H), 1.58 (ddt, *J* = 29.8, 12.4, 6.8 Hz, 2H), 1.44 – 1.37 (m, 1H), 1.34 (s, 9H), 1.24 (dq, *J* = 16.7, 4.2 Hz, 9H).

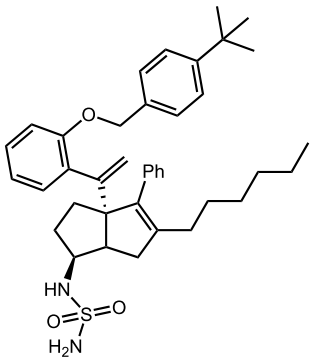

N-(3a-(1-(2-((4-tert-butylbenzene)oxy)phenyl)vinyl)-5-hexyl-4-phenyl-1,2,3,3a,6,6a-hexahydropentalen-1-yl)sulfamide (Ant_4): S17(9.7 mg, 0.02 mmol, 1.0 equiv) was dissolved in EtOH (354 μL) followed by the addition of H_2O (177 μL), triethylamine (7.0 μL, 0.05 mmol, 3.0 equiv), and sulfamide (8.6 mg, 0.0.9 mmol, 5.0 equiv). The reaction vial was heated to 80 °C overnight. After the reaction was cooled to room temperature, the reaction was concentrated. The crude reaction mixture was redissolved in a 1:1 solution of THF/H_2O. After stirring at ambient temperatures for 2 hrs, the reaction was diluted in EtOAc. The organic layer was collected, dried with $NaSO_4$, filter and concentrated before being purified by flash chromatography (30-50% EtOAc/Hex) to afford the title compound (6.1 mg, 50% yield) as a yellow oil.

^{1}H NMR (500 MHz, cdcl$_3$) δ 5.27 (d, *J* = 1.8 Hz, 1H), 5.08 (d, *J* = 1.8 Hz, 1H), 5.05 – 4.99 (m, 2H), 4.69 (s, 3H), 4.30 (q, *J* = 7.1 Hz, 3H), 4.19 (s, 3H), 3.75 – 3.67 (m, 1H), 2.82 (t, *J* = 8.2 Hz, 1H), 2.36 – 2.32 (m, 2H), 2.14 (t, *J* = 7.9 Hz, 2H), 1.79 (ddd, *J* = 11.7, 9.4, 5.8 Hz, 1H), 1.65 – 1.54 (m, 10H), 1.42 (t, *J* = 7.1 Hz, 4H), 1.34 (s, 10H).

LRMS (**APCI**) m/z $[M+H]^+$ calc'd for 627.4, found 627.3

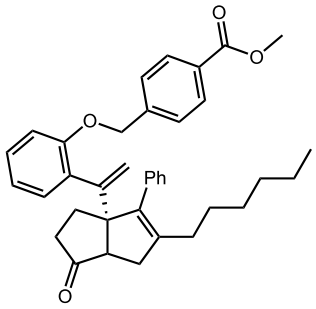

methyl 4-((2-(1-((3a*R*)-5-hexyl-1-oxo-4-phenyl-2,3,6,6a-tetrahydropentalen-3a(1*H*)-yl)vinyl)phenoxy)methyl)benzoate (S18): To a flame-dried screw top vial with a stir bar backfilled (3x) was added **S15** (55.3 mg, 0.14 mmol, 1.0 equiv) methyl-4-(bromomethyl) benzoate (38.9 mg, 0.17 mmol, 1.2 equiv), and K_2CO_3 (95.4 mg, 0.69 mmol, 5 equiv) in MeCN (1.4 mL).

The reaction stirred for 20hrs at 75 °C before being cooled to room temperature. The crude mixture was diluted with EtOAc before being washed with water (2x). The organic layer was dried with Na_2SO_4, filtered, and concentrated. The crude material was purified via flash chromatography (5% EtOAc/Hex) to give the title compound (52 mg, 62% yield) as a clear oil.

^{1}H NMR (500 MHz, cdcl$_3$) δ 8.05 – 8.00 (m, 2H), 7.43 (d, *J* = 8.1 Hz, 2H), 7.34 – 7.30 (m, 2H), 7.26 – 7.22 (m, 5H), 7.10 (dd, *J* = 7.7, 1.8 Hz, 1H), 6.90 (t, *J* = 7.3 Hz, 2H), 5.34 (d, *J* = 1.7 Hz, 1H), 5.13 (d, *J* = 1.6 Hz, 1H), 5.10 (d, *J* = 3.9 Hz, 2H), 3.93 (s, 3H), 2.66 (d, *J* = 7.2 Hz, 1H), 2.35 (d, *J* = 16.3 Hz, 1H), 2.11 – 1.94 (m, 5H), 1.20 – 1.14 (m, 6H), 0.91 – 0.86 (m, 20H).

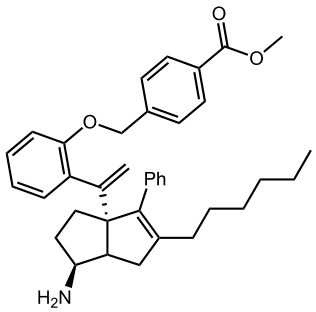

methyl 4-((2-(1-((1*S*,3a*R*)-1-amino-5-hexyl-4-phenyl-2,3,6,6a-tetrahydropentalen-3a(1*H*)-yl)vinyl)phenoxy)methyl)benzoate (S19): To a flame-dried screw top test tube charged with a stir bar backfilled (3x) was added **S18** (47.8 mg, 0.09 mmol, 1.0 equiv.) and ethanol (1.0 mL). Ammonia (7 M in methanol, 260 μL, 1.8 mmol, 20.0 equiv) then titanium(IV) isopropoxide (40 μL, 0.14 mmol, 1.5 equiv) were added via syringe and stirred at room temperature for 6 hours. The test tube cap was then removed and sodium borohydride (10.2 mg, 0.27 mmol, 3.0 equiv) added portion-wise. The resulting solution was stirred at room temperature for 30 minutes before being diluted with EtOAc. Saturated Rochelle's salt was added and the layers were separated and the aqueous layer was extracted 3x with EtOAc. The combined organic layers were then dried over

Na_2SO_4, filtered, and concentrated in vacuo before being purified by flash chromatography (50% EtOAc/Hex + 1% TEA) to give the title compound (15.7 mg, 33% yield) as a clear oil.

^{1}H NMR (500 MHz, cdcl$_3$) δ 8.05 – 8.01 (m, 2H), 7.45 (d, *J* = 8.1 Hz, 2H), 7.32 (dd, *J* = 6.6, 3.1 Hz, 2H), 7.23 – 7.17 (m, 4H), 7.11 (dd, *J* = 7.7, 1.8 Hz, 1H), 6.87 (ddd, *J* = 7.5, 3.4, 2.3 Hz, 2H), 5.24 (d, *J* = 1.8 Hz, 1H), 5.09 (d, *J* = 4.4 Hz, 2H), 5.06 (d, *J* = 1.9 Hz, 1H), 3.93 (s, 3H), 3.20 (td, *J* = 9.6, 6.1 Hz, 1H), 2.57 (d, *J* = 8.8 Hz, 1H), 2.34 (d, *J* = 17.3 Hz, 1H), 2.10 (td, *J* = 7.7, 4.1 Hz, 2H), 1.81 – 1.71 (m, 1H), 1.66 (ddd, *J* = 12.9, 6.1, 2.1 Hz, 1H), 1.57 (td, *J* = 12.3, 5.9 Hz, 1H), 1.32 – 1.16 (m, 13H).

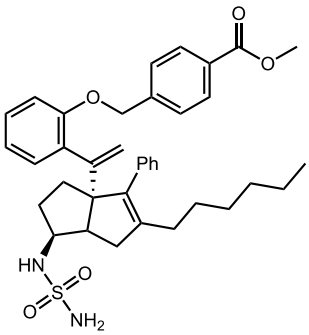

methyl 4-((2-(1-((1*S*,3a*R*)-5-hexyl-4-phenyl-1-(sulfamoylamino)-2,3,6,6a-tetrahydropentalen-3a(1*H*)-yl)vinyl)phenoxy)methyl)benzoate (Ant_6): S19 (15.7 mg, 0.03 mmol, 1.0 equiv) was dissolved in EtOH (571 μL) followed by the addition of H_2O (285 μL), triethylamine (13 μL, 0.09 mmol, 3.0 equiv), and sulfamide (14 mg, 0.15 mmol, 5.0 equiv). The reaction vial was heated to 80 °C overnight. After the reaction was cooled to room temperature, the reaction was concentrated. The crude reaction mixture was redissolved in a 1:1 solution of THF/H_2O. After stirring at ambient temperatures for 2 hrs, the reaction was diluted in EtOAc. The organic layer was collected, dried with $NaSO_4$, filter and concentrated before being purified by

flash chromatography (20-50% EtOAc/Hex) to afford the title compound (3.4 mg, 19% yield) as a yellow oil.

^{1}H NMR (500 MHz, cdcl$_3$) δ 8.03 (d, *J* = 8.0 Hz, 3H), 7.47 (d, *J* = 8.0 Hz, 2H), 7.30 (dd, *J* = 7.0, 3.1 Hz, 3H), 7.21 (dd, *J* = 6.7, 2.6 Hz, 5H), 7.06 (d, *J* = 7.4 Hz, 1H), 6.88 (d, *J* = 7.7 Hz, 2H), 5.27 (d, *J* = 1.8 Hz, 1H), 5.12 (s, 1H), 5.11 – 5.09 (m, 2H), 4.34 (s, 2H), 4.21 (d, *J* = 8.9 Hz, 1H), 3.93 (s, 3H), 3.70 (dt, *J* = 16.8, 8.9 Hz, 1H), 2.78 (t, *J* = 8.5 Hz, 1H), 2.35 (d, *J* = 17.4 Hz, 1H), 2.23 (dd, *J* = 17.4, 8.1 Hz, 1H), 2.10 (t, *J* = 7.9 Hz, 2H), 1.89 – 1.81 (m, 1H), 1.61 (d, *J* = 28.6 Hz, 9H), 1.42 – 1.30 (m, 2H), 1.24 (d, *J* = 21.0 Hz, 10H).

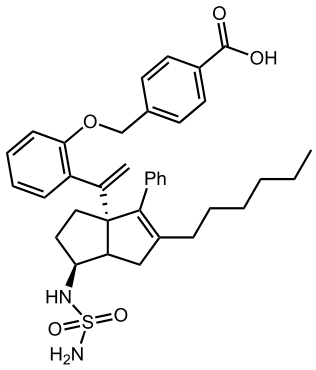

4-((2-(1-((1*S*,3a*R*)-5-hexyl-4-phenyl-1-(sulfamoylamino)-2,3,6,6a-tetrahydropentalen-3a(1*H*)-yl)vinyl)phenoxy)methyl)benzoic acid (Ant_5): S19 (15.7 mg, 0.03 mmol, 1.0 equiv) was dissolved in EtOH (571 μL) followed by the addition of H_2O (285 μL), triethylamine (13 μL, 0.09 mmol, 3.0 equiv), and sulfamide (14 mg, 0.15 mmol, 5.0 equiv). The reaction vial was heated to 80 °C overnight. After the reaction was cooled to room temperature, the reaction was concentrated. The crude reaction mixture was redissolved in a 1:1 solution of THF/H_2O. After stirring at ambient temperatures for 2 hrs, the reaction was diluted in EtOAc. The organic layer was collected, dried with $NaSO_4$, filter and concentrated before being purified by flash

chromatography (20-50% EtOAc/Hex) to afford the title compound (4.6 mg, 25% yield) as a yellow oil.

^{1}H NMR (500 MHz, cdcl$_3$) δ 7.46 (d, *J* = 8.0 Hz, 2H), 7.24 – 7.16 (m, 3H), 7.10 – 7.00 (m, 1H), 6.86 (q, *J* = 8.1 Hz, 2H), 5.24 (s, 1H), 5.08 (s, 3H), 3.65 (s, 1H), 2.75 (s, 1H), 2.34 (d, *J* = 16.8 Hz, 1H), 2.18 (d, *J* = 24.6 Hz, 2H), 2.07 (s, 2H), 1.88 – 1.83 (m, 2H), 1.61 (s, 2H), 1.36 (d, *J* = 20.5 Hz, 1H), 1.21 (d, *J* = 22.7 Hz, 6H).

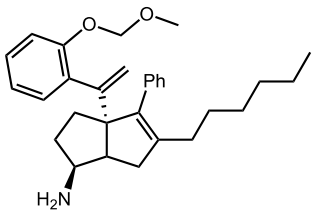

(1*S*,3a*R*)-5-hexyl-3a-(1-(2-(methoxymethoxy)phenyl)vinyl)-4-phenyl-1,2,3,3a,6,6a-hexahydropentalen-1-amine (S20): To a flame-dried screw top test tube charged with a stir bar backfilled (3x) was added **S14** (637.7 mg, 1.4 mmol, 1.0 equiv.) and ethanol (14 mL). Ammonia (7 M in methanol, 4.0 mL, 2.2 mmol, 20.0 equiv) then titanium(IV) isopropoxide (651 μL, 2.2 mmol, 1.5 equiv) were added via syringe and stirred at room temperature for 6 hours. The test tube cap was then removed and sodium borohydride (158.9 mg, 4.2 mmol, 3.0 equiv) added portion-wise. The resulting solution was stirred at room temperature for 30 minutes before being diluted with EtOAc. Saturated Rochelle's salt was added and the layers were separated and the aqueous layer was extracted 3x with EtOAc. The combined organic layers were then dried over Na_2SO_4, filtered, and concentrated in vacuo before being purified by flash chromatography to give the title compound.

^{1}H NMR (500 MHz, cdcl$_3$) δ 7.39 (d, *J* = 7.6 Hz, 2H), 7.31 (t, *J* = 7.4 Hz, 3H), 7.28 – 7.23 (m, 1H), 7.22 – 7.17 (m, 1H), 7.13 – 7.06 (m, 3H), 6.90 (t, *J* = 7.5 Hz, 1H), 5.24 (d, *J* = 2.0 Hz, 1H),

5.06 (s, 2H), 5.01 (d, *J* = 2.0 Hz, 1H), 3.40 (s, 4H), 3.25 (td, *J* = 9.6, 6.1 Hz, 1H), 2.56 (t, *J* = 8.7 Hz, 1H), 2.44 (d, *J* = 17.1 Hz, 1H), 2.16 (dq, *J* = 28.5, 7.9 Hz, 3H), 1.76 – 1.69 (m, 1H), 1.65 – 1.58 (m, 1H), 1.50 (td, *J* = 12.3, 5.9 Hz, 1H), 1.41 (q, *J* = 7.6 Hz, 4H), 1.32 – 1.12 (m, 6H).

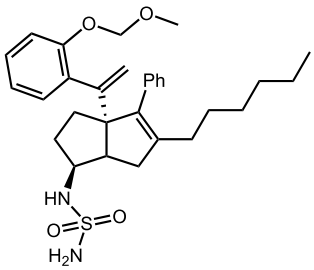

(1*S*,3a*R*)-5-hexyl-(3a-(1-(2-(methoxymethoxy)phenyl)vinyl)-4-phenyl-1,2,3,3a,6,6a-hexahydropentalen-1-yl)sulfamide (S21): S20 (136 mg, 0.31 mmol, 1.0 equiv) was dissolved in EtOH (6.1 mL) followed by the addition of H_2O (3.1 mL), triethylamine (128 μL, 0.92 mmol, 3.0 equiv), and sulfamide (146 mg, 1.52 mmol, 5.0 equiv). The reaction vial was heated to 80 °C overnight. After the reaction was cooled to room temperature, the reaction was concentrated before being purified by flash chromatography (20-50% EtOAc/Hex) to afford the title compound (81.7 mg, 50% yield) as a yellow oil.

^{1}H NMR (600 MHz, $CDCl_3$) δ 7.39 – 7.36 (m, 2H), 7.34 (dd, *J* = 8.3, 6.6 Hz, 2H), 7.30 (d, *J* = 6.8 Hz, 0H), 7.25 – 7.21 (m, 1H), 7.09 – 7.04 (m, 2H), 6.95 – 6.91 (m, 1H), 5.29 (d, *J* = 1.8 Hz, 1H), 5.12 (d, *J* = 2.4 Hz, 2H), 5.07 (d, *J* = 1.7 Hz, 1H), 4.84 (s, 1H), 4.56 (s, 2H), 4.39 – 4.28 (m, 2H), 3.85 (qd, *J* = 9.1, 6.2 Hz, 1H), 3.45 (d, *J* = 0.6 Hz, 3H), 2.84 (td, *J* = 8.4, 2.1 Hz, 1H), 2.47 – 2.34 (m, 2H), 2.16 (t, *J* = 7.9 Hz, 2H), 1.86 (dtd, *J* = 12.1, 6.1, 2.8 Hz, 1H), 1.64 (ttd, *J* = 11.8, 6.3, 3.1 Hz, 2H), 1.56 (ddd, *J* = 13.1, 11.2, 6.1 Hz, 1H), 1.46 – 1.34 (m, 5H).

^{13}C NMR (151 MHz, $CDCl_3$) δ 154.49, 150.77, 142.85, 139.37, 136.98, 132.62, 130.11, 129.89, 128.20, 127.66, 126.63, 121.25, 115.71, 113.91, 94.49, 69.28, 67.65, 57.01, 56.26, 49.25, 34.75, 32.96, 31.61, 30.93, 29.84, 29.46, 28.21, 22.61, 14.64, 14.08.

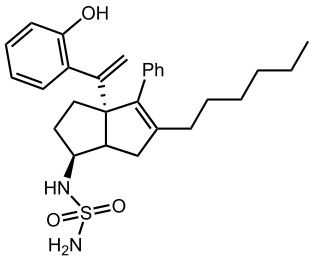

(1*S*,3a*R*)-5-hexyl-(3a-(1-(2-phenol)vinyl)-4-phenyl-1,2,3,3a,6,6a-hexahydropentalen-1-yl)sulfamide (S22): A reaction vial was charged with a stir bar and **S21** (82.6 mg, 0.16 mmol, 1.0 equiv) dissolved in dioxane (1.6 mL) and a few drops of concentrated HCl was then added. The reaction was gradually heated to 40 °C before being diluted with EtOAc and washed with 3 x 5 mL 0.5 M aqueous HCl, 5 ml water, and 5 mL brine. The organic layer was then dried over Na_2SO_4, filtered, and concentrated in vacuo to give the title compound (27.7 mg, 35% yield) after flash chromatography (50% EtOAc/Hex).

^{1}H NMR (600 MHz, $CDCl_3$) δ 7.37 – 7.28 (m, 3H), 7.21 (dd, *J* = 6.8, 1.6 Hz, 2H), 7.16 (td, *J* = 7.7, 1.7 Hz, 1H), 7.11 (dd, *J* = 7.7, 1.7 Hz, 1H), 6.91 (dd, *J* = 8.2, 1.2 Hz, 1H), 6.79 (td, *J* = 7.5, 1.3 Hz, 1H), 5.56 (s, 1H), 5.35 (d, *J* = 1.5 Hz, 1H), 5.25 (d, *J* = 1.4 Hz, 1H), 4.69 (s, 3H), 4.47 (d, *J* = 8.0 Hz, 1H), 3.84 (dtd, *J* = 10.5, 8.4, 6.1 Hz, 1H), 2.58 (td, *J* = 8.9, 1.8 Hz, 1H), 2.38 (dd, *J* = 17.7, 1.9 Hz, 1H), 2.06 (dt, *J* = 23.1, 8.4 Hz, 4H), 1.98 (dtd, *J* = 11.7, 5.8, 1.9 Hz, 1H), 1.75 (ddd, *J* = 12.9, 6.2, 2.1 Hz, 1H), 1.69 (td, *J* = 12.5, 5.7 Hz, 1H), 1.46 (qd, *J* = 11.5, 6.1 Hz, 1H), 1.39 – 1.15 (m, 7H), 0.86 (t, *J* = 7.0 Hz, 3H).

^{13}C NMR (151 MHz, $CDCl_3$) δ 152.27, 149.86, 144.42, 138.00, 136.71, 129.79, 128.78, 128.50, 128.35, 128.15, 127.17, 119.86, 118.11, 115.37, 69.52, 57.09, 48.13, 35.40, 32.38, 31.90, 31.72, 29.93, 29.62, 28.07, 22.73, 14.21.

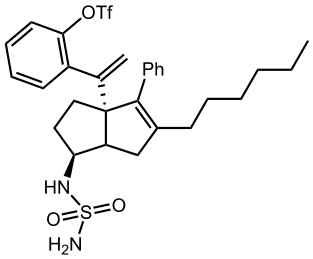

2-(1-((1*S*,3a*R*)-5-hexyl-4-phenyl-1-(sulfamoylamino)-2,3,6,6a-tetrahydropentalen-3a(1*H*)-yl)vinyl)phenyl trifluoromethanesulfonate (S23): An oven-dried one-dram vial was charged with a stir bar and **S22** (21.1 mg, 44.0 µmol) then nitrogen cycled 4 times. A solution of Et_3N (9.2 µL, 66 µmol) in dry DCM (400 µL) was used to dissolve the **S22** then the vial was cooled to -78 °C and a solution of Tf_2O (7.7 µL, 46 µmol) in dry DCM (100 µL) was added slowly. After 1 h, the starting material had been consumed, as judged by TLC, and the reaction solution was diluted with EtOAc and washed twice with aqueous NH_4Cl then twice with H_2O and brine. The organic layer was dried over Na_2SO_4, filtered, and filtrate concentrated under reduced pressure to collect the crude material. This crude material was purified by flash chromatography on silica to collect the title compound (14.6 mg, 54% yield).

^{1}H NMR (600 MHz, $CDCl_3$) δ 7.37 – 7.21 (m, 7H), 7.16 – 7.14 (m, 2H), 5.26 (s, 1H), 5.24 (s, 1H), 4.49 (s, 2H), 4.36 (d, *J* = 7.6 Hz, 1H), 3.85 (dddd, *J* = 10.9, 8.8, 7.6, 5.9 Hz, 1H), 2.72 (t, *J* = 8.7 Hz, 1H), 2.42 (dd, *J* = 17.7, 2.3 Hz, 1H), 2.19 (dd, *J* = 17.6, 8.9 Hz, 1H), 2.06 – 2.00 (m, 2H), 1.97 (ddd, *J* = 11.7, 5.8, 1.9 Hz, 1H), 1.80 (ddd, *J* = 12.9, 5.9, 1.8 Hz, 1H), 1.67 – 1.53 (m, 2H), 1.51 – 1.41 (m, 1H), 1.41 – 1.32 (m, 2H), 1.28 – 1.16 (m, 5H), 0.86 (t, *J* = 7.2 Hz, 3H).

^{13}C NMR (151 MHz, $CDCl_3$) δ 147.15, 143.69, 139.19, 136.91, 136.54, 130.21, 130.07, 128.90, 127.99, 127.92, 127.13, 121.51, 120.33, 118.65 (q, *J* = 320.23 Hz), 12.9, 5.9, 1.8 Hz,69.27, 57.10, 35.35, 32.68, 32.03, 31.71, 29.89, 29.53, 28.12, 22.74, 14.21.

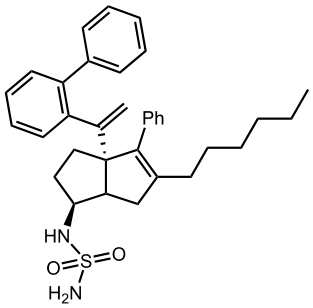

N-(3a-(1-([1,1'-biphenyl]-2-yl)vinyl)-5-hexyl-4-phenyl-1,2,3,3a,6,6a-hexahydropentalen-1-yl)sulfamide (Ant_2): A 1 mL vial was charged with a stir bar **S23** (14.0 mg, 20 µmol), XPhos G3 Pd precatalyst (3.4 mg, 4 µmol), XPhos (3.8 mg, 8 µmol), and phenylboronic acid (3.6 mg, 30 µmol). The vial was then nitrogen cycled 4 times and degassed THF (200 µL) then a degassed solution of K_3PO_4 (0.5M, 80 µL) added. The reaction was stirred at 23 °C for 16 h under nitrogen before exposing to air and putting through a silica plug. The concentrated eluent was purified by preparative HPLC then a second silica plug to remove grease to give the title compound (5.6 mg, 45%).

^{1}H NMR (600 MHz, $CDCl_3$) δ 7.43 – 7.17 (m, 12H), 7.05 – 7.02 (m, 2H), 5.08 (s, 2H), 4.35 (s, 2H), 4.20 (d, *J* = 8.2 Hz, 1H), 3.37 (s, 1H), 2.45 (s, 1H), 2.30 – 2.27 (m, 2H), 1.99 (tt, *J* = 9.7, 5.3 Hz, 2H), 1.76 – 1.67 (m, 1H), 1.46 (d, *J* = 8.6 Hz, 1H), 1.40 – 1.31 (m, 1H), 1.32 – 1.14 (m, 9H), 0.85 (t, *J* = 7.2 Hz, 3H).

^{13}C NMR (151 MHz, $CDCl_3$) δ 151.56, 142.89, 142.44, 141.66, 140.93, 139.84, 136.88, 130.44, 130.33, 130.20, 129.03, 127.92, 127.80, 127.01, 126.83, 126.80, 118.98, 69.60, 56.62, 34.89, 32.44, 31.96, 31.73, 29.85, 29.79, 29.45, 28.21, 22.74, 14.22.

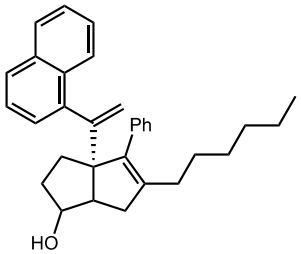

(3a*R*)-5-hexyl-3a-(1-(naphthalen-1-yl)vinyl)-4-phenyl-1,2,3,3a,6,6a-hexahydropentalen-1-ol (**S24**): A slight modification of the procedure of Flynn et al. was used. Prior to use in the reaction, all reagents were dried by azeotropic removal of water using benzene. A dry round bottom flask containing bis(cyclopentadienyl)zirconium(IV) dichloride (409.3 mg, 1.4 mmol, 1.2 equiv) under nitrogen, was dissolved in anhydrous, degassed tetrahydrofuran (THF, 5 mL/mmol enyne) and cooled to -78 °C. The resulting solution was treated with *n*-BuLi (1.12 mL, 2.8 mmol, 2.4 equiv.) and the light yellow solution was stirred for 50 minutes. A solution of tert-butyldimethyl((7-phenylhept-1-en-6-yn-3-yl)oxy)silane (348.6 mg, 1.16mmol, 1.0 equiv) in anhydrous, degassed THF (5 mL/mmol) was added. The resulting salmon-colored mixture was stirred at -78 °C for 45 minutes, the cooling bath removed, and the reaction mixture was allowed to warm to ambient temperature with stirring (2.5 hours total). The reaction mixture was then cooled to -78 °C for 15 minutes and 1,1-dibromoheptane (330.2 mg, 1.28 mmol, 1.1 equiv) was added as a solution in anhydrous THF (5 mL/mmol) followed by freshly prepared lithium diisopropylamide (LDA, 1.28 mL, 1.28 mmol, 1.0 M, 1.1 equiv.). After 30 minutes, a solution of 1-ethynylnaphthalene (**S8**) (0.64 g, 4.2 mmol, 3.6 equiv.) in anhydrous THF (2 mL/mmol) was deprotonated with 1.0 equiv. of *n*BuLi at -78 °C then added dropwise and the resulting rust-colored solution was stirred at -78

°C for 1 hour. The reaction was quenched with methanol and saturated aqueous sodium bicarbonate and allowed to warm to room temperature, affording a light yellow slurry that stirred overnight. The slurry was then poured onto water and extracted with ethyl acetate four times. The combined organic layers were washed with brine, dried with Na_2SO_4, filtered, and concentrated *in vacuo* to afford a crude mixture. The resulting crude mixture was dissolved in 30 mL of 1:2 DCM:MeOH in a round bottom flask then five drops of concentrated HCl added. The resulting solution was stirred at room temperature for 2.5 hours before concentrating *in vacuo* and subjecting to silica gel chromatography to afford the title compound as a yellow oil and 1.7:1 mixture of diastereomers used in the next step without separation. (254.0 mg, 50% over 2 steps).

^{1}H NMR (500 MHz, $CDCl_3$) δ 8.03 (d, *J* = 8.3 Hz, 1H), 7.83 (d, 1H), 7.76 (d, *J* = 8.1 Hz, 1H), 7.49 – 7.27 (m, 9H), 5.29 (d, *J* = 1.6 Hz, 1H), 5.10 (d, *J* = 1.5 Hz, 1H), 3.84 (s, 1H), 2.18 – 2.08 (m, 2H), 1.99 (dd, *J* = 10.1, 7.0 Hz, 2H), 1.93 (d, *J* = 20.7 Hz, 1H), 1.82 (dd, *J* = 13.3, 5.2 Hz, 1H), 1.76 – 1.63 (m, 2H), 1.33 – 1.14 (m, 9H), 0.86 (t, *J* = 7.1 Hz, 3H).

LRMS (**APCI**) m/z $[M+H]^+$ calc'd for 437.6, found 437.3.

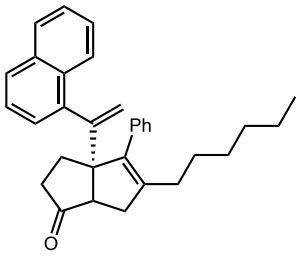

(3a*R*)-5-hexyl-3a-(1-(naphthalen-1-yl)vinyl)-4-phenyl-3,3a,6,6a-tetrahydropentalen-1(2*H*)-one (**S25**): A scintillation vial was charged with a stir bar, **S24** (0.58 mmol, 254.0 mg), and MeCN (6 ml). The resulting solution stirred at 23 ºC then TPAP (0.058 mmol, 20.4 mg) and NMO (5.8 mmol, 679.5 mg) added. The reaction solution continued to stir for 1.5 h before eluting through a

plug of silica. The resulting crude material was then purified by flash chromatography on silica to collect the title compound (156.4 mg, 62%).

^{1}H NMR (600 MHz, $CDCl_3$) δ 7.95 (d, *J* = 8.3 Hz, 1H), 7.86 – 7.83 (m, 1H), 7.79 (dt, *J* = 7.5, 1.7 Hz, 1H), 7.49 – 7.31 (m, 9H), 5.51 (d, *J* = 1.6 Hz, 1H), 5.25 (d, *J* = 1.6 Hz, 1H), 2.38 (d, *J* = 7.5 Hz, 1H), 2.30 (td, *J* = 11.2, 10.1, 3.0 Hz, 1H), 2.21 – 2.07 (m, 3H), 1.99 (t, *J* = 8.0 Hz, 2H), 1.55 – 1.46 (m, 1H), 1.25 – 1.11 (m, 9H), 0.84 (td, *J* = 7.2, 1.5 Hz, 3H).

^{13}C NMR (126 MHz, $CDCl_3$) δ 223.32, 148.78, 145.27, 139.88, 137.95, 136.92, 134.06, 132.46, 129.38, 128.43, 128.27, 127.56, 127.28, 126.16, 126.00, 125.77, 125.46, 124.73, 117.40, 66.84, 55.01, 38.59, 37.59, 32.53, 30.06, 29.45, 28.78, 27.80, 22.64, 14.16.

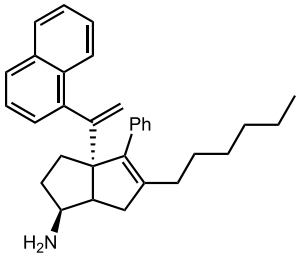

(1*S*,3a*R*)-5-hexyl-3a-(1-(naphthalen-1-yl)vinyl)-4-phenyl-1,2,3,3a,6,6a-hexahydropentalen-1-amine (**S26**): A 1-dram reaction vial was charged with a stir bar, **S25** (0.265 mmol, 115.1 mg), and EtOH (1.89 ml). A solution of NH_3 in MeOH (7N, 5.29 mmol, 0.76 mL) followed immediately by $Ti(O^iPr)_4$ (0.397 mmol, 120 µl) was added and the vial sealed. The resulting solution was stirred at 23 ºC for 7.5 h before unsealing vial and adding $NaBH_4$ (0.79 mmol, 29.9 mg) and continuing stirring at 23 ºC for 16 h. Reaction was then diluted with EtOAc and saturated aqueous Rochelle's salt and sonicated for 5 min. The resulting slurry was washed twice with saturated aqueous Rochelle's salt, twice with H_2O, then brine. The organic layer was dried over Na_2SO_4, filtered, and filtrate concentrated under reduced pressure to collect the crude material. Crude material purified by flash chromatography on silica to collect the title compound (63 mg, 55%).

^{1}H NMR (600 MHz, Chloroform-*d*) δ 7.95 (d, *J* = 8.5 Hz, 1H), 7.83 (d, *J* = 8.2 Hz, 1H), 7.76 (d, *J* = 8.1 Hz, 1H), 7.38 (tdd, *J* = 31.1, 14.6, 7.3 Hz, 9H), 5.31 (s, 1H), 5.11 (s, 1H), 3.27 (td, *J* = 10.0, 5.9 Hz, 1H), 2.30 (t, *J* = 9.0 Hz, 1H), 2.24 (d, *J* = 17.1 Hz, 1H), 2.05 (t, *J* = 7.9 Hz, 2H), 1.88 – 1.80 (m, 2H), 1.73 (dd, *J* = 12.4, 5.6 Hz, 1H), 1.67 (dd, *J* = 17.3, 8.8 Hz, 1H), 1.28 – 1.17 (m, 10H), 0.83 (s, 3H).

^{13}C NMR (151 MHz, $CDCl_3$) δ 151.25, 143.59, 140.53, 138.28, 137.32, 133.52, 132.60, 129.96, 128.09, 127.66, 126.83, 126.59, 126.17, 125.62, 125.36, 124.69, 124.45, 116.86, 70.50, 55.08, 47.89, 34.70, 33.91, 32.67, 31.58, 29.76, 29.63, 29.38, 27.95, 22.55, 14.02.

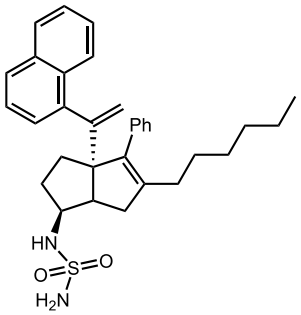

N-(5-hexyl-3a-(1-(naphthalen-1-yl)vinyl)-4-phenyl-1,2,3,3a,6,6a-hexahydropentalen-1-yl)sulfamide (Ant_1): S26 (66.1 mg, 0.15 mmol, 1.0 equiv) was dissolved in EtOH (3.0 mL) followed by the addition of H_2O (1.5 mL), triethylamine (64 μL, 0.46 mmol, 3.0 equiv), and sulfamide (73 mg, 0.76 mmol, 5.0 equiv). The reaction vial was heated to 80 °C overnight. After the reaction was cooled to room temperature, the reaction was concentrated before being purified by flash chromatography (30% EtOAc/Hex) to afford the title compound (62.9 mg, 81% yield) as a yellow oil.

^{1}H NMR (400 MHz, $CDCl_3$) δ 7.89 (d, *J* = 8.4 Hz, 1H), 7.86 – 7.81 (m, 1H), 7.77 (d, *J* = 7.7 Hz, 1H), 7.49 – 7.29 (m, 9H), 5.37 (d, *J* = 1.5 Hz, 1H), 5.15 (d, *J* = 1.5 Hz, 1H), 4.32 (s, 2H), 4.19 (d, *J* = 8.4 Hz, 1H), 3.78 (dt, *J* = 16.9, 9.2 Hz, 1H), 2.52 (t, *J* = 8.7 Hz, 1H), 2.21 (d, *J* = 17.5 Hz, 1H),

2.03 (s, 3H), 1.88 – 1.78 (m, 1H), 1.72 (td, *J* = 12.4, 5.9 Hz, 1H), 1.46 (tt, *J* = 10.9, 5.6 Hz, 1H), 1.37 – 1.16 (m, 9H), 0.87 (t, *J* = 6.8 Hz, 3H).

^{13}C NMR (101 MHz, $CDCl_3$) δ 150.70, 143.69, 140.18, 138.69, 137.07, 133.75, 132.73, 130.03, 128.39, 128.07, 127.31, 127.10, 126.20, 126.01, 125.71, 124.93, 124.87, 117.57, 70.01, 57.27, 49.03, 35.21, 33.07, 32.08, 31.74, 29.95, 29.61, 28.20, 22.75, 14.24.

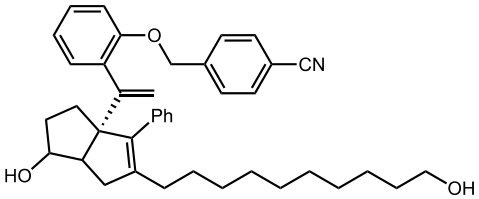

4-((2-(1-((3a*R*)-1-hydroxy-5-(10-hydroxydecyl)-4-phenyl-2,3,6,6a-tetrahydropentalen-3a(1*H*)-yl)vinyl)phenoxy)methyl)benzonitrile (**S27**): Hexahydropentalene formation was accomplished through slight modification of Whitby's procedure. Prior to cyclization, all non-volatile reagents were dried by azeotropic removal of water using benzene. A dry round bottom flask containing bis(cyclopentadienyl)zirconium(IV) dichloride (1.05 g, 3.6 mmol, 1.2 equiv) under nitrogen, was dissolved in anhydrous, degassed tetrahydrofuran (THF, 8 mL/mmol enyne) and cooled to -78 °C. The resulting mixture was treated with n-BuLi (2.9 mL, 7.2 mmol, 2.4 equiv) and the light yellow solution was stirred for 45 minutes. A solution of (tertbutyldimethyl((7-phenylhept-1-en-6-yn-3-yl)oxy)silane) (901.5 mg, 3 mmol, 1.0 equiv) in anhydrous, degassed THF (8 mL/mmol) was added. The resulting salmon-colored mixture was stirred at -78 °C for 45 minutes before the cooling bath was removed. The reaction mixture continued to stir at room temperature for an additional 2.5 hours. The reaction mixture was then cooled to -78 °C and the required 1,1-dibromoheptane (1.9 g, 3.3 mmol, 1.1 equiv) was added as a solution in anhydrous THF (8 mL/mmol enyne) followed by freshly prepared lithium diisopropylamide (LDA, 1.0 M,

1.1 equiv.). After 15 minutes, a freshly prepared solution of lithium 4-((2-ethynylphenoxy)methyl)benzonitrile (**S3**) (2.5 g, 10.8 mmol, 3.6 equiv) in anhydrous THF (8 mL/ mmol enyne) was added dropwise and the resulting black solution was stirred at -78 °C for 1.5 hours. The reaction was quenched with methanol and saturated aqueous sodium bicarbonate slowly warming to room temperature, affording a light yellow slurry. The slurry was poured onto water and extracted with ethyl acetate four times. The combined organic layers were washed with brine, dried withNa_2SO_4, and concentrated in vacuo. The resulting yellow oil was passed through a short plug of silica (100% EtOAc eluent) and concentrated. The crude product was dissolved in THF and treated with either HCl or TBAF. The resulting solution stirred at room temperature for 16 h. The reaction mixture was concentrated and the diastereomers were purified and separated by flash chromatography (20% EtOAc/Hex). The mixture of stereoisomers (957.5 mg, 54% yield) were moved forward without further purification.

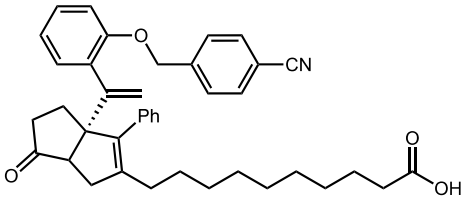

10-((3a*R*)-3a-(1-(2-((4-cyanobenzyl)oxy)phenyl)vinyl)-6-oxo-3-phenyl-1,3a,4,5,6,6a-hexahydropentalen-2-yl)decanoic acid (RMS-V-30**S28**): To a solution **S27** (916.7 mg, 1.5 mmol, 1.0 equiv) in acetonitrile (25 mL) was added tetrapropylammonium perruthenate (TPAP) (47.3 mg, 0.15 mmol, 0.1 equiv), N-methylmorpholine N-oxide (NMO) (1.8 g, 15 mmol, 10 equiv), and water (270 μL, 15 mmol, 10 equiv) and stirred at room temperature overnight. The reaction solution was then filtered through a pad of silica with (100% EtOAc) and concentrated.

The resulting mixture was purified by flash chromatography (30% EtOAc/Hex) to give the title compound (170.1 mg, 20% yield).

^{1}H NMR (500 MHz, cdcl$_3$) δ 7.62 (d, *J* = 7.9 Hz, 2H), 7.44 (d, *J* = 8.0 Hz, 2H), 7.30 – 7.26 (m, 2H), 7.22 (dd, *J* = 8.0, 2.7 Hz, 1H), 7.09 (dt, *J* = 7.4, 1.4 Hz, 1H), 6.90 (t, *J* = 7.5 Hz, 1H), 6.86 (d, *J* = 8.3 Hz, 1H), 5.33 (s, 1H), 5.11 (s, 1H), 5.07 (d, *J* = 3.6 Hz, 2H), 2.65 (d, *J* = 7.0 Hz, 1H), 2.37 – 2.27 (m, 2H), 2.12 – 1.94 (m, 6H), 1.62 (t, *J* = 7.3 Hz, 2H), 1.33 – 1.17 (m, 12H).

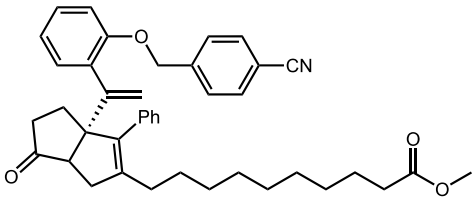

methyl 10-((3a*R*)-3a-(1-(2-((4-cyanobenzyl)oxy)phenyl)vinyl)-6-oxo-3-phenyl-1,3a,4,5,6,6a-hexahydropentalen-2-yl)decanoate (**S29**): To a solution of the desired **S28** (78.3 mg, 0.13 mmol, 1.0 equiv) in methanol (1.3 mL) was added three drops of concentrated HCl and stirred at room temperature overnight. Reaction solution was then concentrated in vacuo and filtered through a pad of silica to collect the title compound (40.3 mg, 50% yield).

^{1}H NMR (400 MHz, CDCl$_3$) δ 7.67 (d, *J* = 7.8 Hz, 2H), 7.49 (d, *J* = 7.7 Hz, 2H), 7.35 – 7.29 (m, 6H), 7.14 (dd, *J* = 7.4, 1.6 Hz, 1H), 6.94 (t, *J* = 7.4 Hz, 1H), 6.90 (d, *J* = 8.2 Hz, 1H), 5.38 (d, *J* = 1.6 Hz, 1H), 5.16 (d, *J* = 1.5 Hz, 1H), 5.11 (s, 2H), 3.68 (s, 3H), 2.65 (d, *J* = 7.0 Hz, 1H), 2.37 – 2.27 (m, 2H), 2.12 – 1.94 (m, 6H), 1.62 (t, *J* = 7.3 Hz, 2H), 1.33 – 1.17 (m, 12H).

^{13}C NMR (101 MHz, CDCl$_3$) δ 174.39, 155.35, 148.77, 145.00, 142.49, 136.55, 132.46, 131.55, 130.80, 129.21, 128.55, 127.97, 127.49, 126.95, 120.82, 118.70, 116.15, 111.92, 111.68, 69.24,

66.11, 55.41, 51.52, 37.91, 37.53, 34.13, 30.00, 29.64, 29.32, 29.29, 29.23, 29.13, 27.91, 27.85, 24.96.

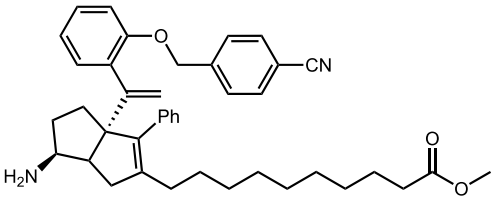

methyl 10-((3a*R*,6*S*)-6-amino-3a-(1-(2-((4-cyanobenzyl)oxy)phenyl)vinyl)-3-phenyl-1,3a,4,5,6,6a-hexahydropentalen-2-yl)decanoate (**S30**): To a flame-dried screw top test tube charged with a stir bar backfilled (3x) was added **S29** (42.9 mg, 0.07 mmol, 1.0 equiv.) and ethanol (700 μL). Ammonia (7 M in methanol, 200 μL, 1.4 mmol, 20.0 equiv) then titanium(IV) isopropoxide (33 μL , 0.11 mmol, 1.5 equiv) were added via syringe and stirred at room temperature for 6 hours. The test tube cap was then removed and sodium borohydride (7.9 mg, 0.21 mmol, 3.0 equiv) added portion-wise. The resulting solution was stirred at room temperature for 30 minutes before being diluted with EtOAc. The solution was adjusted to a pH of 1 with 1M HCl. The layers were separated and the aqueous layer was extracted 3x with EtOAc. The combined organic layers were then dried over Na_2SO_4, filtered, and concentrated in vacuo before being purified by flash chromatography (50% EtOAc/Hex then 10% MeOH/DCM) to give the title compound (19.3 mg, 45% yield).

^{1}H NMR (400 MHz, $CDCl_3$) δ 7.69 – 7.64 (m, 2H), 7.47 (d, *J* = 8.3 Hz, 2H), 7.40 – 7.36 (m, 2H), 7.26 – 7.18 (m, 6H), 7.10 (dd, *J* = 7.5, 1.8 Hz, 1H), 6.92 – 6.83 (m, 2H), 5.32 (d, *J* = 1.7 Hz, 1H), 5.12 (d, *J* = 1.6 Hz, 1H), 5.10 (s, 2H), 3.67 (s, 3H), 2.86 – 2.78 (m, 1H), 2.36 – 2.27 (m, 5H), 2.27 – 2.19 (m, 1H), 1.74 (d, *J* = 7.6 Hz, 1H), 1.60 (dd, *J* = 14.1, 6.8 Hz, 6H), 1.38 – 1.26 (m, 11H).

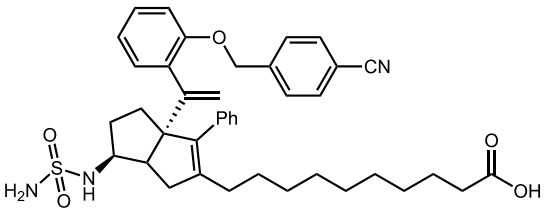

10-((3a*R*,6*S*)-3a-(1-(2-((4-cyanobenzyl)oxy)phenyl)vinyl)-3-phenyl-6-(sulfamoylamino)-1,3a,4,5,6,6a-hexahydropentalen-2-yl)decanoic acid (**ANT3-10CA**): **S30** (9.6 mg, 0.02 mmol, 1.0 equiv) was dissolved in EtOH (311 μL) followed by the addition of H_2O (156 μL), triethylamine (7.0 μL , 0.05 mmol, 3.0 equiv), and sulfamide (7.7 mg, 0.08 mmol, 5.0 equiv). The reaction vial was heated to 80 °C overnight. After the reaction was cooled to room temperature, the reaction was concentrated. The crude oil was then redissolve in 50% H_2O/THF before the addition of excess LiOH. After consumption of starting material the reaction was extracted with EtOAc (2x). The organic layer was dried with Na_2SO_4, filtered, and concentrated before being purified by flash chromatography (50% EtOAc/Hex) to afford the title compound (3.0 mg, 15% yield) as a yellow oil.

^{1}H NMR (400 MHz, $CDCl_3$) δ 7.69 – 7.64 (m, 2H), 7.47 (d, *J* = 8.3 Hz, 2H), 7.40 – 7.36 (m, 2H), 7.26 – 7.18 (m, 6H), 7.10 (dd, *J* = 7.5, 1.8 Hz, 1H), 6.92 – 6.83 (m, 2H), 5.22 (s, 1H), 5.19 (s, 1H), 5.07 (d, *J* = 10.5 Hz, 2H), 5.02 (s, 2H), 4.34 – 4.28 (m, 1H), 2.36 – 2.27 (m, 5H), 2.27 – 2.19 (m, 1H), 1.74 (d, *J* = 7.6 Hz, 1H), 1.60 (dd, *J* = 14.1, 6.8 Hz, 6H), 1.38 – 1.26 (m, 11H).

Chapter 5: Radical Spirocyclization and photoredox hydroarylation

5.1 Spirocycles in biologically active compounds

Spirocyclic scaffolds are considered to be a privileged scaffold in medicinal chemistry.[81,82] Defined as ring systems with two or more rings linked by one common atom, these structures are advantageous due to higher fraction of sp^3 (Fsp^3 = number of sp^3 hybridized carbons/total carbon count). Due to added three-dimensionality of the structures this leads to a larger advantage with conformational flexibility over flat aromatic compounds as well as improvements in absorption and permeability from linear scaffolds.[82–84] Lovering and coworkers claimed that this "escape from flatland" will increase the probability of success for a compound to transition into the clinic.[82,85]

The evidence of their utility is apparent in natural products. Nature evolved to make specific spirocycles, such as griseofulvin used as an antifungal drug (Figure 5.1), with a variety of ring systems ranging from three to eight carbons.[86] This has led chemists to involve a diverse range of spirocycles in new synthetic pharmaceuticals. In 1957, a spirolactone was noted as a breakthrough development for a mineralocorticoid receptor (MR) antagonist.[87] These spirolactones have since been added to a variety of different drugs including digitoxin and drospirenone, a progesterone analogue.[82,87] Peaking in 2008, the keyword spiro in medicinal chemistry journals has been published hundreds of times over the past decade. Even more recently spirocycles are being used in modern technologies, such as GSK's spiropiperidine in their DNA-encoded library.[88]

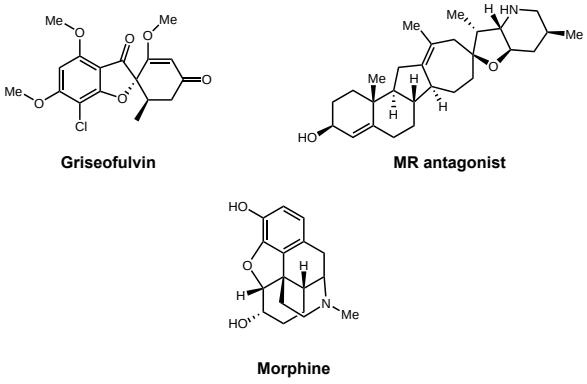

Figure 5.1: Select spirocyclic compounds from natural products and pharmaceuticals

Piperidines are specifically a desirable heterocycle in drug scaffolds.[81,89] Due to their saturated ring, there is an increased flexibility for hydrogen bonding to amino acids. Key spiropiperidines are found in various drug scaffolds, but most notably is the key structural component to give morphine its high potency.[90,91] Therefore, there is a great desire and need to be able to form spirocyclic piperidines.

5.2 The use of catalysis in order to make hard to form bonds

Nature has evolved to form complex and strained bond structures through the utilization of enzymes. These enzymes commonly use metal atoms or radicals to assemble complex molecules.[92] Through studying enzymes, chemists have been able to mimic enzymatic activity by developing their own chemical reactions to form a variety of different substrates using various metals, temperatures, atmospheres, and energy sources.[93,94] Although chemists are close to synthesizing molecules as effectively as enzymes in nature, they are still struggling with the environmental toxicity of reagents and catalysts that are needed in order to achieve the same products as enzymes.[94,95]

Photoredox catalysis offers a mild strategy to make high energy bond transformations.[96] Utilizing light, both visible and ultraviolet, an electron from the ground state of a photocatalyst (PC) can be excited to a high-energy singlet state. Following intersystem crossing, the electrons form a long-lived triplet excited state to give the active species, PC*. This excited species can now be utilized as either an oxidant or a reductant based on the reaction environment. With the ability to manipulate the mechanistic pathway, a reductant can sacrificially give an electron to the PC* via reductive quenching to give the ground state radical anion $PC^{\bullet-}$. The $PC^{\bullet-}$ now can

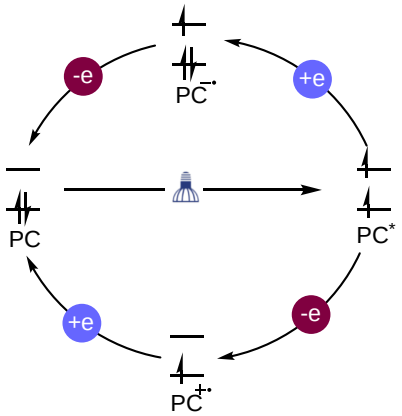

Figure 5.2: Excitation diagram for photocatalysts

act as the reductant to reduce the substrate, returning the catalyst to the neutral ground state and completing the catalytic cycle. In another pathway, the triplet excited state (PC*) could initially reduce the substrate, turning the catalyst into an oxidant ($PC^{\bullet+}$). After subsequent oxidation of a reductant would in turn return the catalyst to ground state (PC).[96,97] Through tuning the associated redox potentials of the catalyst we have the ability to control radicals within a system.

Stephenson and coworkers showed in 2012 the utility of using this mechanistic route when they successfully reduced aryl iodides that subsequently underwent an intramolecular cyclization by adding into linked alkene substrates to produce bicyclic structures in high yields.[98] Based on this work, the Jui lab created a series of both intra- and intermolecular hydroarylation methods that selectivity react with electron- poor, -rich, and -neutral olefins. The first systems developed by Aycock and Boyington used $[Ir(ppy)_2dtbbpy]^+$ to create the pyridyl radical which in turn engages with alkenes to either give conjugate addition or the anti-Markovnikov product, respectively.[99,100] These methods utilized a mild, safe, flexible method to create previously hard to form bonds. McDaniel and Flynn in 2020 published a hydroarylation method that involves the dearomatization of benzene rings.[101] Although they sought to also apply this method to pyridines in order to make

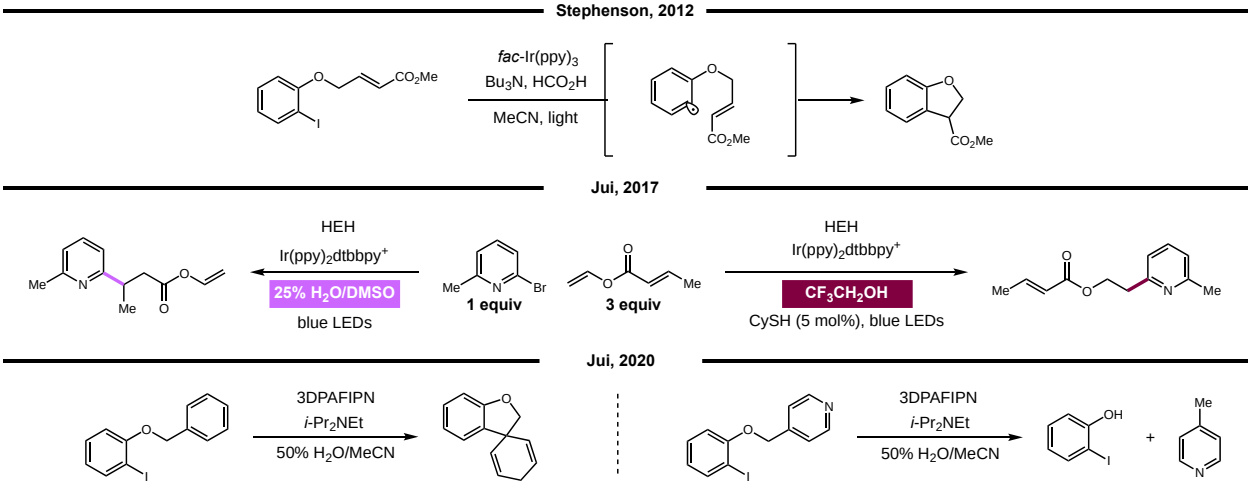

Figure 5.3: Hydroarylation reactions developed over the years

the desired spiropiperidine, it instead resulted in mesolytic cleavage of the pyridine ring. We sought to use this knowledge in order to make various spiropiperidine complexes.

Chapter 6: Synthesis of Spirocyclic Piperidines via Radical Hydroarylation

Adapted and Reprinted in part with permission from *Synlett*. **2021**, 32(2), 211-214

DOI: 10.1055/a-1315-1014

Abstract: Reported here are conditions for the construction of spirocyclic piperidines from linear aryl halide precursors. These conditions employ a strongly-reducing organic photoredox catalyst, in combination with a trialkylamine reductant, to achieve formation of aryl radical species. Regioselective cyclization followed by hydrogen atom transfer afforded a range of complex spiropiperidines. This system efficiently operates under mild conditions, without the need for toxic reagents or precious metals.

6.1 Introduction

Heterocycles play central roles in the development of pharmaceuticals and agrichemicals.[89,102] Among the many nitrogen-containing heterocyclic scaffolds of value, piperidine is the most widely represented in FDA approved drugs.[89] Within this family, spirocyclic piperidines are particularly interesting to us because of their rigidity, structural complexity, and utility as pharmacophore templates across a range of different biological targets. Shown in Figure 6.1 is a select collection of bioactive spiropiperidines, where the piperidine units are bound with different saturated heterocycles.[103–105] While the embedded spirocyclic systems are very similar in nature, their respective synthetic routes differ significantly. For example, the oxindole RSV fusion inhibitor was prepared using enolate arylation,[103] and the spiroindoline growth hormone secretagogue arises via a Fisher-type condensation/rearrangement sequence of a hydrazine building block.[104] Assembly of the

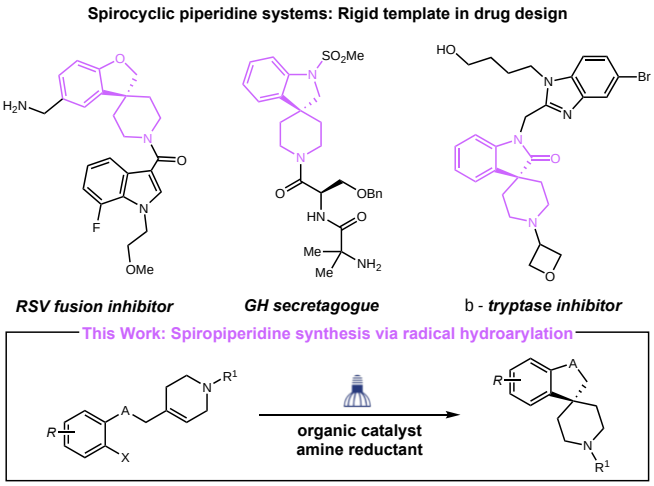

Figure 6.1: Practical metal-free approach to spirocyclic piperidines

spirocyclic framework in the β-tryptase inhibitor (shown in Figure 6.1) was performed using a tin-mediated radical chain mechanism.[105,106] We questioned whether the salient mechanistic feature of this pathway (i.e. regioselective aryl radical cyclization) could be accessed via organic photoredox catalysis.[96] If successful, this would provide a flexible route to a diverse array of spiropiperidines without the need for harsh conditions, toxic reagents, or precious metals.

Our lab has developed a series of olefin hydroarylation methods that leverage the highly-reactive nature of aryl radicals.[99,100,107] Through reduction of aryl and heteroaryl halides by photoredox catalysts,[98] the resulting radical species can be intercepted with olefinic substrates to deliver a wide range of biorelevant alkylation products. To apply this principle toward the synthesis of spirocyclic piperidines, we envisioned the general strategy that is outlined in Figure 6.1. More specifically, a range of linear aryl halide substrates, easily accessible through heteroatom alkylation, would undergo radical formation via catalytic single electron transfer (SET). Regioselective cyclization and radical termination via hydrogen atom transfer (HAT) would furnish the desired scaffolds. This net reductive machinery is appealing, in part, because it would be driven by visible light and a commercial, nontoxic amine.

6.2 Results and Discussion

To evaluate this idea, we constructed a series of linear substrates through alkylation of 2-iodophenol derivatives with a collection of allyl halide electrophiles. In the presence of blue light, 5 mol% of a Zeitler organic photoredox catalyst **P1**,[108] and Hünig's base as reductant (5 equiv), the aryl iodides underwent activation and *exo*-selective radical cyclization to form the desired spirocyclic products that are shown in Table 6.1. Under this protocol, ether-linked substrates were transformed to the corresponding dihydrofuran-fused piperidine structures like **1** (81% yield); this

scaffold has been evaluated extensively for its ability to modulate opioid receptors.[109,110] In addition, nitrogen and sulfur-linked systems smoothly cyclized to afford indoline **2** and dihydrothianapthene **3** in direct fashion. As expected, other cyclic olefin systems could be utilized

Table 6.1: Organic photoredox spirocyclization: Substrate scope

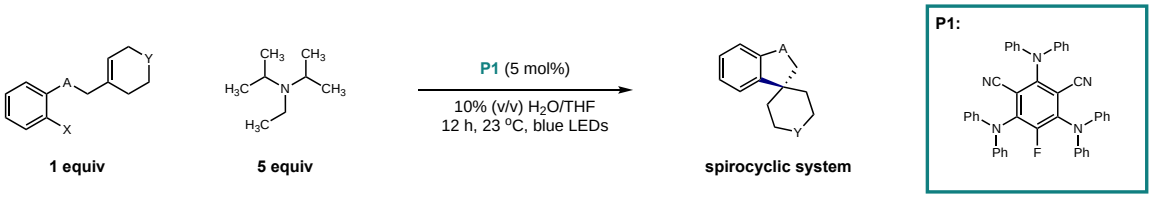

aryl halide	product		aryl halide	product	
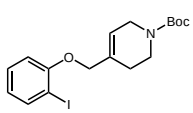	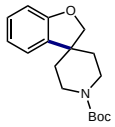	**1: 81%**	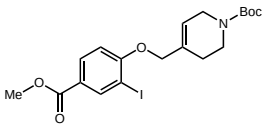	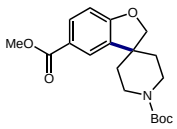	**7: 77%**[b]
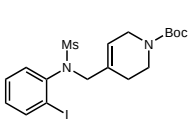	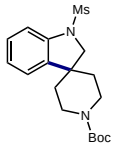	**2: 81%**	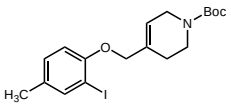	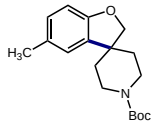	**8: 65%**
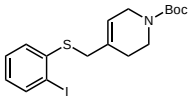	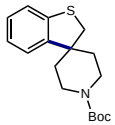	**3: 37%**	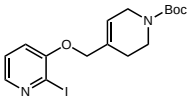	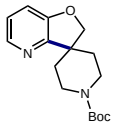	**9: 84%**
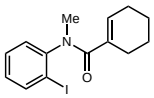	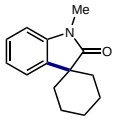	**4: 51%**	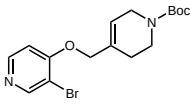	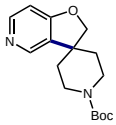	**10: 37%**
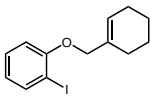	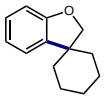	**5: 94%**	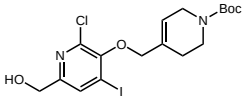	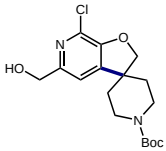	**11: 67%**
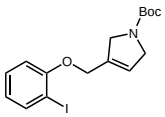	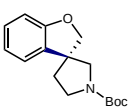	**6: 68%**	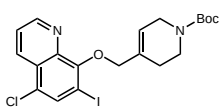	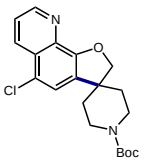	**12: 38%**

[a]Conditions: (het)aryl halide (0.3 mmmol), 3DPAFIPN (5.0 mol %), *i*-Pr$_2$NEt (1.5 mmol) 10% H$_2$O/THF is (6 mL), blue LEDs, 23ºC, 12 h, isolted yields shown.
[b]Ran on a 0.24 scale.

here, where *exo*-selective hydroarylation of cyclohexene and dihydropyrrole substrates gave rise to the desired products (**4**–**6**) in 51–94% yield. Iodophenol derivatives bearing substitution at the

4-position were good substrates under the standard conditions, where **7** and **8** were produced in 77% and 65% yield, respectively. In the same manner, reduction of pyridyl substrates with halogenation at the 2, 3, and 4-positions triggered reductive cyclization to afford the complex tri-heterocyclic systems (**9**–**11**, 37–84% yield). The formation of complex pyridine **11** demonstrates: (i) the ability of this approach to chemoselectively activate the Ar–I function in preference to the Ar–Cl (based on C–X bond strength)[111] and (ii) the inherent tolerance of the key radical intermediates to couple with olefins in the presence of acidic/polar functional groups like alcohols. The former is underscored by the reductive cyclization of 7-iodo-5- chloroquinoline **12**.

Shown in Figure 6.2 is a proposed mechanism for this transformation. Photoexcitation of the donor-acceptor cyanoarene catalyst **P1** (3DPAFIPN) would be followed by reductive quenching with Hünig's base, E1/2° = 0.84 V vs. SCE (**P1***: E1/2° = +1.09 V vs. SCE).[108,112] Single electron transfer (SET) from the resulting ground state reductant (**P1**$^{\bullet-}$: E1/2°= –1.59 V vs. SCE)[108] to aryl halide **13**, followed by rapid halide expulsion from the aryl radical anion, would give rise to radical species **14**. Radical cyclization through the *exo*-mode would furnish intermediate **15**, thus forging the spirocyclic scaffold. Radical termination via hydrogen atom transfer would deliver the desired hydroarylation product **1**. Support for this proposal includes a high observed rate of **P1*** luminescence quenching by the amine base (KSV ~1700), indicating that radical formation likely occurs via reductive quenching.[101] To probe the nature of radical termination in this process, we conducted a

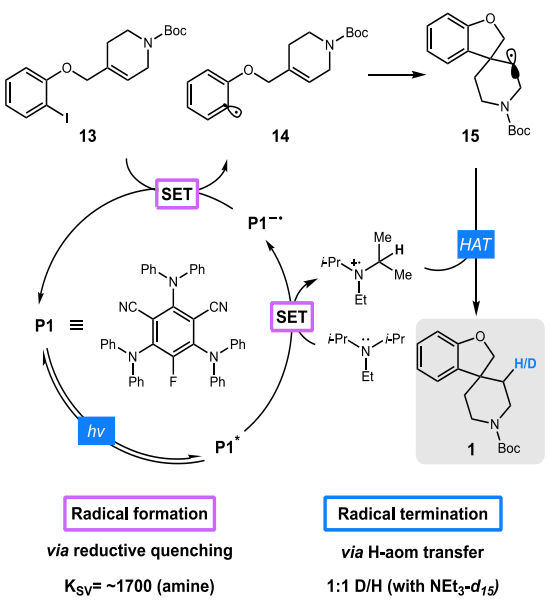

Figure 6.2: Metal free hydroarylation mechanistic proposal

series of isotopic labeling studies. We found that, when the amine reductant was substituted with triethylamine-*d15*, we observed deuterium transfer from the amine to the product **1**, albeit with moderate fidelity (~1:1 D/H). Here, proton incorporation presumably occurs through hydrogen atom abstraction from THF. Though radical termination could, in principle, occur through reductive radical-polar crossover and protonation of the resulting anion, deuterium incorporation was not observed when the reaction was conducted in the presence of D2O.

6.3 Conclusions

In summary, we have developed a photoredox strategy for spiropiperidine synthesis. Here, light-driven reduction of linear aryl halides to the corresponding radical species is accomplished by an organic catalyst. Regioselective cyclization and radical termination via hydrogen atom transfer afford the desired scaffolds, where substitution of the aryl radical precursor, linking alkyl unit, and cyclic olefin was well-tolerated, affording a wide range of complex spiro-fused heterocycles.

6.4 Supporting Information

6.4.1 General Information

Solvents used in anhydrous reactions were purified by passing over activated alumina and storing under argon. Reagents were purchased from Sigma-Aldrich, Alfa Aesar, Combi-Blocks, Oakwood Chemicals, TCI America, and Cambridge Isotopes and used as received, unless stated otherwise. Organic solutions were concentrated under reduced pressure on a rotary evaporator using a water bath. Chromatographic purification of products was accomplished using forced-flow chromatography on 230–400 mesh silica gel. Eluents used were unmodified unless otherwise stated. Thin-layer chromatography (TLC) was performed on 250 μm SiliCycle silica gel F-254 plates. Visualization of the developed chromatogram was performed by fluorescence quenching or staining using a $KMnO_4$ stain. Solvent was degassed by sonication under mild vacuum for 15 minutes. Photoredox catalysts 3DPAFIPN, was prepared according to the literature procedure.[108] All yields refer to chromatographically and spectroscopically (^{1}H NMR) homogenous materials. New compounds were characterized by NMR and LCMS. ^{1}H and ^{13}C NMR spectra were obtained from the Emory University NMR facility and recorded on a Bruker Avance III HD 600 equipped with cryo-probe (600 MHz), INOVA 600 (600 MHz), INOVA 400 (400 MHz), or VNMR 400 (400 MHz), and are internally referenced to residual protio solvent signals. Data for ^{1}H NMR are reported as follows: chemical shift (ppm), multiplicity (s = singlet, d = doublet, t = triplet, q = quartet, m = multiplet, dd = doublet of doublets, dt = doublet of triplets, ddd= doublet of doublet of doublets, b= broad), coupling constant (Hz), and integration, when applicable. Data for decoupled ^{13}C NMR are reported in terms of chemical shift and multiplicity when applicable. Liquid Chromatography Mass Spectrometry (LC-MS) was performed on an Agilent 6120 mass spectrometer with an Agilent 1220 Infinity liquid chromatography inlet.

6.4.2. General Procedures

6.4.2.1 General Coupling Procedure A: A round bottom flask was charged with aryl halide (1.1 equiv) and K_2CO_3 (2.0 equiv). The round bottom was equipped with a stir bar and was sealed with a red septum stopper. The atmosphere was exchanged by applying vacuum and backfilling with nitrogen (this process was conducted a total of three times). Under nitrogen atmosphere, DMF (0.1 M) was added via syringe followed by *tert*-butyl 4- (chloromethyl-3,6-dihydropyridine- 1(*2H*)-carboxylate (1.0 equiv). The resulting mixture was stirred at 70 °C for 12 h before being cooled to room temperature. The reaction mixture was diluted with ethyl acetate and washed with water (1x 100 mL) and brine (3x 100 mL). The organic layer was dried over sodium sulfate, filtered, and concentrated via rotary evaporation. The residue was purified on silica using the indicated solvent mixture as eluent to afford the product.

6.4.2.2 General Coupling Procedure B: A round bottom flask was charged with aryl halide (1.1 equiv) and K_2CO_3 (2.0 equiv). The round bottom was equipped with a stir bar and was sealed with a red septum stopper. The atmosphere was exchanged by applying vacuum and backfilling with nitrogen (this process was conducted a total of three times). Under nitrogen atmosphere, DMF (0.1 M) was added via syringe followed by *tert*-butyl 4- (chloromethyl-3,6-dihydropyridine- 1(*2H*)-carboxylate (1.0 equiv). The resulting mixture was stirred at 70 °C for 12 h before being cooled to room temperature. The reaction mixture was diluted with ethyl acetate and washed with water (1x 100 mL), 1M NaOH (2x 100mL), and brine (3x 100mL). The organic layer was dried over sodium sulfate, filtered, and concentrated via rotary evaporation to give the title compound with no further purification required.

6.4.2.3 General Photoredox Procedure: A 16 mL screw-top test tube was charged with substrate (0.3 mmol, 1.0 equiv) and photocatalyst (0.015 mmol, 5 mol%). The tube was equipped with a stir bar and was sealed with a PTFE/silicon septum. The atmosphere was exchanged by applying vacuum and backfilling with nitrogen (this process was conducted a total of three times). Under nitrogen atmosphere, separated degassed solvent was added via syringe (5.4 mL of THF and 0.6 mL of DI H_2O to give a 0.05 M solution), followed by diisopropylethylamine (1.5 mmol, 5.0 equiv). The resulting mixture was stirred at 800 RPM for 16 h under the irradiation by blue LEDs. The reaction mixture was then diluted with water and extracted with ethyl acetate (3x 20 mL). The organic layer was dried over sodium sulfate, filtered, and concentrated via rotary evaporation. The residue was purified on silica using the indicated solvent mixture as eluent to afford the product.

6.4.3 Spectral Data and Procedures for Starting Material Preparation

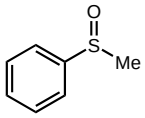

(methylsulfinyl)benzene (S1): The title compound was prepared according to the reported procedure and the NMR data were consistent with those previously reported.[113]

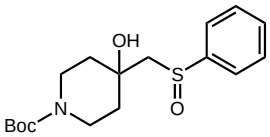

***tert*-butyl 4-hydroxy-4-((phenylsulfinyl)methyl)piperidine-1-carboxylate (S2):** The title compound was prepared according to the reported procedure and the NMR data were consistent with those previously reported.[114]

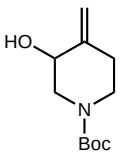

***tert*-butyl 3-hydroxy-4-methylenepiperidine-1-carboxylate (S3):** The title compound was prepared according to the reported procedure and the NMR data were consistent with those previously reported.[114]

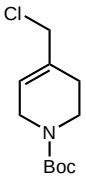

***tert*-butyl 4-(chloromethyl)-3,6-dihydropyridine-1(2*H*)-carboxylate (S4):** The title compound was prepared according to the reported procedure and the NMR data were consistent with those previously reported.[114]

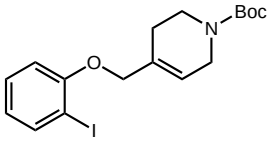

***tert*-butyl 4-((2-iodophenoxy)methyl)-3,6-dihydropyridine-1(2*H*)-carboxylate (S5):** Following general procedure A, the reaction of 2-iodophenol (209 mg, 0.95 mmol, 1.1 equiv), K_2CO_3 (357 mg, 2.6 mmol, 2.0 equiv), *tert*-butyl 4-(chloromethyl)-3,6-dihydropyridine-1(2*H*)-carboxylate (200.1 mg, 0.86 mmol, 1.0 equiv), and DMF (8.6 mL) provided the title compound (270 mg, 76% yield) as a white solid after purification by flash column chromatography (10-20% EtOAc/Hex eluent).

^{1}H NMR (600 MHz, $CDCl_3$) δ 7.76 (d, *J* = 7.7 Hz, 1H), 7.27 (t, *J* = 8.7, 7.5 Hz, 1H), 6.80 (d, *J* = 8.3 Hz, 1H), 6.71 (td, *J* = 7.6, 2.3 Hz, 1H), 5.85 (s, 1H), 4.47 (s, 2H), 3.95 (s, 2H), 3.56 (s, 2H), 2.25 (s, 2H), 1.47 (s, 9H).

^{13}C NMR (151 MHz, $CDCl_3$) δ 157.06, 154.91, 139.51, 132.09, 129.42, 122.76, 112.41, 86.66, 79.67, 72.04, 43.35, 39.87 28.49, 25.83.

LRMS (APCI) m/z: $[M+H]^+$ calc'd. for $C_{17}H_{23}INO_3$: 416.1, found 316.1 (**S5**-Boc)

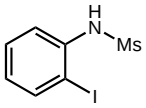

***N*-(2-iodophenyl)methanesulfonamide (S6):** The title compound was prepared according to the reported procedure and the NMR data were consistent with those previously reported.[115]

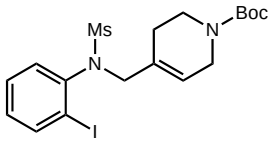

***tert*-butyl 4-((*N*-(2-iodophenyl)methylsulfonamido)methyl)-3,6-dihydropyridine-1(2*H*)-carboxylate (S7):** Following general procedure A, the reaction of *N*-(2-iodophenyl) methanesulfonamide (328 mg, 1.1 mmol, 1.1 equiv), K_2CO_3 (276 mg, 2.0 mmol, 2.0 equiv), *tert*-butyl 4- (chloromethyl)-3,6-dihydropyridine-1(2*H*)-carboxylate (231.7 mg, 1.0 mmol, 1.0 equiv), and DMF (10 mL) provided the title compound (318 mg, 65% yield) as a yellow oil after purification by flash column chromatography (20-50% EtOAc/Hex eluent).

^{1}H NMR (600 MHz, $CDCl_3$) δ 7.92 (t, *J* = 6.8 Hz, 1H), 7.35 (m, 2H), 7.06 (d, *J* = 7.1 Hz, 1H), 5.37 (s, 1H), 4.30 (d, *J* = 14.7 Hz, 1H), 4.13 (d, *J* = 14.0 Hz, 1H), 3.75 (t, *J* = 18.0 Hz, 2H), 3.50 (d, *J* = 12.6 Hz, 1H), 3.42 (s, 1H), 3.08 (s, 3H), 2.27(s, 2H), 1.44 (s, 9H)

^{13}C NMR (151 MHz, $CDCl_3$) δ 154.97, 140.75, 132.78, 130.32, 129.32, 100.52, 79.80, 60.53, 56.64, 41.28, 31.73, 29.71, 28.59, 27.06, 22.79, 14.26.

LRMS (APCI) m/z: $[M+H]^+$ calc'd. for $C_{18}H_{26}IN_2O_4S$: 493.1, found 393.0 (**S7**-Boc)

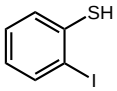

2-iodobenzenethiol (S8): The title compound was prepared according to the reported procedure and the NMR data were consistent with those previously reported.[116]

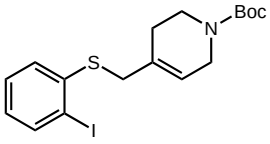

***tert*-butyl 4-(((2-iodophenyl)thio)methyl)-3,6-dihydropyridine-1(2*H*)-carboxylate (S9):** Following general procedure A, the reaction of 2-iodobenzenethiol (924 mg, 3.9 mmol, 1.3 equiv), K_2CO_3 (801 mg, 5.8 mmol, 2.0 equiv), *tert*-butyl 4- (chloromethyl)-3,6-dihydropyridine-1(2*H*)-carboxylate (671.9 mg, 2.9 mmol, 1.0 equiv), and DMF (29 mL) provided the title compound (964 mg, 77% yield) as a clear oil after purification by flash column chromatography (10-20% EtOAc/Hex eluent).

^{1}H NMR (600 MHz, $CDCl_3$) δ 7.83 (dd, *J* = 7.9, 1.3 Hz, 1H), 7.37 – 7.26 (m, 2H), 6.88 (td, *J* = 7.3, 1.8 Hz, 1H), 5.52 (s, 1H), 3.82 (s, 2H), 3.53 (s, 2H), 3.49 (s, 2H), 2.25 (s, 2H), 1.46 (s, 9H).

^{13}C NMR (151 MHz, $CDCl_3$) δ 154.66, 140.83, 139.43, 131.11, 129.33, 128.42, 127.32, 123.49, 122.31, 101.31, 79.46, 41.24, 40.89, 28.33, 27.37.

LRMS (APCI) m/z: $[M+H]^+$ calc'd. for $C_{17}H_{23}INO_2S$: 432.0, found 376.1 (**S9**-*t*Bu)

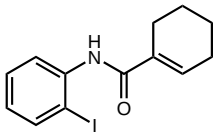

***N*-(2-iodophenyl)cyclohex-1-ene-1-carboxamide (S10):** The title compound was prepared according to the reported procedure and the NMR data were consistent with those previously reported.[117]

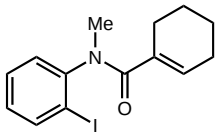

***N*-(2-iodophenyl)-*N*-methylcyclohex-1-ene-1-carboxamide (S11):** The title compound was prepared according to the reported procedure and the NMR data were consistent with those previously reported.[117]

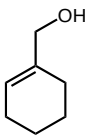

cyclohex-1-en-1-ylmethanol (S12): The title compound was prepared according to the reported procedure and the NMR data were consistent with those previously reported.[118]

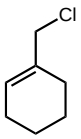

1-(chloromethyl)cyclohex-1-ene (S13): The title compound was prepared according to the reported procedure and the NMR data were consistent with those previously reported.[118]

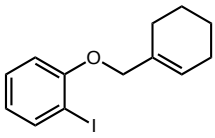

1-(cyclohex-1-en-1-ylmethoxy)-2-iodobenzene (S14): The title compound was prepared according to the reported procedure and the NMR data were consistent with those previously reported.[119]

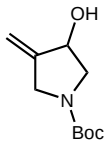

***tert*-butyl 3-hydroxy-4-methylenepyrrolidine-1-carboxylate (S15):** The title compound was prepared according to the reported procedure and the NMR data were consistent with those previously reported.[120]

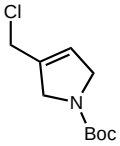

***tert*-butyl 3-(chloromethyl)-2, 5-dihydro-1*H*-pyrrole-1-carboxylate (S16):** The title compound was prepared according to the reported procedure and the NMR data were consistent with those previously reported.[121]

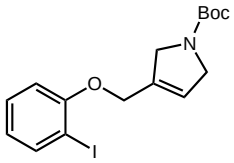

***tert*-butyl 3-((2-iodophenoxy)methyl)-2,5-dihydro-1*H*-pyrrole-1-carboxylate (S17):** Following general procedure A, the reaction of 2-iodophenol (873 mg, 3.97 mmol, 1.2 equiv), K_2CO_3 (914 mg, 6.62 mmol, 2.0 equiv), *tert*-butyl 3-(chloromethyl)-2,5-dihydro-1*H*-pyrrole-1-carboxylate (720.2 mg, 3.30 mmol, 1.0 equiv), and DMF (33 mL) provided the title compound (682.1 mg, 52% yield) as a clear oil after purification by flash column chromatography (10% EtOAc/Hex eluent).

^{1}H NMR (600 MHz, $CDCl_3$) δ 7.75 (d, *J* = 7.3 Hz, 1H), 7.25 (t, *J* = 7.0 Hz, 1H), 6.78 (d, *J* = 7.9 Hz, 1H), 6.70 (t, *J* = 6.7 Hz, 1H), 5.87 (d, *J* = 17.8 Hz, 1H), 4.61 (s, 2H), 4.20 (dd, *J* = 18.6, 12.8 Hz, 3H), 4.13 (s, 1H), 1.45 (s, 9H).

^{13}C NMR (151 MHz, $CDCl_3$) δ 156.75, 154.12, 139.50, 134.85, 129.37, 122.92, 122.66, 112.07, 86.49, 79.41, 65.96, 53.32, 52.97, 28.42.

LRMS (APCI) m/z: $[M+H]^+$ calc'd. for $C_{16}H_{21}INO_3$: 402.1, found 345.8 (**S17**-*t*Bu)

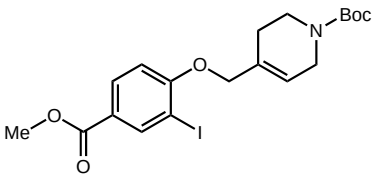

***tert*-butyl-4-((2-iodo-4-(methoxycarbonyl)phenoxy)methyl)-3,6-dihydropyridine-1(2*H*)-carboxylate (S18):** Following general procedure B, the reaction of 4-hydroxy-3-iodobenzoate (306 mg, 1.1 mmol, 1.1 equiv), K_2CO_3 (276 mg, 2.0 mmol, 2.0 equiv), *tert*-butyl 4-(chloromethyl)-3,6-dihydropyridine-1(2*H*)-carboxylate (231.72 mg, 1.0 mmol, 1.0 equiv), and DMF (10 mL) provided the title compound (391 mg, 83% yield) as a clear oil.

^{1}H NMR (400 MHz, $CDCl_3$) δ 8.41 (d, *J* = 2.1 Hz, 1H), 7.95 (d, *J* = 8.6 Hz, 1H), 6.77 (dd, *J* = 8.7, 2.8 Hz 1H), 5.84 (s, 1H), 4.50 (s, 2H), 3.93 (s, 2H), 3.85 (s, 3H), 3.53 (s, 2H), 2.21 (s, 2H), 1.44 (s, 9H) ppm.

^{13}C NMR (151 MHz, $CDCl_3$) δ 165.28, 160.36, 154.68, 140.81, 131.38, 131.33, 124.29, 122.67, 121.77, 116.22, 110.98, 85.69, 79.55, 72.01, 51.95, 28.29, 25.58.

LRMS (APCI) m/z: $[M+H]^+$ calc'd. for $C_{19}H_{25}INO_5$: 474.1, found 417.6 (**S18**-*t*Bu)

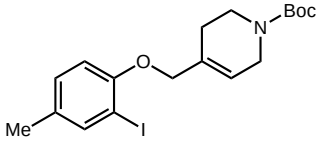

***tert*-butyl 4-((2-iodo-4-methylphenoxy)methyl)-3,6-dihydropyridine-1(2*H*)-carboxylate (S19):** Following general procedure B, the reaction of 2-iodo-4-methylphenol (257 mg, 1.1 mmol, 1.1 equiv), K_2CO_3 (276 mg, 2.0 mmol, 2.0 equiv), *tert*-butyl 4- (chloromethyl)-3,6-dihydropyridine-1(2*H*)-carboxylate (231.72 mg, 1.0 mmol, 1.0 equiv), and DMF (10 mL) provided the title compound (359 mg, 84% yield) as a clear oil.

^{1}H NMR (600 MHz, $CDCl_3$) δ 7.58 (s, 1H), 7.05 (d, *J* = 8.1 Hz, 1H), 6.68 (d, *J* = 8.5 Hz, 1H), 5.84 (s, 1H), 4.41 (s, 2H), 3.94 (s, 2H), 3.55 (s, 2H), 2.24 (m, 5H), 1.46 (s, 9H).

^{13}C NMR (151 MHz, $CDCl_3$) δ 154.87, 154.72, 139.63, 132.18, 132.08, 129.70, 121.08, 112.16, 86.36, 79.46, 72.05, 43.20, 40.12, 39.28, 28.33, 25.68.

LRMS (APCI) m/z: $[M+H]^+$ calc'd. for $C_{18}H_{25}INO_3$: 430.1, found 373.7 (**S19**-*t*Bu)

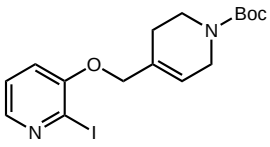

***tert*-butyl 4-(((2-iodopyridin-3-yl)oxy)methyl)-3,6-dihydropyridine-1(2*H*)-carboxylate (S20):** Following general procedure B, the reaction of 2-iodopyridin-3-ol (243 mg, 1.1 mmol, 1.1 equiv), K_2CO_3 (304 g, 2.2 mmol, 2.2 equiv), *tert*-butyl 4- (chloromethyl)-3,6-dihydropyridine-1(2*H*)-carboxylate (231.72 mg, 1.0 mmol, 1.0 equiv), and DMF (10 mL) provided the title compound (348 mg, 84% yield) as an off-white solid.

^{1}H NMR (600 MHz, $CDCl_3$) δ 7.94 (s, 1H), 7.12 (m, 1H), 6.94 (dd, *J* = 8.1, 1H), 5.81 (s, 1H), 4.45 (s, 2H), 3.91 (s, 2H), 3.51 (s, 2H), 2.19 (s, 2H), 1.42 (s, 9H).

^{13}C NMR (151 MHz, $CDCl_3$) δ 154.83, 154.18, 142.84, 131.36, 123.44, 122.19, 118.30, 112.22, 79.74, 72.16, 43.31, 39.37, 28.48, 25.77.

LRMS (APCI) m/z: $[M+H]^+$ calc'd. for $C_{16}H_{22}IN_2O_3$: 417.1, found 416.7

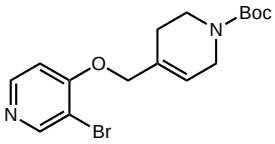

***tert*-butyl 4-(((3-bromopyridin-4-yl)oxy)methyl)-3,6-dihydropyridine-1(2*H*)-carboxylate (S21):** Following general procedure A, the reaction of 3-bromopyridin-4-ol (396.7 mg, 2.28 mmol, 1.2 equiv), K_2CO_3 (525.2 mg, 3.8 mmol, 2.0 equiv), *tert*-butyl 4-(chloromethyl)-3,6-dihydropyridine-1(2*H*)-carboxylate (430.4 mg, 1.9 mmol, 1.0 equiv), and DMF (19 mL) provided the title compound (107.2 mg, 15% yield) as a yellow oil after purification by flash column chromatography (20-100% EtOAc/Hex eluent).

^{1}H NMR (600 MHz, $CDCl_3$) δ 8.58 (s, 1H), 8.36 (d, *J* = 5.3 Hz, 1H), 6.79 (d, *J* = 5.7 Hz, 1H), 5.83 (s, 1H), 4.54 (s, 2H), 3.95 (s, 2H), 3.47 (s, 2H), 2.21 (s, 2H), 1.46 (s, 9H).

^{13}C NMR (101 MHz, $CDCl_3$) δ 160.65, 154.62, 152.36, 149.74, 130.84, 122.00, 110.30, 108.27, 79.63, 71.46, 28.26, 28.15, 27.87, 25.41.

LRMS (APCI) m/z: $[M+H]^+$ calc'd. for $C_{16}H_{22}BrN_2O_3$: 369.1, found 369.1

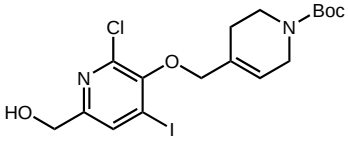

***tert*-butyl 4-(((2-chloro-6-(hydroxymethyl)-4-iodopyridin-3-yl)oxy)methyl)-3,6-dihydropyridine-1(2*H*)-carboxylate (S22):** Following general procedure A, the reaction of 2-chloro-6-(hydroxymethyl)-4-iodopyridin-3-ol (236 mg, 0.825 mmol, 1.1 equiv), K_2CO_3 (207 mg, 1.5 mmol, 2.0 equiv), *tert*-butyl 4-(chloromethyl)-3,6-dihydropyridine-1(2*H*)-carboxylate (174 mg, 0.75 mmol, 1.0 equiv), and DMF (7.5 mL) provided the title compound (184 mg, 51% yield) as a clear oil after purification by flash column chromatography (20-50% EtOAc/Hex eluent).

^{1}H NMR (600 MHz, $CDCl_3$) δ 7.73 (t, *J* = 0.7 Hz, 1H), 5.58 (s, 1H), 4.68 (dd, *J* = 5.7, 0.7 Hz, 2H), 4.43 (s, 2H), 3.98 (s, 2H), 3.60 (t, *J* = 5.7 Hz, 2H), 2.66 (t, *J* = 5.7 Hz, 1H), 2.41 (s, 2H), 1.46 (s, 9H).

^{13}C NMR (151 MHz, $CDCl_3$) δ 155.79, 154.79, 150.46, 143.81, 130.40, 105.13, 80.29, 76.37, 68.92, 62.46, 43.01, 39.27 28.42, 26.29, 25.55.

LRMS (APCI) m/z: $[M+H]^+$ calc'd. for $C_{17}H_{23}ClN_2O_4$: 481.0, found 481.0

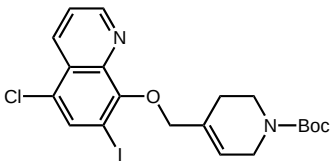

***tert*-butyl 4-(((5-chloro-7-iodoquinolin-8-yl)oxy)methyl)-3,6-dihydropyridine-1(2*H*)-carboxylate (S23):** Following general procedure A, the reaction of 5-chloro-7- iodoquinolin-8-ol (336 mg, 1.1 mmol, 1.1 equiv), K_2CO_3 (276 mg, 2.0 mmol, 2.0 equiv), *tert*-butyl 4-(chloromethyl)-3,6-dihydropyridine-1(2*H*)-carboxylate (231.72 mg, 1.0 mmol, 1.0 equiv), and DMF (10 mL)

provided the title compound (378 mg, 76% yield) as a green oil after purification by flash column chromatography (30% EtOAc/Hex eluent).

^{1}H NMR (400 MHz, $CDCl_3$) δ 8.99 (m, 1H), 8.53 (dd, *J* = 8.6, 1.7 Hz, 1H), 8.04 (s, 1H), 7.55 (dd, *J* = 8.6, 4.1 Hz, 1H), 5.87 (s, 1H), 4.83 (s, 2H), 3.92 (s, 2H), 3.61 (s, 2H), 2.59 (s, 2H), 1.46 (s, 9H).

^{13}C NMR (101 MHz, $CDCl_3$) δ 154.70, 150.22, 142.28, 134.95, 133.33, 132.82, 128.16, 127.32, 126.37, 122.12, 90.08, 79.36, 77.63, 77.04, 43.64, 40.73, 28.33, 26.40.

LRMS (APCI) m/z: $[M+H]^+$ calc'd. for $C_{20}H_{23}ClIN_2O_3$: 501.0, found 500.5

Ch.4.4 Spectral Data and Procedures for Products from Substrate Table

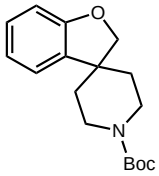

***tert*-butyl 2*H*-spiro[benzofuran-3,4'-piperidine]-1'-carboxylate (1):** Following general procedure C, the reaction of *tert*-butyl 4-((2- iodophenoxy)methyl)-3,6-dihydropyridine-1(2*H*)-carboxylate (**S5**) (124.5 mg, 0.3 mmol, 1.0 equiv), N,N-diisopropylethylamine (0.26 mL, 1.5 mmol, 5 equiv), and 3DPAFIPN (10 mg, 5 mol%) provided the product (70.3 mg, 81% yield) as an off-white solid after purification by flash chromatography (10-50% EtOAc/Hex eluent).

^{1}H NMR (600 MHz, $CDCl_3$) δ 7.15 (td, *J* = 7.7, 2.2 Hz, 1H), 7.11 (dd, *J* = 7.5, 2.2 Hz, 1H), 6.89 (td, *J* = 7.5, 2.4 Hz, 1H), 6.82 (dd, *J* = 8.0, 2.5 Hz, 1H), 4.40 (s, 2H), 4.07 (s, 2H), 2.90 (t, *J* = 13.1 Hz, 2H), 1.85 (m, 2H), 1.73 (d, *J* = 13.6 Hz, 2H), 1.49 (d, *J* = 2.6 Hz, 9H).

^{13}C NMR (151 MHz, $CDCl_3$) δ 159.29, 154.77, 134.30, 128.50, 122.90, 120.61, 109.84, 79.77, 79.70, 44.53, 35.16, 28.38.

LRMS (APCI) m/z: $[M+H]^+$ calc'd. for $C_{17}H_{24}NO_3$: 290.2, found 233.9 (**1**-*t*Bu)

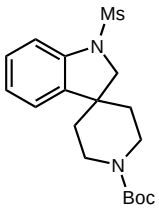

***tert*-butyl 1-(methylsulfonyl)spiro[indoline-3,4'-piperidine]-1'-carboxylate (2):** Following general procedure C, the reaction of *tert*-butyl 4-((*N*-(2-iodophenyl)methylsulfonamido)methyl)-3,6-dihydropyridine-1(2*H*)-carboxylate (**S7**) (153 mg, 0.3 mmol, 1.0 equiv), N,N-diisopropylethylamine (0.26 mL, 1.5 mmol, 5 equiv), and 3DPAFIPN (10 mg, 5 mol%) provided the product (89.1 mg, 81% yield) as a yellow solid after purification by flash chromatography (50% EtOAc/Hex eluent).

^{1}H NMR (600 MHz, $CDCl_3$) δ 7.39 (d, *J* = 8.1 Hz, 1H), 7.23 (td, *J* = 7.7, 1.3 Hz, 1H), 7.14 (dd, *J* = 7.6, 1.3 Hz, 1H), 7.06 (td, *J* = 7.5, 1.0 Hz, 1H), 4.13 (s, 2H), 3.84 (s, 2H), 2.91 (s, 3H), 2.89 – 2.82 (m, 2H), 1.84 (q, *J* = 13.9 Hz, 2H), 1.75 – 1.64 (m, 2H), 1.48 (s, 9H).

^{13}C NMR (151 MHz, $CDCl_3$) δ 154.72, 140.95, 138.29, 128.82, 123.85, 123.27, 113.36, 79.94, 59.10, 42.97, 36.10, 34.19, 28.45.

LRMS (APCI) m/z: $[M+H]^+$ calc'd. for $C_{18}H_{27}N_2O_4S$: 367.2, found 311.1(**2**-*t*Bu)

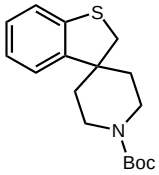

***tert*-butyl 2*H*-spiro[benzo[*b*]thiophene-3,4'-piperidine]-1'-carboxylate (3):** Following general procedure C, the reaction of *tert*-butyl 4-(((2-iodophenyl)thio)methyl)-3,6-dihydropyridine-1(2*H*)-carboxylate (**S9**) (129.4 mg, 0.3 mmol, 1.0 equiv), N,N-diisopropylethylamine (0.26 mL, 1.5 mmol, 5 equiv), and 3DPAFIPN (10 mg, 5 mol%) provided the product (33.9 mg, 37% yield) as a yellow oil after purification by preparative TLC (20% EtOAc/Hex eluent).

^{1}H NMR (400 MHz, $CDCl_3$) δ 7.22 – 7.18 (m, 1H), 7.14 (td, *J* = 7.7, 7.2, 1.9 Hz, 1H), 7.10 – 7.03 (m, 2H), 4.11 (s, 2H), 3.32 (s, 2H), 2.91 (s, 2H), 1.82 (m, 4H), 1.49 (s, 9H).

^{13}C NMR (126 MHz, $CDCl_3$) δ 154.75, 148.57, 141.56, 128.40, 125.41, 123.52, 122.49, 79.62, 50.58, 40.81, 36.79, 28.84.

LRMS (APCI) m/z: $[M+H]^+$ calc'd. for $C_{17}H_{24}NO_2S$: 306.2, found 251.9 (**3**-*t*Bu)

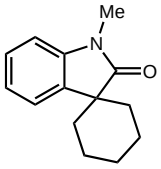

1'-methylspiro[cyclohexane-1,3'-indolin]-2'-one (8): Following general procedure C, the reaction of *N*-(2-iodophenyl)cyclohex-1-ene-1-carboxamide (**S11**) (102.4 mg, 0.3 mmol, 1.0 equiv), N,N-diisopropylethylamine (0.26 mL, 1.5 mmol, 5 equiv), and 3DPAFIPN (10 mg, 5 mol%) provided the product (32.9 mg, 51% yield) as a yellow solid after purification by flash

chromatography (50% EtOAc/Hexanes). The physical properties and spectral data were consistent with the reported values. The NMR data were consistent with those previously reported.[122]

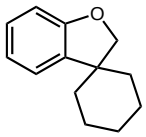

2*H*-spiro[benzofuran-3,1'-cyclohexane] (5): Following general procedure C, the reaction of 1-(cyclohex-1-en-1-ylmethoxy)-2- iodobenzene (**S14**) (94.3 mg, 0.3 mmol, 1.0 equiv), N,N-diisopropylethylamine (0.26 mL, 1.5 mmol, 5.0 equiv), and 3DPAFIPN (10 mg, 5 mol%) provided the product (53.1 mg, 94% yield) as a white solid after purification by flash chromatography (0-10% EtOAc/Hex eluent).

^{1}H NMR (600 MHz, $CDCl_3$) δ 7.15-7.10 (m, 2H), 6.87 (td, *J* = 7.4, 1.0 Hz, 1H), 6.80 (dd, *J* = 8.3, 1.0 Hz, 1H), 4.36 (s, 2H), 1.81 – 1.71 (m, 5H), 1.65 (td, *J* = 13.3, 4.5 Hz, 2H), 1.45-1.28 (m, 3H).

^{13}C NMR (151 MHz, $CDCl_3$) δ 159.23, 136.21, 127.94, 122.82, 120.28, 109.53, 80.90, 46.04, 36.66, 25.36, 23.23.

LRMS (APCI) m/z: $[M+H]^+$ calc'd. for $C_{13}H_{17}O$: 189.1, found 188.1

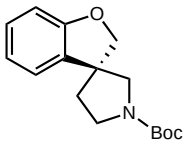

***tert*-butyl (*R*)-2*H*-spiro[benzofuran-3,3'-pyrrolidine]-1'-carboxylate (6):** Following general procedure C, the reaction of *tert*-butyl 3-((2-iodophenoxy)methyl)-2,5-dihydro-1*H*-pyrrole-1-carboxylate (**S17**) (120.4 mg, 0.3 mmol, 1.0 equiv), N,N-diisopropylethylamine (0.26 mL, 1.5

mmol, 5.0 equiv), and 3DPAFIPN (10 mg, 5 mol%) provided the product (56.2 mg, 68% yield) as a yellow oil after purification by flash chromatography (5-50% EtOAc/Hex eluent).

^{1}H NMR (600 MHz, $CDCl_3$)δ 7.17 (t, *J* = 7.8 Hz, 1H), 7.12 (d, *J* = 7.5 Hz, 1H), 6.90 (t, *J* = 7.4 Hz, 1H), 6.83 (d, *J* = 8.0 Hz, 1H), 4.49-4.28 (m, 2H), 3.74-3.37 (m, 4H), 2.18 (dt, *J* = 17.0, 8.8 Hz, 1H), 2.05 (ddd, *J* = 12.3, 7.4, 4.0 Hz, 1H), 1.48 (s, 9H).

^{13}C NMR (151 MHz, $CDCl_3$) *reported as a mix of rotomers* δ 171.00, 159.80, 154.37, 130.29, 128.89, 122.67, 120.86, 109.82, 81.71, 79.56, 60.26, 56.84, 56.05, 51.54, 51.12, 45.23, 44.91, 38.17, 36.96, 28.37.

LRMS (APCI) m/z: $[M+H]^+$ calc'd. for $C_{16}H_{22}NO_3$: 276.2, found 220.1 (**6**-*t*Bu)

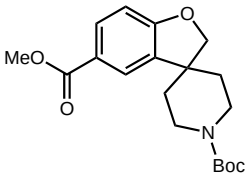

1'-(*tert*-butyl) 5-methyl 2*H*-spiro[benzofuran-3,4'-piperidine]-1',5-dicarboxylate (7): Following general procedure C, the reaction of *tert*-butyl 4-((2-iodo-4-(methoxycarbonyl)phenoxy)methyl)-3,6-dihydropyridine-1(2*H*)- carboxylate (**S18**) (114 mg, 0.24 mmol, 1.0 equiv), N,N-diisopropylethylamine (0.20 mL, 1.2 mmol, 5.0 equiv), and 3DPAFIPN (7.0 mg, 5 mol%) provided the product (64.2 mg, 77% yield) as a light yellow oil after purification by flash chromatography (20% EtOAc/Hex eluent).

^{1}H NMR (400 MHz, $CDCl_3$) δ 7.89 (dd, *J* = 8.4, 1.9 Hz, 1H), 7.79 (d, *J* = 1.9 Hz, 1H), 6.80 (d, *J* = 8.4 Hz, 1H), 4.46 (s, 2H), 4.08 (s, 2H), 3.85 (s, 3H), 2.87 (d, *J* = 13.5 Hz, 2H), 1.87 (td, *J* = 12.9, 4.6 Hz, 2H), 1.71 (d, *J* = 13.6 Hz, 2H), 1.47 (s, 9H).

^{13}C NMR (151 MHz, $CDCl_3$) δ 166.65, 163.42, 152.97, 134.75, 131.45, 124.88, 122.93, 114.17, 109.53, 80.80, 79.76, 51.76, 44.17, 35.90, 28.33.

LRMS (APCI) m/z: $[M+H]^+$ calc'd. for $C_{19}H_{26}NO_5$: 348.2, found 291.8 (**7**-*t*Bu)

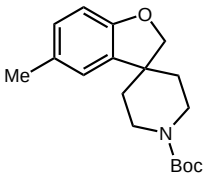

***tert*-butyl 5-methyl-2*H*-spiro[benzofuran-3,4'-piperidine]-1'-carboxylate (8):** Following general procedure C, the reaction of *tert*-butyl 4-((2-iodo-4- methylphenoxy)methyl)-3,6-dihydropyridine-1(2*H*)-carboxylate (**S19**) (129 mg, 0.3 mmol, 1.0 equiv), N,N-diisopropylethylamine (0.26 mL, 1.5 mmol, 5.0 equiv), and 3DPAFIPN (10 mg, 5 mol%) provided the product (59.2 mg, 65% yield) as a yellow oil after purification by flash chromatography (10% EtOAc/Hex eluent).

^{1}H NMR (600 MHz, $CDCl_3$) δ 6.95 (ddd, *J* = 8.1, 1.9, 0.8 Hz, 1H), 6.91 (dt, *J* = 1.9, 0.7 Hz, 1H), 6.70 (d, *J* = 8.1 Hz, 1H), 4.37 (s, 2H), 4.07 (s, 2H), 3.15 – 2.73 (m, 2H), 2.29 (s, 3H), 1.89-1.77 (m, 2H), 1.75 – 1.64 (m, 2H), 1.49 (s, 9H).

^{13}C NMR (151 MHz, $CDCl_3$) δ 157.16, 154.70, 134.28, 129.86, 128.84, 123.43, 114.50, 109.32, 79.84, 79.61, 44.54, 35.78, 28.36, 20.76.

LRMS (APCI) m/z: $[M+H]^+$ calc'd. for $C_{18}H_{26}NO_3$: 304.2, found 248.2 (**8**-*t*Bu)

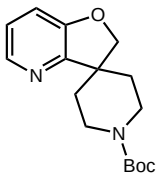

***tert*-butyl 2*H*-spiro[furo[3,2-*b*]pyridine-3,4'-piperidine]-1'-carboxylate (9):** Following general procedure C, the reaction of *tert*-butyl 4-(((2-iodopyridin-3- yl)oxy)methyl)-3,6-dihydropyridine-1(2*H*)-carboxylate (**S20**) (125.3 mg, 0.3 mmol, 1.0 equiv), N,N-diisopropylethylamine (0.26 mL, 1.5 mmol, 5 equiv), and 3DPAFIPN (10 mg, 5 mol%) provided the product (73.2 mg, 84% yield) as a yellow solid after purification by flash chromatography (50% EtOAc/Hex eluent).

^{1}H NMR (400 MHz, $CDCl_3$) δ 8.06 (d, *J* = 2.6 Hz, 1H), 7.01 (d, *J* = 2.0 Hz, 2H), 4.43 (s, 2H), 4.07 (s, 2H), 3.05 (t, *J* = 11.7 Hz, 2H), 2.01 (td, *J* = 12.1, 10.3, 3.6 Hz, 2H), 1.66 (d, *J* = 13.4 Hz, 2H), 1.45 (s, 9H).

^{13}C NMR (151 MHz, $CDCl_3$) δ 155.44, 154.56, 153.06, 141.69, 122.62, 116.08, 80.61, 79.48, 43.66, 40.01 34.38, 28.34.

LRMS (APCI) m/z: $[M+H]^+$ calc'd. for $C_{16}H_{23}N_2O_3$: 291.2, found 291.2

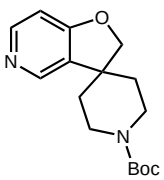

***tert*-butyl 2*H*-spiro[furo[3,2-*c*]pyridine-3,4'-piperidine]-1'-carboxylate (10):** Following general procedure C, the reaction of *tert*-butyl 4-(((3-bromopyridin-4-yl)oxy)methyl)-3,6-dihydropyridine-1(2*H*)-carboxylate (**S21**) (110.5 mg, 0.3 mmol, 1.0 equiv), N,N-diisopropylethylamine (0.26 mL, 1.5 mmol, 5 equiv), and 3DPAFIPN (10 mg, 5 mol%) provided the product (32.2 mg, 37% yield) as a clear oil after purification by flash chromatography (60-100% EtOAc/Hex eluent).

^{1}H NMR (400 MHz, $CDCl_3$) δ 8.26 (m, 2H), 6.71 (d, *J* = 5.5 Hz, 1H), 4.40 (s, 2H), 3.95 (d, *J* = 14.1 Hz, 2H), 2.92 (t, *J* = 12.5 Hz, 2H), 1.82 (ddd, *J* = 13.6, 11.2, 4.5 Hz, 2H), 1.71 (m, 2H), 1.42 (s, 9H).

^{13}C NMR (101 MHz, $CDCl_3$) δ 166.13, 154.54, 150.20, 144.60, 131.00, 106.07, 81.06, 79.85, 77.05, 43.35, 35.54, 28.26.

LRMS (APCI) m/z: $[M+H]^+$ calc'd. for $C_{16}H_{23}N_2O_3$: 291.2, found 291.2

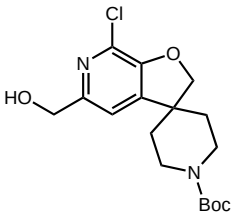

***tert*-butyl 7-chloro-5-(hydroxymethyl)-2*H*-spiro[furo[2,3-*c*]pyridine-3,4'-piperidine]-1'-carboxylate (11):** Following general procedure C, the reaction of *tert*-butyl 4-(((2-chloro-6-(hydroxymethyl)-4-iodopyridin-3-yl)oxy)methyl)-3,6-dihydropyridine-1(2*H*)-carboxylate (**S22**) (150 mg, 0.3 mmol, 1.0 equiv), N,N-diisopropylethylamine (0.26 mL, 1.5 mmol, 5 equiv), and

3DPAFIPN (10 mg, 5 mol%) provided the product (71.3 mg, 67% yield) as a yellow oil after purification by flash chromatography (20% EtOAc/Hex eluent).

^{1}H NMR (600 MHz, $CDCl_3$) δ 7.07 (s, 1H), 4.68 (d, *J* = 5.0 Hz, 2H), 4.55 (s, 2H), 4.07 (s, 2H), 2.96 – 2.88 (m, 3H), 1.88-1.80 (m, 2H), 1.79 – 1.72 (m, 2H), 1.48 (s, 9H).

^{13}C NMR (151 MHz, $CDCl_3$) δ 154.55, 152.82, 151.39, 146.12, 132.91, 131.44, 114.66, 80.89, 80.10, 64.33, 45.97,m40.52, 35.84, 35.24, 28.34.

LRMS (APCI) m/z: $[M+H]^+$ calc'd. for $C_{17}H_{24}ClN_2O_4$: 355.1, found 355.1

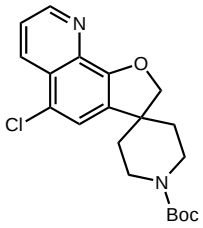

***tert*-butyl 5-chloro-2*H*-spiro[furo[3,2-*h*]quinoline-3,4'-piperidine]-1'-carboxylate (12):** Following general procedure C, the reaction of *tert*-butyl 4-(((5-chloro-7-iodoquinolin-8-yl)oxy)methyl)-3,6-dihydropyridine-1(2*H*)-carboxylate (**S23**) (150 mg, 0.3 mmol, 1.0 equiv), N,N-diisopropylethylamine (0.26 mL, 1.5 mmol, 5.0 equiv), and 3DPAFIPN (10 mg, 5 mol%) provided the product (42.7 mg, 38% yield) as a brown oil after purification by flash chromatography (10-50% EtOAc/Hex eluent).

^{1}H NMR (600 MHz, $CDCl_3$) δ 8.89 (dd, *J* = 4.2, 1.6 Hz, 1H), 8.50 (dd, *J* = 8.6, 1.6 Hz, 1H), 7.48 (dd, *J* = 8.6, 4.1 Hz, 1H), 7.39 (s, 1H), 4.71 (s, 2H), 4.15 (s, 2H), 2.89 (s, 2H), 1.93 (m, 2H), 1.82 (d, *J* = 13.4 Hz, 2H), 1.49 (s, 9H).

^{13}C NMR (151 MHz, $CDCl_3$) δ 154.62, 153.71, 150.29, 136.22, 133.19, 131.75, 126.53, 122.26, 121.88, 121.58, 116.25, 81.08, 79.87, 46.04, 35.94, 28.36.

LRMS (APCI) m/z: $[M+H]^+$ calc'd. for $C_{20}H_{24}ClN_2O_3$: 375.1, found 374.8

References

(1) Santos, R.; Ursu, O.; Gaulton, A.; Bento, A. P.; Donadi, R. S.; Bologa, C. G.; Karlsson, A.; Al-Lazikani, B.; Hersey, A.; Oprea, T. I.; Overington, J. P. A Comprehensive Map of Molecular Drug Targets. *Nat. Rev. Drug Discov.* **2016**, *16* (1), 19–34. https://doi.org/10.1038/nrd.2016.230.

(2) Ghadermarzi, S.; Li, X.; Li, M.; Kurgan, L. Sequence-Derived Markers of Drug Targets and Potentially Druggable Human Proteins. *Front. Genet.* **2019**, *10* (November), 1–18. https://doi.org/10.3389/fgene.2019.01075.

(3) Bull, S. C.; Doig, A. J. Properties of Protein Drug Target Classes. *PLoS One* **2015**, *10* (3), 1–44. https://doi.org/10.1371/journal.pone.0117955.

(4) Germain, P.; Staels, B.; Dacquet, C.; Spedding, M.; Laudet, V. Overview of Nomenclature of Nuclear Receptors. *Pharmacol. Rev.* **2006**, *58* (4), 685–704. https://doi.org/10.1124/pr.58.4.2.

(5) Giguère, V. Transcriptional Control of Energy Homeostasis by the Estrogen-Related Receptors. *Endocr. Rev.* **2008**, *29* (6), 677–696. https://doi.org/10.1210/er.2008-0017.

(6) Weikum, E. R.; Liu, X.; Ortlund, E. A. The Nuclear Receptor Superfamily: A Structural Perspective. *Protein Sci.* **2018**, *27* (11), 1876–1892. https://doi.org/10.1002/pro.3496.

(7) Gujral, P.; Mahajan, V.; Lissaman, A. C.; Ponnampalam, A. P. Histone Acetylation and the Role of Histone Deacetylases in Normal Cyclic Endometrium. *Reprod. Biol. Endocrinol.* **2020**, *18* (1), 1–11. https://doi.org/10.1186/s12958-020-00637-5.

(8) Bannister, A. J.; Kouzarides, T. Regulation of Chromatin by Histone Modifications. *Cell Res.* **2011**, *21* (3), 381–395. https://doi.org/10.1038/cr.2011.22.

(9) Jin,Linhua; Li, Y. Structural and Functional Insights into Nuclear Receptor Signaling. *Adv Drug Deliv Rev* **2010**, *62* (13), 1218–1226. https://doi.org/10.1038/nature08365.Reconstructing.

(10) O'Malley, B. W.; Tsai, M. J. Molecular Pathways of Steroid Receptor Action. *Biol. Reprod.* **1991**, *46* (2), 163–167. https://doi.org/10.1095/biolreprod46.2.163.

(11) Gronemeyer, H.; Moras, D. Nuclear Receptors. How to Finger DNA. *Nature* **1995**, *375*, 190–191.

(12) Sever, R.; Glass, C. K. Signaling by Nuclear Receptors. *Cold Spring Harb. Perspect. Biol.* **2013**, *5* (3), 1–4. https://doi.org/10.1101/cshperspect.a016709.

(13) Mangelsdorf, D. J.; Thummel, C.; Beato, M.; Herrlich, P.; Schütz, G.; Umesono, K.; Blumberg, B.; Kastner, P.; Mark, M.; Chambon, P.; Evans, R. M. The Nuclear Receptor Superfamily: The Second Decade. *Cell* **1995**, *83* (6), 835–839. https://doi.org/10.1016/0092-8674(95)90199-X.

(14) Weikum, E. R.; Tuntland, M. L.; Murphy, M. N.; Ortlund, E. A. A Structural Investigation into Oct4 Regulation by Orphan Nuclear Receptors, Germ Cell Nuclear Factor (GCNF), and Liver Receptor Homolog-1 (LRH-1). *J. Mol. Biol.* **2016**, *428* (24), 4981–4992. https://doi.org/10.1016/j.jmb.2016.10.025.

(15) Little, T. H.; Zhang, Y.; Matulis, C. K.; Weck, J.; Zhang, Z.; Ramachandran, A.; Mayo, K. E.; Radhakrishnan, I. Sequence-Specific Deoxyribonucleic Acid (DNA) Recognition by Steroidogenic Factor 1: A Helix at the Carboxy Terminus of the DNA Binding Domain Is Necessary for Complex Stability. *Mol. Endocrinol.* **2006**, *20* (4), 831–843. https://doi.org/10.1210/me.2005-0384.

(16) Lang, A.; Isigkeit, L.; Schubert-Zsilavecz, M.; Merk, D. The Medicinal Chemistry and Therapeutic Potential of LRH-1 Modulators. *J. Med. Chem.* **2021**, *64* (23), 16956–16973. https://doi.org/10.1021/acs.jmedchem.1c01663.
(17) Fayard, E.; Auwerx, J.; Schoonjans, K. LRH-1: An Orphan Nuclear Receptor Involved in Development, Metabolism and Steroidogenesis. *Trends Cell Biol.* **2004**, *14* (5), 250–260. https://doi.org/10.1016/j.tcb.2004.03.008.
(18) Sun, Y.; Demagny, H.; Schoonjans, K. Emerging Functions of the Nuclear Receptor LRH-1 in Liver Physiology and Pathology. *Biochim. Biophys. Acta - Mol. Basis Dis.* **2021**, *1867* (8), 166145. https://doi.org/10.1016/j.bbadis.2021.166145.
(19) Gu, P.; Goodwin, B.; Chung, A. C.-K.; Xu, X.; Wheeler, D. A.; Price, R. R.; Galardi, C.; Peng, L.; Latour, A. M.; Koller, B. H.; Gossen, J.; Kliewer, S. A.; Cooney, A. J. Orphan Nuclear Receptor LRH-1 Is Required To Maintain Oct4 Expression at the Epiblast Stage of Embryonic Development. *Mol. Cell. Biol.* **2005**, *25* (9), 3492–3505. https://doi.org/10.1128/mcb.25.9.3492-3505.2005.
(20) Schwaderer, J.; Phan, T. S.; Glöckner, A.; Delp, J.; Leist, M.; Brunner, T.; Delgado, M. E. Pharmacological LRH-1/Nr5a2 Inhibition Limits pro-Inflammatory Cytokine Production in Macrophages and Associated Experimental Hepatitis. *Cell Death Dis.* **2020**, *11* (2). https://doi.org/10.1038/s41419-020-2348-9.
(21) Michalek, S.; Brunner, T. Nuclear-Mitochondrial Crosstalk: On the Role of the Nuclear Receptor Liver Receptor Homolog-1 (NR5A2) in the Regulation of Mitochondrial Metabolism, Cell Survival, and Cancer. *IUBMB Life* **2021**, *73* (3), 592–610. https://doi.org/10.1002/iub.2386.
(22) Cai, Z.; Wang, S.; Li, J. Treatment of Inflammatory Bowel Disease: A Comprehensive Review. *Front. Med.* **2021**, *8* (December), 1–24. https://doi.org/10.3389/fmed.2021.765474.
(23) Adolph, T. E.; Meyer, M.; Schwärzler, J.; Mayr, L.; Grabherr, F.; Tilg, H. The Metabolic Nature of Inflammatory Bowel Diseases. *Nat. Rev. Gastroenterol. Hepatol.* **2022**, *19* (12), 753–767. https://doi.org/10.1038/s41575-022-00658-y.
(24) Zerlotin, R.; Arconzo, M.; Piccinin, E.; Moschetta, A. Another One Bites the Gut: Nuclear Receptor Lrh-1 in Intestinal Regeneration and Cancer. *Cancers (Basel).* **2021**, *13* (4), 1–17. https://doi.org/10.3390/cancers13040896.
(25) Coste, A.; Dubuquoy, L.; Barnouin, R.; Annicotte, J. S.; Magnier, B.; Notti, M.; Corazza, N.; Antal, M. C.; Metzger, D.; Desreumaux, P.; Brunner, T.; Auwerx, J.; Schoonjans, K. LRH-1-Mediated Glucocorticoid Synthesis in Enterocytes Protects against Inflammatory Bowel Disease. *Proc. Natl. Acad. Sci. U. S. A.* **2007**, *104* (32), 13098–13103. https://doi.org/10.1073/pnas.0702440104.
(26) Mays, S. G.; D'Agostino, E. H.; Flynn, A. R.; Huang, X.; Wang, G.; Liu, X.; Millings, E. J.; Okafor, C. D.; Patel, A.; Cato, M. L.; Cornelison, J. L.; Melchers, D.; Houtman, R.; Moore, D. D.; Calvert, J. W.; Jui, N. T.; Ortlund, E. A. A Phospholipid Mimetic Targeting LRH-1 Ameliorates Colitis. *Cell Chem. Biol.* **2022**, *29* (7), 1174-1186.e7. https://doi.org/10.1016/j.chembiol.2022.03.001.
(27) Heng, J. C. D.; Feng, B.; Han, J.; Jiang, J.; Kraus, P.; Ng, J. H.; Orlov, Y. L.; Huss, M.; Yang, L.; Lufkin, T.; Lim, B.; Ng, H. H. The Nuclear Receptor Nr5a2 Can Replace Oct4 in the Reprogramming of Murine Somatic Cells to Pluripotent Cells. *Cell Stem Cell* **2010**, *6* (2), 167–174. https://doi.org/10.1016/j.stem.2009.12.009.
(28) Nadolny, C.; Dong, X. Liver Receptor Homolog-1 (LRH-1): A Potential Therapeutic

Target for Cancer. *Cancer Biol. Ther.* **2015**, *16* (7), 997–1004. https://doi.org/10.1080/15384047.2015.1045693.

(29) Ataollahi, M. R.; Sharifi, J.; Paknahad, M. R.; Paknahad, A. Breast Cancer and Associated Factors: A Review. *J. Med. Life* **2015**, *8* (Spec Iss 4), 6–11.

(30) Liu, Y.; Yao, J. ERα, A Key Target for Cancer Therapy.Pdf. **2020**, 2183–2191.

(31) Ortlund, E. A.; Lee, Y.; Solomon, I. H.; Hager, J. M.; Safi, R.; Choi, Y.; Guan, Z.; Tripathy, A.; Raetz, C. R. H.; McDonnell, D. P.; Moore, D. D.; Redinbo, M. R. Modulation of Human Nuclear Receptor LRH-1 Activity by Phospholipids and SHP. *Nat. Struct. Mol. Biol.* **2005**, *12* (4), 357–363. https://doi.org/10.1038/nsmb910.

(32) Krylova, I. N.; Sablin, E. P.; Moore, J.; Xu, R. X.; Waitt, G. M.; MacKay, J. A.; Juzumiene, D.; Bynum, J. M.; Madauss, K.; Montana, V.; Lebedeva, L.; Suzawa, M.; Williams, J. D.; Williams, S. P.; Guy, R. K.; Thornton, J. W.; Fletterick, R. J.; Willson, T. M.; Ingraham, H. A. Structural Analyses Reveal Phosphatidyl Inositols as Ligands for the NR5 Orphan Receptors SF-1 and LRH-1. *Cell* **2005**, *120* (3), 343–355. https://doi.org/10.1016/j.cell.2005.01.024.

(33) Lee, J. M.; Lee, Y. K.; Mamrosh, J. L.; Busby, S. A.; Griffin, P. R.; Pathak, M. C.; Ortlund, E. A.; Moore, D. D. Antidiabetic Actions of a Phosphatidylcholine Ligand for Nuclear Receptor LRH-1. *Nature* **2011**, *474* (7352), 506–510. https://doi.org/10.1038/nature10111.Antidiabetic.

(34) Whitby, R. J.; Dixon, S.; Maloney, P. R.; Delerive, P.; Goodwin, B. J.; Parks, D. J.; Willson, T. M. Identification of Small Molecule Agonists of the Orphan Nuclear Receptors Liver Receptor Homolog-1 and Steroidogenic Factor-1. *J. Med. Chem.* **2006**, *49* (23), 6652–6655. https://doi.org/10.1021/jm060990k.

(35) Whitby, R. J.; Stec, J.; Blind, R. D.; Dixon, S.; Leesnitzer, L. M.; Orband-Miller, L. A.; Williams, S. P.; Willson, T. M.; Xu, R.; Zuercher, W. J.; Cai, F.; Ingraham, H. A. Small Molecule Agonists of the Orphan Nuclear Receptors Steroidogenic Factor-1 (SF-1, NR5A1) and Liver Receptor Homologue-1 (LRH-1, NR5A2). *J. Med. Chem.* **2011**, *54* (7), 2266–2281. https://doi.org/10.1021/jm1014296.

(36) Mays, S. G.; Okafor, C. D.; Whitby, R. J.; Goswami, D.; Stec, J.; Flynn, A. R.; Dugan, M. C.; Jui, N. T.; Griffin, P. R.; Ortlund, E. A. Crystal Structures of the Nuclear Receptor, Liver Receptor Homolog 1, Bound to Synthetic Agonists. *J. Biol. Chem.* **2016**, *291* (49), 25281–25291. https://doi.org/10.1074/jbc.M116.753541.

(37) Musille, R.M.; Pathak, M.; Lauer, J.L.; Hudson, W.H; Griffin, P.R.; Ortlund, E. A. Antidiabetic Phospholipid- Nuclear Receptor Complex Reveals the Mechanism for Phospholipid Driven Gene Regulation. *Nat. Struct. Mol. Biol.* **2014**, *19* (5), 532–536. https://doi.org/10.1038/nsmb.2279.Antidiabetic.

(38) Flynn, A. R.; Mays, S. G.; Ortlund, E. A.; Jui, N. T. Development of Hybrid Phospholipid Mimics as Effective Agonists for Liver Receptor Homologue-1. *ACS Med. Chem. Lett.* **2018**, *9* (10), 1051–1056. https://doi.org/10.1021/acsmedchemlett.8b00361.

(39) Mays, S. G.; Flynn, A. R.; Cornelison, J. L.; Okafor, C. D.; Wang, H.; Wang, G.; Huang, X.; Donaldson, H. N.; Millings, E. J.; Polavarapu, R.; Moore, D. D.; Calvert, J. W.; Jui, N. T.; Ortlund, E. A. Development of the First Low Nanomolar Liver Receptor Homolog-1 Agonist through Structure-Guided Design. *J. Med. Chem.* **2019**, *62* (24), 11022–11034. https://doi.org/10.1021/acs.jmedchem.9b00753.

(40) Cato, M. L.; Cornelison, J. L.; Spurlin, R. M.; Courouble, V. V.; Patel, A. B.; Flynn, A. R.; Johnson, A. M.; Okafor, C. D.; Frank, F.; D'Agostino, E. H.; Griffin, P. R.; Jui, N. T.;

Ortlund, E. A. Differential Modulation of Nuclear Receptor LRH-1 through Targeting Buried and Surface Regions of the Binding Pocket. *J. Med. Chem.* **2022**, No. Figure 1. https://doi.org/10.1021/acs.jmedchem.2c00235.

(41) Corzo, C. A.; Mari, Y.; Chang, M. R.; Khan, T.; Kuruvilla, D.; Nuhant, P.; Kumar, N.; West, G. M.; Duckett, D. R.; Roush, W. R.; Griffin, P. R. Antiproliferation Activity of a Small Molecule Repressor of Liver Receptor Homolog 1. *Mol. Pharmacol.* **2015**, *87* (2), 296–304. https://doi.org/10.1124/mol.114.095554.

(42) Benod, C.; Carlsson, J.; Uthayaruban, R.; Hwang, P.; Irwin, J. J.; Doak, A. K.; Shoichet, B. K.; Sablin, E. P.; Fletterick, R. J. Structure-Based Discovery of Antagonists of Nuclear Receptor LRH-1. *J. Biol. Chem.* **2013**, *288* (27), 19830–19844. https://doi.org/10.1074/jbc.M112.411686.

(43) Rey, J.; Hu, H.; Kyle, F.; Lai, C. F.; Buluwela, L.; Coombes, R. C.; Ortlund, E. A.; Ali, S.; Snyder, J. P.; Barrett, A. G. M. Discovery of a New Class of Liver Receptor Homolog-1 (LRH-1) Antagonists: Virtual Screening, Synthesis and Biological Evaluation. *ChemMedChem* **2012**, *7* (11), 1909–1914. https://doi.org/10.1002/cmdc.201200307.

(44) Sablin, E. P.; Krylova, I. N.; Fletterick, R. J.; Ingraham, H. A. Structural Basis for Ligand-Independent Activation of the Orphan Nuclear Receptor LRH-1. *Mol. Cell* **2003**, *11* (6), 1575–1585. https://doi.org/10.1016/S1097-2765(03)00236-3.

(45) Ikeda, Y. SF-1: A Key Regulator of Development and Function in the Mammalian Reproductive System. *Pediatr. Int.* **1996**, *38* (4), 412–419. https://doi.org/10.1111/j.1442-200X.1996.tb03516.x.

(46) Sbiera, S.; Schmull, S.; Assie, G.; Voelker, H. U.; Kraus, L.; Beyer, M.; Ragazzon, B.; Beuschlein, F.; Willenberg, H. S.; Hahner, S.; Saeger, W.; Bertherat, J.; Allolio, B.; Fassnacht, M. High Diagnostic and Prognostic Value of Steroidogenic Factor-1 Expression in Adrenal Tumors. *J. Clin. Endocrinol. Metab.* **2010**, *95* (10), 161–171. https://doi.org/10.1210/jc.2010-0653.

(47) Lewis, S. R.; Hedman, C. J.; Ziegler, T.; Ricke, W. A.; Jorgensen, J. S. Steroidogenic Factor 1 Promotes Aggressive Growth of Castration-Resistant Prostate Cancer Cells by Stimulating Steroid Synthesis and Cell Proliferation. *Endocrinology* **2014**, *155* (2), 358–369. https://doi.org/10.1210/en.2013-1583.

(48) Willson, T. M.; Kliewer, S. A. PXR, Car and Drug Metabolism. *Nat. Rev. Drug Discov.* **2002**, *1* (4), 259–266. https://doi.org/10.1038/nrd753.

(49) Oladimeji, P. O.; Chen, T. PXR: More than Just a Master Xenobiotic Receptor. *Mol. Pharmacol.* **2018**, *93* (2), 119–127. https://doi.org/10.1124/mol.117.110155.

(50) D'Agostino, E. H.; Flynn, A. R.; Cornelison, J. L.; Mays, S. G.; Patel, A.; Jui, N. T.; Ortlund, E. A. Development of a Versatile and Sensitive Direct Ligand Binding Assay for Human NR5A Nuclear Receptors. *ACS Med. Chem. Lett.* **2020**, *11* (3), 365–370. https://doi.org/10.1021/acsmedchemlett.9b00442.

(51) Lipinski, C. A. Drug-like Properties and the Causes of Poor Solubility and Poor Permeability. *J. Pharmacol. Toxicol. Methods* **2000**, *44* (1), 235–249. https://doi.org/10.1016/S1056-8719(00)00107-6.

(52) Cozzini, P.; Spyrakis, F. Exercise I . 12 Hydrophobicity in Drug Design. *Biochemistry* **2006**, No. December, 1–33.

(53) Alavijeh, M. S.; Chishty, M.; Qaiser, M. Z.; Palmer, A. M. Drug Metabolism and Pharmacokinetics, the Blood-Brain Barrier, and Central Nervous System Drug Discovery. *NeuroRx* **2005**, *2* (4), 554–571. https://doi.org/10.1602/neurorx.2.4.554.

(54) Leibman, K. C. Metabolism and Toxicity of Styrene. *Environ. Health Perspect.* **1975**, *11* (June), 115–119. https://doi.org/10.1289/ehp.7511115.
(55) Shen, Shuijie; Li, Lei; Ding, Xinxin; Zheng, J. Metabolism of Styrene to Styrene Oxide and Vinylphenols in Cytochrom P450 2F2- and P450 2E1-Knockout Mouse Liver and Lung Microsomes. *Chem Res Toxicol* **2014**, *27* (1), 27–33. https://doi.org/10.1038/nature08365.Reconstructing.
(56) Davis, Jeremy; Whitby, R. J.-C. A. Convergent Synthesis of Aminobicyclo[3.3.0]Octenes Using Zirconium Chemistry An Unusual Anti-1,3-Amine Shift. *Synlett Lett.* **1993**, 110–112.
(57) Cornelison, J. L.; Cato, M. L.; Johnson, A. M.; D'Agostino, E. H.; Melchers, D.; Patel, A. B.; Mays, S. G.; Houtman, R.; Ortlund, E. A.; Jui, N. T. Development of a New Class of Liver Receptor Homolog-1 (LRH-1) Agonists by Photoredox Conjugate Addition. *Bioorganic Med. Chem. Lett.* **2020**, *30* (16), 127293. https://doi.org/10.1016/j.bmcl.2020.127293.
(58) Yamashita, M.; Yamashita, T.; Aoyagi, S. Toward the Racemic Total Synthesis of Hederacines A and B: Construction of an Advanced Tricyclic Intermediate. *Org. Lett.* **2011**, *13* (9), 2204–2207. https://doi.org/10.1021/ol2004353.
(59) Ovung, A.; Bhattacharyya, J. Sulfonamide Drugs: Structure, Antibacterial Property, Toxicity, and Biophysical Interactions. *Biophys. Rev.* **2021**, *13* (2), 259–272. https://doi.org/10.1007/s12551-021-00795-9.
(60) Mays, S. G.; Stec, J.; Liu, X.; D'Agostino, E. H.; Whitby, R. J.; Ortlund, E. A. Enantiomer-Specific Activities of an LRH-1 and SF-1 Dual Agonist. *Sci. Rep.* **2020**, *10* (1), 1–14. https://doi.org/10.1038/s41598-020-79251-9.
(61) Jahromi, A. H.; Fu, Y.; Miller, K. A.; Nguyen, L.; Luu, L. M.; Baranger, A. M.; Zimmerman, S. C. Developing Bivalent Ligands to Target CUG Triplet Repeats, the Causative Agent of Myotonic Dystrophy Type 1. *J. Med. Chem.* **2013**, *56* (23), 9471–9481. https://doi.org/10.1021/jm400794z.
(62) LaFrate, A. L.; Carlson, K. E.; Katzenellenbogen, J. A. Steroidal Bivalent Ligands for the Estrogen Receptor: Design, Synthesis, Characterization and Binding Affinities. *Bioorganic Med. Chem.* **2009**, *17* (10), 3528–3535. https://doi.org/10.1016/j.bmc.2009.04.016.
(63) Sakamoto, K. M.; Kim, K. B.; Kumagai, A.; Mercurio, F.; Crews, C. M.; Deshaies, R. J. Protacs: Chimeric Molecules That Target Proteins to the Skp1-Cullin-F Box Complex for Ubiquitination and Degradation. *Proc. Natl. Acad. Sci. U. S. A.* **2001**, *98* (15), 8554–8559. https://doi.org/10.1073/pnas.141230798.
(64) Burslem, G. M.; Crews, C. M. Small-Molecule Modulation of Protein Homeostasis. *Chem. Rev.* **2017**, *117* (17), 11269–11301. https://doi.org/10.1021/acs.chemrev.7b00077.
(65) Moreau, K.; Coen, M.; Zhang, A. X.; Pachl, F.; Castaldi, M. P.; Dahl, G.; Boyd, H.; Scott, C.; Newham, P. Proteolysis-Targeting Chimeras in Drug Development: A Safety Perspective. *Br. J. Pharmacol.* **2020**, *177* (8), 1709–1718. https://doi.org/10.1111/bph.15014.
(66) Qi, S. M.; Dong, J.; Xu, Z. Y.; Cheng, X. D.; Zhang, W. D.; Qin, J. J. PROTAC: An Effective Targeted Protein Degradation Strategy for Cancer Therapy. *Front. Pharmacol.* **2021**, *12* (May), 1–13. https://doi.org/10.3389/fphar.2021.692574.
(67) Bondeson, D. P.; Smith, B. E.; Burslem, G. M.; Buhimschi, A. D.; Hines, J.; Jaime-Figueroa, S.; Wang, J.; Hamman, B. D.; Ishchenko, A.; Crews, C. M. Lessons in

PROTAC Design from Selective Degradation with a Promiscuous Warhead. *Cell Chem. Biol.* **2018**, *25* (1), 78-87.e5. https://doi.org/10.1016/j.chembiol.2017.09.010.

(68) Békés, M.; Langley, D. R.; Crews, C. M. PROTAC Targeted Protein Degraders: The Past Is Prologue. *Nat. Rev. Drug Discov.* **2022**, *21* (3), 181–200. https://doi.org/10.1038/s41573-021-00371-6.

(69) Kedra Cyrus,†, Marie Wehenkela,†, Eun-Young Choib, Hyeong-Jun Hana, Hyosung Leea, Hollie Swansonb, and K.-B. K. Impact of Linker Length on the Activity of PROTACs. **2013**, *7* (2). https://doi.org/10.1039/b000000x/Cyrus.

(70) Zou, L.; Braegelman, A. S.; Webber, M. J. Spatially Defined Drug Targeting by in Situ Host-Guest Chemistry in a Living Animal. *ACS Cent. Sci.* **2019**, *5* (6), 1035–1043. https://doi.org/10.1021/acscentsci.9b00195.

(71) Bhushan, B.; Lin, Y. A.; Bak, M.; Phanumartwiwath, A.; Yang, N.; Bilyard, M. K.; Tanaka, T.; Hudson, K. L.; Lercher, L.; Stegmann, M.; Mohammed, S.; Davis, B. G. Genetic Incorporation of Olefin Cross-Metathesis Reaction Tags for Protein Modification. *J. Am. Chem. Soc.* **2018**, *140* (44), 14599–14603. https://doi.org/10.1021/jacs.8b09433.

(72) Guo, Z.; Sun, Y.; Liang, L.; Lu, W.; Luo, B.; Wu, Z.; Huo, B.; Hu, Y.; Huang, P.; Wu, Q.; Wen, S. Design and Synthesis of Dual EZH2/BRD4 Inhibitors to Target Solid Tumors. *J. Med. Chem.* **2021**. https://doi.org/10.1021/acs.jmedchem.1c01876.

(73) Nakamura, T.; Noguchi, T.; Kobayashi, H.; Miyachi, H.; Hashimoto, Y. Mono- and Dihydroxylated Metabolites of Thalidomide: Synthesis and TNF-α Production-Inhibitory Activity. *Chem. Pharm. Bull.* **2006**, *54* (12), 1709–1714. https://doi.org/10.1248/cpb.54.1709.

(74) Zhang, C.; Han, X. R.; Yang, X.; Jiang, B.; Liu, J.; Xiong, Y.; Jin, J. Proteolysis Targeting Chimeras (PROTACs) of Anaplastic Lymphoma Kinase (ALK). *Eur. J. Med. Chem.* **2018**, *151*, 304–314. https://doi.org/10.1016/j.ejmech.2018.03.071.

(75) Crew, A. P.; Raina, K.; Dong, H.; Qian, Y.; Wang, J.; Vigil, D.; Serebrenik, Y. V.; Hamman, B. D.; Morgan, A.; Ferraro, C.; Siu, K.; Neklesa, T. K.; Winkler, J. D.; Coleman, K. G.; Crews, C. M. Identification and Characterization of von Hippel-Lindau-Recruiting Proteolysis Targeting Chimeras (PROTACs) of TANK-Binding Kinase 1. *J. Med. Chem.* **2018**, *61* (2), 583–598. https://doi.org/10.1021/acs.jmedchem.7b00635.

(76) Paech, K.; Webb, P.; Kuiper, G. G.; Nilsson, S.; Gustafsson, J.; Kushner, P. J.; Scanlan, T. S.; Ramsey, T. L.; Risinger, K. E.; Jernigan, S. C.; Mattingly, K. A.; Klinge, C. M.; Filant, J.; Spencer, T. E. Differential Ligand Activation of Estrogen Receptors ERalpha and ERbeta at AP1 Sites. **2013**, *277*; *145;* (September), 1508; 149–1510; 160.

(77) Okamoto, Y.; Shibutani, S. Development of Novel and Safer Anti-Breast Cancer Agents, SS1020 and SS5020, Based on a Fundamental Carcinogenic Research. *Genes Environ.* **2019**, *41* (1), 1–6. https://doi.org/10.1186/s41021-019-0124-9.

(78) Pearce, S. T.; Liu, H.; Jordan, V. C. Modulation of Estrogen Receptor α Function and Stability by Tamoxifen and a Critical Amino Acid (Asp-538) in Helix 12. *J. Biol. Chem.* **2003**, *278* (9), 7630–7638. https://doi.org/10.1074/jbc.M211129200.

(79) Tsang, K. Y.; Brimble, M. A. Synthesis of Aromatic Spiroacetals Related to γ-Rubromycin Based on a 3H-Spiro[1-Benzofuran-2,2′-Chromane] Skeleton. *Tetrahedron* **2007**, *63* (26), 6015–6034. https://doi.org/10.1016/j.tet.2007.02.033.

(80) He, M. X.; Mo, Z. Y.; Wang, Z. Q.; Cheng, S. Y.; Xie, R. R.; Tang, H. T.; Pan, Y. M. Electrochemical Synthesis of 1-Naphthols by Intermolecular Annulation of Alkynes with 1,3-Dicarbonyl Compounds. *Org. Lett.* **2020**, *22* (2), 724–728.

https://doi.org/10.1021/acs.orglett.9b04549.
(81) Griggs, S. D.; Tape, D. T.; Clarke, P. A. Strategies for the Last Synthesis of Spiropiperdines- a Review of the Last 10 Years. *Org. Biomol. Chem.* **2018**, *16* (36), 6620–6633. https://doi.org/10.1039/c8ob01271g.
(82) Hiesinger, K.; Dar'In, D.; Proschak, E.; Krasavin, M. Spirocyclic Scaffolds in Medicinal Chemistry. *J. Med. Chem.* **2021**, *64* (1), 150–183. https://doi.org/10.1021/acs.jmedchem.0c01473.
(83) Wei, W.; Cherukupalli, S.; Jing, L.; Liu, X.; Zhan, P. Fsp3: A New Parameter for Drug-Likeness. *Drug Discov. Today* **2020**, *25* (10), 1839–1845. https://doi.org/10.1016/j.drudis.2020.07.017.
(84) Talele, T. T. Opportunities for Tapping into Three-Dimensional Chemical Space through a Quaternary Carbon. *J. Med. Chem.* **2020**, *63* (22), 13291–13315. https://doi.org/10.1021/acs.jmedchem.0c00829.
(85) Lovering, F.; Bikker, J.; Humblet, C. Escape from Flatland: Increasing Saturation as an Approach to Improving Clinical Success. *J. Med. Chem.* **2009**, *52* (21), 6752–6756. https://doi.org/10.1021/jm901241e.
(86) Chupakhin, E.; Babich, O.; Prosekov, A.; Asyakina, L.; Krasavin, M. Spirocyclic Motifs in Natural Products. *Molecules* **2019**, *24* (22). https://doi.org/10.3390/molecules24224165.
(87) Garthwaite, S. M.; McMahon, E. G. The Evolution of Aldosterone Antagonists. *Mol. Cell. Endocrinol.* **2004**, *217* (1–2), 27–31. https://doi.org/10.1016/j.mce.2003.10.005.
(88) Kazmierski, W. M.; Xia, B.; Miller, J.; De La Rosa, M.; Favre, D.; Dunham, R. M.; Washio, Y.; Zhu, Z.; Wang, F.; Mebrahtu, M.; Deng, H.; Basilla, J.; Wang, L.; Evindar, G.; Fan, L.; Olszewski, A.; Prabhu, N.; Davie, C.; Messer, J. A.; Samano, V. DNA-Encoded Library Technology-Based Discovery, Lead Optimization, and Prodrug Strategy toward Structurally Unique Indoleamine 2,3-Dioxygenase-1 (IDO1) Inhibitors. *J. Med. Chem.* **2020**, *63* (7), 3552–3562. https://doi.org/10.1021/acs.jmedchem.9b01799.
(89) Vitaku, E.; Smith, D. T.; Njardarson, J. T. Analysis of the Structural Diversity, Substitution Patterns, and Frequency of Nitrogen Heterocycles among U.S. FDA Approved Pharmaceuticals. *J. Med. Chem.* **2014**, *57* (24), 10257–10274. https://doi.org/10.1021/jm501100b.
(90) Szczepańska, K.; Podlewska, S.; Dichiara, M.; Gentile, D.; Patamia, V.; Rosier, N.; Mönnich, D.; Ruiz Cantero, M. C.; Karcz, T.; Łażewska, D.; Siwek, A.; Pockes, S.; Cobos, E. J.; Marrazzo, A.; Stark, H.; Rescifina, A.; Bojarski, A. J.; Amata, E.; Kieć-Kononowicz, K. Structural and Molecular Insight into Piperazine and Piperidine Derivatives as Histamine H3 and Sigma-1 Receptor Antagonists with Promising Antinociceptive Properties. *ACS Chem. Neurosci.* **2022**, *13* (1), 1–15. https://doi.org/10.1021/acschemneuro.1c00435.
(91) Goldberg, J. S. Stereochemical Basis for a Unified Structure Activity Theory of Aromatic and Heterocyclic Rings in Selected Opioids and Opioid Peptides. *Perspect. Medicin. Chem.* **2010**, *2010* (4), 1–10. https://doi.org/10.4137/pmc.s3898.
(92) Andreini, C.; Bertini, I.; Cavallaro, G.; Holliday, G. L.; Thornton, J. M. Metal Ions in Biological Catalysis: From Enzyme Databases to General Principles. *J. Biol. Inorg. Chem.* **2008**, *13* (8), 1205–1218. https://doi.org/10.1007/s00775-008-0404-5.
(93) Bell, E. L.; Finnigan, W.; France, S. P.; Green, A. P.; Hayes, M. A.; Hepworth, L. J.; Lovelock, S. L.; Niikura, H.; Osuna, S.; Romero, E.; Ryan, K. S.; Turner, N. J.; Flitsch, S. L. Biocatalysis. *Nat. Rev. Methods Prim.* **2021**, *1* (1), 1–21.

https://doi.org/10.1038/s43586-021-00044-z.
(94) Yi, D.; Bayer, T.; Badenhorst, C. P. S.; Wu, S.; Doerr, M.; Höhne, M.; Bornscheuer, U. T. Recent Trends in Biocatalysis. *Chem. Soc. Rev.* **2021**, *50* (14), 8003–8049. https://doi.org/10.1039/d0cs01575j.
(95) Jegannathan, K. R.; Nielsen, P. H. Environmental Assessment of Enzyme Use in Industrial Production-a Literature Review. *J. Clean. Prod.* **2013**, *42*, 228–240. https://doi.org/10.1016/j.jclepro.2012.11.005.
(96) Romero, N. A.; Nicewicz, D. A. Organic Photoredox Catalysis. *Chem. Rev.* **2016**, *116* (17), 10075–10166. https://doi.org/10.1021/acs.chemrev.6b00057.
(97) Prier, C. K.; Rankic, D. A.; MacMillan, D. W. C. Visible Light Photoredox Catalysis with Transition Metal Complexes: Applications in Organic Synthesis. *Chem. Rev.* **2013**, *113* (7), 5322–5363. https://doi.org/10.1021/cr300503r.
(98) Nguyen, J. D.; D'Amato, E. M.; Narayanam, J. M. R.; Stephenson, C. R. J. Engaging Unactivated Alkyl, Alkenyl and Aryl Iodides in Visible-Light-Mediated Free Radical Reactions. *Nat. Chem.* **2012**, *4* (10), 854–859. https://doi.org/10.1038/nchem.1452.
(99) Aycock, R. A.; Wang, H.; Jui, N. T. A Mild Catalytic System for Radical Conjugate Addition of Nitrogen Heterocycles. *Chem. Sci.* **2017**, *8* (4), 3121–3125. https://doi.org/10.1039/c7sc00243b.
(100) Boyington, A. J.; Riu, M. L. Y.; Jui, N. T. Anti-Markovnikov Hydroarylation of Unactivated Olefins via Pyridyl Radical Intermediates. *J. Am. Chem. Soc.* **2017**, *139* (19), 6582–6585. https://doi.org/10.1021/jacs.7b03262.
(101) Flynn, A. R.; Mcdaniel, K. A.; Hughes, M. E.; Vogt, D. B.; Jui, N. T. Hydroarylation of Arenes via Reductive Radical-Polar Crossover. *J. Am. Chem. Soc.* **2020**, *142* (20), 9163–9168. https://doi.org/10.1021/jacs.0c03926.
(102) Martins, P.; Jesus, J.; Santos, S.; Raposo, L. R.; Roma-Rodrigues, C.; Baptista, P. V.; Fernandes, A. R. Heterocyclic Anticancer Compounds: Recent Advances and the Paradigm Shift towards the Use of Nanomedicine's Tool Box. *Molecules* **2015**, *20* (9), 16852–16891. https://doi.org/10.3390/molecules200916852.
(103) Waldstreicher, J. WO1997041879A1.Pdf. WO1997041879A1, 1997.
(104) Maligres, P. E.; Houpis, I.; Rossen, K.; Molina, A.; Sager, J.; Upadhyay, V.; Wells, K. M.; Reamer, R. A.; Lynch, J. E.; Askin, D.; Volante, R. P.; Reider, P. J.; Houghton, P. Synthesis of the Orally Active Spiroindoline-Based Growth Hormone Secretagogue, MK-677. *Tetrahedron* **1997**, *53* (32), 10983–10992. https://doi.org/10.1016/S0040-4020(97)00359-1.
(105) Liang, G.; Choi-Sledeski, Y. M.; Poli, G. B.; Chen, X.; Minnich, A.; Wang, Q.; Tsay, J.; Sides, K.; Vaz, R. J. Structure-Based Design, Synthesis, and Profiling of a β-Tryptase Inhibitor with a Spiro-Piperidineamide Scaffold, Benzylamine P1 Group, and a Substituted Indole P4 Group. *Medchemcomm* **2011**, *2* (8), 794–799. https://doi.org/10.1039/c1md00104c.
(106) Chen, M.; Abrahamt, J. A. Free Radical Method for the Synthesis of Spiro-Piperidinyl Heterocycles Abstract : A General Approach to Spiro-Piperidinyl Heterocycles (1 , X = S , O , NH , NAc) Was Obtained from the Key Intermediate 3 via an Efficient Radical Reaction . Copyright © 1. *Tetrahedron Lett.* **1996**, *37* (30), 5233–5234.
(107) Aycock, R. A.; Vogt, D. B.; Jui, N. T. A Practical and Scalable System for Heteroaryl Amino Acid Synthesis. *Chem. Sci.* **2017**, *8* (12), 7998–8003. https://doi.org/10.1039/c7sc03612d.

(108) Speckmeier, E.; Fischer, T. G.; Zeitler, K. A Toolbox Approach to Construct Broadly Applicable Metal-Free Catalysts for Photoredox Chemistry: Deliberate Tuning of Redox Potentials and Importance of Halogens in Donor-Acceptor Cyanoarenes. *J. Am. Chem. Soc.* **2018**, *140* (45), 15353–15365. https://doi.org/10.1021/jacs.8b08933.

(109) Cheng, C.-Y.; Hsin, L.-W.; Liou, J.-P. Copyright © 1996 Elsevier Science. *Tetrahedron* **1996**, *52* (33), 10935–10944.

(110) Pasternak, G. W.; Pan, Y. X. Mu Opioids and Their Receptors: Evolution of a Concept. *Pharmacol. Rev.* **2013**, *65* (4), 1257–1317. https://doi.org/10.1124/pr.112.007138.

(111) Pause, L.; Robert, M.; Savéant, J. M. Can Single-Electron Transfer Break an Aromatic Carbon - Heteroatom Bond in One Step? A Novel Example of Transition between Stepwise and Concerted Mechanisms in the Reduction of Aromatic Iodides [5]. *J. Am. Chem. Soc.* **1999**, *121* (30), 7158–7159. https://doi.org/10.1021/ja991365q.

(112) Chen, J-M., Ho, T-I., Mou, C.-Y. DIPEA Ox Pot.Pdf. *J. Phys. Chem.* **1990**, *94*, 2889–2896.

(113) Feghhi, A.; Malakooti, R.; Malakooti, S. Scaled-up, Selective and Green Synthesis of Sulfoxides under Mild Conditions Using (CeIII-MoVI)Ox/Aniline Hybrid Rods as an Efficient Catalyst. *Appl. Organomet. Chem.* **2019**, *33* (12), 1–11. https://doi.org/10.1002/aoc.5237.

(114) Costanzo, Michael J.; Yabut, Stephen, C.; Tounge, Brett; Maryanoff, Bruce, E.; Zhang, H.-C. WO 2009067202. *WO 2009067202* **2013**.

(115) Varela-Fernández, A.; Varela, J. A.; Saá, C. Formation of Indoles, Dihydroisoquinolines, and Dihydroquinolines by Ruthenium-Catalyzed Heterocyclizations. *Synth.* **2012**, *44* (21), 3285–3295. https://doi.org/10.1055/s-0032-1316539.

(116) Xiao, W. J.; Alper, H. Regioselective Carbonylative Heteroannulation of O-Iodothiophenols with Allenes and Carbon Monoxide Catalyzed by a Palladium Complex: A Novel and Efficient Access to Thiochroman-4-One Derivatives. *J. Org. Chem.* **1999**, *64* (26), 9646–9652. https://doi.org/10.1021/jo9913098.

(117) Seashore-Ludlow, B.; Somfai, P. Domino Carbopalladation-Carbonylation: Generating Quaternary Stereocenters While Controlling β-Hydride Elimination. *Org. Lett.* **2010**, *12* (17), 3732–3735. https://doi.org/10.1021/ol1009703.

(118) Hanessian, S.; Szychowski, J.; Pablo Maianti, J. Synthesis and Comparative Antibacterial Activity of Verdamicin C2 and C2a. A New Oxidation of Primary Allylic Azides in Dihydro[2H]Pyrans. *Org. Lett.* **2009**, *11* (2), 429–432. https://doi.org/10.1021/ol802421d.

(119) Ishizaki, M.; Ozaki, K.; Kanematsu, A.; Isoda, T.; Hoshino, O. Synthetic Approaches toward Spiro[2,3-Dihydro-4H-1-Benzopyran-4,1′-Cyclohexan]-2-One Derivatives via Radical Reactions: Total Synthesis of (±)-Lycoramine. *J. Org. Chem.* **1993**, *58* (15), 3877–3885. https://doi.org/10.1021/jo00067a019.

(120) Brnardic, E. J.; Ye, G.; Brooks, C.; Donatelli, C.; Barton, L.; McAtee, J.; Sanchez, R. M.; Shu, A.; Erhard, K.; Terrell, L.; Graczyk-Millbrandt, G.; He, Y.; Costell, M. H.; Behm, D. J.; Roethke, T.; Stoy, P.; Holt, D. A.; Lawhorn, B. G. Discovery of Pyrrolidine Sulfonamides as Selective and Orally Bioavailable Antagonists of Transient Receptor Potential Vanilloid-4 (TRPV4). *J. Med. Chem.* **2018**, *61* (21), 9738–9755. https://doi.org/10.1021/acs.jmedchem.8b01317.

(121) Aponick, A.; Dietz, A. L.; Pearson, W. H. 2-(3-Pyrrolin-1-Yl)-1,4-Naphthoquinones: Photoactivated Alkylating Agents. *European J. Org. Chem.* **2008**, No. 25, 4264–4276. https://doi.org/10.1002/ejoc.200800482.

(122) Shaughnessy, K. H.; Hamann, B. C.; Hartwig, J. F. Palladium-Catalyzed Inter- and Intramolecular α-Arylation of Amides. Application of Intramolecular Amide Arylation to the Synthesis of Oxindoles. *J. Org. Chem.* **1998**, *63* (19), 6546–6553. https://doi.org/10.1021/jo980611y.